TO INVESTIGATE THE PHENOMENON OF SURFACE MODIFICATION IN DIE STEELS USING EDM PROCESS

A THESIS

Submitted in fulfilment of the requirements

for the award of the degree

of

DOCTOR OF PHILOSOPHY

in

MECHANICAL ENGINEERING

By

SANJEEV KUMAR

DEPARTMENT OF MECHANICAL ENGINEERING

THAPAR UNIVERSITY

PATIALA – 147 004, PUNJAB, INDIA.

December, 2008

CERTIFICATE

Certified that the work which is being presented in this thesis entitled **"To investigate the phenomenon of surface modification in die steels using EDM Process"** by Mr. Sanjeev Kumar in fulfillment of the requirements for the award of degree of **Doctor of Philosophy** and submitted to the **Department of Mechanical Engineering, Thapar University, Patiala**, is an authentic record of research work carried out by him under our guidance. The matter contained in this thesis work has not been submitted for the award of any other degree.

Dated 4/12/08

(Dr. T. P. Singh)

Director
Rayat Institute of Engg. and
Information Tech., Nawanshahar.
Formerly Professor
Deptt. of Mechanical Engg.
Thapar University, Patiala,
Punjab, INDIA.

(Dr. B. L. Sethi)

Director
Guru Nanak Institute of Tech.
Mullana (Distt. Ambala),
Haryana, INDIA.

ACKNOWLEDGEMENT

I express my sincere gratitude to my supervisors, Dr. T. P. Singh and Dr. B. L. Sethi for their deep involvement, invaluable help, guidance and words of inspiration at every stage of this thesis work.

I am indebted to the college authorities of Thapar University, Patiala for providing me with various workshop, laboratory and computer facilities required for this work. In particular, I am grateful to Dr. S. K. Mohapatra, Dr. Ajay Batish, Sh. Sukhdev Chand, Sh. Trilok Singh and Sh. Purushottam Singh who were always so willing to help me in the various activities related to this thesis work.

I am thankful to Dr. A. S. Arora and Sh. Harmesh Kansal of Sant Longowal Institute of Engineering & Technology for helping me in carrying out the micro-hardness testing. I am also thankful to Sh. Suresh Kumar for his help in arranging the various electrode materials and metallic powders for the experimentation.

No words are sufficient to describe my gratitude to Sh. B. S. Sangha and Sh. Sanjeev Katoch of Institute of Autoparts Technology, Ludhiana for the help and care provided by them during my numerous visits to that institute. Sh. Siddharth Thakkar deserves a special mention for helping me in writing the thesis.

I also gratefully acknowledge the help provided by Dr. O. P. Pandey, Dr. Rupinder Singh and Dr. Ravinderjit Singh Walia during the analysis of the results. I am indebted to Sh. Dhiraj Mahajan, Research Scholar at Indian Institute of Technology, Kanpur, for his help in arranging the literature.

In the end, I express my heartfelt thanks to my family members and friends for their continuous encouragement and support.

Dated : 4th December, 2008

(SANJEEV KUMAR)

ABSTRACT

Electrical Discharge Machining (EDM) has established itself as one of the most versatile machining process in the manufacture of press tools, dies and punches. In this process, a tool (electrode) cuts the work material by a series of electrical sparks generated in a dielectric medium and produces a mirror image of itself by advancing into the workpiece. Some of the reasons for the tremendous popularity of this process are its ability to machine complex internal shapes in hardened materials, negligible cutting forces because of absence of any physical contact between the tool and work material, distortion-free accurate machining, easy fabrication of the tool and simple operation of the machine.

Though EDM is essentially a material removal process, a number of phenomena observed during machining make it a suitable technology for application in the field of surface improvement. Each spark generates a temperature in the range of 8,000 to 12,000 ^{0}C and creates a plasma channel; causing fusion or partial vapourization of the workpiece material, tool electrode and the dielectric fluid at the point of discharge. As the plasma channel collapses towards the end of the machining cycle, some of these constituents may get deposited on the machined surface under appropriate process conditions. Suitable alloying elements may be introduced in the tool electrode bodies or added to the dielectric medium in the form of fine powders for specific surface modifications. These elements may migrate to the machined surface either in free form or as carbides by combining with carbon generated from the breakdown of the hydrocarbon dielectric. The changes in chemical composition of the surface and its quenching by the flowing dielectric bring about desirable improvements in properties. Additive powders in the dielectric medium also change the sparking pattern and hence, significantly affect the properties of the machined surface.

This research work has investigated the effect of EDM process on surface properties under machining conditions favouring material transfer to the workpiece surface from electrode bodies as well as from powders suspended in the dielectric medium. The experimentation was conducted on three of the most widely used die steel materials; namely Oil-Hardening Non-Shrinkable (OHNS type O2) die steel, High- Carbon High-Chromium (type D2) die steel and Hot work (type H13) die Steel. These materials were machined in two stages – first

with four different electrode materials, and then with four different powders mixed in the dielectric medium. The four electrode materials were copper, graphite, copper-tungsten and inconel (an alloy of nickel, chromium and iron as main constituents). The four powders used for experimentation were graphite, manganese, silicon and tungsten.

The study of existing literature in this area reveals that no work has been done on OHNS die steel which is a very important tool material for cold working applications. Inconel alloy has only been used as work material in EDM. If it is used as an electrode material, this alloy may contribute chromium and nickel to the plasma channel and consequently, to the workpiece surface. Likewise, no research work is available on the use of manganese powder in the dielectric. The effect of powder-mixed dielectric on output parameters such as material removal rate, tool wear rate and surface finish has been studied extensively but very few researchers have used this method for surface modification. Amongst the input process parameters, the effect of pulse off-time has been investigated as part of duty cycle and not as an independent variable.

The most significant machining parameters and their ranges for this work were selected on the basis of pilot experimentation. Machining was carried out by using L9 orthogonal array of Taguchi experimental design. The input process parameters that constituted the orthogonal array were Peak current, Pulse on-time and Pulse off-time. Work material was not included as one of the factors in orthogonal array because the pattern of response of each work material to surface modification was expected to be different. The set of nine experiments were repeated for each combination of electrode material and work material during the first stage; and then for each combination of powder and work material during the second stage of experimentation. As the objective of the work was to study surface modification of die steels, no attempt was made to measure conventional output parameters such as material removal rate and tool wear rate etc.

Micro-hardness and surface roughness measurements were carried out on all the machined samples and the data was analyzed as per Taguchi method to find out the best values of input process parameters for each combination of work material, electrode material and powder. Analysis of Variance (ANOVA) of the data revealed the significance and percentage contribution of the three factors. Confirmation experiments were conducted where the

desirable machining parameters did not constitute one of the rows of the orthogonal array. Optimum values and relative contribution of the three input process parameters for each electrode material or the type of powder suspended in the dielectric medium were found to be almost same irrespective of the work material. On the other hand, the best values of micro-hardness and surface roughness achieved, depended on the work material.

Peak current emerged as the most significant factor in all the experiments (more than 50 % contribution in all cases), followed by pulse on-time and then pulse off-time. However, in two cases, when machining was carried out with inconel electrode and with tungsten powder suspended in the dielectric medium, the contribution of pulse off-time was found to be more than pulse on-time. The improvement in micro-hardness in both these cases turned out to be very high. Good improvement in micro-hardness was also noticed when machining was carried out with copper-tungsten electrode and with manganese powder. Amongst the four electrode materials, copper-tungsten resulted in the best combination of micro-hardness and surface roughness. Machining with inconel electrode resulted in the transfer of nickel and chromium to the workpiece surface and an improvement in micro-hardness by as much as 88%. However, it was accompanied by a substantial deterioration of surface finish.

Very good surface finish (of the order of 1 μm) was obtained when machining was carried out with graphite powder and also with silicon powder. Both the powders substantially improved R_a and R_z values of surface roughness, produced a crack-free surface and had some positive effect on micro-hardness. The measurements on surfaces obtained after machining with copper electrode (without any powder) served as reference values. However, the performance of graphite powder on both the counts was found to be better than silicon powder. Machining with graphite powder also resulted in free graphite on the workpiece surface which can be expected to provide self-lubricating property to it.

The samples showing high values of micro-hardness or very good surface finish were further subjected to X-ray Diffraction analysis and then chemical composition analysis on Optical Emission Spectrometer to find out the phases and constituents of the surfaces. The microstructures were studied under a Scanning Electron Microscope. The results showed significant material transfer from the electrode bodies as well as from the powders suspended in the dielectric medium. In general, it was observed that less current and more pulse on-time

were required for material transfer from suspended powders as compared to material transfer from electrode bodies. An increase in the percentage of carbon in the work materials was observed under all machining conditions and it was found that this carbon came from the pyrolysis of the hydrocarbon dielectric. An examination of the migration of carbon and tungsten by the two methods of surface modification was also done.

Tungsten was found in the workpiece surfaces in the form of intermetallic compounds with iron (Fe_2W, Fe_7W_6); as carbides (WC, W_2C); or in the form of alloyed cementite [$(FeW)_3C$]. All the three work materials showed more than 100 % improvement in micro-hardness when machining was carried out with tungsten powder mixed in the dielectric medium. Different forms of manganese carbide ($Mn_4C_{1.06}$, Mn_7C_3 and Mn_5C_2) were observed in the workpiece surface when manganese powder was added to the dielectric medium. Inconel alloy electrode contributed chromium and nickel to the workpiece surface in the form of an intermetallic compound (FeCrNi) and a solid solution (Fe-Ni). Some traces of silicon in elemental form and as a solid solution with iron (Fe-Si) were seen but formation of silicon carbide did not take place by this method.

It can be concluded from this research work that surface modification of die steels by electrical discharge machining is technically feasible and simple modifications in the existing set-ups can lead to substantial improvement in surface properties. Higher surface hardness and better abrasion resistance will enhance the working life of dies and press tools.

INDEX

LIST OF FIGURES

LIST OF TABLES

NOMENCLATURE AND ACRONYMS

NOMENCLATURE

Symbol	Notation	Units
HV	Vickers Hardness Number	-
I_p	Peak Current	Amperes
m	Mean of S/N ratio	dB
m_{A1}	Mean of S/N data for factor A at level 1	dB
m_{B1}	Mean of S/N data for factor B at level 1, etc.	dB
P_{on}	Pulse on-time	micro-seconds
P_{off}	Pulse off-time	micro-seconds
R_a	Average Surface roughness value	µm
R_z	Mean peak-to-valley Surface roughness value	µm
$\overline{T}_{MH}$	Overall mean of micro hardness	HV
$\overline{T}_{SR}$	Overall mean of surface roughness (R_a)	µm
y_{opt}	Calculated value of Response characteristic under optimum values of process parameters	HV for micro-hardness/ µm for surface roughness
η	Signal-to-Noise ratio	dB
η_{opt}	S/N ratio under optimum values of process parameters	dB

ACRONYMS

ANOVA	Analysis of Variance
EDM	Electrical Discharge Machining
EDS	Energy Dispersive Spectroscopy
EL1	Copper Electrode
EL2	Graphite Electrode
EL3	Copper-tungsten Electrode

EL4	Inconel Electrode
I1, I2, I3	Levels of Peak Current
L1, L2, L3	Levels of Input Process Parameters
MRR	Material Removal Rate
MSD	Mean Square Deviation
OA	Orthogonal Array
P/M	Powder Metallurgy
$P_{on}1$, $P_{on}2$, $P_{on}3$	Levels of Pulse on-time
$P_{off}1$, $P_{off}2$, $P_{off}3$	Levels of Pulse off-time
PW1	Graphite Powder
PW2	Manganese Powder
PW3	Silicon Powder
PW4	Tungsten Powder
S/N	Signal-to-Noise ratio
SEM	Scanning Electron Microscope
TWR	Tool Wear Rate
W1	OHNS Die Steel
W2	D2 High-Carbon High-Chromium Die Steel
W3	H13 Hot Die Steel
XRD	X-Ray Diffraction

CHAPTER - 1
INTRODUCTION

The last decade has seen an increasing interest in the novel applications of Electrical Discharge Machining (EDM) process, with particular emphasis on the potential of this process for surface modification. Since EDM is already being used extensively for the manufacture of press tools, dies and punches where a hard and abrasion-resistant machined surface is a major requirement, researchers are exploring various ways to adapt this technique for surface hardening of workpieces. Efforts are being made to create new, harder alloys on the surface of machined components with the aim of increasing their working life and wear resistance [1]. With the advancement of technology, there is an ever-increasing need for harder materials with surfaces that are able to withstand stringent applications. Such hard and wear resisting surfaces are required in the case of cutting tools also. Forging dies need to retain surface characteristics and dimensional accuracy at elevated temperatures [2]. Moreover, there are instances where the designer would like the same component to have different properties at different locations. It is all the more demanding in the case of aerospace mechanisms and structures because of weight and space limitations. The purview of surface modification may be stated to include:

(a) Improving the surface characteristics by varying the input machining parameters within the existing process.

(b) Altering the microstructure by changing the rate of melting and cooling.

(c) Deposition of new metals and compounds (such as carbides and nitrides) on the machined surface.

EDM is a machining process that removes metal with sparks between a tool electrode and the workpiece. The tool electrode made of graphite or copper gradually makes a cavity that is a mirror image of its shape. There is no direct contact between the electrode and the workpiece. The sparks travel through a dielectric fluid (typically a light oil) at a controlled distance. Both electrode and the workpiece must be electrically conductive [3-5]. A number of phenomena observed during the EDM process make it a high potential technology for

application in the field of surface modification. Each spark generates a temperature of the order of 8,000 to 12,000 ^{0}C and creates a plasma channel, causing fusion or partial vapourization of the workpiece, tool electrode and the dielectric fluid at the point of discharge [6]. As the spark duration is only a few micro-seconds, this surface is immediately quenched by the flowing dielectric. Variation in process parameters such as pulse wave form, current intensity, flushing, type of dielectric and electrode material properties such as thermal conductivity, electrical resistivity and heat diffusivity have considerable impact on surface finish, hardness and dimensional accuracy of the machined surface [7-8]. Some powder additives suspended in the dielectric fluid also significantly affect the properties of the machined surface. These particles facilitate the ignition process by creating a higher discharge probability and lowering the breakdown strength of the insulating dielectric. This results in a strong corrosion resistant surface having high micro-hardness and less micro-cracks [9-10].

While removing material from the workpiece surface, the spark also erodes some material from the tool electrode. Most of this material is carried away by the dielectric but some of it gets deposited back on the workpiece and the tool electrode. Many research works have reported the presence of the constituents of tool electrode in the machined workpiece surface and vice-versa [11-13]. The formation of plasma channel, pyrolysis of the dielectric and metal vapours aid the process of material deposition [14]. As the dissolution of the electrode takes place during the process, the constituents of the electrode material may be deposited on the machined surface by varying the process parameters towards the end of the machining cycle for specific surface modifications. Suitable alloying elements may also be added to the dielectric in the form of fine metal powders and they may get deposited on the machined surface either in the free form or as carbides by combining with carbon from the break-down of the dielectric [15-16].

1.1 NEED FOR SURFACE MODIFICATION

Main criteria of the functional workpiece quality are the geometrical surface integrity (surface roughness, dimensional and form accuracy) and physical surface integrity (microstructure, hardness, residual stresses). The conditions (surface topography, heat transfer and friction) at the die / material interface affect not only the surface and appearance

of the finished product but also influence the input process parameters; especially in metal forming operations. Thus surface finish and coating of the dies play an important role in improving lubrication, metal flow and operational life of the die [17]. Surface modification has been defined as "The alteration of surface composition or structure by the use of energy or particle beams. Elements may be added to influence the surface characteristics of the substrate by the formation of alloys, metastable alloys or phases, or amorphous layers. Surface – modified layers are distinguished from conversion or coating layers by their greater similarity to metallurgically alloying as compared to chemically reacted, adhered or physically bonded layers. However, surface structures are produced that differ significantly from those obtained by conventional metallurgical processes. This latter characteristic further distinguishes surface modification from other conventional processes such as amalgamation or thermal diffusion" [18]. Surface modification may be necessary to:

- Improve resistance to wear, erosion and indentation.
- Reduce friction, improve lubrication.
- Improve resistance to corrosion and oxidation.
- Improve fatigue resistance.

A vast number of engineering components degrading or failing catastrophically in service, due to surface related phenomena such as wear, fatigue, corrosion etc. can be made to serve longer by the optimal use of surface modification. Several techniques are available for mechanically improving the surface properties of mechanically functional components. It starts with the definition of functional requirements of the surface to ensure certain performance of the component, identification of the failure mechanism, choice of appropriate material for the component and the surface modification process which will ensure economics of processing and conservation process of raw materials / environment [18]. In the case of dies, punches and other press tools, it is desirable to introduce suitable alloying elements and their compounds in the machined surfaces only and not in the base material due to the following very important reasons:

- The contribution of alloying elements in improving mechanical and physical properties is desired at the interacting surfaces only and material going into the rest of component body adds a substantial cost to it.
- The presence of these alloying elements significantly affects the heat treatment behaviour of die steels. For example, most carbide forming elements (Mn, Cr, W, Mo, V and Ti) impede carbon diffusion in austenite and make the process of transformation of pearlite into austenite slower [19]. They also increase the stability of supercooled austenite in the pearlitic region to a much greater degree which results in a large amount of retained austenite instead of the desirable martensite [20]. Hence, it becomes imperative that alloying elements are introduced after the heat treatment cycle.
- It may not be metallurgically feasible to add some of the elements (such as refractory materials) in molten state to the whole liquid material.

A list of the surface modification processes presently available and the surface properties enhanced by them is given in Table 1.1. These processes are applied as separate secondary processes on to the finished components and involve substantial cost and time additions. Two types of surface modification methods commonly employed for dies and moulds are ion implantation and laser surface processing [21-22]. In the ion implantation process, charged ions, accelerated to 100-400 keV energies, are directed to the surface of the material. In laser surface processing, a limited area of the die surface is melted using high energy laser radiation. A "path" is created by the feed motion of the workpiece in relation to the laser beam, laying several tracks alongside one another. A range of different materials (in powder form) can be fed to harden and coat a specific portion of the die. However, both these processes are characterized by poor surface finish and require final machining on EDM. Another hindrance is the enormous cost of the equipment [23]. Thus, if surface modification can be incorporated into the EDM process itself, it will result in substantial economic benefits to the tool and die making industry.

Table 1.1 Surface Modification Processes for achieving various surface properties [18]

S. No.	Surface Property Enhanced	Surface Modification Process
1.	Hardness, Wear resistance, decorative appeal.	Electroplating, Anodisation, Tin deposition by Physical Vapour Deposition (PVD)
2.	Hardness, wear resistance	Electroplating, Anodisation, Ceramic coating by Chemical or Physical Vapour Deposition, Plasma spraying, Carburizing & Nitriding etc.
3.	Wear resistance, corrosion and oxidation resistance.	Metal spraying, Pack cementation, Laser Surface Processing and PVD
4.	Corrosion resistance	Electroplating, Galvanizing, Chromating, Painting etc.
5.	Wear resistance	Plasma nitriding, Ion implantation, Diffusion bonding, High pressure carburizing & nitriding etc.

1.2 ELECTRICAL DISCHARGE MACHINING PROCESS

A bolt of lightning striking the ground represents the working force of EDM in its most primitive form; the cloud being the tool electrode and atmospheric air acting as the dielectric medium. This heat energy of the spark has been harnessed to remove material from the workpiece and EDM has emerged as one of the most versatile machining processes being used by the tool and die making industry. In this process, two metal electrodes, one being the tool of a pre-determined shape, and other being the workpiece, are immersed in a liquid dielectric which is generally kerosene or any other hydrocarbon oil (Fig. 1.1). Both the electrodes should be made of conductive materials. A servo mechanism maintains a gap of about 0.0005 to 0.001 inch (0.01 to 0.02 mm) between the electrode and workpiece, preventing them from coming in contact with each other. A series of voltage pulses, usually

of rectangular form, having magnitude of about 80 Volts and frequency of the order of 200-5000 Hz, is applied between the two electrodes [24].

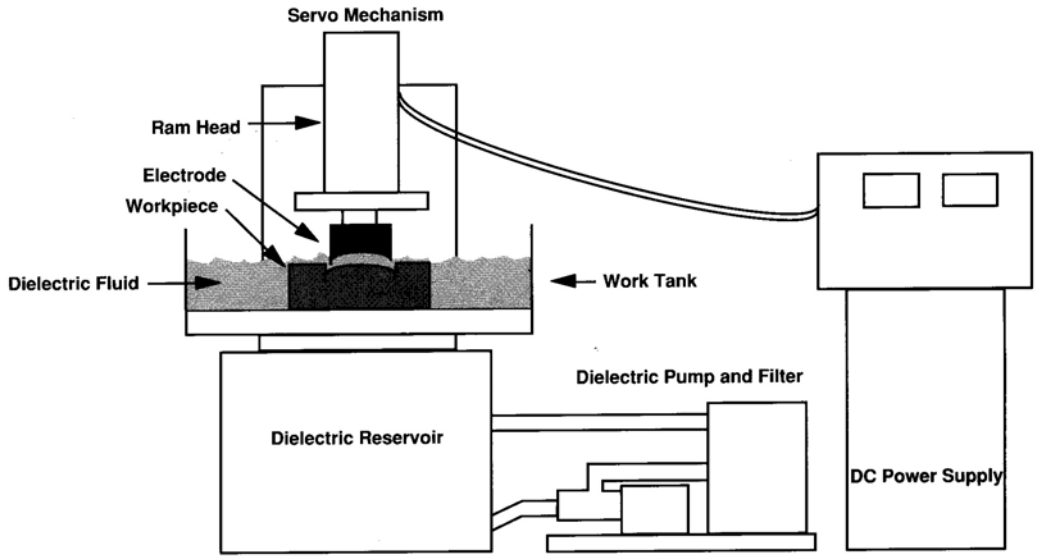

Figure 1.1 Basic EDM system [25]

Localized breakdown of the dielectric occurs and sparks are generated across the inter-electrode gap, generally at regions of minimum separation. Each spark erodes a tiny amount of material from the surface of both the electrodes. The high frequencies at which voltage pulses are supplied, together with the forward movement of the tool electrode towards the workpiece by means of a servomechanism, enables the sparking action to be eventually achieved over the entire area of the electrodes in contact. The process can be controlled such that substantially more metal is removed from the workpiece than from the tool electrode [26]. As machining proceeds, image shape of the tool-electrode is gradually reproduced to a fine accuracy on the workpiece. Flowing dielectric fluid flushes out the chips and confines the sparks to a narrow region [27]. More recent developments such as orbiting EDM, wire-cut EDM, computerized numerical control, rotating quills, automatic tool changers and adaptive controls represent the evolution of EDM to an accepted and rapidly developing technology [28]. These advances have made EDM machines much easier to operate and have improved the accuracy and surface finish that can be produced. Since material removal is realized by sparks and not mechanical action, the rate of machining is not limited by the

hardness of the workpiece. These attractive features of EDM have led to its widespread industrial use, particularly in the manufacture of dies and moulds.

1.2.1 Phenomenon of material transfer

While several theories of how EDM works have been advanced over the years, most of the evidence supports the thermoelectric model [29-30]. The four illustrations given in Fig. 1.2 (a), (b), (c) and (d) show the steps during a single EDM cycle. It also explains how material transfer to the machined workpiece surface may take place from the electrode material or from the dielectric medium or both. The graphs below the illustrations show the relative values of voltage and current at the point depicted.

As the charged electrode is brought near the workpiece, electrical field is strongest at the point where distance between the electrode and workpiece is the least. Even though the dielectric fluid is a good insulator, a large enough electrical potential can cause it to break

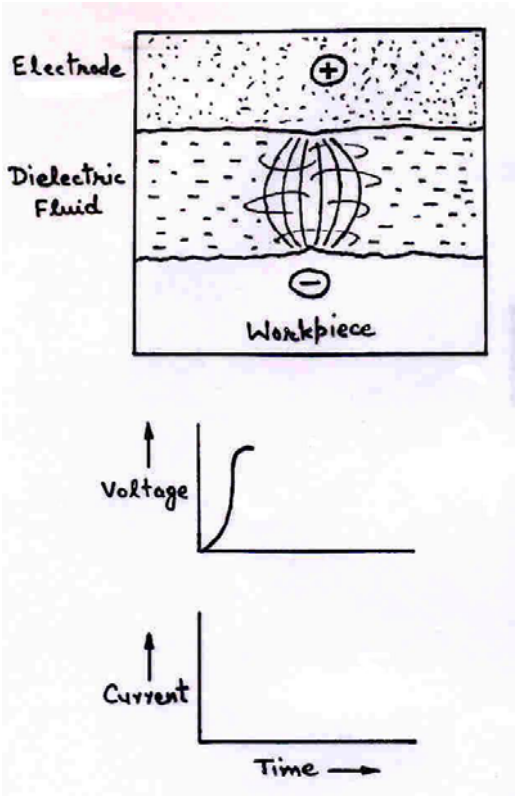

Fig. 1.2 (a) First stage of a single EDM cycle

down into ionic (charged) fragments, allowing an electrical current to pass from electrode to the workpiece [31]. The presence of conductive particles can aid this electrical transfer [10].

In Fig. 1.2 (a), voltage is increasing and ionization of the fluid is beginning to happen, but current is still zero. As the voltage reaches its peak, insulating properties of the dielectric fluid begin to decrease along a narrow channel centered in the strongest part of the field. A current is established as the number of ionic particles increase and the fluid becomes less of an insulator. This stage is depicted in Fig. 1.2 (b).

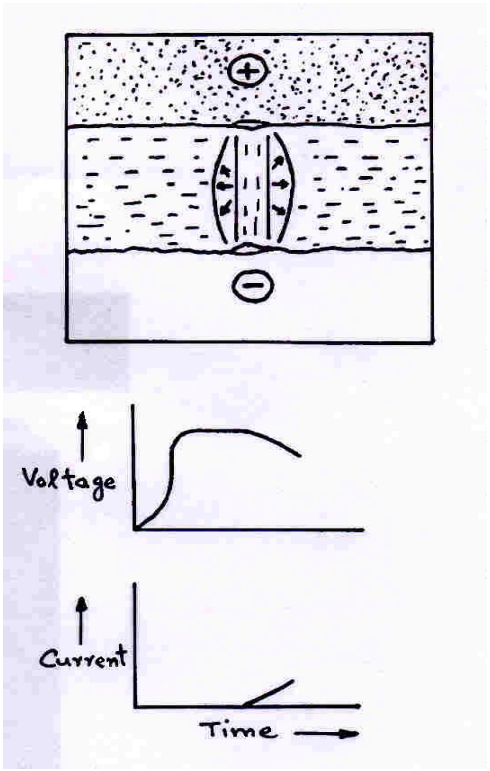

Fig. 1.2 (b) Second stage of a single EDM cycle

Heat builds up rapidly as current increases, and voltage continues to drop. It vapourizes some of the fluid, workpiece and the tool electrode. A discharge channel is formed consisting of superheated plasma made up of vapourized material from the electrode as well as workpiece; and carbon and other elements from the dielectric fluid. This vapour bubble tries to expand outwards, but its expansion is limited by a rush of ions towards the discharge channel. These ions are attracted by the extremely intense electromagnetic field that has built up. Voltage and current stabilizes towards the end of pulse on-time [Fig. 1.2 (c)]. As the off-time starts,

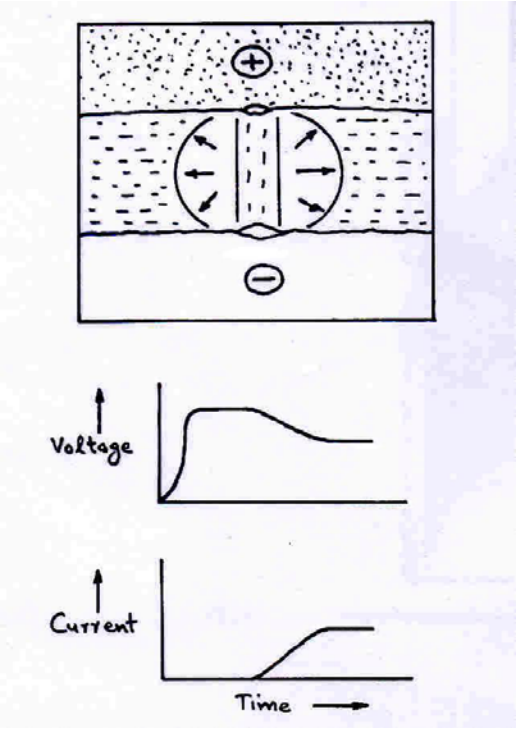

Fig. 1.2 (c) Third stage of a single EDM cycle

heat and pressure within the plasma channel have reached their maximum. The layer of material directly under the discharge column is in the molten state, but is held in place by the pressure of vapour bubble. More material is vapourized from the surfaces of workpiece and tool electrode. In the superheated plasma, various elements may react with each other or with the carbon (that has come from the breakdown of the hydrocarbon dielectric) to form their carbides. As the voltage and current drop to zero, temperature decreases rapidly and the plasma channel collapses, causing the molten material to be taken away by the flowing dielectric [Fig. 2 (d)]. It is at this stage that some of the elements or their compounds from the plasma channel may get deposited on the workpiece surface under appropriate machining conditions. Fresh dielectric fluid now rushes in, flushing away the debris (particles eroded from the electrodes) and quenching the surface of the workpiece. Without a sufficient pulse off-time, debris may accumulate in the machining area and make the spark unstable. This situation can create a DC arc which may damage the electrode and workpiece surfaces. This complete on / off sequence represents one EDM cycle and the frequency of sparking may be as high as thousands of sparks per second [3].

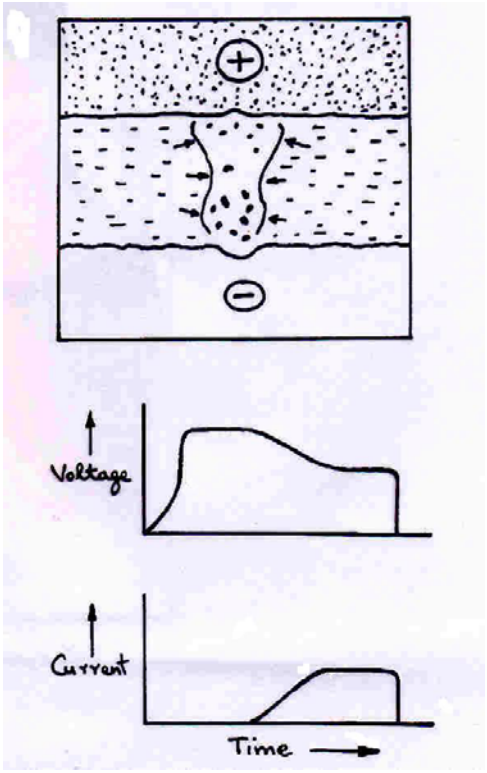

Fig. 1.2 (d) Final stage of a single EDM cycle

1.3 WORK MATERIALS

Three of the most widely used die steel materials by the tool and mould making industry have been chosen as work materials for this experimental work. These are Oil-Hardening Non-Shrinkable (OHNS) type O2 die steel, High Carbon High Chromium (HC-HCr) type D2 die steel and Hot work type H13 die Steel. The composition limits of these work materials [17] are given in Table 1.2.

Oil hardening cold work tool steels, designated as group 'O' steels in the AISI classification system, derive their high hardness and wear resistance from high carbon and modest alloy contents. The high carbon content makes possible the formation of martensite of high hardness, and the alloying elements provide sufficient hardenability to make possible hardening of sections of reasonable size by oil quenching. However, alloy content is insufficient to provide the alloy carbides necessary for cutting at high speeds or for hot-working applications, therefore these steels are used for cold working applications only. The

O2 type OHNS die steel is used for making dies and punches for blanking, trimming, flanging and forming; broaches, reamers, knurling tools, slitting saws and coining dies.

Table 1.2 Composition limits of the three work materials [17]

Composition	Work Materials		
	O2 (OHNS)	**D2 (HC-HCr)**	**H13 (Hot Die Steel)**
% Carbon	0.85-0.95	1.40-1.60	0.32-0.45
% Silicon	0.50 max	0.60 max	0.80-1.20
% Manganese	1.40-1.80	0.60 max	0.20-0.50
% Chromium	0.50 max	11.00-13.00	4.75-5.50
% Molybdenum	0.30 max	0.70-1.20	1.10-1.75
% Vanadium	0.30 max	1.10 max	0.80-1.20
% Tungsten	-	-	-
% Nickel	0.30 max	0.30 max	0.30 max
% Cobalt	-	-	-

High-carbon high-chromium tool steels, designated as group ‘D’ steels in the AISI classification system, are the most highly alloyed cold-work steels. In view of their high carbon and alloy contents, all the D steels are deep hardening. They are hardenable by air cooling from austenitizing temperatures and they have very low susceptibility to distortion and cracking [17, 32]. The D2 type HC-HCr tool steels find wide usage as the raw material for blanking & deep drawing dies, thread rolling & forming dies, burnishing tools, shear & slitter knives.

Tool steels for hot work applications, designated as group ‘H’ steels in the AISI classification system, have the capacity to resist softening during long or repeated exposures to high temperatures needed to hot work or for die-casting other materials. The outstanding

characteristics of these tool steels are high toughness and shock resistance. They have air hardening capability from relatively low austenitizing temperatures and exhibit minimum scaling tendency during air cooling. H13 hot work steel is the best material for hot die work of all kinds, particularly dies for the extrusion of aluminium and magnesium, as well as die casting dies, forging dies, mandrels and hot shears; because of its ability to retain dimensional accuracy and surface characteristics at elevated temperatures. This material also possesses high resistance to erosion.

The workpieces made from these three die steel materials were hardened and tempered using standard heat treatment procedures before experimentation to bring them at par with the state in which they are actually used in the industry.

1.4 OBJECTIVES & SCOPE OF THE WORK

Properties of surface layers after EDM are affected by quenching due to flowing dielectric and by chemical composition which, in EDM, might change under the influence of material transfer from the tool electrode or from the dielectric media in which machining is taking place or both. Suitable materials may be introduced either in the electrode bodies or suspended in the dielectric fluid for carrying out desirable surface modifications [7].

A comparison of the basic characteristics of the three die steel materials selected for this work is given in Table 1.3. The important characteristics from the point of view of their application in the tool making industry and the desired surface modification are toughness, wear resistance and resistance to the softening effect of heat. These characteristics can be improved by the addition of silicon, tungsten, manganese, nickel and chromium etc. which may be transferred from the eroding tool electrode bodies or contributed by the powders suspended in the dielectric medium. For example, it is observed from this table that D2 die steel has low toughness which can be improved by adding silicon, nickel or vanadium to the surface. It is also well known that H13 hot work die steel can retain its hot hardness up to 425 ^{0}C but with the addition of tungsten, it can retain this hardness up to 620 ^{0}C [19]. Hence, its resistance to softening effect of heat can be enhanced. Similarly, both OHNS and H13 die steels have low wear resistance which can be improved by adding manganese, chromium and carbon to the surface.

Table 1.3 Comparison of basic characteristics of the three work materials [17]

Property	Work Material			Remarks
	OHNS	D2	H13	
Non-deforming	Good	High	Good	
Toughness	Medium	Low	Very High	**Can be improved by adding Si, Ni and V**
Resistance to softening effect of heat	Low	Fair	Good	**Can be improved by adding Co, Mo and W**
Wear resistance	Fair	Very High	Fair	**Can be improved by adding Mn, Cr and C**
Hardening response	Medium	Deep	Deep	
Resistance to cracking	High	Good	Very High	
Approx. hardness (HRC)	57-62	54-61	38-53	
Machinability	High	Low	Medium to High	

Besides this, some elements have a strong influence on the properties of tool steels when they are used in combination with some other specific elements. For example, when manganese is added to a tool steel containing chromium, silicon and molybdenum, it increases the strength, toughness and hardness. The effect of manganese is then greater than that of chromium. It also increases the hardenability of alloy steels. When nickel is combined with molybdenum, the resulting steel has ductility, strength, improved machinability and deep hardness. When silicon is used in percentages up to 2 %, it intensifies the effects of molybdenum, manganese and chromium and increases the resistance of steel to oxidation [33].

To provide some of these elements, the three work materials were machined by using copper, graphite, copper-tungsten and inconel (an alloy of nickel, chromium and iron as main constituents) as electrode materials; followed by machining in powder suspended dielectric medium using graphite, manganese, silicon and tungsten powders. The experimental results thus obtained were analyzed to find out the desirable input process parameters of electrical discharge machining, by which it might be possible to improve the composition and properties of the surfaces of these die steel materials by material transfer from the electrode bodies or from the powders suspended in the dielectric medium.

1.5 METHODOLOGY

The overall methodology for the study has been divided into five phases:

- Detailed literature review
- Pilot experimentation and design of study
- Experimentation with different electrode materials
- Experimentation with powders mixed in the dielectric medium
- Analysis of the results

A large number of input process parameters can be varied in the EDM process, each having its own impact on output parameters such as material removal rate, tool wear rate, hardness of the machined surface, surface finish, dimensional accuracy and overall surface integrity. However, for the purpose of this experimentation, it was not considered necessary to vary all these parameters because the impact of some of them has already been well established by previous research work available in literature. Detailed literature review was carried out to find the significance of various input process parameters for the phenomenon of material transfer and their effective ranges. For example, in the case of polarity (which can be positive or negative), it was clearly known that negative electrode polarity favoured high tool wear [1], which was desirable for this work. Hence, by default, negative electrode polarity was used in the experimentation and this variable was excluded from the design of experiment.

After this, pilot experimentation was conducted on OHNS die steel to find out the most significant machining parameters and their levels that were conducive for material transfer to take place. Commercial grade kerosene was used as the dielectric medium and the time for

each cut was fixed at 10 minutes. The criterion for material transfer was taken as an increase in the micro-hardness of the machined surface. The experimental results of the workpieces machined with copper electrode served as reference values. Some of the workpieces which showed considerable increase in micro-hardness were subjected to Energy Dispersive Spectroscopy (EDS) analysis to find out the presence of additional alloying elements as a result of electrical discharge machining.

Based on the results of pilot experimentation, input machining parameters and their levels for actual experimentation on all the three work materials were finalized. Taguchi method was used for the design of study. The fractional factorial method developed by Taguchi is a technique that allows a process to yield most information using relatively few experiments when there are a large number of input variables [34-35]. For this, Taguchi defines a set of orthogonal arrays, each of which can be used in many experimental situations, and provides a standard method for analysis of the results. For this work, L9 orthogonal array was found to be most suitable. After constructing the control log, the set of nine experiments were repeated for each combination of the work material, electrode material and the powder. A specially designed tank was used for conducting experiments with powder mixed in the dielectric medium. This tank confined the powder to a very small region and isolated it from the main dielectric circulating and filtering system. A stirrer was used in this tank to maintain the circulation and consistency of the powder in the machining area.

All the machined surfaces thus obtained were subjected to micro-hardness tests and surface roughness measurements. Workpieces showing considerable improvement in these parameters were subjected to:

- X-ray diffraction (XRD) analysis to find out the presence of additional elements and their phases;
- Composition testing on Optical Emission Spectrophotometer to confirm material transfer and for quantitative analysis of the changes in the constituents of the machined surfaces;
- Scanning electron microscopy to analyze the microstructure.

The results confirm the efficacy of the selected process parameters for carrying out surface modification of the three die steel materials. Analysis of the experimental data establishes the significance and relative contribution of the process parameters.

1.6 ORGANIZATION OF THE THESIS

The thesis has been divided into seven chapters. Brief description of the contents of each chapter is given below:

Chapter - 1 highlights the need for surface modification of die steels, gives introduction to the process of electrical discharge machining and how it may be utilized for selective surface alloying. Basic characteristics and applications of the work materials have been given. The significance of various alloying elements and their effects on the properties of tool and die steels have been described. Objectives, scope and overall methodology of the experimental work have been outlined.

Chapter - 2 presents an account of available literature on the status of research in the field of surface modification by EDM process using composite electrodes and by suspending various powders in the dielectric medium. The impact of various input process parameters such as peak current, pulse on-time, pulse off-time, polarity of machining and duty factor on electrode wear and material transfer has been discussed. After an elaborate scrutiny of the published work on surface modification, the gaps in this research area have been listed.

Chapter - 3 gives a detailed account of the design of study, Taguchi approach for design of experiments and the selection of various input process parameters and response characteristics. While the relevance of low discharge current and low pulse duration on the phenomenon of material transfer has been established through literature review, the actual impact of these parameters and their ranges has been investigated through pilot experimentation conducted by varying one-parameter-at-a-time approach. The impact of change in pulse off-time has also been included. After considering all the variables, L9 orthogonal array was selected for the experimentation. The factors included in the array are peak current, pulse on-time and pulse off-time. The experimentation has been divided into two distinct stages, namely, experimentation with four different electrode materials and

experimentation with four different powders mixed in the dielectric medium. Machining time, voltage, type of flushing, polarity and powder concentration were kept fixed for all the experiments. The effect has been studied on the response characteristics of micro-hardness and surface roughness.

Chapter - 4 discusses the experimental procedure for machining with different electrode materials and setting up of various input process parameters. The set of nine experiments was repeated three times for each work material with copper, graphite, copper-tungsten and inconel as electrode materials. Micro-hardness and surface roughness tests were carried out on all the samples. The significance and relative contribution of peak current, pulse on-time and pulse off-time towards each response characteristic have been obtained. Confirmation experiments were conducted with the optimum values of various input parameters as obtained from Taguchi analysis. The chapter establishes the governing input process parameters for material transfer by each of the electrode material.

Chapter - 5 explains the design of machining set-up for experimentation with powder-mixed dielectric. A specially designed tank was used for this stage of experimentation which allowed machining with powder mixed in the dielectric medium without disturbing the routine operation of the machine. Each work material was machined with graphite, manganese, silicon and tungsten powders suspended in the dielectric medium; using copper as the electrode material. The desirable machining conditions for each combination of workpiece and powder and the results of confirmation experiments have been presented.

Chapter - 6 takes a collective view of the results obtained by machining with different electrode materials and with powders suspended in the dielectric medium. It presents the comparative analysis with the help of graphs. The results obtained with copper electrode served as reference values for both stages of experimentation. The impact of each method on the response characteristics of micro-hardness and surface roughness has been discussed. Microstructure, X-ray diffraction pattern and chemical composition of the machined surfaces after confirmation experiments and some other samples showing high values of micro-hardness or good surface finish have been given.

Chapter - 7 lists down the conclusions of this research work. Recommendations for future work in this area have also been given.

This chapter is followed by references and appendices.

CHAPTER - 2

LITERATURE REVIEW

The use of Electric Discharge Machining is growing rapidly in tool rooms, die shops and even in general shop floors of modern industries to facilitate complex machining problems in difficult-to-machine materials and provide better surface integrity. Development of wire-EDM has added a new dimension to this technology. EDM, in its two variations, that is die-sinking and wire-EDM, is now the fourth most popular machining process after milling, turning and grinding. The factors that have contributed to its popularity are:

- Absence of any physical contact between the tool and work piece
- Accurate and distortion-free machining of hardened work pieces
- Negligible cutting forces
- Machining of difficult-to-machine materials
- Generation of complicated internal geometries
- The process is burr-free

A variety of research work has been carried out on different aspects of EDM such as tool material-workpiece combination, type of dielectric, pulse train, flushing techniques and hybridization of EDM with other non-conventional techniques such as ultrasonic machining, electro-chemical machining and abrasive machining. In addition to this, detailed literature is available on the surface properties of heat treated steels after spark machining. Electro-spark toughening of cutting tools and steel components has also been explored. This chapter presents a comprehensive review of available literature on technological aspects of the process, active research areas and future trends of its applications.

2.1 BRIEF HISTORY OF EDM PROCESS

The origin of EDM dates back to 1770 when English scientist Joseph Priestly discovered the erosive effect of electrical discharges. During the 1930s, attempts were made for the first time to machine metals and diamonds with electrical discharges. Erosion was caused by intermittent arc discharges occuring in air between the tool electrode and workpiece connected to a DC power supply. These processes were not very precise due to overheating

of the machining area and may be defined as “arc machining” rather than “spark machining” [28-29].

Pioneering work on electrical discharge machining was carried out in 1943 during World War II by two Russian scientists, B.R. and N.I. Lazarenko at the Moscow University [36]. They channelised the destructive effect of an electrical discharge and developed a controlled process for machining materials that were conductors of electricity. They introduced the RC (resistance-capacitance) relaxation circuit in the 1950s, providing the first consistent dependable control of pulse times and also a simple servo control circuit to automatically find and hold a given gap between the electrode (tool) and the workpiece. The RC circuit was widely used in the 1950s and later served as the model for successive developments in EDM technology.

There have been similar claims made at about the same time when three American employees came up with the notion of using electrical discharges to remove broken taps and drills from hydraulic valves. Their work became the basis for the vacuum tube EDM machine and an electronic circuit servo system that automatically provided the proper electrode-to-workpiece spacing (spark gap) for sparking, without the electrode contacting the workpiece [37]. However, It was only in the 1980s with the advent of Computer Numerical Control (CNC) in EDM that brought about tremendous advancement in improving the efficiency of the machining operation. Due to continuous process improvement, modern EDM machines have become so stable that these can be operated round the clock under monitoring by an adaptive control system. This process enables machining of any material, which is electrically conductive, irrespective of its hardness, shape or strength [38]. The growing merits of EDM have since then been intensely sought by the manufacturing sector yielding enormous economic benefits and generating keen research interests.

2.2 WORKING PRINCIPLE OF EDM PROCESS

Although the technique of material erosion employed in EDM is still arguable [39-40], the widely accepted principle is the conversion of electrical energy into thermal energy through a series of discrete electrical discharges occurring between the electrode and workpiece immersed in a dielectric fluid. The insulating effect of the dielectric is important in avoiding electrolysis of the electrodes during the EDM process. Spark is initiated at the point of

smallest inter-electrode gap by a high voltage, overcoming the dielectric breakdown strength of the small gap (Fig. 2.1). Erosion of metal from both electrodes takes place there.

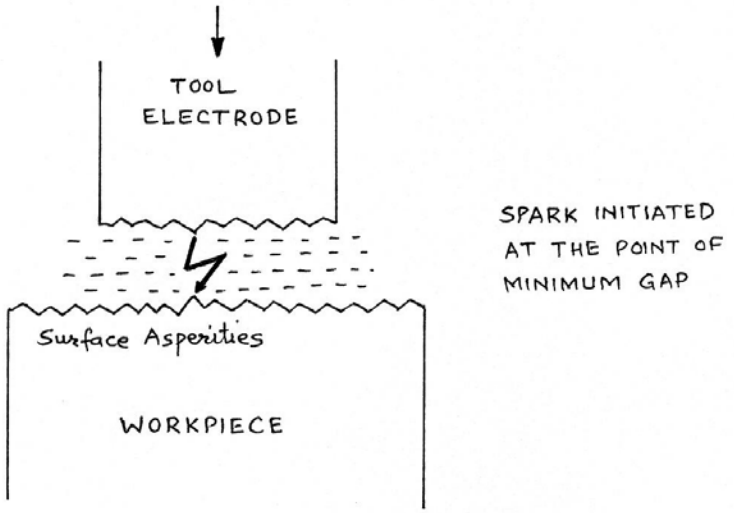

Fig. 2.1 Spark initiation in EDM process

After each discharge, the capacitor is recharged from the DC source through a resistor (Fig. 2.2), and the spark that follows is transferred to the next narrowest gap. The cumulative effect of a succession of sparks spread over the entire workpiece surface leads to its erosion, or machining to a shape which is approximately complementary to that of the tool.

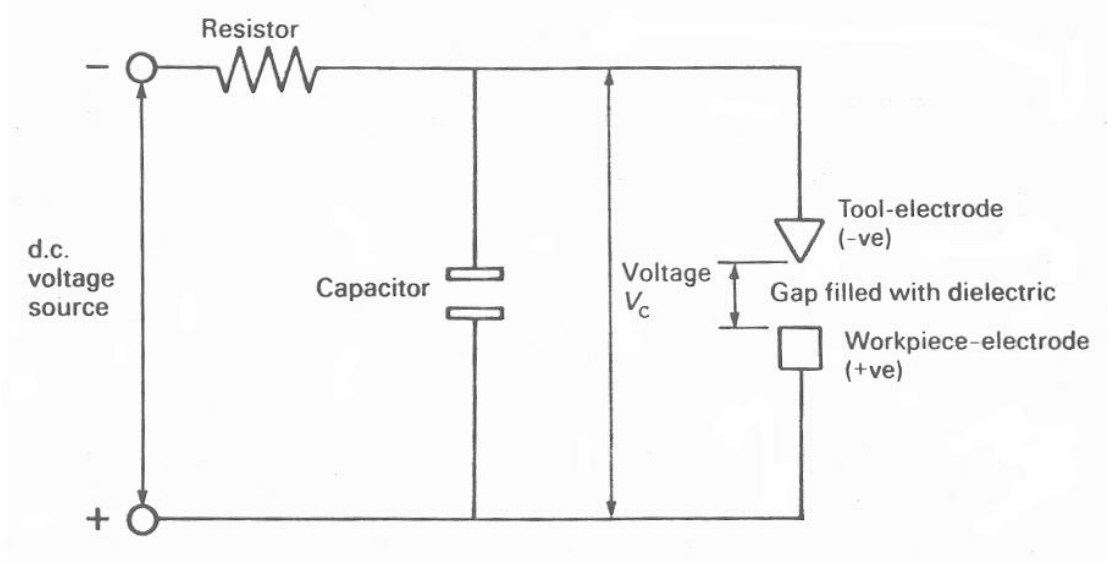

Fig. 2.2 The Lazarenko RC Circuit [41]

The dielectric serves to concentrate the discharge energy into a channel of very small cross-sectional area. It also cools the two electrodes, and flushes away the products of machining from the gap. The electrical resistance of the dielectric influences the discharge energy and the time of spark initiation. If the resistance is low, an early discharge will occur. If it is large, the capacitor will attain a higher value of charge before the discharge spark occurs. As the workpiece is spark-eroded, the tool has to be advanced through the dielectric towards it. A servo system, which compares the gap voltage with a reference value, is employed to ensure that the electrode moves at a proper rate to maintain the right spark gap, and to retract the electrode if short-circuiting occurs.

The Lazarenko RC circuit does not give good material removal rate (MRR), and higher MRR is possible only by sacrificing surface finish. A major portion of the machining time is spent on charging the capacitors (Fig. 2.3). There is a very high peak value of current at the instant of spark initiation, followed by a rapid rate of decline. The spark temperature resulting from this high current peak is much higher than that needed to remove material and results in thermal damage to the tool electrode.

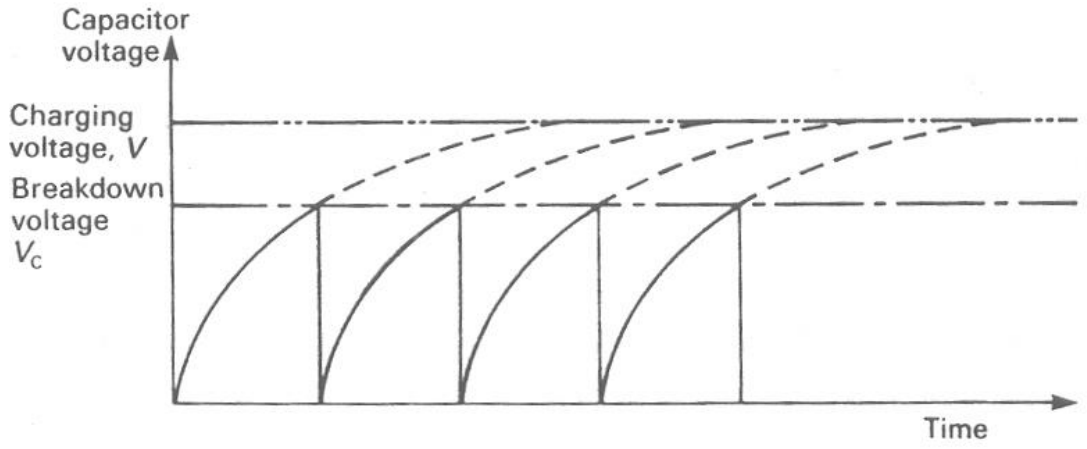

Fig. 2.3 Variation of capacitor voltage with time in RC circuit [41]

It is obvious that reduction in peak current and increase in spark duration would result in lower electrode wear and improved machining efficiency. This has been achieved with the advent of controlled pulse generator. Its typical waveform is shown in Fig. 2.4. In comparison to the RC circuit, there is less peak current value, shortened idle period and an increase in pulse duration.

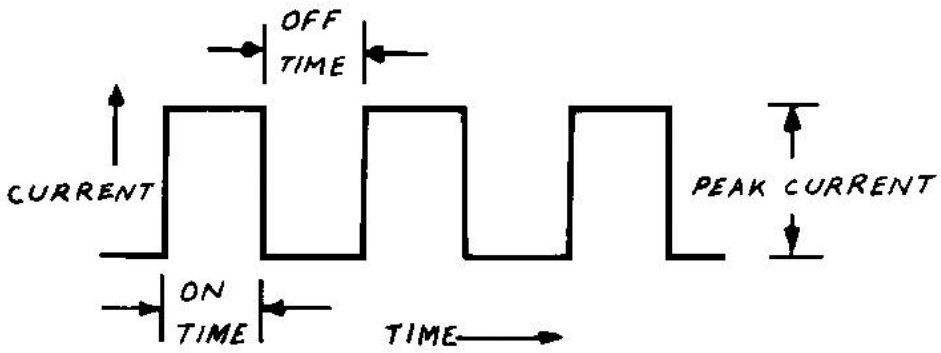

Fig. 2.4 Pulse waveform of controlled pulse generator

Spark energy is the product of peak current and on-time. Since these process variables can be readily adjusted, machining conditions can be selected for particular effects needed. However, the process is more complex than what is depicted in Fig. 2.4. When the electrode is separated from the workpiece, the potential is the open circuit voltage, usually having a value of about 100 Volts. As the dielectric begins to ionize, current starts flowing and the potential drops to a level of about 35 V. Plotting voltage and current as a function of time, Fig. 2.5 gives a more detailed picture, 'a' is ionization time, 'b' is discharge time, 'c' is deionization time and 'd' is idle time.

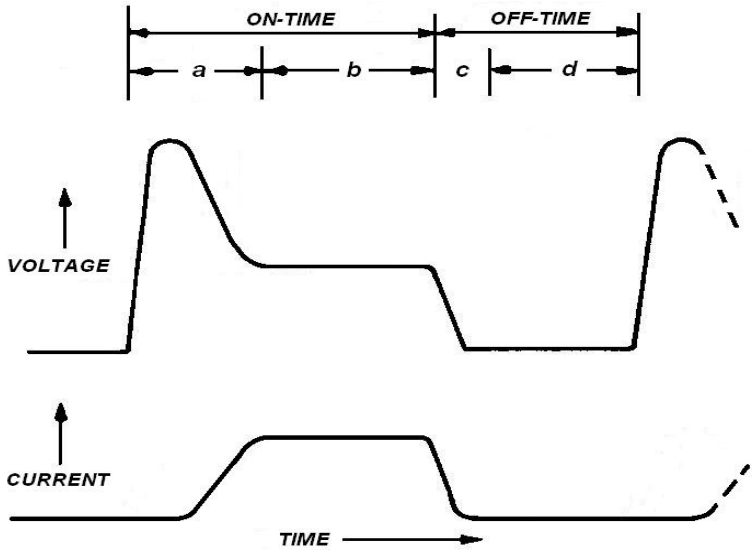

Fig. 2.5 Actual profile of a single EDM pulse

Most of the electrode wear occurs during the ionization time. While the RC circuit usually employed negative polarity for the tool electrode, positive polarity is preferred with pulse generator power supply [41].

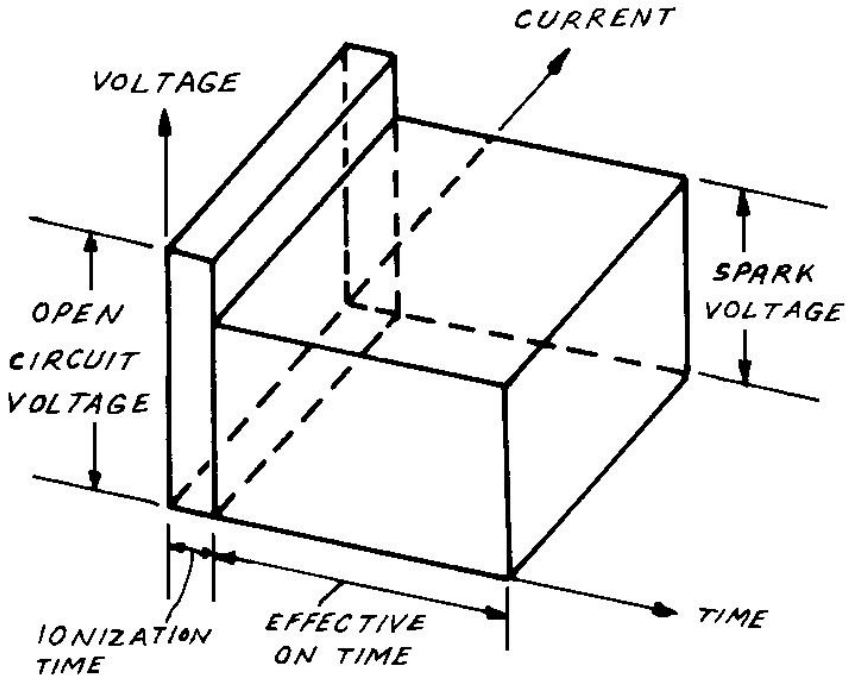

Fig. 2.6 Three-dimensional schematic of the EDM spark [3]

Another depiction of the spark energy is shown in Fig. 2.6. Although the spark energy available for material removal is proportional to the product of effective on-time, current and sparking voltage, these constituent variables do not individually contribute to material removal in a straightforward manner [42]. Only the time following ionization is effective in removing material. As an approximation, it may be stated that crater diameter is proportional to the applied current, and the depth is proportional to the on-time.

2.3 EDM PROCESS PARAMETERS

2.3.1 Discharge Voltage

Discharge voltage in EDM is related to the spark gap and breakdown strength of the dielectric. Before current can flow, the open gap voltage increases until it has created an ionization path through the dielectric. Once the current starts to flow, voltage drops and stabilizes at the working gap level. The preset voltage determines the width of the spark gap

between the leading edge of the electrode and workpiece. Higher voltage settings increase the gap, which improves the flushing conditions and helps to stabilize the cut. MRR, TWR and surface roughness increase with increasing open circuit voltage, because electric field strength increases. However, the impact of changing open circuit voltage on surface hardness after machining has been found to be only marginal.

2.3.2 Peak Current

This is the amount of power used in discharge machining, measured in units of amperage, and is the most important machining parameter in EDM. During each on-time pulse, the current increases until it reaches a preset level, which is expressed as the peak current. In both die-sinking and wire-EDM applications, the maximum amount of amperage is governed by the surface area of the cut. Higher amperage is used in roughing operations and in cavities or details with large surface areas. Higher currents will improve MRR, but at the cost of surface finish and tool wear. This is all the more important in EDM because the machined cavity is a replica of tool electrode and excessive wear will hamper the accuracy of machining. New improved electrode materials, especially graphite, can work on high currents without much damage.

2.3.3 Pulse On-time & Off-time

Each cycle has an on-time and off-time that is expressed in units of microseconds. Since all the work is done during on-time, the duration of these pulses and the number of cycles per second (frequency) are important. Metal removal is directly proportional to the amount of energy applied during the on-time. This energy is controlled by the peak amperage and the length of the on-time. The longer the on-time pulse is sustained, the more workpiece material will be melted away. The resulting crater will be broader and deeper than a crater produced by a shorter on-time. These large craters will create a rougher surface finish. Extended on-times also allow more heat to sink into the workpiece and spread, which means the recast layer will be larger and the heat affected zone will be deeper. Excessive on-times can be counter-productive. When the optimum on-time for each electrode – work material combination is exceeded, material removal rate starts to decrease. A long on-time can also put the electrode into a no-wear situation. Once that point is reached, increasing pulse on-time further causes the electrode to grow due to plating build-up.

The cycle is completed when sufficient off-time is allowed before the start of the next cycle. Off-time will affect the speed and stability of the cut. In theory, the shorter the off-time, the faster will be the machining operation. However, if the off-time is too short, the ejected work piece material will not be swept away by the flow of the dielectric and the fluid will not be deionized. This will cause the next spark to be unstable. Unstable conditions cause erratic cycling and retraction of the advancing servo. This slows down cutting more than long, stable off-times. Off-time must be greater than the deionization time to prevent continued sparking at one point. Modern power supplies allow independent setting of pulse on-times and off-times. Typical ranges are from 2 to 1000 μsec.

Ideally, each pulse creates a spark. However, it is seen practically that many pulses fail if on-time and off-time are not properly set, causing a loss of the machining efficiency. Such pulses are known as "open pulses".

2.3.4 Pulse Waveform

The pulse shape is normally rectangular, but generators with other pulse shapes have also been developed. Using a generator which can produce trapezoidal pulses, De Bruyn [43] succeeded in reducing relative tool wear to very low values. Other types of generators introduce an initial pulse of high voltage but low current and of a few micro-seconds duration, before the main pulse, which facilitates ignition.

2.3.5 Polarity

The polarity of the electrode can be either positive or negative. The current passing the gap creates high temperatures causing material evaporation at both electrode spots. The plasma channel is composed of ion and electron flows. As the electron processes (smaller mass than anions) show quicker reaction, the anode material is worn out predominantly. This effect causes minimum wear to the tool electrodes and becomes of importance under finishing operations with shorter on-times. However, while running longer discharges, the early electron process predominance changes to positron process (proportion of ion flow increases with pulse duration), resulting in high tool wear. In general, polarity is determined by experiments and is a matter of tool material, work material, current density and pulse length combinations. Modern power supplies insert an opposite polarity **"swing pulse"** at fixed intervals to prevent arcing. A typical ratio is 1 swing pulse for every 15 standard pulses.

2.3.6 Electrode Gap

The tool servo-mechanism is of considerable importance in the efficient working of EDM, and its function is to control responsively the working gap to the set value. Mostly electro-mechanical (DC or stepper motors) and electro-hydraulic systems are used, and are normally designed to respond to average gap voltage. The most important requirements for good performance are gap stability and the reaction speed of the system; the presence of backlash is particularly undesirable. The reaction speed must be high in order to respond to short circuits or open gap conditions. Gap width is not measurable directly, but can be inferred from the average gap voltage [42].

2.3.7 Type of Dielectric Flushing

Basic characteristics required of a dielectric in EDM are high dielectric strength and quick recovery after breakdown, effective quenching and flushing ability. Tool wear and MRR are affected by the type of dielectric and the method of its flushing [44]. Most dielectric fluids are hydrocarbon compounds or water. Deionized water is used for wire-EDM and high precision die-sinking because of its low viscosity and carbon-free characteristics. The dielectric fluid is flushed through the spark gap to remove gaseous and solid debris during machining and to maintain the dielectric temperature well below its flash point. Flushing methods can be broadly divided into four categories – normal flow, reverse flow, jet flushing and immersion flushing. In normal flow, which is used in this experimental work, the dielectric fluid is fed to the inter-electrode gap either from the side (side flushing), or through an opening in the tool or the workpiece. Other means of improving flushing conditions involve some form of relative motion between tool and workpiece. A control feature that is available on many machines to facilitate chip removal is vibration or cyclic reciprocation (as in this case) of the servo-controlled tool electrode to create a hydraulic pumping action.

Orbiting of the tool or workpiece has also been found to assist flushing and improve machining conditions. Orbiting EDM permits machining to proceed from roughing to finishing using only a single electrode, with suitable control of the orbit and machining conditions [45].

2.4 BASIC EDM SETTINGS

The polarity, pulse on-time, pulse off-time and peak current are the basic machine settings. These parameters can also be expressed as duty cycle, frequency and average current.

2.4.1 Duty Cycle

Duty cycle is a percentage of the on-time relative to the total cycle time. Generally, the higher duty cycles mean increased cutting efficiency. Duty cycle is calculated in percentage by dividing the on-time by the total cycle time (on-time + off-time).

$$\text{Duty Cycle (\%)} = \frac{\text{On-time (}\mu\text{sec)}}{\text{Total cycle time (}\mu\text{sec)}} \times 100$$

2.4.2 Frequency

Frequency is the number of cycles produced across the gap in one second. The higher the frequency, finer is the surface finish that can be obtained. As the number of cycles per second increases, the length of the on-time decreases. Short on-times remove very little metal and create smaller craters. This produces a smoother surface finish with less thermal damage to the workpiece. Frequency is calculated by dividing 1000 by the total cycle time (on-time + off-time) in microseconds.

$$\text{Frequency (kHz)} = \frac{1000}{\text{Total cycle time (}\mu\text{sec)}}$$

2.4.3 Average Current

Peak current is the maximum current available for each pulse from the power supply / generator. Average current is the average of the amperage in the spark gap measured over a complete cycle. It is calculated by multiplying peak current by duty cycle.

$$\text{Average Current (amperes)} = \text{Duty Cycle (\%)} \times \text{Peak Current}$$

2.5 EDM SURFACE LAYERS

The examination of a section of the surface layer produced by EDM (Fig. 2.7) reveals that there is a top white layer which crystallizes from the liquid cooled at high speed. The depth of this top melted zone depends on the pulse energy and duration. Below the top layer is a chemically affected layer with changes in the average chemical composition and possible phase changes. After this, there is a plastically deformed zone with micro and macro strains characterized by the presence of twinning, slip and phase changes.

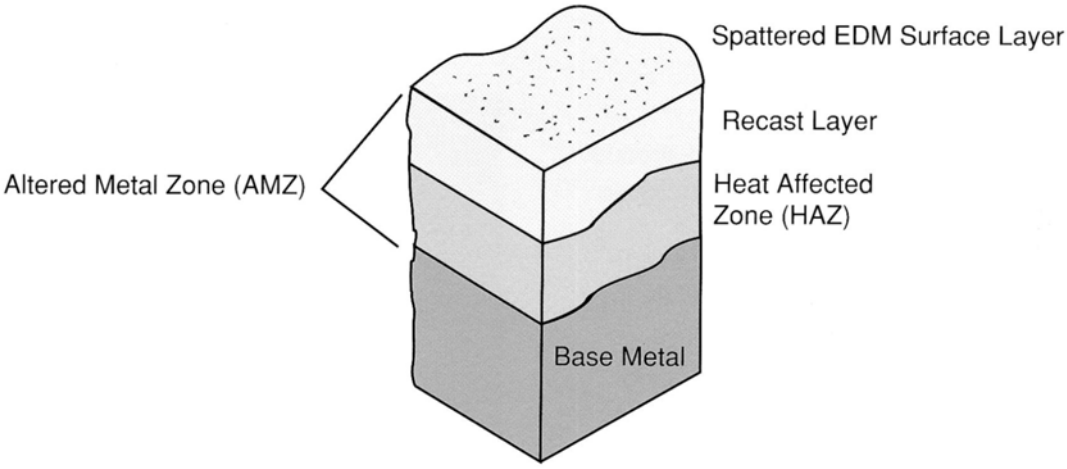

Fig. 2.6 Surface layers after electrical discharge machining

The EDM process changes not only the surface of the workpiece metal, but also the sub-surface. Three layers are created on top of the unaffected workpiece metal. The spattered EDM surface layer is created when expelled molten metal and small amounts of electrode material form spheres and spatter the surface of the workpiece. This spattered material is easily removed.

The next layer is the recast (white) layer. The action of EDM has actually altered the metallurgical structure and characteristics in the recast layer. This layer is formed by the unexpelled molten metal solidifying in the crater. The molten metal is rapidly quenched by the dielectric. Micro-cracks can form in this very hard, brittle layer. If this layer is too thick or is not reduced or removed by polishing, the effects of this layer can cause premature failure of the part in some applications.

The last layer is the heat affected zone (HAZ) or annealed layer, which has only been heated, not melted. The depth of the recast layer and the heat affected zone is determined by the heat sinking ability of the material and the power used for the cut. This altered metal zone influences the quality of the surface integrity. Automatic finishing circuits available on CNC machines greatly reduce the recast layer, but do not eliminate the heat affected zone.

2.6 ALLOYING ELEMENTS IN TOOL AND DIE STEELS

Steels used for tool and die applications cover a wide range of ferrous alloys. A tool or die steel is any steel used to make tools for cutting, forming, or otherwise shaping a material into a part or component adapted to a definite use. Plain carbon steels, if used as cutting tools, lack certain characteristics such as red hardness and hot strength toughness, which are necessary for such applications [17]. Some elements added to plain carbon steels as alloying elements overcome many of the shortcomings. These elements may dissolve in the ferrite phase and increase its hardness and strength by the principle of solid solution strengthening. They may also form hard carbides or intermetallic compounds. Elements like nickel, aluminum, silicon, copper and cobalt are all found largely dissolved in ferrite. Others like manganese, chromium, tungsten, molybdenum, vanadium and titanium have a tendency to form carbides if sufficient carbon is available. While all the carbides found in steel are hard and brittle, chromium and vanadium carbides are outstanding in hardness and wear resistance [33]. The alloying elements may also exist as intermetallic compounds such as FeCr, Fe_2W, FeMo, Fe_3Ti, Fe_3Mo_2 etc. The effect of some of these alloying elements on the properties of tool and die steels [19] relevant to this research work is discussed below.

Carbon is the most important alloying element in steels. Hardness increases as the carbon content is increased. But if carbon content increases above 0.85 %, it leads to a lowering of strength and the hardness remains almost constant. Upon quenching, the maximum hardness attainable also increases with increasing carbon content, but above a value of 0.6 %, the rate of increase is very small. In the 0.85 to 1.4 % carbon range, an increase in carbon content increases the wear resistance at the expense of toughness. The increase in wear resistance is due to the presence of undissolved hard carbides in the hardened matrix.

Chromium increases the hardenability, wear and abrasion resistance, and toughness of steel. Its effectiveness as a carbide former is between tungsten and manganese. The carbides that

are formed have high wear resistance and high hardness. When added to steel in amounts of 10 % or more, the corrosion resistance of the material becomes very high.

Manganese increases the depth of hardness and counters the brittleness caused by sulphur. It also improves the ductility properties of steel without sacrificing strength and wear resistance. Its carbide forming ability is greater than that of ferrite but less than that of chromium. It is most effective in high carbon steels and improves the hot working properties.

Silicon in percentages of up to 0.25 % has little effect as an alloying element. In percentages of up to 2 %, it intensifies the effect of manganese, chromium and molybdenum. It increases the hardenability and oxidation resistance of steel. When combined with manganese, the strength and toughness of steels improve substantially. Its carbide forming effect is less than that of ferrite.

Nickel is one of the oldest and most fundamental alloying elements in steel. It is highly soluble in both ferrite and gamma iron, thus it contributes to the strength and toughness of these phases. When alloyed in steels having high chromium content, it improves hardenability.

When **tungsten** is used in high-carbon steels in amounts of about 4 %, it imparts hardness and wear resistance to steel. It is a strong carbide former and improves the abrasion resistance of tool steels. It also provides red hardness and hot strength to steels.

2.7 SURFACE MODIFICATION USING EDM

Though EDM is essentially a material removal process, efforts have been made to use it as a surface treatment method and / or an additive process. Many surface changes have been reported ever since the process established itself in the toolrooms of manufacturing industry [46]. White layers generated on a steel workpiece machined by EDM using hydrocarbon dielectric have higher carbon content than the base material and hence show increased resistance to abrasion and corrosion [47-48]. Carbon in the white layer appears as iron carbide (Fe_3C) having columnar, dendritic structures. Under the high temperature of discharge column, this white layer can absorb carbon from the gases formed in the discharge column by the breakdown of hydrocarbon dielectric. The available literature on surface modification may be divided into two categories – surface modification by electrode

materials (this includes contribution by the pyrolysis of the dielectric also) and surface modification by powder – mixed dielectric.

2.7.1 Surface Modification by Electrode Materials

Sukahara and Sone [9] carried out surface hardening of titanium using EDM process and obtained a crack less layer of titanium carbide with relatively short pulse duration at low peak current range under negative electrode polarity. The EDMed surface indicated various effective improvements such as hardness, tribological properties and corrosion resistance.

Marafona and Wykes [11] used 75/25 tungsten copper electrode and D2 tool steel workpieces and optimized the parameters such as MRR, TWR and surface roughness Ra. It was found that a black layer of carbon was deposited on the tool when low current intensity and a long pulse duration was used. This layer inhibits further tool wear and a higher current intensity can then be used to improve MRR without corresponding increase in TWR. SEM showed that a layer was formed on the surface of the tool with a high carbon content as well as D2 steel elements such as iron and chromium. It is likely that the carbon comes from the dielectric. Further, energy dispersive X-ray (EDX) analysis was used to measure the composition of the tool.

Mohri et al.. [12] carried out surface modification on workpieces of carbon steel and aluminium using composite electrodes of copper, aluminium, tungsten carbide and titanium in hydrocarbon oil. It was revealed that there existed the electrode material in the work surface layer and the characteristics of the surface layer changed remarkably. These surfaces had less cracks and higher corrosion and wear resistance.

Soni and Chakraverti [13] observed that change in chemical composition of the machined surface occurs due to migration of material from electrode to workpiece material of HCHCr die steel. The experiments were conducted by varying discharge current and electrode rotation to study the effect of these parameters on alloying of tool and workpiece surfaces. The investigation was made on variation of micro-hardness, depth of resolidified layer and heat affected zone.

Kruth [49] reported the possibility of depositing thick layers of material with a traditional EDM machine. This was obtained by using porous electrodes with negative polarity favouring high tool wear. Aluminium on steel and TiC on aluminium were deposited using Al and Ti-Al green compact electrodes respectively.

Mohri et al. [50] used 0.1 mm diameter wires of tungsten, copper and brass as electrodes on AISI-1049 steel workpiece material to observe the effects of electrode materials on material accretion process using EDM. Under the same machining conditions, tungsten was deposited on the workpiece while the workpiece was drilled with copper and brass electrodes.

Roethel and Garbajs [51] observed that the properties of machined surfaces depended on the properties of alloys which were formed in the surface layers due to diffusion of the tool electrode material and breakdown of the dielectric. By microprobe analysis, it was possible to study the phase changes of the material in the surface layers. The working conditions in the gap played a highly significant role in deciding the chemical structure and the properties of the melted and consequently solidified layer.

The surface characteristics of the machined surface were investigated extensively by Lee et al. [52] and attempts were made to quantify the depth of white (or damaged) layer with respect to the process parameters and surface roughness after EDM. It was found that with a fixed dielectric and flushing condition, the damaged layer correlates well with the pulse energy irrespective of the tool steel material. High surface hardness, excellent thermal stability and better wear resistance of the white layer and its phase transformation has also been reported by Venkatesh and Parasnis [53]. The white layer is a complex alloy carbide which can retain its hardness at elevated temperatures. Two distinct types of transformed layers were revealed on etching – a white layer unattacked by the common etchants and devoid of structure, and thermally affected zone below.

Jeswani and Basu [54] carried out electron microprobe analysis for surface deposition and diffusion of tool material on mild steel, high carbon steel and high speed steel with copper and brass tool electrodes using distilled water and kerosene as dielectric media. It was observed that high energy machining results in lower surface deposition but more depth of diffusion. High speed steel had the best deposition followed by high carbon steel and mild steel showed the least deposition. Machining in distilled water at high pulse energy resulted

in lower surface deposition and depth of diffusion as compared to machining in kerosene. Pulse energy (and thus, peak current) was found to be the most important factor aiding surface deposition as compared to tool material, work material or the dielectric fluid.

Kuneida and Yoshida [55] experimented with copper as tool electrode and steel as workpiece by using high pressure air flow supplied through a thin-walled pipe electrode and found that workpiece material can be removed and flushed out of the working gap without being re-attached to the electrode surfaces. The tool electrode wear ratio is almost zero for any pulse duration. Hence a 3D shape can be machined very precisely using a special NC tool path which can supply a uniform high velocity air flow over the working gap. A planetary motion with radius one-tenth of the wall thickness of tool electrode was superimposed in the X-Y plane perpendicular to the axis of the tool electrode because short circuits occurred frequently without this planetary motion. It was found that in the case of EDM in air, the tool electrode wear ratio is much lower and MRR much higher when tool electrode is negative. In contrast, in the case of EDM in a liquid, there is less tool electrode wear and higher MRR when the polarity of the tool electrode is positive.

Barash and Kahlon [56] found that when mild steel was eroded in liquid medium paraffin using a copper electrode, the workpiece was coated with a very hard layer which was difficult to remove by filing. This was attributed to the carburization of the layer due to hydrocarbon medium and its subsequent quenching. The material transfer was found to be a function of the various electrical parameters of the circuit. The addition of doping elements to the dielectric medium can be used to impart the desired properties to the top layer of the workpiece [57]. The carbon in the hydrocarbon dissociates and combines with the doping element to form their respective carbides. The workpiece is positive and the tool electrode is negative for such applications. The two main parameters that influence the doping characteristics are pulse current and pulse duration. Erden and Bilgin [58] observed that that there is practically no change in machining rate during machining of mild steel with copper electrode when the dielectric is artificially contaminated with metallic powders. However, when brass electrode was used, there was a significant increase in machining rate. This is due to the short time lag in case of copper electrodes and long time lags in case of brass electrodes. The impurities decrease the time lag and some of the open circuit pulses are replaced by erosive electrical discharges.

Gangadhar et al. [59] used bronze compacts having 90 % copper and 10 % tin in reverse polarity on mild steel and studied the work surface using electron microscopy and X-ray diffraction analysis and found that surface topography becomes modified by the process. The major phase present in the surface was Cu_3Sn while other phases such as Cu_6Sn_5 and CuSn were also present. They concluded that it was possible to alter the metallurgical and physico-chemical nature of the surface by a suitable change in the ingredients and compositions of the powder compact. Similarly, they used tungsten carbide powder compact electrode containing 40 % WC and 60 % Fe to improve the wear resistance of mild steel work material [60]. Energy dispersive analysis of the surface confirmed the transfer of tungsten carbide. Other than WC and W_2C phases, iron carbide was also present in the deposited layer in the form of FeC, $(Fe_3C)H$ and Fe_3C phases. They reported an improvement of 25 to 60 % in abrasive wear resistance and 20 to 50 % reduction in cutting forces with WC-coated HSS tools. Fabrication of tungsten micro-electrode by single discharge of EDM has also been reported when the tungsten wire electrode is connected to the cathode of the generator [61].

Tsunekawa et al. [62] carried out surface modification of aluminum using powder compact electrode containing 64 % Ti and 36 % Al and found the formation of fine dendritic precipitates of titanium carbide. The electrode was connected to negative polarity and kerosene was used as the working fluid. The average diameter and alloyed depth of discharge craters increased with increase in pulse width, the other important factor being the discharge current. It was found that the forming pressure of the powder metallurgy electrodes did not affect material transfer. Transfer of copper and chromium particles from copper-chromium sintered electrodes under negative polarity has also been reported by Tsai et al. [63].

In a case of surface modification of steel not involving the EDM process, Miyazaki et al. [64] applied a plasma arc produced through a small diameter nozzle on steel. Ceramic powder of silicon carbide was supplied to the processing region with argon as shielding gas. The initial and running cost of plasma arc is much cheaper than laser beam but the former is generally used in industry for cutting and welding applications. It was possible to obtain a hardness of 1000 HV for AISI 1010 steel by self-quenching without any powder and 1200 HV with silicon carbide particles.

Comparison of the performance of powder metallurgy (P/M) tool electrodes with conventional electrodes in normal electrical discharge machining (using straight polarity and not in machining conditions favouring surface modification) has been done by Samuel and Philip [65]. The impact of P/M electrodes on material removal rate, electrode wear was found to be different than conventional electrodes and they were more sensitive to changes in pulse current and pulse duration. The study established that P/M electrodes were technically viable for EDM machining and their related properties could be controlled by varying compaction and sintering variables. It was also found that under certain processing and operating conditions, P/M electrodes could cause net material addition instead of material removal.

Pantelis et al. [66] machined 0.4 % carbon steel with a tool electrode containing 70 % Fe and 30 % WC using both positive and negative polarity. The work surfaces were subjected to optical metallography, SEM, EDS, X-ray diffraction analysis, surface roughness measurements and micro-hardness testing. The commonly described white layer was found along the surface of machined specimens for all the pulse energies tested, regardless of the polarity used. Tungsten rich zones were found in the alloyed white layer but high pulse energies during machining led to extensive cracking and surface defects. It was concluded that EDM could become a useful and cheap alternative process for surface modification and major research efforts were required in this direction. However, many issues related to the accretion process have not been understood properly [67].

A combined machining process using EDM with ball burnishing has also been used to achieve surface modification of Al-Zn-Mg alloy using copper electrode fitted with two 5 mm diameter ZrO_2 balls [68-69]. The significant parameters and optimum combination level of machining parameters were obtained by Taguchi method. It was found that negative polarity of the tool resulted in better hardness of the surface. By this combined process, it was possible to remove micro-cracks and pores from the machined surface. The technique of surface modification has been successfully used in texturing of rolls [70-71] where greater consistency / repeatability of specified roughness and texture has been achieved. Texturing of rolls has traditionally been done using cross-grinding and shot blasting. When using a negative polarity, higher concentration of Ti and W were consistently found at the EDT (Electrical Discharge Texturing) roll surface. Formation of hard carbides such as WC, W_3C and Fe_3C and increase in hardness of up to 100 % in case of AISI H13 work material has also

been reported [72]. The topography of the machined surface typically comprises overlapping craters, which substantially increases the apparent surface area [73]. A significantly reduced coefficient of friction was obtained with alloyed EDT surfaces as compared to similar EDT surfaces machined with standard copper or graphite electrodes.

Wang et al. [74] suggested the application of this method to surface repairing and strengthening of cutting tools and moulds and called it "electrical discharge coating (EDC)". They conducted experiments on carbon steel with Ti powder compact electrodes using negative polarity of the tool and a machining time of 18 minutes. It was found that low values of discharge current (2 to 10 A) and low pulse on-time (2 to 12 μsec) gave a content of TiC as high as 51% and more than three times increase in hardness. Maximum value of micro-hardness was achieved at 2.2 A discharge current and 2 μsec pulse on-time. Other studies with Ti powder compact electrode report an increase in working life of the die by three to seven times [75-76].

Surface modification of H13 hot work tool steel has been attempted using WC / Cobalt electrodes and L8 fractional factorial Taguchi design to identify the effect of key operating factors [77]. The alloyed / modified layer had relatively few micro-cracks, an average thickness of 30 μm and surface hardness of 1319 HK, up from 640 HK. Open gap voltage has been shown to have little effect on workpiece micro-hardness. Bai and Koo [78] used distilled water and kerosene as dielectric media to carry out surface modification of superalloy Haynes 230 using Al-Mo composite electrode. Each sample was machined for 6 minutes. Distilled water gave higher hardness whereas kerosene gave better surface finish, finer surface morphology, thicker alloyed layer and slower oxidation rate. The best R_a value of surface roughness obtained was 2.62 μm. Current density at the negative electrode was higher than the positive electrode. They concluded that surface alloying effect in kerosene is better than that in distilled water.

In one of the recent research works on surface modification in India, Patowari et al. [79] used WC / Cu powder metallurgy electrode on C-40 grade steel and found the presence of both WC and copper on the workpiece surface. The deposition was achieved in only three minutes and significant factors were analyzed using Taguchi L8 orthogonal array. Surface

examination on SEM revealed relatively few micro-cracks and an increase in hardness from 200-220 HV to 1200-1632 HV.

Review of some other research works not directly studying the phenomenon of surface modification but relevant to the application of this process are also presented below.

Shankar and Krishnan [26] studied the effect of work function of the cathode on the spark current pulse width at which preferential erosion switches from anode to cathode in spark machining. In metals with low work function, reversal occurs at large pulse widths. Apart from the EDM process parameters, growth of the plasma channel and energy sharing by the two electrodes depend on thermo-physical properties of electrode materials, dielectric medium and polarity of the electrodes [80]. When using copper as tool electrode and workpiece both, erosion of cathode was found to be about 2 to 3 times more than the erosion of anode and it increases with increase in pulse duration till it attains the maximum value at about 200 μsec. The governing physical process includes breakdown of liquid dielectric that surrounds the two electrodes, followed by electron avalanche and mobility of positive ions leading to ionization and vapourization of dielectric and electrodes forming a high-energy plasma [81-82]. Plasma channel containing high energy plasma shows unequal spatial variation at both ends leading to unequal energy flux available for conduction into the matrix of the electrodes [83].

Shankar et al. [84] carried out a fundamental study of electric discharge machining based on the physics of an arc and heat transfer theory. The field equations for electric potential and temperature in the spark region are simultaneously solved by employing the finite element method. Using the criterion of constant current at any cross-section of a spark, the arc radii at different cross-sections are corrected until convergence. The final spark shape obtained is non-cylindrical, and has different radii at different cross-sections. Also, the percent of heat input absorbed by cathode, anode and dielectric has been calculated. The computed relative electrode wear has been compared with experimental results.

Kaldes [85] established the effectiveness of flushing on MRR, tool wear and accuracy, especially in finishing operations when pulse energies are low and small local products can quickly develop causing short circuits and generally impairing working efficiency. If the dielectric fluid is forced at low velocity through the gap, these local products are flushed.

However, higher velocity of flushing hinders the formation of ionized bridges across the gap and result in higher ignition delay. The relationship of inlet pressure of dielectric fluid with MRR and TWR has been given in the study.

George and Venkatesh [86] investigated optimum machining conditions for EDM of 5 Cr die steel and found out that each electric spark discharge produces a spherical crater in the workpiece, the value of which is directly related to the energy contained in the spark. The depth of crater defines the surface finish that in turn depends on the discharge current, frequency and surface finish of the electrode. It was also observed that high frequency and low amperage settings give the best surface finish.

Altan et al. [2] covered the various aspects of the use of EDM for Die and Mold manufacturing such as wire-EDM, orbital EDM, EDM milling, unattended and high speed EDM, use of non-inflammable dielectric fluids, increasing machining accuracy and reduction and control of electrode wear. Significant improvements in machining time have been reported by using graphite as electrode material and glycerine as an additive to water. Copper is used predominantly for EDMing small and precision dies, used in cold forging and coining. Studies with graphite electrode on inconel work material [87] and for minimizing the spark gap have also been conducted [88].

Van Dijck [89] performed multiple discharge tests on tool steel workpieces with a copper tool to verify the results of theoretical predictions on metal erosion obtained using a thermal model. He explained change in metal erosion with pulse duration on the basis of current density variations in the spark channel. For each combination of workpiece and tool, constant metal erosion graphs can be derived to determine appropriate machine settings. Wide variation in results reported is indicative of the uncertainties involved in the EDM process.

Raghunathan [90] investigated the EDM process with an SAE 1035 steel workpiece, electro carb EC-4 tool and a static impulse generator power supply. The electrohydraulic feed control mechanism and the support equipment used were comparable to a commercially marketed system. This experimental investigation provided the basis for a regression model which represented the EDM process performance. Performance measures and significant machining parameters were identified for the particular combination of tool, workpiece and power supply. Existing optimization techniques were used to optimize the process for

maximizing the machining rate under constraints of surface roughness and tool wear. Trade-off curves were developed showing maximum machining rate as a function of allowable surface roughness.

Soni and Chakraverty [91] studied the effect of electrode material properties on surface roughness and dimensional accuracy in electric discharge machining of HCHCr die steel. They made efforts to investigate the effect of variation of discharge current, electrode material properties such as thermal conductivity, electrical resistivity and heat diffusivity constant with different electrode polarities on surface roughness and dimensional accuracy. The electrodes used were copper, brass, copper-tungsten, graphite and titanium. They observed that surface roughness and dimensional accuracy increase with increase of thermal conductivity. It was also found that copper-tungsten is the best electrode material for finish machining whereas for rough machining graphite is better. Size of crater increases with increase of current which ultimately affects the surface finish.

Toren et al. [31] suggested that in electric discharge machining operation the workpiece as well as the tool (electrode) experience an intense local heating in the vicinity of plasma channel. The high power density would result in the erosion of a part of the material both from the workpiece and the electrode by the local melting and heating. When high material removal rate is desirable with good surface quality, erosion of electrode is unwanted. So a proper selection of tool material and choice of process parameters like pulse power, width and polarity were envisaged.

George and Philip [92] analyzed the EDM performance and tool wear in copper and die-steel system. The large number of input process parameters together with the complex interaction of some of them present difficulty in controlling the EDM output data such as MRR, TWR and surface integrity. The various process parameters studied were discharge current, polarity, pulse energy, pulse width and flushing method.

2.7.2 Surface Modification by Powder – Mixed Dielectric

The suspended particles facilitate the ignition process by creating a higher discharge probability and lowering the breakdown strength of the insulating dielectric fluid. As a result,

MRR is increased, TWR is lowered and sparking efficiency is improved. Conductive powders enlarge the gap distance and improve the surface finish by reducing the spark energy and dispersing the discharges more randomly throughout the surface [93-94]. Thickness of the recast layer is smaller and micro-cracks are reduced. Consequently, the corrosion resistance of the machined surface is substantially improved. Pecas and Henriques [95] found that presence of silicon powder in the dielectric almost eliminates undesirable machining conditions Smooth and highly reflective craters were formed and the improvement in surface roughness depended on the electrode surface area. These powders may combine with carbon at high temperatures of the plasma (from the breakdown of the hydrocarbon dielectric) to form hard carbides on the machined surface. The hardness of the modified surface becomes higher with an increase in discharge duration and powder concentration [96].

Most of the research work using powder – mixed dielectric focuses on improving the process parameters such as MRR, TWR and surface roughness. Lower electrode wear with water dielectrics containing a powder suspension has been reported [97-98]. Abrasive powders such as silicon carbide and alumina have been mixed in the dielectric to improve the material removal rate. Kerosene as well as deionized water has been used as dielectrics [99]. Tool electrode wear decreased sharply and improvement in surface roughness (both R_a and R_z values) was also reported. Such a process has been named PMEDM (powder mixed EDM) [100] in which machining efficiency can be significantly increased by selecting proper discharge parameters. Jeswani [101] conducted experiments with addition of 4 g/liter of fine graphite powder in the dielectric and found that MRR improved by 60 % and electrode wear ratio reduced by about 15 %. However, the impact of such machining on surface modification has been studied by very few researchers and most of it is of recent origin only. An inverse or reverse polarity arrangement is universally recommended and the powders used are Ni, Co, Fe, Al, Cr, Cu, Ti, C (graphite), Si and Mo with quoted grain sizes between 1 to 100 μm.

Uno et al. [102] conducted experiments on aluminum bronze work material (used for making plastic moulds and shell mould cores) with nickel powder mixed in the dielectric and obtained a surface of high wear resistance and good surface finish as compared to conventional EDM due to the presence of nickel. Machining parameters used were 3 amp

discharge current, 2 μsec pulse on-time and negative polarity for the electrode. The nickel content was measured by glow discharge spectroscopy (GDS) and the machined surface was found to be crack-free. Furutani [16] used titanium powder in kerosene dielectric and obtained titanium carbide layer of hardness 1600 HV on carbon steel with a negatively polarized copper electrode, 3 amp peak current and 2 μsec pulse duration. Rotating disk electrode kept the powder concentration high in the machining area. Both titanium and titanium carbide were found in the X-ray diffraction analysis of the machined surface and it was concluded that carbon came from the breakdown of the dielectric.

Lahiri et al. [14] estimated the loss of energy in the pyrolysis or decomposition of dielectric based on a quantitative determination of carbon (a product of pyrolysis) yielded per pulse and a determination of the heat of dissociation of the dielectric. It was found that pyrolysis occurred only during the first few microseconds of the discharge and there was low increment in carbon yield per pulse with increase in pulse width. Loss of energy in pyrolysis in roughing operation was less than 1% whereas it was considerable in finishing operations.

A deposition method for solid lubricant layer of molybdenum disulphide by suspending its powder in the dielectric to produce parts for ultra high vacuum applications (such as space environment) has been proposed by Furutani and Shimizu [103]. They used high open circuit voltage, low discharge current, short pulse duration and medium pulse interval to deposit the lubricant layer on carbon steel and stainless steel. The process is not without its drawbacks, which include the difficulty in ensuring that the powder is held in suspension. This is easier with more viscous dielectrics but at the cost of reduced flushing efficiency [72]. By adding urea to distilled water as the dielectric medium for machining titanium, Yan et al. [104] obtained TiN on the work surface which exhibited improved friction and wear characteristics. Both MRR and TWR declined with an increase in pulse duration. Micro-hardness values of the order of 250 HK were achieved. In order to address the problem of powder settling, Wu et al. [105] added a surfactant along with aluminum powder in the dielectric and observed a more apparent discharge distribution effect which resulted in a surface roughness R_a value of less than 0.2 μm.

It has been possible to achieve near mirror-finish using conductive powders (such as graphite and aluminum) and semi-conductive silicon powders [106]. It has been shown that there is a

great influence of work material and powder properties on the response parameters such as MRR, TWR and surface roughness, besides the appropriate settings of electrode polarity and pulse parameters. Whilst aluminum powder gave mirror-finish on SKH-51 work material, it failed to give the same in case of SKH-54 work material. The use of negative electrode polarity was found to be essential for achieving mirror-finish condition. Tzeng and Chen [107] conducted experiments on SKD-11 steel with aluminum, chromium, copper and silicon carbide powders and found that aluminum powder gave the best surface finish followed by chromium, whereas copper powder generated the worst surface characteristics. Particle size, concentration as well as its properties such as density, electrical resistivity and thermal conductivity affected the performance. Using High Speed Framing Camera (HSFC) technique, Klocke et al. [108] found a larger plasma channel with aluminum powder-mixed dielectric in contrast to the standard dielectric. With a pulse on-time of 100 μsec, photos were taken after a delay of 60 μsec, in order to snapshot a fully developed plasma channel, Thus, it could be concluded that the discharge energy got distributed on a bigger workpiece surface.

Fredriksson and Hogmark [109] performed EDM of tool steel at various dielectric fluid temperatures using both copper and graphite electrodes. The dielectrics investigated were silicone oil, a hydrocarbon based fluid and liquid nitrogen. The type of dielectric fluid used was found to have a greater influence on the microstructure and surface layers than its temperature. The only beneficial effect of changing the temperature was a reduced hardness in the layer beneath the recast layer when the tool steel was machined at an elevated temperature. MRR was found to be very low when machining was carried out in liquid nitrogen. Instead, a recast layer rich in material from the electrode was produced. Hence, electrode material had a great influence on the properties and composition of surface layers in this case. No significant difference in the thickness of affected layer was found when varying the temperature, dielectric or the electrode material.

A hybrid machining process combining EDM and ultrasonic machining (USM) has also been used to achieve surface modification of an aluminum alloy using copper electrode and silicon carbide abrasive particles of 20 μm diameter [110]. The dielectric fluid was circulated by an agitator to ensure that the abrasive particles were uniformly suspended in the dielectric fluid. The surface machined by negative polarity was coarser than the surface machined by positive polarity. The modified layer depth increased with the gap voltage, reaching a peak when the

voltage was about 80-100 Volts and it contained SiC particles as well as Al-Si solid solution strengthening structure. It was concluded that the combined process could produce a hardened layer which was very different from the layer produced by conventional EDM.

2.8 TAGUCHI'S EXPERIMENTAL DESIGN AND ANALYSIS

A properly planned and executed experiment is of utmost importance for deriving clear and accurate conclusions from the experimental observations. Design of experiments is considered to be a very useful strategy for accomplishing these tasks [111]. All engineering experiments involve setting values of a large number of process variables. Technical experience, together with experiments through prototype hardware models or computer simulations, is needed to come up with the most advantageous decisions about these variables. This leads to a very long and expensive time span for completing the design process. Hence, the need arises for scientifically designing the experiments such that complete information is obtained about the process with relatively fewer experiments and redundant data is eliminated.

The science of statistical experimental design originated with the work of Sir Ronald Fisher in England in the 1920s. Fischer founded the basic principles of experimental design and the associated data analysis technique called Analysis of Variance (ANOVA) during his efforts to improve the yield of agricultural crops. The theory and applications of experimental design and the related technique of Response Surface Methodology (RSM) have been advanced by many statistical researchers [112]. Various types of matrices are used for planning experiments to study several decision variables simultaneously. Over a period of time, several innovations such as Full Factorial Design, Fractional Factorial Design and Taguchi method etc. have been introduced to extract maximum possible usage from the concept.

2.8.1 Orthogonal Arrays

The Taguchi Robust Design method uses a mathematical tool called Orthogonal Arrays (OAs) to study a large number of process variables with a small number of experiments [113-114]. OAs are "fractional factorial designs" which are symmetrical sub-sets of all combinations of treatments in the corresponding full factorial designs (that is, when all levels of all the factors are taken into consideration one by one). If experiments are conducted by taking one level of each parameter at a time, the number of experiments will run into

thousands, making it a very time consuming and expensive process. Another major disadvantage of one-parameter-at-a-time approach is that it fails to consider any possible interaction between the parameters [115]. An interaction is the failure of one parameter to produce the same effect on the response at different levels of another parameter.

As the name Orthogonal Array suggests, the columns of the array are mutually orthogonal. It means that for any pair of columns, all combinations of factor levels occur and they occur an equal number of times. This is called the balancing property and it implies orthogonality. The number of rows of an orthogonal array represents the number of experiments. The number of columns of an array represents the maximum number of factors that can be studied using that array. A number of standard OAs are available and one of these can be selected for a particular experiment by knowing the following details [116-117]:

- How many factors are to be studied?
- How many treatment levels are possible for each factor?
- What specific 2-factor interactions are to be investigated?
- Would one encounter any particular difficulty during the runs (for example, some factors may not permit frequent treatment changes)?

There exists a large variety of industrial experiments. Each experiment has a different number of factors. Some factors have two levels, some three levels and some even more. Taguchi has tabulated 18 basic orthogonal arrays that are called standard orthogonal arrays. Depending upon the number of factors and their levels, it is generally possible to select one of these for a specific requirement. However, the standard orthogonal arrays can also be modified to suit complicated designs.

The first step in selecting the appropriate OA involves the counting of the total degrees of freedom (DOF) present in the study. As per Taguchi's method, the total DOF of the selected OA must be greater than or equal to the total DOF required for the experiment. Then the levels of various factors to be included in the study are finalized. The next task is the assignment of process parameters and interactions of interest to the appropriate columns. The use of linear graphs and triangular tables suggested by Taguchi makes the assignment of parameters simple. The array forces all experimenters to design almost identical experiments.

The control log for the experiment is then prepared by assigning the levels of each parameter to various rows of the OA. Such designed experiments are called *matrix experiments* and individual experiment constituting one row of the orthogonal array is called *run* or *treatment*. Settings are also referred to as *levels* and parameters as *factors* [112].

Experiments are performed at random by setting the value of each process parameter according to a single row of the orthogonal array. Three repetitions of each setting are desirable. The results of the experiments are analyzed to achieve one or more of the following objectives:

- To estimate the best or the optimum condition for a product or process.
- To estimate the contribution of individual parameters and their significance for a stated level of confidence.
- To estimate the response under the optimum condition.

2.8.2 Analysis of Variance

Taguchi suggests two different routes to carry out complete analysis of the experimental data. In the first approach, results of a single run or the average of repetitive runs are processed through main effect and ANOVA analysis of the raw data. The second approach, which Taguchi strongly recommends, is to use Signal-to-Noise (S/N) ratios for the same steps of the analysis [112]. The S/N ratio is generally represented by η and is a concurrent quality metric linked to the loss function. By maximizing the S/N ratio, the loss associated with the process can be minimized. The S/N ratio determines the most robust set of operating conditions from variation within the results. It is treated as a response parameter (transform of raw data) of the experiment. For this study, the second approach has been used for analysis of the data.

The primary goal of conducting a matrix experiment is to optimize the product or process design – that is, to determine the best or the optimum level for each factor. The optimum level for a factor is the level that gives the highest value of η in the experimental region. Thus, the optimum level for each factor can be obtained but this best setting may not correspond to one of the rows in the matrix experiment. In such cases, the value of η realized for the predicted best setting is better than the best among the rows of the matrix experiment.

Taguchi recommends that a confirmation experiment should be conducted at the best setting and its result should be compared with the theoretical value predicted by the analysis.

2.9 GAPS IN LITERATURE

From the literature survey, it is observed that the field of surface modification using EDM process is still at the experimental stage. A number of research studies have been carried out and feasibility of the process is well established. Experiments conducted on titanium and various carbon steels reveal that migration of material through the plasma channel does take place from the electrode under appropriate machining conditions. If hydrocarbon oil is used as dielectric, its pyrolysis contributes carbon to the plasma channel which may form carbides with the elements of the machined surface and alter its microstructure. However, the area of surface modification of common die steel materials by limiting the significant process parameters using Taguchi methods and thereby evolving a practical approach for commercial use has not been fully investigated. The effect of changing pulse off-time on surface modification has also not been studied. The recast layer formed during the EDM process is another problem area in die steels and as of now, a secondary process to remove this layer is the only solution which results in additional costs and time delays.

After an elaborate scrutiny of the published work on surface modification, the following gaps have been observed:

- No research work on surface modification has been done using OHNS die steel as work material which is a popular tool material for cold working applications.
- Though Inconel has been used as a work material by some researchers, no one has yet attempted to use it as a tool electrode with reverse polarity in which the electrode wear is higher. The dissolution of this material contributes chromium and nickel to the plasma channel.
- Most of the available research work on EDM with powder-mixed dielectric has studied the impact of machining on material removal rate, surface roughness and tool wear rate etc. using normal polarity. The emphasis on surface modification by this method using reverse polarity is missing.

- No work has been reported about surface modification using manganese powder in the dielectric medium.
- The effect of discharge current and pulse on-time has been taken into consideration in various research works but variation in pulse off-time has not been investigated or it has been taken into consideration in conjunction with pulse on-time by way of duty cycle. There is a need to independently study the effect of this important input process parameter also on the phenomenon of surface modification.
- In the available literature, the constituents of modified surface layers after EDM have been analyzed by EDS (Energy Dispersive Spectroscopy) analysis and EPMA (Electron Probe Micro Analyzer) techniques in which the weight percentage of elements is calculated over a very small area of the surface (diameter in microns) where the electron beam is focused. There is a need to find out the weight percentage of the constituents as an average over a much wider area of the machined surface using some suitable analytical technique such as Optical Emission Spectrometry.
- A comparative analysis of the two methods of surface modification; that is material transfer from electrode bodies and material transfer from powders suspended in the dielectric medium; is missing in the available literature.

All these aspects have been addressed in this research work.

CHAPTER - 3
DESIGN OF STUDY

A large number of input process parameters can be varied in the EDM process, each having its own impact on output parameters such as material removal rate, tool wear rate, hardness of the machined surface, surface finish, dimensional accuracy and overall surface integrity. These input machining parameters are:

(a) Discharge voltage
(b) Peak current
(c) Pulse waveform
(d) Pulse on-time and off-time
(e) Pulse frequency
(f) Polarity
(g) Electrode gap
(h) Type of dielectric flushing

The effect of each of these parameters on EDM process in general, and on the phenomenon of material transfer in particular, has been discussed in detail in the preceding literature review. It is also known from previous research work that out of the above listed parameters, four parameters directly affect the phenomenon of surface modification in electrical discharge machining. These four parameters are **peak current, pulse on-time, pulse off-time and polarity** [77-78]. These parameters have been investigated thoroughly in this research work. The value of any of these parameters can be easily changed from the control panel switches of most of the EDM machines that are currently being used by the tool and die making industry.

The range of first three process parameters for this experimental work was to be decided on the basis of the results of pilot experimentation conducted by 'varying one parameter at a time' approach. But the fourth parameter was fixed as **reverse polarity** (electrode negative) for all the experiments because it was the desirable setting for material transfer to occur [79-80]. With straight polarity, the energy available per discharge at work surface is higher as

compared to the tool electrode and consequently, material removal rate is also higher. No deposition on the workpiece surface can take place under such machining conditions.

3.1 OVERALL EXPERIMENTAL DESIGN STRATEGY

As the objective of this research work is to develop a method of surface modification for common die steel materials through material transfer either from electrode bodies or from powder suspended in the dielectric medium by changing the various input machining process parameters, the design variables can be summarized as follows:

(a) Three die steel materials; namely OHNS die steel, D2 high-carbon high-chromium die steel and H13 hot work die steel (referred as W1, W2 and W3)

(b) Four electrode materials; namely Copper, Graphite, Copper-Tungsten and Inconel (referred as EL1, EL2, EL3 and EL4)

(c) Four powders to be suspended in the dielectric one by one; namely Graphite, Manganese, Silicon and Tungsten (referred as PW1, PW2, PW3 and PW4)

(d) Three levels of peak current to be used (referred as I1, I2 and I3); because the non-linear behaviour of process parameters can only be studied if more than two levels of a parameter are used.

(e) Three levels of pulse on-time to be used (referred as $P_{on}1$, $P_{on}2$ and $P_{on}3$)

(f) Three levels of pulse off-time to be used (referred as $P_{off}1$, $P_{off}2$ and $P_{off}3$)

For conducting the experiments, it was decided to follow the Taguchi method of experimental design and an appropriate orthogonal array was to be selected after taking into consideration the above design variables. Since the pattern of response of each work material to surface modification was expected to be independent of each other which could not be predicted at that stage, it was decided not to include the work material as one of the variables of Taguchi orthogonal array. For example, the hardening range achievable by each work material varies significantly (refer Table 1.3) which may skew the Taguchi design analysis unduly in favour of a particular material if work material is included as part of the array. Moreover, the effect of each electrode material and suspended powder on the phenomenon of surface modification was to be studied separately in order to correctly understand its behaviour. Hence, it was decided to conduct experiments with each combination of work

material, electrode material and powder. Consequently, the experimental work was divided into two distinct stages:

Stage – I : Experimentation with different electrode materials

Stage – II : Experimentation with powder – mixed dielectric

Out of the above listed design variables, the orthogonal array was then to be selected for three design variables (namely peak current, pulse on-time and pulse off-time; also called 'factors') at three levels each (I1, I2, I3, $P_{on}1$, $P_{on}2$, $P_{on}3$, $P_{off}1$, $P_{off}2$ and $P_{off}3$) which would constitute the orthogonal array.

The two most important output process parameters for dies and press tools are micro-hardness and surface roughness of the machined surfaces and the same have been selected as response parameters for this research work also. Micro-hardness directly influences the life of the tools and surface roughness is significant from the point of view of lubrication retention and quality of the products made from these tools. Moreover, when a study involves surface changes due to coatings, carburizing, nitriding etc. or surface modifications affecting hardness, micro-hardness testing is preferred over bulk or macro-hardness [118]. This is done because the depth of indentation during measurement of micro-hardness is much less (around 70 μm) as compared to the depth of indentation during measurement of macro-hardness (which is of the order of 500 μm). As this study is concerned with surface modifications, micro-hardness is an appropriate indicator of the changes taking place in the machined surface. The effect of the variation in input process parameters needs to be studied on these two response parameters and the experimental data to be analyzed as per Taguchi method to find out the optimum machining conditions and percentage contribution of each factor.

The machining parameters that were kept fixed throughout the experimentation are listed in Table 3.1. Electrode quill movement is the periodic lifting of the tool electrode to facilitate the flushing of accumulated debris in the machining area. Machining time of 10 minutes was considered adequate for the surface changes to take effect over the entire region. Spark energy is generally kept low for smaller values of peak current and pulse on-time to ensure stability of the machining process.

Table 3.1 Fixed Input Process Parameters

S. No.	Machining Parameter	Fixed Value
1.	Open Circuit Voltage	135 ± 5% Volts
2.	Polarity	Reverse
3.	Machining Time	10 minutes
4.	Type of Dielectric	Kerosene
5.	Electrode Quill Movement	10 : 4
6.	Powder Concentration in dielectric	15 g/liter
7.	Spark Energy	Low (position 3)

3.1.1 Selection of Orthogonal Array & Parameter Assignment

In this experiment, there are three parameters at three levels each. The degrees of freedom (DOF) of a three level parameter is 2 (number of levels - 1), hence total DOF for the experiment is 6. The DOF of an orthogonal array selected for an experiment should be more than the total DOF for that experiment. The difference should also not be very high, otherwise the cost and effort involved in conducting the extra experiments is wasted. Out of the standard orthogonal arrays available in Taguchi design, L9 orthogonal array has 8 degrees of freedom and it can accommodate three levels of up to four parameters, so it has been selected for this work. The array has been shown in Table 3.2. The fourth column of the array can be left blank. The orthogonality of an array is not lost if one or more columns are not used [92].

Linear graph of L9 orthogonal array indicates interaction between column 1 and 2 (Appendix-D). It means that if interaction between any two factors is anticipated and needs to be studied, they should be assigned to these two columns. Columns 3 and 4 are to be left blank in that case because the interaction effect is reflected in these columns. However, Taguchi recommends that study of interaction should be avoided, if possible, by proper assignment of the factors. Amongst the parameters of this design, it is well known from previous research work that in EDM, the impact of variation in peak current and pulse on-

time on output parameters is independent of each other and there is no interaction between them. Hence, they have been assigned to columns 1 and 2. The third factor, that is pulse off-time, has been assigned to column 3. The levels of these factors have been decided on the basis of the results of pilot experimentation.

Table 3.2 Standard L9 orthogonal array of Taguchi Design

Experiment Number	Column			
	1	**2**	**3**	**4**
1	1	1	1	1
2	1	2	2	2
3	1	3	3	3
4	2	1	2	3
5	2	2	3	1
6	2	3	1	2
7	3	1	3	2
8	3	2	1	3
9	3	3	2	1

Each row of the orthogonal array represents the set of values of input process parameters with which a particular experiment is to be conducted. Thus, a total of nine experiments are required for one phase of a study. Taguchi also recommends that the experiments of an OA should be conducted at random and that each experiment should be repeated three times to minimize the effect of uncontrollable factors. For this experimentation, the set of these nine experiments were repeated three times for each combination of electrode material and work material for the first stage; and for each combination of powder and work material for the second stage of experimentation. However, the following exceptions were taken:

- D2 work material is already rich in carbon (nominal value 1.4 to 1.6% carbon, measured value 1.57% carbon) and adding any more carbon does not improve its properties as a tool steel material [19, 119]. Hence this material was not machined with graphite powder suspended in the dielectric or by graphite electrode.

- Inconel alloy was intended to provide chromium and nickel to the machined surface. But addition of nickel to a chromium and carbon rich die steel results in retention of austenite phase and deterioration of properties [19, 120]. Hence, D2 work material (containing 1.57 % carbon and 12.38 % chromium) was not machined using inconel alloy as electrode.

3.1.2 Signal-to-Noise Ratio for Response Characteristics

The parameters that influence the output can be categorized into two classes, namely controllable (or design) factors and uncontrollable (or noise) factors [111]. Controllable factors are those factors whose values can be set and easily adjusted by the designer or process engineer. Uncontrollable factors are the sources of variation often associated with production or operational environment. The best settings of control factors as they influence the output parameters are determined through experiments. Quality is measured by the deviation of a functional characteristic from its target value. Noises are the uncontrollable factors which can cause such deviations resulting in loss of quality. Taguchi methods seek to remove the effect of these noises and the robust design lends itself well for optimization through the macro- modeling approach.

At the heart of the Taguchi philosophy is the quality loss function. The loss function promotes efforts to continually reduce the variation in a product's functional characteristics [113]. The loss function is further transformed into a signal-to-noise (S/N) ratio. The change in quality characteristic of a product under investigation in response to a factor introduced in the experimental design is the 'signal' of the desired effect. The effect of external factors (uncontrollable factors) on the outcome of quality characteristic is termed as 'noise'. Thus, signal-to-noise ratio measures the sensitivity of the quality characteristic being investigated in a controlled manner, to those external influencing factors (noise factors) not under control. The aim of any experiment is always to determine the highest possible S/N ratio for the result irrespective of the quality characteristics. A high value of S/N implies that signal is much higher than the random effects of noise factors.

Finding a correct objective function to maximize in an engineering design problem is very important. Depending upon the type of response, the following three types of S/N ratios are employed in practice:

(1) Higher the better:

$(S/N)_{HB} = -10 \log (MSD_{HB})$

where $MSD_{HB} = \frac{1}{R} \sum_{j=1}^{R} (1/y_j^2)$ (3.1)

MSD_{HB} = Mean Square Deviation for Higher-the-better response

(2) Lower the better:

$(S/N)_{LB} = -10 \log (MSD_{LB})$

where $MSD_{LB} = \frac{1}{R} \sum_{j=1}^{R} (y_j^2)$ (3.2)

MSD_{LB} = Mean Square Deviation for Lower-the-better response

(3) Nominal the best:

$(S/N)_{NB} = -10 \log (MSD_{NB})$

where $MSD_{NB} = \frac{1}{R} \sum_{j=1}^{R} (y_j - y_o)^2$ (3.3)

MSD_{NB} = Mean Square Deviation for Nominal-the-best response

And, y_j = Observed value of the response characteristic

y_o = Nominal or target value of the results

R = Number of repetitions

For smaller-the-better type, target value is zero. For larger-the-better type, inverse of each large value becomes a small value and again the target value is zero. For nominal-the-best type of characteristic, the standard definition of MSD has been used. Therefore, for all the three expressions, the smallest magnitude of MSD is being sought. The constant 10 has been purposely used to magnify S/N ratio for each analysis and negative sign is used to set S/N ratio of larger-the-better type relative to the square deviation of smaller-the-better type [115].

For this experimental work, the response characteristics have been studied as under:

(1) Response Name : Micro-hardness

	Response Type	:	Higher-the better
	Units	:	HV (Vickers Hardness Number)
(2)	Response Name	:	Surface Roughness
	Response Type	:	Lower-the better
	Units	:	R_a value in microns

Thus, for micro-hardness, higher values are considered optimal and Equation (3.1) was used to calculate S/N ratio. The S/N data was then analyzed to find out that combination of the machining conditions which resulted in the highest value of micro-hardness for a given situation. For surface roughness, lower values are considered optimal and Equation (3.2) was used to calculate S/N ratio and subsequently, the data was analyzed to find out that combination of the machining conditions which resulted in the lowest value of surface roughness for a given situation.

3.2 DESCRIPTION OF THE EDM MACHINE

The experiments have been conducted on Electric Discharge Machine model T – 3822M of Victory Electromech (India) available at Thapar University, Patiala. A pictorial view of the machine is shown in Fig. 3.1.

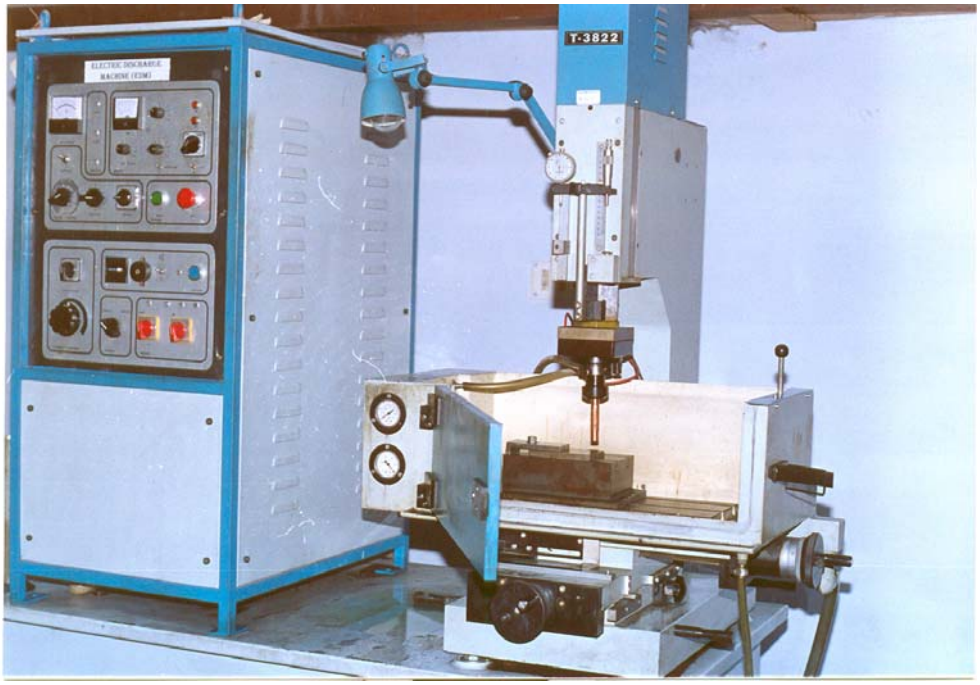

Fig. 3.1 EDM machine used for the experimentation

Important technical data of the machine has been summarized in Appendix – A. The x-axis and y-axis movements are given to the work table and the z-axis movement is on the tool holder. A servo-mechanism controls the downward movement of the tool holder during machining. Commercial grade kerosene is used as the dielectric medium. The dielectric tank has a capacity of 150 liters. A dielectric level indicator maintains the pre-set level (minimum 40 mm above sparking point) during machining and switches off the machine if it falls below that level due to any reason. The setting of erosive pulse parameters [121] is obtained by selection of DURATION (pulse on-time), BASE (pulse off-time which decides the duty factor), IGNITION and AVERAGE MACHINING CURRENT. These parameters can be set from the control panel of the machine which is shown in Fig. 3.2.

Fig. 3.2 Control Panel of the EDM machine

If the pulse duration is longer, more energy is available per discharge and the craters produced are deeper and the resultant surface finish is coarser. At the same time, shorter pulse on-times result in more electrode wear. Pulse off-time determines the spacing of the pulses. Ignition can be set by a 4-position rotary switch which controls the energy of ignition in the discharge channel. This energy is maximum at position 1 and decreases progressively. Excessive ignition of the discharge channel provokes arcing tendency and instability of the machining process. The position of this switch has been kept fixed at position 3 for this experimentation. Machining current can be increased gradually by means of a knob and rotary switch. Both these switches should be at the minimum position when the sparking is started. A toggle switch 'SOFT PULSE' has been provided for the purpose of smoothening the discharge pulses which are very strong when the average machining current is more than 2 to 3 amperes. Normal setting of this switch is position '1' and the same has been used for this experimentation.

3.3 PILOT EXPERIMENTATION

Having established the relevance of low discharge current and low pulse duration on the phenomenon of material transfer through literature review, the actual impact of these parameters and their ranges was investigated through pilot experimentation. The impact of variation in pulse off-time as an independent parameter (it has been used as part of duty cycle along with pulse on-time) was missing in the available literature and this aspect needed further exploration. Though the two response characteristics selected for the experimentation were micro-hardness and surface roughness; a third characteristic, namely electrode wear, was also studied as part of the pilot experimentation. Electrode wear is an important parameter when material transfer is to take place from the electrode bodies. It was calculated as the percentage loss in weight of the electrode after machining. Thus the effect of variation in peak current, pulse on-time and pulse off-time was studied on three response characteristics. OHNS die steel was used as the work material for pilot experimentation. The work material was hardened and tempered as per standard heat treatment procedure and its micro-hardness before machining was measured as 607 HV. The values of input process parameters taken from the operation manual of EDM machine [121] for pilot experimentation are as under:

Peak Current	:	2, 4, 6, and 8 Amperes
Pulse on-time	:	5, 10, 20, 50 and 100 µsec
Pulse off-time	:	17, 25, 38, 57 and 85 µsec

The higher side values of pulse off-time were chosen (as permissible in the manual for a particular setting of pulse on-time) with the aim of providing adequate cooling time to the recast material. Moreover, low pulse off-time results in unstable machining and may cause arcing.

3.3.1 Effect on Micro-hardness

The graphs showing the effects of variation of peak current, pulse on-time and pulse off-time on micro-hardness for the four electrode materials are given in Fig. 3.3 to 3.5. It was found during machining that the pulse off-time setting of 17 µsec resulted in unstable machining conditions and arcing tendency. It could be due to less deionization time available to the dielectric and inadequate flushing of the spark gap. Hence this value of pulse off-time was eliminated and experimentation was carried out with the remaining four values. It was also observed during experimentation that stable and continuous machining took place at higher values of pulse off-time and manual adjustment of spark gap was not required.

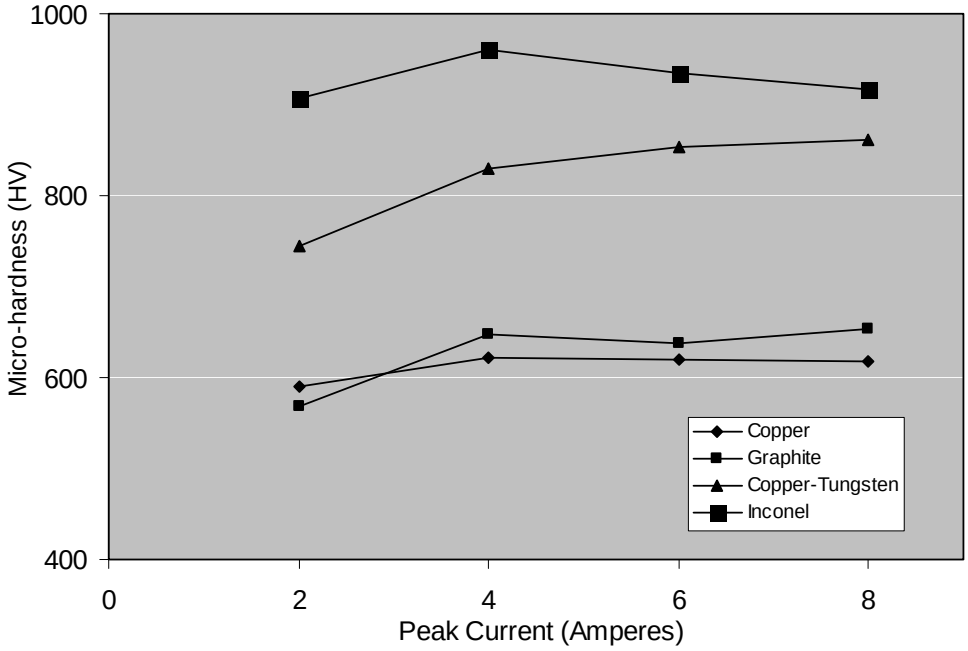

Fig. 3.3 Effect of variation in Peak Current on Micro-hardness for the four electrode materials at Pulse on-time = 10 µsec and Pulse off-time = 38 µsec

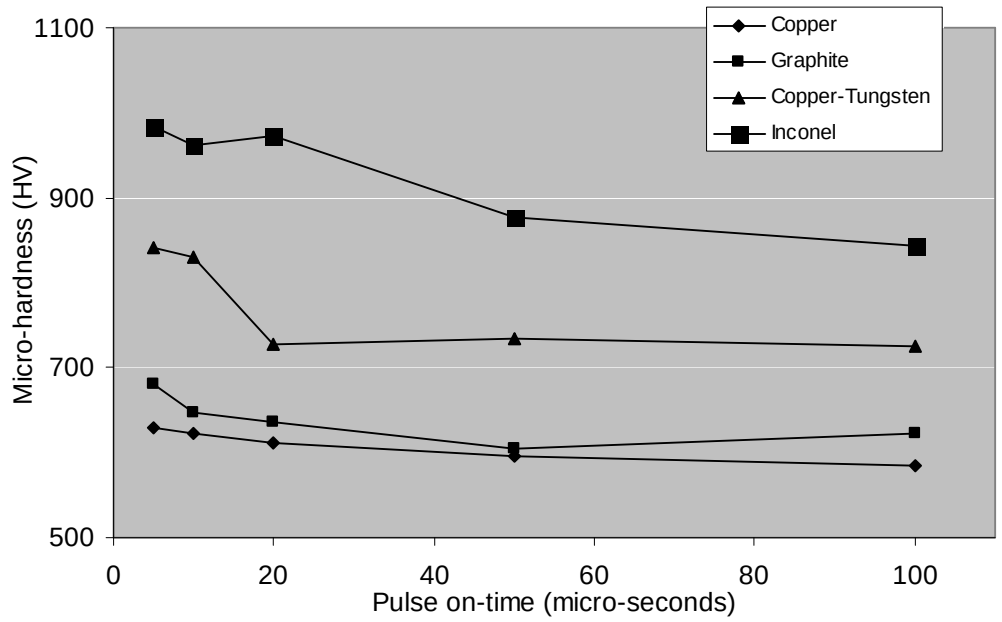

Fig. 3.4 Effect of variation in Pulse on-time on Micro-hardness for the four electrode materials at Peak Current = 4 A and Pulse off-time = 38 µsec

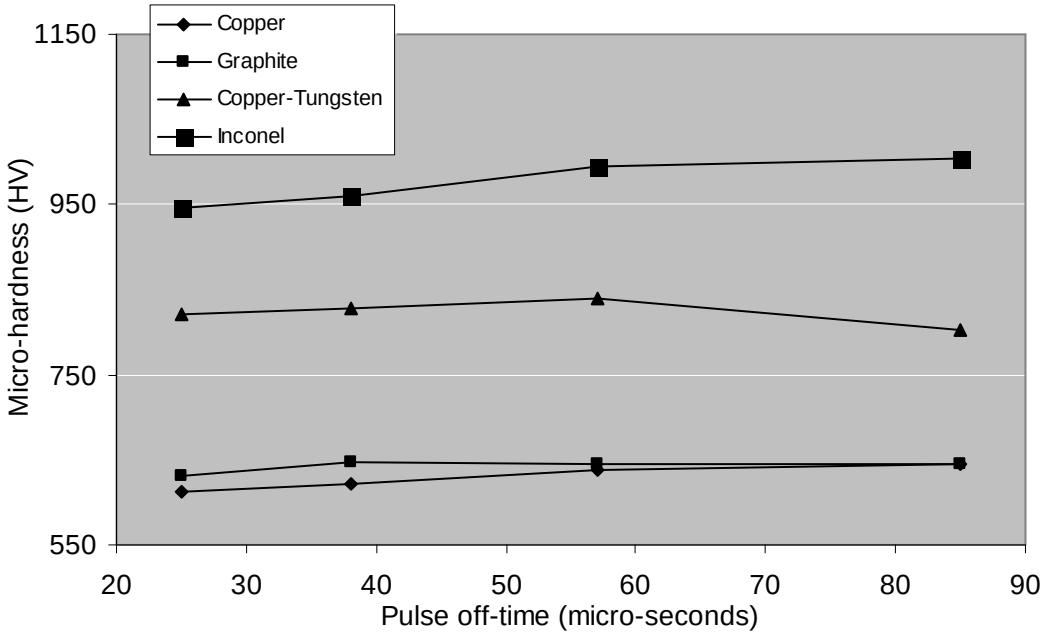

Fig. 3.5 Effect of variation in Pulse off-time on Micro-hardness for the four electrode materials at Peak Current = 4 A and Pulse on-time = 10 µsec

It can be seen from the graphs that maximum variation in micro-hardness takes place at low values of peak current and pulse on-time. Moreover, changes in micro-hardness are more pronounced at low values of pulse on-time and a steady decrease is observed at higher values. No discernible pattern is observed with changing pulse off-time but a marginal increase in micro-hardness at higher values of pulse off-time can be seen. Maximum increase in micro-hardness is reported by inconel electrode followed by copper-tungsten electrode. While inconel electrode shows a decrease in micro-hardness at higher values of peak current, copper-tungsten electrode shows a steady increase in micro-hardness with increasing peak current. The best value of micro-hardness is achieved at the peak current of 4 A which is due to the transfer of electrode material to the workpiece surface. During EDM, improvement in micro-hardness is achieved by the combined effect of material transfer and hardening due to the heating and quenching cycle. While hardening is more at higher values of peak current, it can be inferred that the maximum impact of material transfer takes place at 4 A peak current in case of inconel electrode. The behaviour of copper and graphite electrodes is almost identical.

Some of the machined surfaces showing high value of micro-hardness were subjected to EDS (Energy Dispersive Spectroscopy) analysis to find out the presence of electrode material. Only some of the positive results of this analysis are shown in Fig. 3.6 to 3.8.

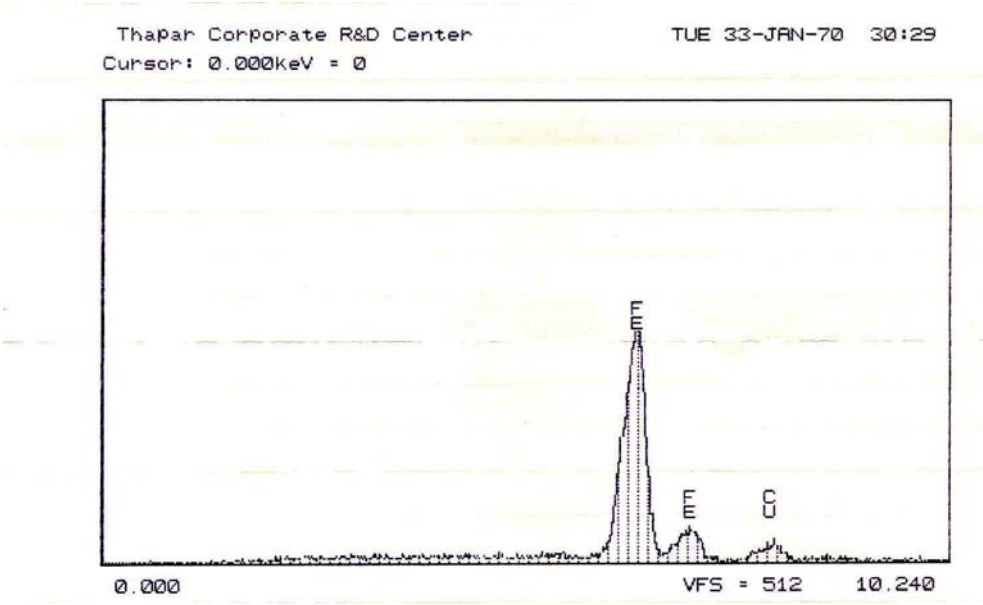

Fig. 3.6 EDS analysis of surface machined with copper electrode at Peak Current = 4 A, Pulse on-time = 5 µsec, Pulse off-time = 38 µsec

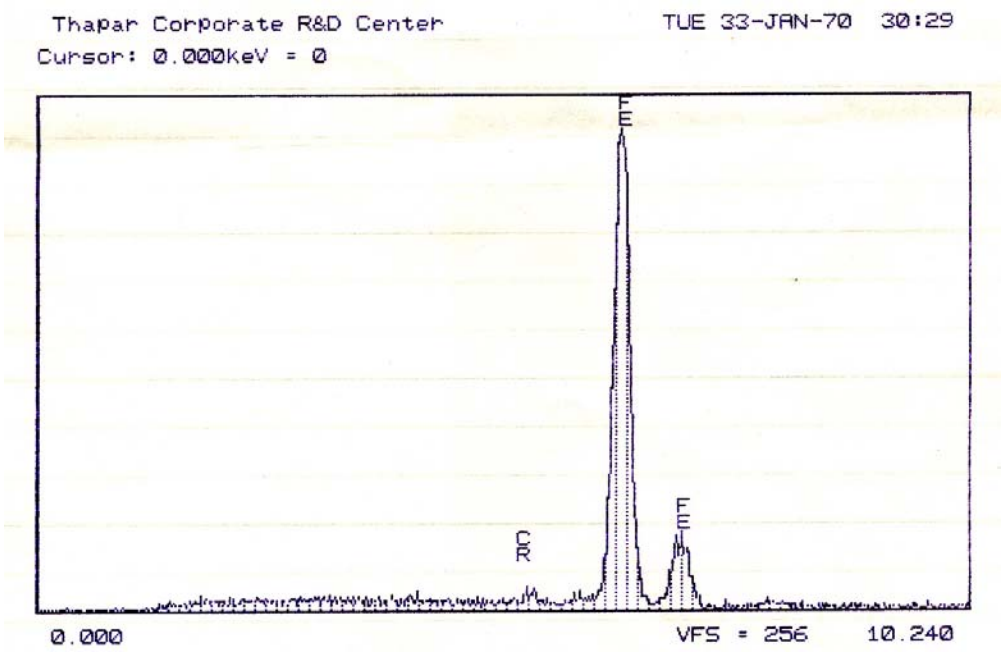

Fig. 3.7 EDS analysis of surface machined with Inconel electrode at Peak Current = 4 A, Pulse on-time = 10 µsec, Pulse off-time = 38 µsec

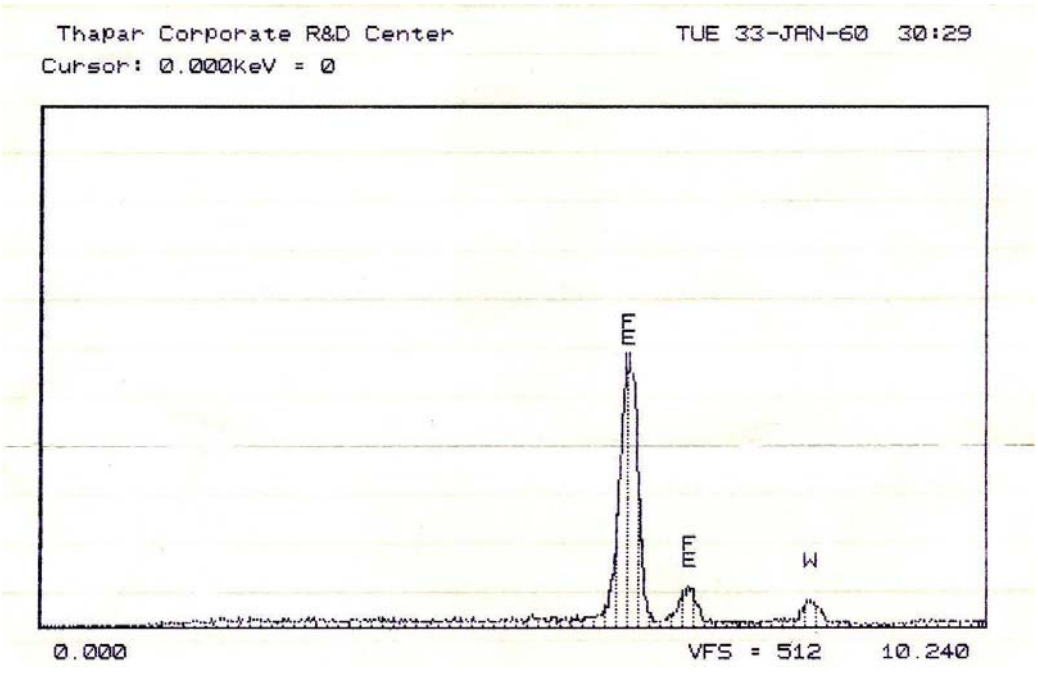

Fig. 3.8 EDS analysis of surface machined with Copper-tungsten electrode at Peak Current = 6 A, Pulse on-time = 10 µsec, Pulse off-time = 38 µsec

It can be seen that machining with inconel electrode results in the presence of chromium (but not nickel) in the machined surface (Fig. 3.7). Similarly, machining with copper-tungsten electrode shows presence of tungsten but not copper (Fig. 3.8). A comparison of the machining parameters reveals that transfer of tungsten has taken place at a higher value of peak current as compared to chromium. Presence of copper and chromium is seen at the peak current value of 4 A whereas the presence of tungsten is seen at 6 A. It is significant to note that even though copper-tungsten electrode has copper as the major constituent; no trace of copper is seen under these machining conditions. Besides lower value of peak current, transfer of copper also requires less pulse on-time which can be attributed to the lower melting point of copper as compared to chromium and tungsten (Appendix – B).

No traces of electrode materials were found in samples machined at settings of 8 Amperes peak current and 100 μsec pulse on-time. However, micro-hardness was relatively high at these values which can be attributed to higher spark energy and consequently, more heating and quenching effect which results in higher hardness. It can be inferred from the EDS analysis that material transfer from the electrode bodies does take place under these machining conditions but no definite conclusions can be drawn. An elaborate and scientifically designed experimentation is required to establish the process parameters.

For subsequent experimentation, EDS analysis has been replaced by a combination of XRD analysis and Optical Emission Spectroscopy due to the following reasons:

(i) The EDS facility is not capable of detecting elements having atomic number less than 11, hence presence of carbon can not be detected by this method.

(ii) The weight percentage of elements in EDS analysis is calculated for a very small area of the surface (diameter in microns) where the electron beam is focused. In comparison to this, the Optical Emission Spectrometer calculates weight percentage as an average over a much wider area of the surface (approximately 5 mm diameter) where the spark is directed.

(iii) The EDS analysis provides information about the constituents of the machined surface only in elemental form whereas XRD analysis gives complete information about the presence of constituents in elemental as well as compound form.

3.3.2 Effect on Surface Roughness (R_a)

The graphs showing the effects of variation of peak current, pulse on-time and pulse off-time on surface roughness (R_a value in microns) for the four electrode materials are given in Fig. 3.9 to 3.11.

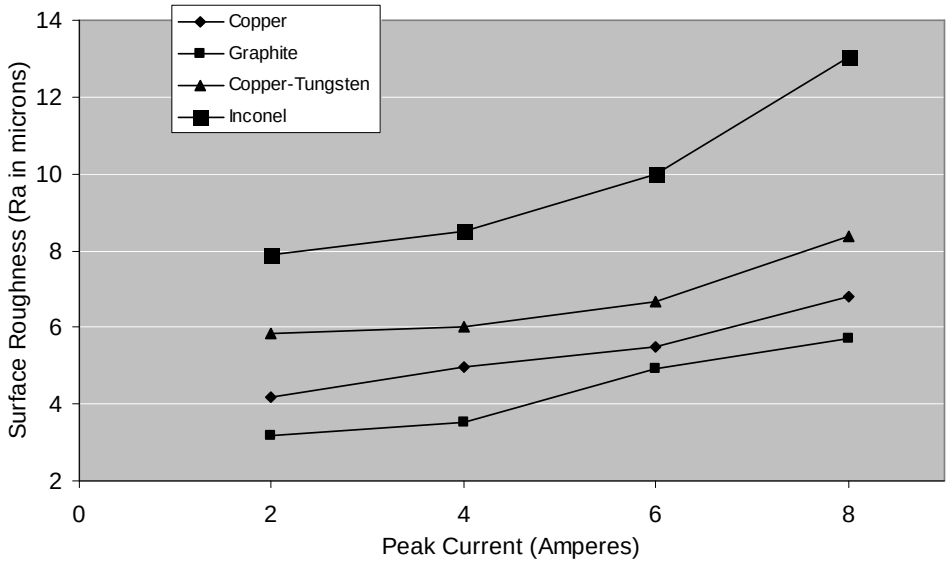

Fig. 3.9 Effect of variation in Peak Current on Surface Roughness for the four electrode materials at Pulse on-time = 10 µsec and Pulse off-time = 38 µsec

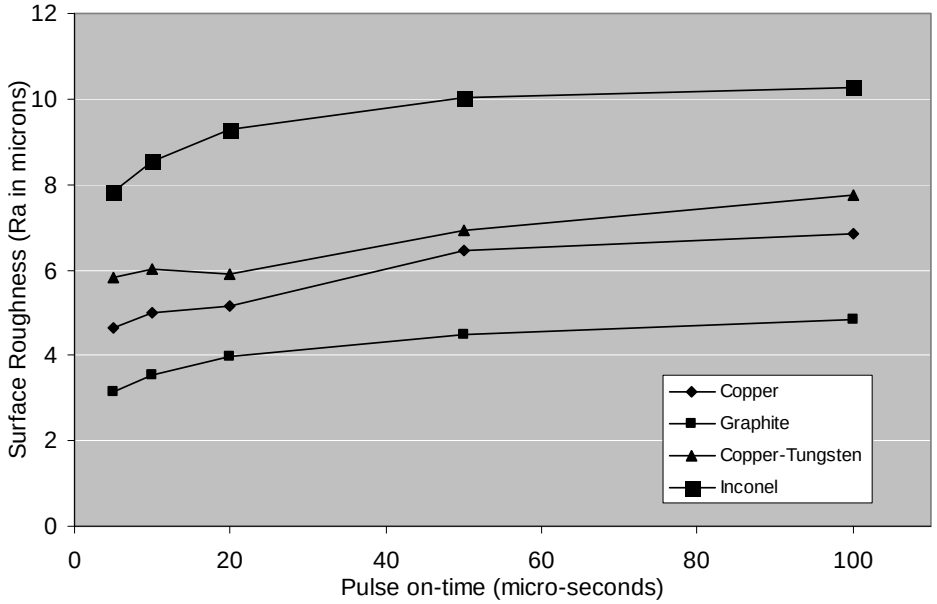

Fig. 3.10 Effect of variation in Pulse on-time on Surface Roughness for the four electrode materials at Peak Current = 4 A and Pulse off-time = 38 µsec

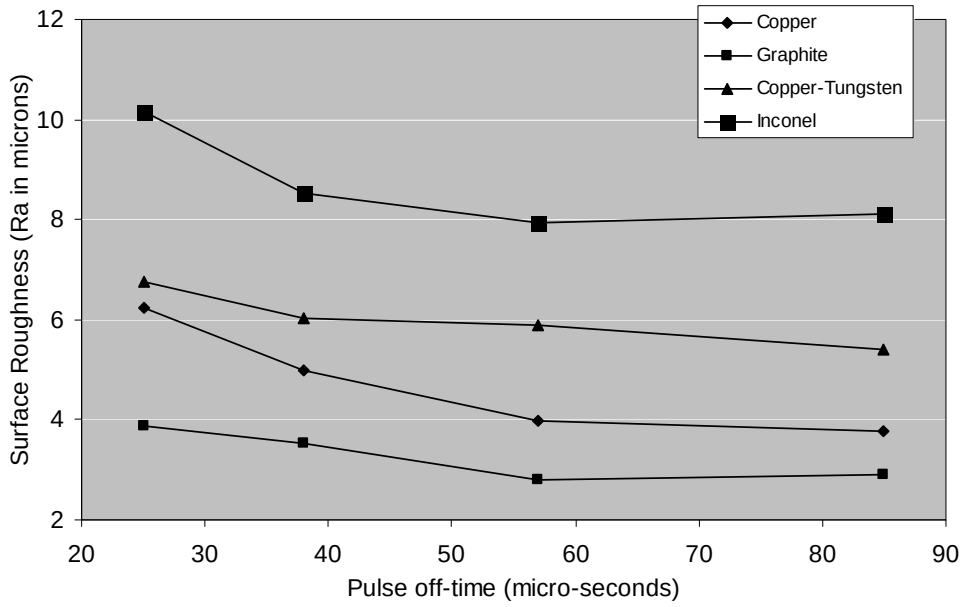

Fig. 3.11 Effect of variation in Pulse off-time on Surface Roughness for the four electrode materials at Peak Current = 4 A and Pulse on-time = 10 µsec

It is observed from the graphs that there is a steady increase in surface roughness with increase in peak current (Fig. 3.9). It is expected because more current means more energy in each discharge and a larger size of the crater. In figure 3.10, abrupt changes in surface roughness are seen at low values of pulse on-time. It has been reported in many research papers that low values of pulse on-time provoke a certain amount of electrode wear and a rougher electrode surface results in a rougher workpiece surface. Surface roughness shows a marked improvement with increase in pulse off-time (Fig. 3.11) which may be due to adequate flushing and sufficient deionization of the dielectric at high pulse off-time. The best surface finish is reported by graphite electrode which approaches a value of 2.81 µm at 4 A peak current, 10 µsec pulse on-time and 57 µsec pulse off-time. The worst performance for this response characteristic is shown by inconel electrode which is due to its high wear.

3.3.3 Effect on Electrode Wear

The graphs showing the effects of variation of peak current, pulse on-time and pulse off-time on electrode wear (calculated as percentage loss in weight) for the four electrode materials are given in Fig. 3.12 to 3.14. As expected, all the four electrode materials show a steady increase in wear with increasing peak current (Fig. 3.12). Reverse polarity results in high tool

wear and inconel electrode reports percentage wear as high as 1.912% at 8 A peak current, 10 µsec pulse on-time and 38 µsec pulse off-time.

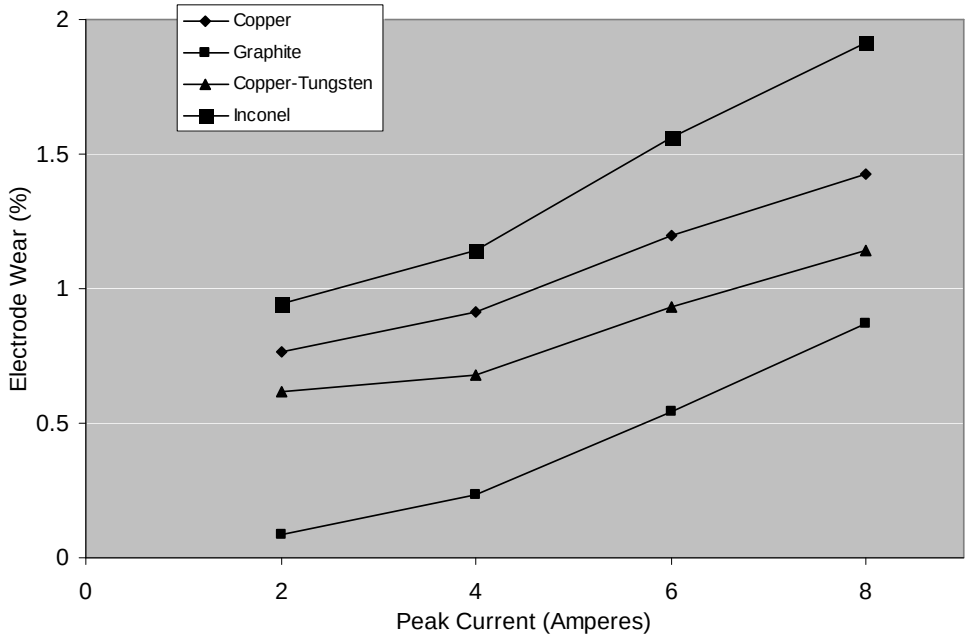

Fig. 3.12 Effect of variation in Peak Current on Electrode Wear (%) for the four electrode materials at Pulse on-time = 10 µsec and Pulse off-time = 38 µsec

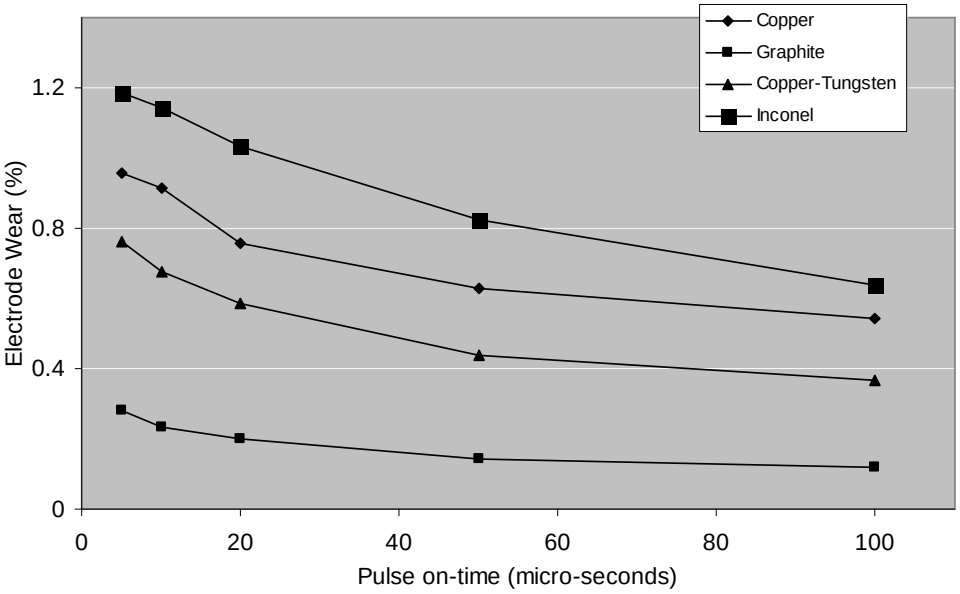

Fig. 3.13 Effect of variation in Pulse on-time on Electrode Wear (%) for the four electrode materials at Peak Current = 4 A and Pulse off-time = 38 µsec

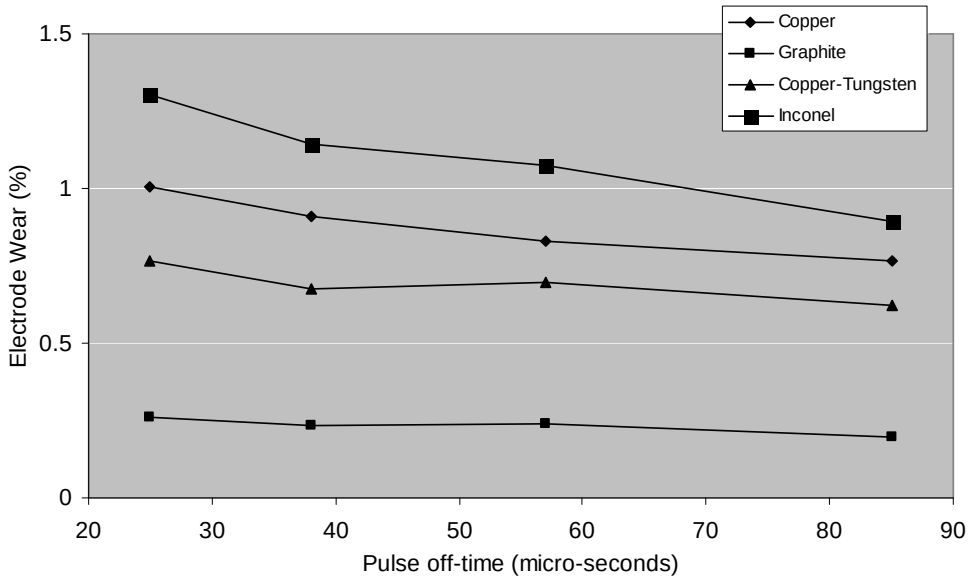

Fig. 3.14 Effect of variation in Pulse off-time on Electrode Wear (%) for the four electrode materials at Peak Current = 4 A and Pulse on-time = 10 µsec

It can be seen from Fig. 3.13 that a decrease in pulse on-time from 10 to 5 µsec results in a sharp increase in electrode wear of all the four electrode materials but it gradually stabilizes with increasing pulse on-time. Hence, it may be concluded that low values of pulse on-time are conducive for material transfer to take place from the electrode bodies. Electrode wear is higher at low values of pulse off-time (Fig. 3.14) also but keeping in mind the stability of the machining operation; to prevent carbon accumulation in the gap and to provide adequate cooling time to the deposited material; higher values of pulse off-time have been selected for subsequent experimentation. It is also observed that graphite electrode shows minimum wear under all conditions followed by copper-tungsten, copper and inconel in that order.

3.3.4 Selection of Input Process Parameters

Based on the observations made during pilot experimentation conducted by varying one parameter at a time, the following levels of input process parameters were selected for subsequent experimentation:

Peak Current	:	2, 4 and 6 Amperes
Pulse on-time	:	5, 10 and 20 µsec
Pulse off-time	:	38, 57 and 85 µsec

Considering the linear graph of L9 orthogonal array (Appendix – D) and in order to avoid interaction between parameters during subsequent experimentation, peak current was assigned to column 1 of the array, pulse on-time to column 2 and pulse off-time to column 3 of the array. Column 4 was left unassigned. The final control log for the experimentation is shown in Table 3.3. Each run was conducted three times at random.

Table 3.3 Control Log for experimentation - L9 orthogonal array (Taguchi Design)

Experiment Number	Column			
	Peak Current	**Pulse On-time**	**Pulse Off-time**	**4 (Unassigned)**
1	I1 (2 Amp)	$P_{on}1$ (5 µsec)	$P_{off}1$ (38 µsec)	-
2	I1 (2 Amp)	$P_{on}2$ (10 µsec)	$P_{off}2$ (57 µsec)	-
3	I1 (2 Amp)	$P_{on}3$ (20 µsec)	$P_{off}3$ (85 µsec)	-
4	I2 (4 Amp)	$P_{on}1$ (5 µsec)	$P_{off}2$ (57 µsec)	-
5	I2 (4 Amp)	$P_{on}2$ (10 µsec)	$P_{off}3$ (85 µsec)	-
6	I2 (4 Amp)	$P_{on}3$ (20 µsec)	$P_{off}1$ (38 µsec)	-
7	I3 (6 Amp)	$P_{on}1$ (5 µsec)	$P_{off}3$ (85 µsec)	-
8	I3 (6 Amp)	$P_{on}2$ (10 µsec)	$P_{off}1$ (38 µsec)	-
9	I3 (6 Amp)	$P_{on}3$ (20 µsec)	$P_{off}2$ (57 µsec)	-

3.4 EXPERIMENTATION WITH POWDER MIXED IN THE DIELECTRIC

For carrying out machining in powder-suspended dielectric, the following important points are to be kept in consideration:

- The powder should not enter the main dielectric tank and the filtering system.
- The machining in powder-suspended dielectric should be confined to a small volume so as to avoid wastage of powder.

- The dielectric should be continuously stirred to prevent settling of the powder.
- Proper conductivity at the tool electrode and workpiece interface must be maintained.

In view of these points, a specially designed tank was used for this stage of experimentation. A pictorial view of the tank is shown in Fig. 3.15.

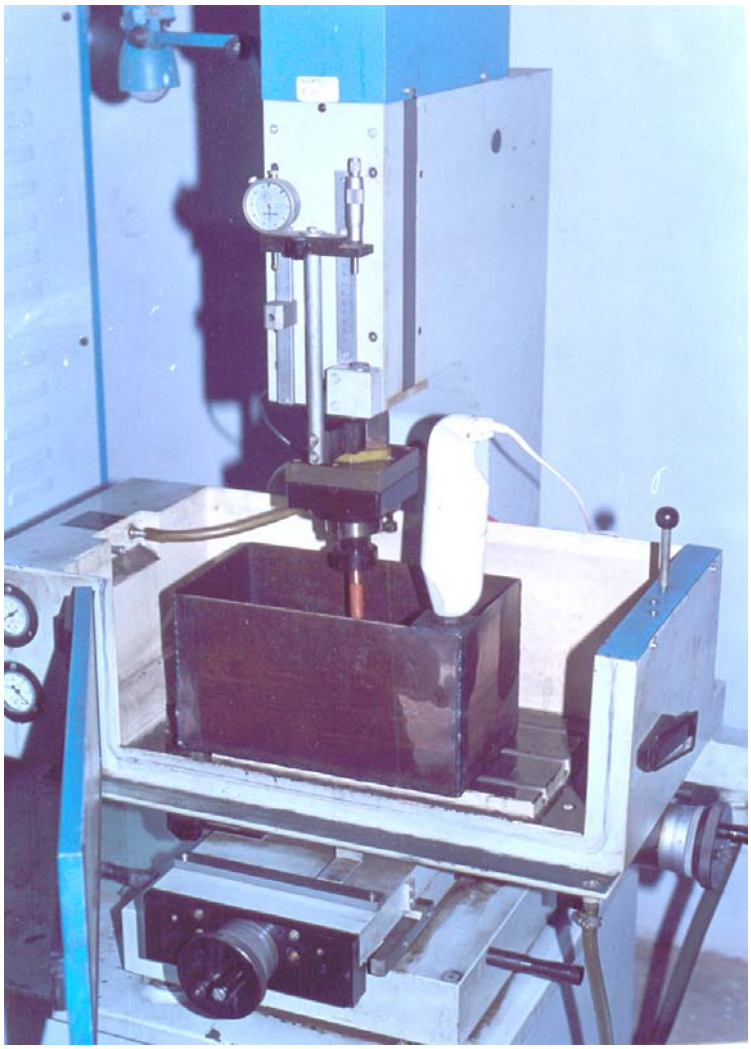

Fig. 3.15 Experimental set-up for machining with powder-mixed dielectric

The inside dimensions of the tank are 330 mm x 180 mm x 187 mm (length x breadth x height) and it was fabricated out of mild steel sheet (to ensure electrical conductivity) of thickness 1.6 mm. The critical dimension of the tank is its height which must be more than

the operating level of the dielectric in the main tank. Capacity of the tank is approximately 9 liters after deducting the volume of fixture and other accessories. This tank was filled by the dielectric flowing through the tool holder chuck that allowed mixing of the powder in a limited volume (9 liters) of the dielectric. A stirrer was provided in the tank for keeping the powder in suspension. On the completion of each cut, the powder-mixed dielectric was siphoned off into a separate container by using a rubber tube. After changing the work piece and machine setting, the tank was filled again with this powder-mixed dielectric. Since the machining time for each cut was only 10 minutes, very little consumption of the powder was expected during each cut. Because reverse polarity was used in machining which resulted in very low MRR, the accumulation of debris would also be negligible. Hence, it was decided to replace the powder after each set of nine experiments.

3.5 INSTRUMENTS USED FOR ANALYSIS

Micro-hardness and surface roughness tests were conducted on all the samples. The analysis of surface properties of selected samples was then performed by such methods as observing the microstructure under scanning electron microscope (SEM), by X-ray diffraction and by chemical composition analysis using an optical emission spectrophotometer. The details of these instruments are as under:

(a) Micro-hardness tests were done on Micro Hardness Tester, model HMV-2 of Shimadzu Corporation, Kyoto, Japan at Sant Longowal Institute of Engineering & Technology, Punjab using a load of 9.807 N for a duration time of 20 seconds. Though the displayed minimum unit of diagonal length in the instrument is 0.5 μm, the actual calculation of hardness is done on a unit of 0.01 μm. The output value is given in the form of both Vickers hardness as well as Rockwell hardness. For this experimentation, Vickers hardness number was used.

(b) Surface roughness tests were done on Perthometer, model M4Pi of Mahr, Germany available at Thapar University, Patiala. The equipment uses the stylus method of measurement, has a profile resolution of 12 nm and can measure a value of up to 100 μm. A tracing length of 4.8 mm and evaluation length of 4.0 mm were used for the tests.

(c) XRD analysis was done on X-Ray Diffractometer System, model ME210LA2 of Rigaku Corporation, Japan available at Thapar Centre for Industrial Research and Development, Patiala. The range of 2θ from 5^0 to 100^0 was used at a scan speed of 5^0/minute for each test.

(d) Chemical composition analysis was done on Optical Emission Spectrometer, model DV-6, make Baird, USA available at Institute for Autoparts Technology, Ludhiana. The equipment uses argon gas and is capable of detecting elements in iron-base, copper-base and aluminum-base materials to an accuracy of 0.0001%.

(e) Microstructure studies were done on Scanning Electron Microscope, model JSM-840A, make JEOL, Japan having the range of magnification from 10x to 3,00,000x. The equipment is available at Thapar Centre for Industrial Research and Development, Patiala and it is fitted with an Energy Dispersive Spectrometer (EDS), model TN-5500 of Tracor Northern make. EDS analysis of the samples during the pilot experimentation stage was carried out on this facility.

CHAPTER - 4

EXPERIMENTATION WITH DIFFERENT ELECTRODE MATERIALS

During the first stage of experimentation, four different electrode materials were used to machine the three workpiece materials. These four electrode materials were copper, graphite, copper-tungsten and Inconel alloy. A pictorial view of the four electrode materials is shown in Fig. 4.1. Before the start of experimentation, the chemical composition of workpieces and electrode materials was measured on an Optical Emission Spectrometer (model DV-6, make Baird, USA) and is given in Tables 4.1 and 4.2 respectively.

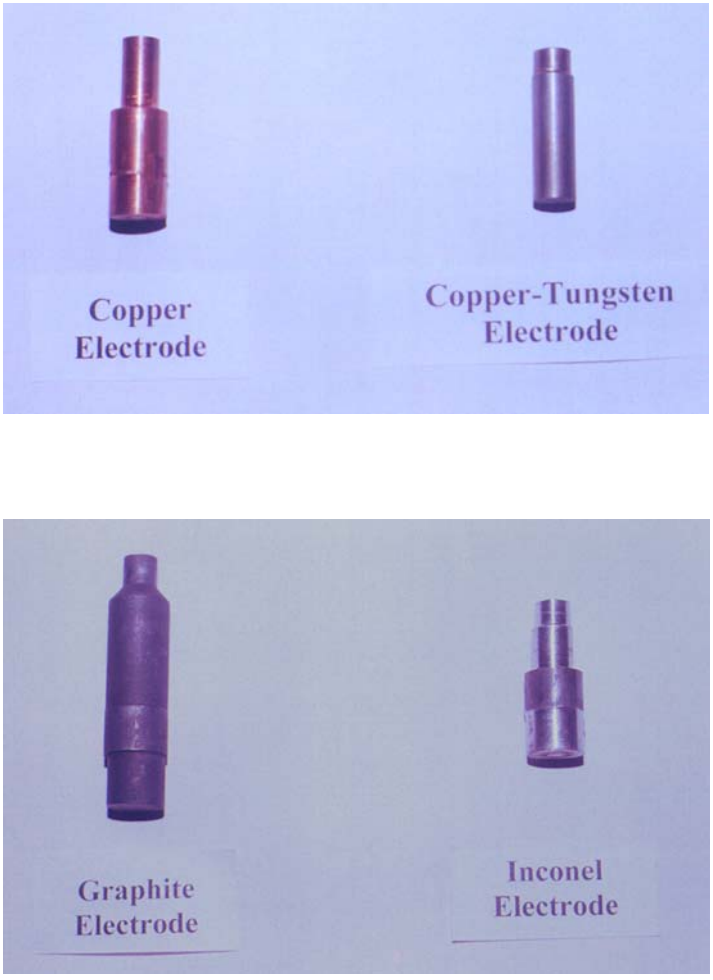

Fig. 4.1 Electrode materials used for experimentation

Table 4.1 Initial Chemical composition of the three work materials

Material Composition	O2 (OHNS)	D2 (HC-HCr)	H13 (Hot Die Steel)
% Carbon	0.82	1.57	0.44
% Silicon	0.18	0.19	1.04
% Manganese	0.52	0.07	0.28
% Chromium	0.49	12.38	5.39
% Molybdenum	0.13	0.761	0.934
% Vanadium	0.19	0.962	1.126
% Tungsten	-	-	-
% Nickel	0.05	0.09	0.19
% Cobalt	-	-	-
% Iron	Balance	Balance	Balance

Table 4.2 Initial Chemical composition of the four electrode materials

Electrode Material	Chemical Composition
Copper	99.77% Copper, 0.09% Zinc, 0.054% Nickel, 0.044% Lead, 0.018% Tin and 0.009% Aluminum.
Graphite	more than 99.9% purity
Copper-tungsten	70.46% Copper, 29.326% Tungsten, 0.121% Nickel, 0.047% Zinc, 0.026% Lead and 0.014% Tin.
Inconel alloy	74.69% Nickel, 15.75% Chromium, 9.03% Iron, 0.5% Manganese, 0.39% Silicon, 0.20% Aluminum, 0.11% Molybdenum and 0.04% Cobalt.

Before machining, the workpieces were subjected to the standard heat treatment cycles of hardening and tempering [17]. The hardening process consisted of pre-heating to a recommended temperature (650 ^{0}C for OHNS die steel and 815 ^{0}C for D2 and H13 die steels) and holding at this temperature for about 30 minutes. This was done to bring about uniformity in temperature to the core because die steels do not possess very good thermal conductivity. OHNS die steel was subsequently heated to a hardening temperature in the range of 760-800 ^{0}C with a holding time of about 20 minutes, followed by oil quenching in an oil bath maintained at 60 ^{0}C. D2 die steel was heated to a hardening temperature in the range of 980-1025 ^{0}C with a holding time of about 30 minutes, followed by quenching in still air. H13 die steel was heated to a hardening temperature in the range of 995-1040 ^{0}C with a holding time of about 30 minutes, followed by quenching in still air. The workpieces were tempered immediately after quenching in the range of 175 to 205 ^{0}C to remove internal stresses and bring about slight refinement in microstructure. Die steels are usually subjected to two cycles of tempering to remove stresses of hardening and to maximize the transformation of austenite to martensite. The surfaces of the workpieces were then ground on a surface grinder to remove surface impurities and minor scaling. Micro-hardness of the workpieces was measured at six different places and average values were noted which are given in Table 4.3.

Table 4.3 Micro-hardness of the three work materials before machining

Material	**O2 (OHNS)**	**D2 (HC-HCr)**	**H13**
Micro-hardness (Vickers Hardness Number, HV)	607	652	465

Machining of the workpieces was then carried out on Electric Discharge Machine model T – 3822M of Victory Electromech (India) available at Thapar University, Patiala. The set of nine experiments as per Taguchi L9 orthogonal array have been repeated three times for each combination of workpiece and electrode material. Negative polarity of the tool electrode and kerosene dielectric with side flushing was used for all the experiments. Time for each machining cut was fixed at 10 minutes. The input machining parameters and their levels used for experimentation are given in Table 4.4.

Table 4.4 Input process parameters and their levels

Parameters	Levels		
	L1	L2	L3
Peak Current (Amperes)	2	4	6
Pulse on-time (μsec)	5	10	20
Pulse off-time (μsec)	38	57	85

A total of 10 sets of experiments (with the exceptions that D2 high-carbon high-chromium work material was not machined using graphite and inconel electrodes as explained in Para 3.1.1) were conducted. The values of peak current, pulse on-time and pulse off-time for each experiment were set from the control panel of the machine according to the control log given in Table 3.3. The effect on the two response parameters of micro-hardness and surface roughness has been studied and presented in this chapter. For calculating S/N ratios, the criteria of "higher-the-better" for micro-hardness and "lower-the-better" for surface roughness as defined in the Taguchi method have been used. The experimental data has been analyzed to find out:

- Optimum values of input process parameters for each response characteristic and for each combination of workpiece and electrode material.
- The percentage contribution of each factor and its significance from ANOVA (Analysis of Variance) of the S/N data.
- The theoretical estimated values of response characteristics for the set of optimum parameters thus obtained.

The formulae used for the analysis are given in Appendix-E. After this, a set of three confirmation experiments were performed with the optimum parameters for each response charactersitic (where the suggested values did not constitute a row of the orthogonal array). The experimental results have been then compared with the theoretical estimated values.

4.1 MACHINING WITH COPPER ELECTRODE (EL1)

4.1.1 Work Material – OHNS die steel (W1)

The observed values of micro-hardness and surface roughness after machining OHNS die steel with copper electrode and calculated values of their S/N ratios are given in Table 4.5.

Table 4.5 Observed values of Micro-hardness and Surface roughness and their calculated S/N ratios (W1 – EL1)

Expt. No.	Micro-hardness (HV)			S/N Ratio (dB)	Surface Roughness (R_a in microns)			S/N Ratio (dB)
	R1	R2	R3		R1	R2	R3	
1	617	598	607	55.666	2.57	2.68	2.76	-8.534
2	595	582	572	55.310	2.63	2.71	2.75	-8.618
3	576	585	598	55.360	3.75	3.91	3.82	-11.658
4	653	658	662	56.360	2.93	3.12	2.98	-9.574
5	651	645	638	56.186	3.83	3.76	3.68	-11.497
6	598	611	623	55.712	5.17	5.28	5.05	-14.266
7	691	685	672	56.682	4.52	4.67	4.38	-13.112
8	608	620	633	55.849	5.37	5.53	5.58	-14.798
9	640	618	622	55.938	5.63	5.72	5.95	-15.221
Total	5629	5602	5627	503.063	36.40	37.38	36.95	-107.278
	$\overline{T}_{MH}$ = Overall mean of micro hardness = 624.37			Mean, m= 55.896	$\overline{T}_{SR}$ = Overall mean of surface roughness = 4.101			Mean, m= -11.9198
R1, R2 and R3 represent the three repetitions.								

From this data, the average values of micro-hardness and the corresponding S/N ratios for the three levels of peak current, pulse on-time and pulse off-time have been calculated and are given in Table 4.6. These average values represent the factor effects of input parameters.

Table 4.6 Average values by factor levels for Micro-hardness (W1 – EL1)

Parameter / Levels	Peak Current (amperes)		Pulse on-time (µsec)		Pulse off-time (µsec)	
	Raw Data	S/N Data	Raw Data	S/N Data	Raw Data	S/N Data
L1	592.22	55.445	649.22	56.236	612.78	55.743
L2	637.67	56.086	616.00	55.782	622.44	55.869
L3	643.22	56.156	607.89	55.670	637.89	56.076

These factor effects have been plotted and presented in Fig. 4.2 (a), (b) and (c).

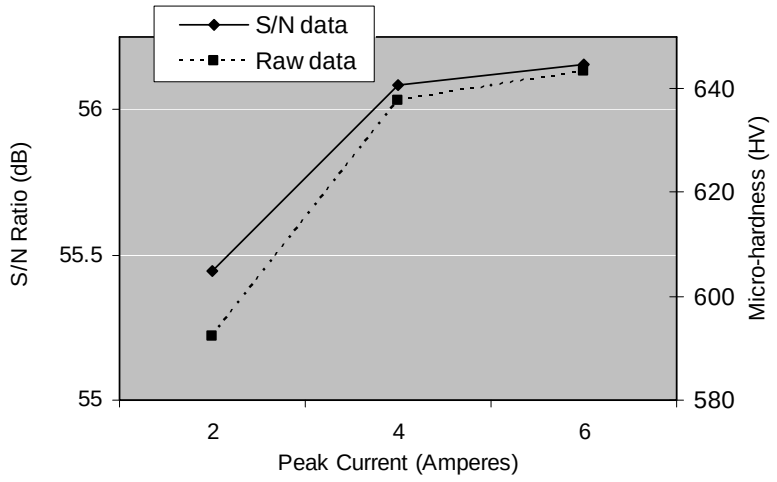

Fig. 4.2 (a) Effect of Peak Current on Micro-hardness and its S/N ratio (W1 – EL1)

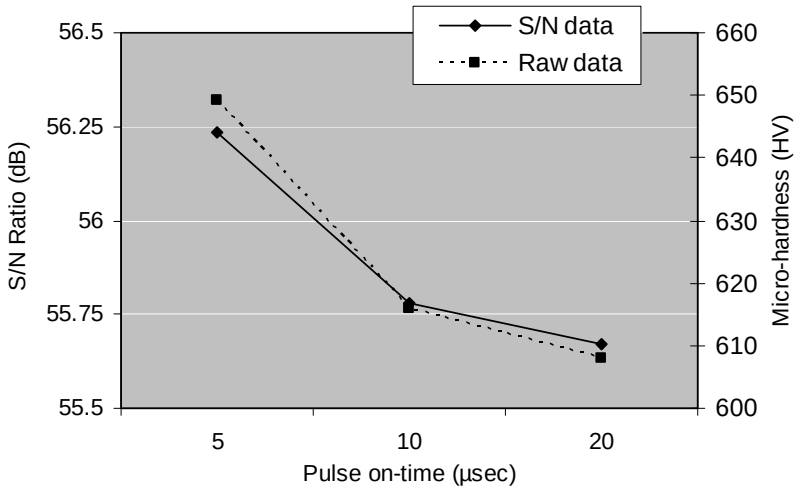

Fig. 4.2 (b) Effect of Pulse on-time on Micro-hardness and its S/N ratio (W1 – EL1)

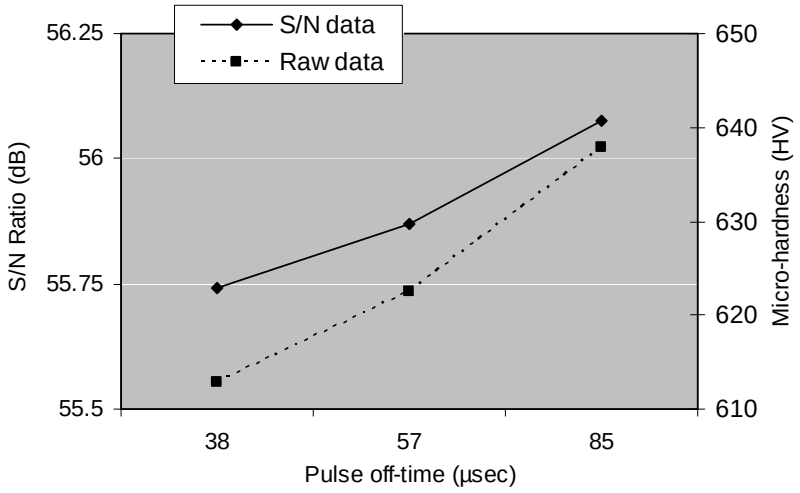

Fig. 4.2 (c) Effect of Pulse off-time on Micro-hardness and its S/N ratio (W1 – EL1)

Micro-hardness is the 'higher-the-better' type of response characteristic. Therefore, higher values of micro-hardness are considered to be optimal. It can be observed from Fig. 4.2 (a), (b) and (c) that the third level of peak current (A_3), first level of pulse on-time (B_1) and the third level of pulse off-time (C_3) give the highest values of micro-hardness. Hence, the optimum condition of input process parameters is $A_3B_1C_3$. Since this combination existed in the orthogonal array (as seventh row), a confirmation experiment was not required. The average value of micro-hardness obtained at this setting of the experiment was 682.67 HV which can be compared with the theoretical value predicted by Taguchi analysis. The theoretical value of η under the optimum conditions, denoted by η_{opt}, is given by:

$$\eta_{opt} = m + (m_{A3} - m) + (m_{B1} - m) + (m_{C3} - m) = 56.677$$

where m is the overall mean of S/N data, m_{A3} is the mean of S/N data for factor A at level 3 and m_{B1} is the mean of S/N data for factor B at level 1, etc.

The corresponding value of micro-hardness is given by

$$y_{opt}^2 = 1 / 10^{-\eta opt / 10}$$

or, y_{opt} = 682.08 HV which is very close to the observed experimental value.

To obtain percentage contribution of the three factors and their significance, analysis of variance (ANOVA) of the S/N data was performed. It is presented in Table 4.7 which shows that all the three factors; namely peak current, pulse on-time and pulse off-time; are significant for the response characteristic of micro-hardness (a factor is significant if the

calculated F-ratio for that factor is more than the tabulated F-ratio). Peak current is the most significant factor with 56.19% contribution followed by pulse on-time and pulse off-time.

Table 4.7 ANOVA Table of S/N data for Micro-hardness (W1 – EL1)

Factor/Source	Sum of Squares	DOF	V	F-ratio	% Contri-bution	Remarks
Peak Current	0.9208	2	0.4604	110.67	56.19	Significant
Pulse on-time	0.5397	2	0.2698	64.86	32.93	Significant
Pulse off-time	0.1700	2	0.0850	20.43	10.37	Significant
Error (Pooled)	0.0083	2	0.0042	-	0.51	-
Total	1.6388	8		-	100	
DOF = Degrees of Freedom, V = Variance, Tabulated F-ratio $_{0.05}$ (2, 2) = 19						

Similar analysis has now been done for surface roughness which is "lower-the-better" type of response characteristic. Therefore, lower values of surface roughness are considered to be optimal. From the experimental data given in Table 4.5, the average values of surface roughness and the corresponding S/N ratios for the three levels of peak current, pulse on-time and pulse off-time have been calculated and are given in Table 4.8. These average values represent the factor effects of input parameters.

Table 4.8 Average values by factor levels for Surface Roughness (W1 – EL1)

Parameter / Levels	Peak Current (Amperes)		Pulse on-time (µsec)		Pulse off-time (µsec)	
	Raw Data	S/N Data	Raw Data	S/N Data	Raw Data	S/N Data
L1	3.06	-9.603	3.40	-10.407	4.44	-12.533
L2	3.98	-11.779	3.98	-11.638	3.82	-11.138
L3	5.26	-14.377	4.92	-13.715	4.04	-12.089

These factor effects have been plotted and presented in Fig. 4.3 (a), (b) and (c).

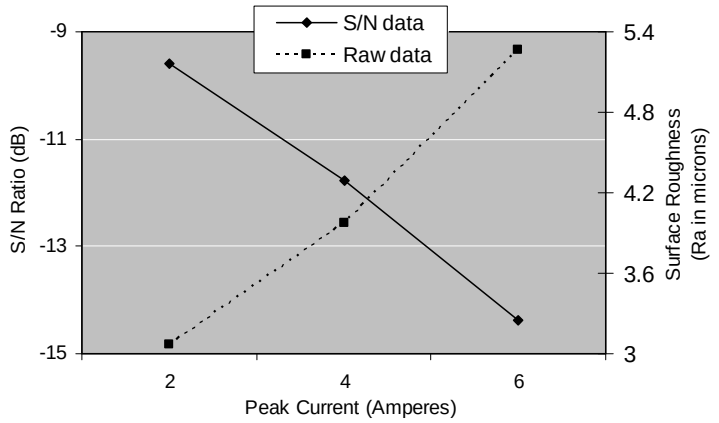

Fig. 4.3 (a) Effect of Peak Current on Surface Roughness and its S/N ratio (W1 – EL1)

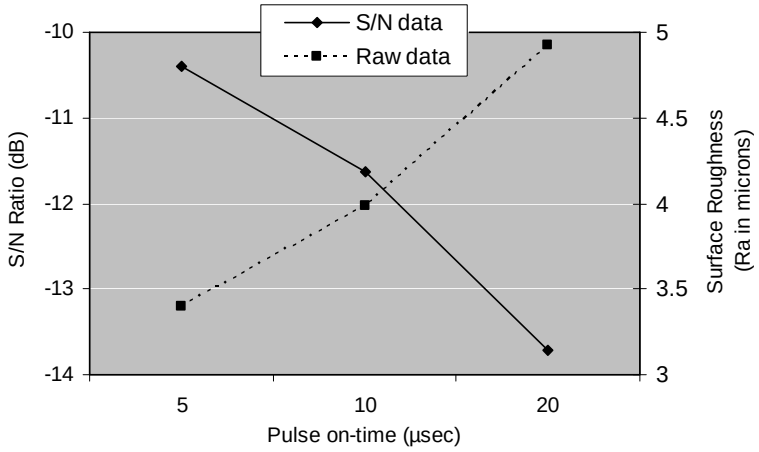

Fig. 4.3 (b) Effect of Pulse on-time on Surface Roughness and its S/N ratio (W1 – EL1)

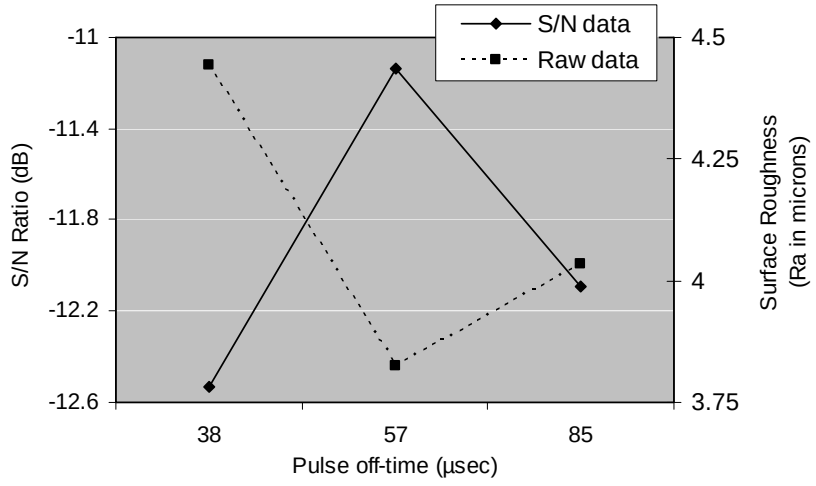

Fig. 4.3 (c) Effect of Pulse off-time on Surface Roughness and its S/N ratio (W1 – EL1)

It is observed from Fig. 4.3 (a), (b) and (c) that the first level of peak current (A_1), first level of pulse on-time (B_1) and the second level of pulse off-time (C_2) give the lowest values of surface roughness. Hence, the optimum condition of input process parameters is $A_1B_1C_2$. The theoretical value of η_{opt} under the optimum conditions is given by:

$$\eta_{opt} = m + (m_{A1} - m) + (m_{B1} - m) + (m_{C2} - m) = -7.3082$$

where m is the overall mean of S/N data, m_{A1} is the mean of S/N data for factor A at level 1 and m_{B1} is the mean of S/N data for factor B at level 1, etc.

The corresponding value of surface roughness is given by

$$y_{opt}^2 = 10^{-\eta opt / 10} \qquad \text{or,} \qquad y_{opt} = 2.32\ \mu m$$

Since this combination of input process parameters did not exist in the orthogonal array, a set of three confirmation experiments were conducted. The average value of surface roughness obtained at this setting of the experiment was 2.46 μm which is very close to the theoretical value predicted by Taguchi analysis.

Analysis of variance (ANOVA) of the S/N data was performed to obtain the percentage contribution of the factors and their significance. It is presented in Table 4.9 which shows that all the three factors; namely peak current, pulse on-time and pulse off-time; are significant for the response characteristic of surface roughness. Peak current emerges as the most significant factor with 63.21 % contribution.

Table 4.9 ANOVA Table of S/N data for Surface Roughness (W1 – EL1)

Factor/Source	**Sum of Squares**	**DOF**	**V**	**F-ratio**	**% Contri-bution**	**Remarks**
Peak Current	34.2721	2	17.1361	265.97	63.21	Significant
Pulse on-time	16.7713	2	8.3856	130.15	30.93	Significant
Pulse off-time	3.0467	2	1.5233	23.64	5.62	Significant
Error (Pooled)	0.1289	2	0.0645	-	0.24	-
Total	54.2190	8		-	100	
DOF = Degrees of Freedom, V = Variance, Tabulated F-ratio $_{0.05}(2, 2) = 19$						

4.1.2 Work Material – D2 High-carbon High-chromium die steel (W2)

The observed values of micro-hardness and surface roughness after machining D2 die steel with copper electrode and calculated values of their S/N ratios are given in Table 4.10.

Table 4.10 Observed values of Micro-hardness and Surface roughness and their calculated S/N ratios (W2 – EL1)

Expt. No.	Micro-hardness (HV)			S/N Ratio (dB)	Surface Roughness (R_a in microns)			S/N Ratio (dB)
	R1	R2	R3		R1	R2	R3	
1	627	648	641	56.103	3.65	3.46	3.51	-10.982
2	676	691	665	56.613	4.03	3.81	3.95	-11.890
3	642	662	651	56.278	4.36	4.52	4.67	-13.100
4	683	668	671	56.572	3.94	3.62	3.68	-11.479
5	711	737	703	57.105	4.65	4.41	4.58	-13.156
6	642	635	658	56.188	4.53	4.75	4.61	-13.313
7	738	747	725	57.343	5.04	5.12	4.86	-13.993
8	731	718	723	57.194	5.71	5.33	5.48	-14.821
9	715	697	711	56.995	5.43	5.58	5.62	-14.876
Total	6165	6203	6148	510.3923	41.34	40.6	40.96	-117.611
	$\overline{T}_{MH}$ = Overall mean of micro hardness = 685.78			Mean, m= 56.7103	$\overline{T}_{SR}$ = Overall mean of surface roughness = 4.552			Mean, m= -13.0679

From this data, the average values of micro-hardness and the corresponding S/N ratios for the three levels of peak current, pulse on-time and pulse off-time have been calculated and are given in Table 4.11. These average values represent the factor effects of input parameters.

Table 4.11 Average values by factor levels for Micro-hardness (W2 – EL1)

Parameter / Levels	Peak Current (amperes)		Pulse on-time (µsec)		Pulse off-time (µsec)	
	Raw Data	S/N Data	Raw Data	S/N Data	Raw Data	S/N Data
L1	655.89	56.331	683.11	56.673	669.22	56.495
L2	678.67	56.622	706.11	56.971	686.33	56.727
L3	722.78	57.178	668.11	56.487	701.78	56.909

These factor effects have been plotted and presented in Fig. 4.4 (a), (b) and (c).

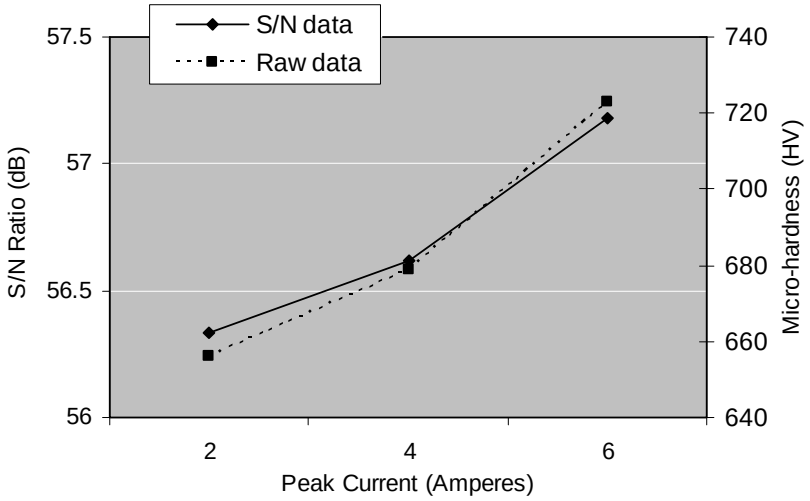

Fig. 4.4 (a) Effect of Peak Current on Micro-hardness and its S/N ratio (W2 – EL1)

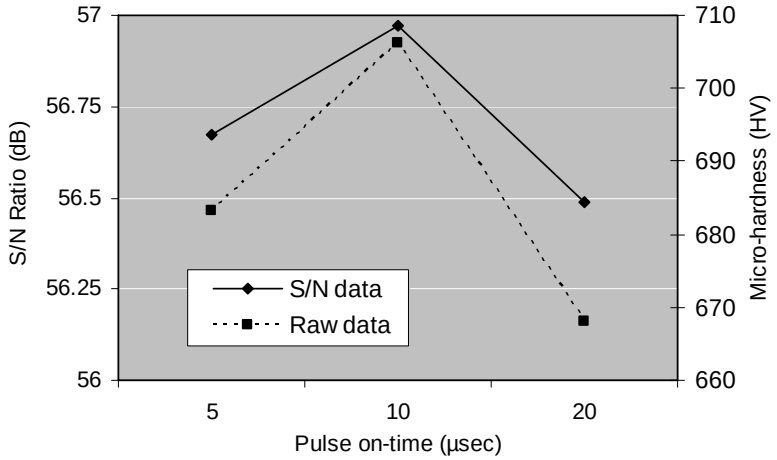

Fig. 4.4 (b) Effect of Pulse on-time on Micro-hardness and its S/N ratio (W2 – EL1)

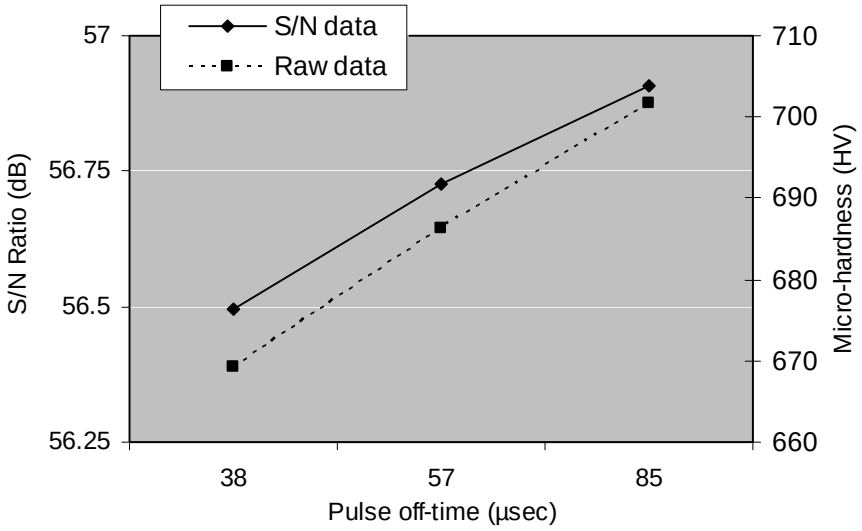

Fig. 4.4 (c) Effect of Pulse off-time on Micro-hardness and its S/N ratio (W2 – EL1)

It is observed from Fig. 4.4 (a), (b) and (c) that micro-hardness increases steadily with increase in peak current and pulse off-time but when pulse on-time changes from level 1 to 2, it increases sharply and then shows a decline. This is contrary to the response of the other two materials where the best value of micro-hardness is achieved at level 1 of pulse on-time. It is also observed that the third level of peak current (A_3), second level of pulse on-time (B_2) and the third level of pulse off-time (C_3) give the highest values of micro-hardness. Hence, the optimum combination of input process parameters is $A_3B_2C_3$. The theoretical value of η_{opt} under this optimum combination is given by:

$$\eta_{opt} = m + (m_{A3} - m) + (m_{B2} - m) + (m_{C3} - m) = 57.6394$$

The corresponding value of micro-hardness is given by

$$y_{opt}^2 = 1 / 10^{-\eta opt / 10}$$

or, $$y_{opt} = 762.03 \text{ HV}$$

Since this combination of input process parameters did not exist in the orthogonal array, a set of three confirmation experiments were conducted using the optimum values of the input parameters. The average value of micro hardness obtained at this setting of the experiment was 749.33 HV which is very close to the theoretical value predicted by Taguchi analysis.

To obtain percentage contribution of the three factors and their significance, analysis of variance (ANOVA) of the S/N data was performed. It is presented in Table 4.12 which

shows that all the three factors; namely peak current, pulse on-time and pulse off-time; are significant for the response characteristic of micro-hardness. Peak current is the most significant factor with 64.16% contribution followed by pulse on-time and pulse off-time. Compared to OHNS dies steel, percentage contribution of pulse off-time for this material is higher. It is important to note that error contribution is less than 1 %.

Table 4.12 ANOVA Table of S/N data for Micro-hardness (W2 – EL1)

Factor/Source	Sum of Squares	DOF	V	F-ratio	% Contri-bution	Remarks
Peak Current	1.1089	2	0.5545	258.48	64.16	Significant
Pulse on-time	0.3568	2	0.1784	83.17	20.65	Significant
Pulse off-time	0.2581	2	0.1291	60.17	14.94	Significant
Error (Pooled)	0.0044	2	0.0022	-	0.25	-
Total	1.7282	8		-	100	
DOF = Degrees of Freedom, V = Variance, Tabulated F-ratio $_{0.05}$ (2, 2) = 19						

Similar analysis has now been done for surface roughness. From the experimental data given in Table 4.10, the average values of surface roughness and the corresponding S/N ratios for the three levels of peak current, pulse on-time and pulse off-time have been calculated and are given in Table 4.13. These average values represent the factor effects of input parameters.

Table 4.13 Average values by factor levels for Surface Roughness (W2 – EL1)

Parameter Levels	Peak Current (Amperes)		Pulse on-time (µsec)		Pulse off-time (µsec)	
	Raw Data	S/N Data	Raw Data	S/N Data	Raw Data	S/N Data
L1	4.00	-11.991	4.10	-12.151	4.556	-13.039
L2	4.301	-12.649	4.66	-13.289	4.401	-12.749
L3	5.35	-14.564	4.90	-13.763	4.69	-13.416

These factor effects have been plotted and presented in Fig. 4.5 (a), (b) and (c).

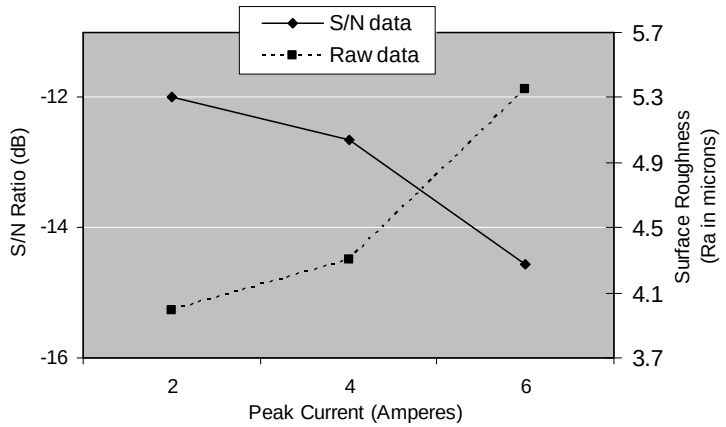

Fig. 4.5 (a) Effect of Peak Current on Surface Roughness and its S/N ratio (W2 – EL1)

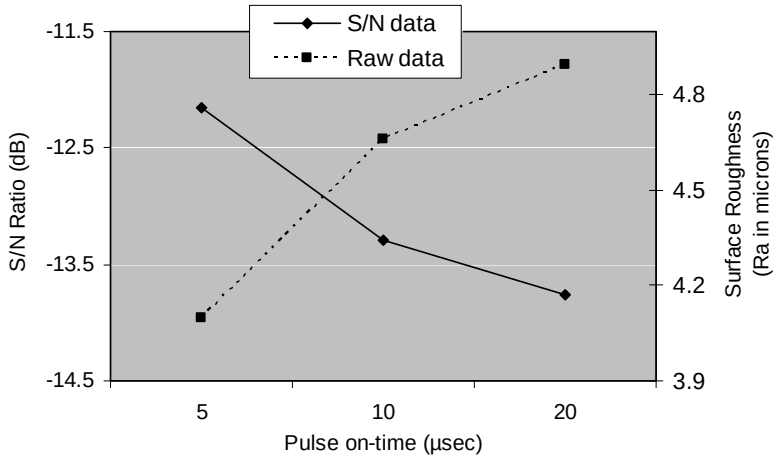

Fig. 4.5 (b) Effect of Pulse on-time on Surface Roughness and its S/N ratio (W2 – EL1)

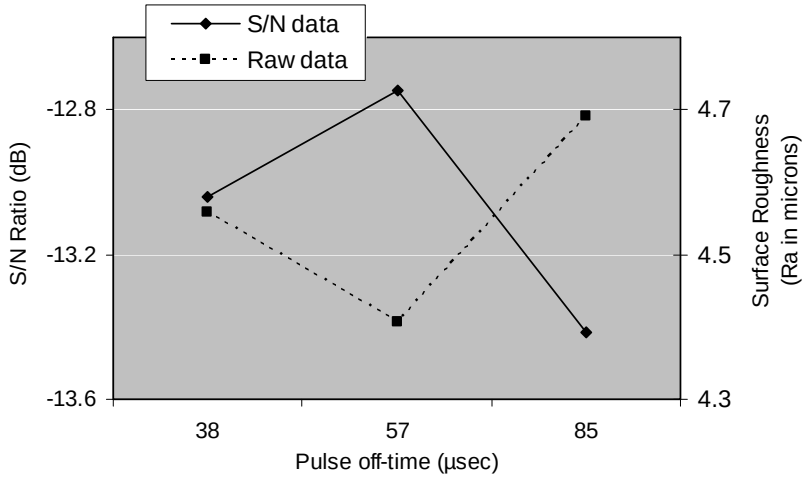

Fig. 4.5 (c) Effect of Pulse off-time on Surface Roughness and its S/N ratio (W2 – EL1)

Surface roughness is "lower-the-better" type of response characteristic. Therefore, lower values of surface roughness are considered to be optimal. It is observed from Fig. 4.5 (a), (b) and (c) that first level of peak current (A_1), first level of pulse on-time (B_1) and the second level of pulse off-time (C_2) give the lowest values of surface roughness. Hence, the optimum condition of input process parameters is $A_1B_1C_2$. The theoretical value of η_{opt} at the optimum condition is given by:

$$\eta_{opt} = m + (m_{A1} - m) + (m_{B1} - m) + (m_{C2} - m) = -10.755$$

The corresponding value of surface roughness is given by

$$y_{opt}^2 = 10^{-\eta opt / 10}$$

or, $$y_{opt} = 3.45\ \mu m$$

Since this combination of input process parameters did not exist in the orthogonal array, a set of three confirmation experiments were conducted. The average value of surface roughness obtained at this setting of the experiment was 3.54 μm which is very close to the theoretical value predicted by Taguchi analysis.

Analysis of variance (ANOVA) of the S/N data was performed to obtain the percentage contribution of the factors and their significance. It is presented in Table 4.14 which shows that all the three factors are significant for the response characteristic of surface roughness. Peak current again emerges as the most significant factor with 69 % contribution.

Table 4.14 ANOVA Table of S/N data for Surface Roughness (W2 – EL1)

Factor/Source	**Sum of Squares**	**DOF**	**V**	**F-ratio**	**% Contri-bution**	**Remarks**
Peak Current	10.7172	2	5.3586	432.82	69.00	Significant
Pulse on-time	4.1169	2	2.0584	166.26	26.51	Significant
Pulse off-time	0.6727	2	0.3363	27.17	4.33	Significant
Error (Pooled)	0.0247	2	0.0124	-	0.16	-
Total	15.5315	8		-	100	
DOF = Degrees of Freedom, V = Variance, Tabulated F-ratio $_{0.05}$ (2, 2) = 19						

4.1.3 Work Material – H13 hot die steel (W3)

The observed values of micro-hardness and surface roughness after machining H13 hot die steel with copper electrode and calculated values of their S/N ratios are given in Table 4.15.

Table 4.15 Observed values of Micro-hardness and Surface roughness and their calculated S/N ratios (W3 – EL1)

Expt. No.	Micro-hardness (HV)			S/N Ratio (dB)	Surface Roughness (R_a in microns)			S/N Ratio (dB)
	R1	R2	R3		R1	R2	R3	
1	465	471	476	53.453	3.12	2.98	3.19	-9.821
2	482	473	467	53.513	3.27	3.21	3.36	-10.319
3	442	451	455	53.049	3.51	3.63	3.58	-11.062
4	529	538	542	54.587	3.23	3.39	3.28	-10.372
5	522	547	535	54.557	3.81	3.63	3.95	-11.593
6	476	487	465	53.548	4.11	3.85	3.97	-11.994
7	591	585	572	55.306	4.08	4.19	4.25	-12.411
8	547	554	561	54.869	4.62	4.53	4.47	-13.142
9	528	542	535	54.566	4.41	4.38	4.58	-12.982
Total	4582	4648	4608	487.448	34.16	33.79	34.63	-103.696
	$\overline{T}_{MH}$ = Overall mean of micro hardness = 512.52			Mean, m= 54.161	$\overline{T}_{SR}$ = Overall mean of surface roughness = 3.799			Mean, m= -11.522
R1, R2 and R3 represent the three repetitions.								

From this data, the average values of micro-hardness and the corresponding S/N ratios for the three levels of peak current, pulse on-time and pulse off-time have been calculated and are given in Table 4.16. These average values represent the factor effects of input parameters.

Table 4.16 Average values by factor levels for Micro-hardness (W3 – EL1)

Parameter / Levels	Peak Current (amperes)		Pulse on-time (µsec)		Pulse off-time (µsec)	
	Raw Data	S/N Data	Raw Data	S/N Data	Raw Data	S/N Data
L1	464.67	53.339	529.89	54.449	500.22	53.956
L2	515.67	54.231	520.89	54.313	515.11	54.222
L3	557.22	54.913	486.78	53.721	522.22	54.304

These factor effects have been plotted and presented in Fig. 4.6 (a), (b) and (c).

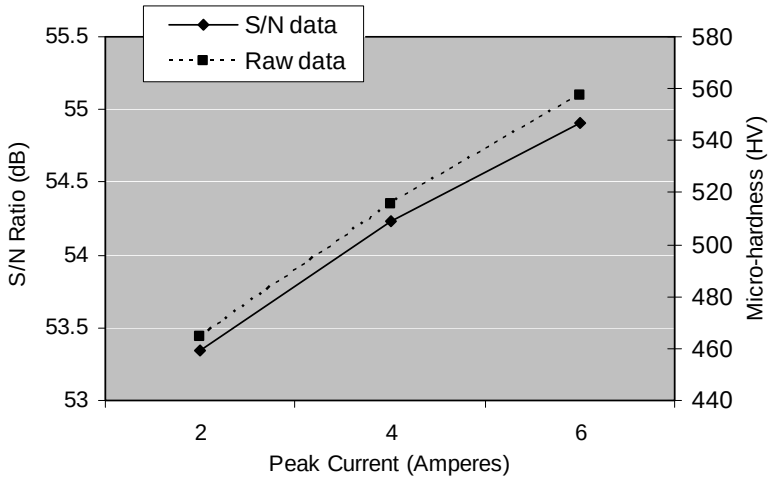

Fig. 4.6 (a) Effect of Peak Current on Micro-hardness and its S/N ratio (W3 – EL1)

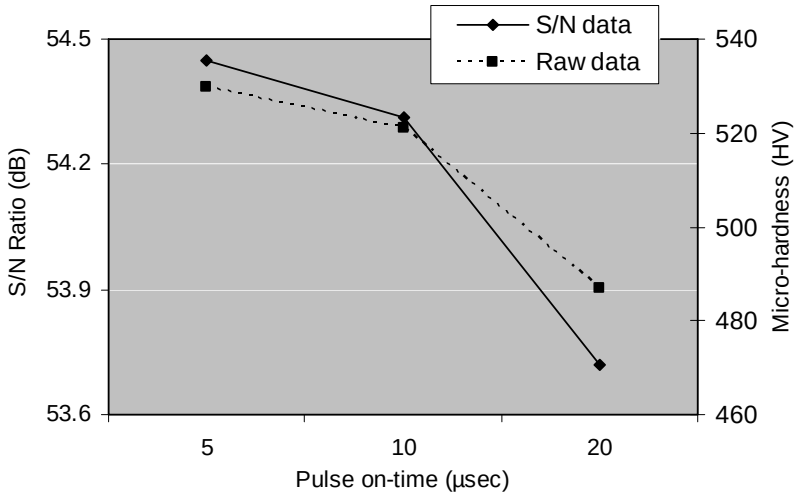

Fig. 4.6 (b) Effect of Pulse on-time on Micro-hardness and its S/N ratio (W3 – EL1)

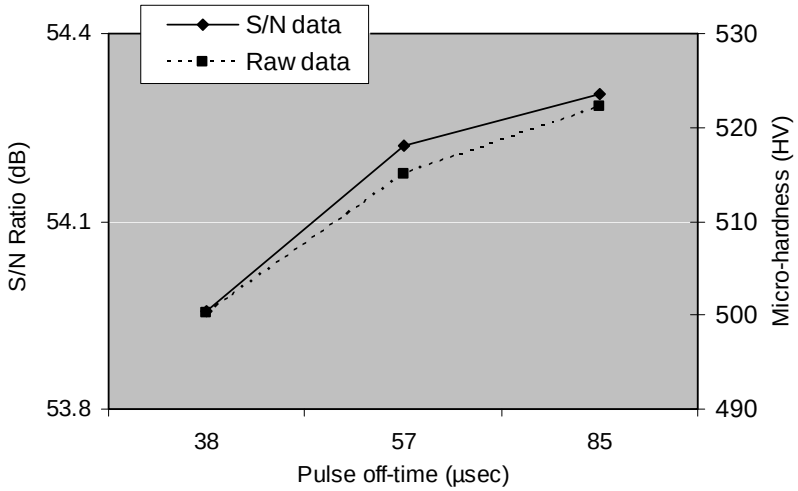

Fig. 4.6 (c) Effect of Pulse off-time on Micro-hardness and its S/N ratio (W3 – EL1)

It is observed from Fig. 4.6 (a), (b) and (c) that there is a steady increase in micro-hardness with increase in peak current and pulse off-time but it decreases with increase in pulse on-time. This response is similar to the response of OHNS die steel for this electrode material. At low values of pulse on-time, electrode wear is high and the ferrite phase is getting strengthened by the induction of copper atoms which form a solid solution with iron. It can also be observed that the third level of peak current (A_3), first level of pulse on-time (B_1) and third level of pulse off-time (C_3) give the highest values of micro-hardness. Hence, the optimum condition of input process parameters is $A_3B_1C_3$. Since this combination exists in the orthogonal array (as seventh row), a confirmation experiment is not required. The average value of micro-hardness obtained at this setting of the experiment is 582.67 HV which can be compared with the theoretical value predicted by Taguchi analysis. The theoretical value of η under the optimum conditions, denoted by η_{opt}, is given by:

$$\eta_{opt} = m + (m_{A3} - m) + (m_{B1} - m) + (m_{C3} - m) = 55.34$$

The corresponding value of micro-hardness is given by

$$y_{opt}^2 = 1 / 10^{-\eta opt / 10}$$

or, $$y_{opt} = 584.66 \text{ HV}$$

which is very close to the observed experimental value.

To obtain percentage contribution of the three factors and their significance, analysis of variance (ANOVA) of the S/N data was performed. It is presented in Table 4.17 which

shows that all the three factors are significant for the response characteristic of micro-hardness. Peak current is the most significant factor with 77.21 % contribution followed by pulse on-time and pulse off-time.

Table 4.17 ANOVA Table of S/N data for Micro-hardness (W3 – EL1)

Factor/Source	Sum of Squares	DOF	V	F-ratio	% Contri-bution	Remarks
Peak Current	3.7420	2	1.8710	497.32	77.21	Significant
Pulse on-time	0.8990	2	0.4495	119.48	18.55	Significant
Pulse off-time	0.1981	2	0.0991	26.33	4.09	Significant
Error (Pooled)	0.0075	2	0.0037	-	0.15	-
Total	4.8466	8		-	100	
DOF = Degrees of Freedom, V = Variance, Tabulated F-ratio $_{0.05}$ (2, 2) = 19						

Similar analysis has now been done for surface roughness which is "lower-the-better" type of response characteristic. Therefore, lower values of surface roughness are considered to be optimal. From the experimental data given in Table 4.15, the average values of surface roughness and the corresponding S/N ratios for the three levels of peak current, pulse on-time and pulse off-time have been calculated and are given in Table 4.18. These average values represent the factor effects of input parameters.

Table 4.18 Average values by factor levels for Surface Roughness (W3 – EL1)

Parameter / Levels	Peak Current (Amperes)		Pulse on-time (µsec)		Pulse off-time (µsec)	
	Raw Data	S/N Data	Raw Data	S/N Data	Raw Data	S/N Data
L1	3.32	-10.401	3.52	-10.868	3.87	-11.652
L2	3.69	-11.320	3.87	-11.685	3.68	-11.224
L3	4.39	-12.845	4.00	-12.013	3.85	-11.689

These factor effects have been plotted and presented in Fig. 4.7 (a), (b) and (c).

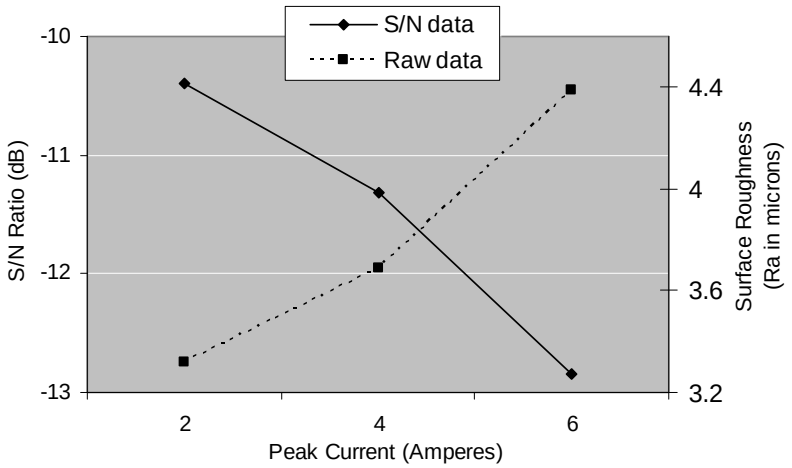

Fig. 4.7 (a) Effect of Peak Current on Surface Roughness and its S/N ratio (W3 – EL1)

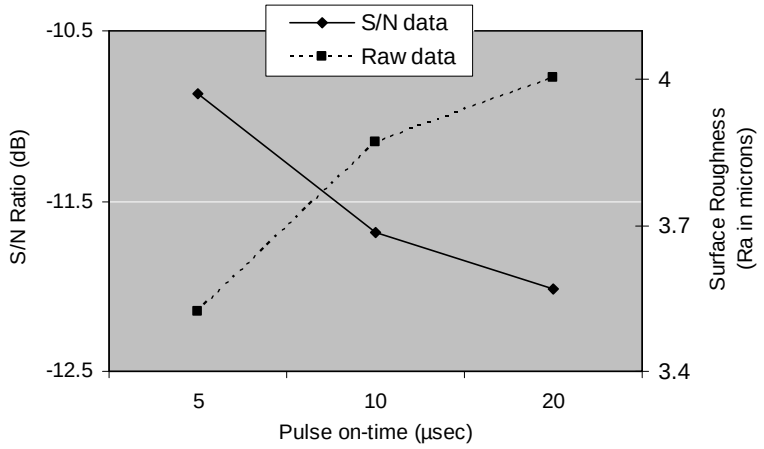

Fig. 4.7 (b) Effect of Pulse on-time on Surface Roughness and its S/N ratio (W3 – EL1)

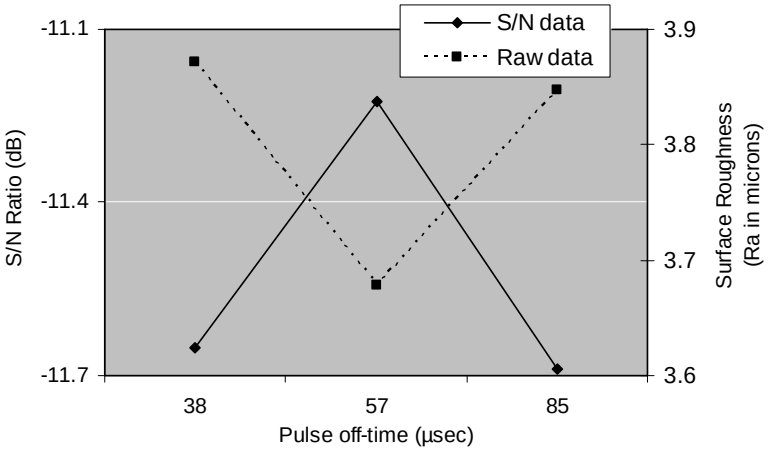

Fig. 4.7 (c) Effect of Pulse off-time on Surface Roughness and its S/N ratio (W3 – EL1)

It is observed from Fig. 4.7 (a), (b) and (c) that the first level of peak current (A_1), first level of pulse on-time (B_1) and the second level of pulse off-time (C_2) give the lowest values of surface roughness. Hence, the optimum combination of input process parameters is $A_1B_1C_2$. It is found to be the same for all the three work materials. The theoretical value of η_{opt} under this optimum combination is given by:

$$\eta_{opt} = m + (m_{A1} - m) + (m_{B1} - m) + (m_{C2} - m) = -9.450$$

The corresponding value of surface roughness is given by

$$y_{opt}^2 = 10^{-\eta opt / 10}$$

or, $$y_{opt} = 2.97\ \mu m$$

Since this combination of input process parameters did not exist in the orthogonal array, a set of three confirmation experiments were conducted. The average value of surface roughness obtained at this setting of the experiment was 3.05 μm which is very close to the theoretical value predicted by Taguchi analysis.

Analysis of variance (ANOVA) of the S/N data is performed to obtain the percentage contribution of the factors and their significance. It is presented in Table 4.19 which shows that all the three factors are significant for the response characteristic of surface roughness. Though pulse off-time is significant, its contribution is found to be only 3.44 %.

Table 4.19 ANOVA Table of S/N data for Surface Roughness (W3 – EL1)

Factor/Source	**Sum of Squares**	**DOF**	**V**	**F-ratio**	**% Contri-bution**	**Remarks**
Peak Current	9.1439	2	4.5719	511.57	78.51	Significant
Pulse on-time	2.0841	2	1.0420	116.60	17.90	Significant
Pulse off-time	0.4002	2	0.2001	22.39	3.44	Significant
Error (Pooled)	0.0179	2	0.0089	-	0.15	-
Total	11.6461	8		-	100	
DOF = Degrees of Freedom, V = Variance, Tabulated F-ratio $_{0.05}$ (2, 2) = 19						

4.2 MACHINING WITH GRAPHITE ELECTRODE (EL2)

4.2.1 Work Material – OHNS die steel (W1)

The observed values of micro-hardness and surface roughness after machining OHNS die steel with graphite electrode and calculated values of their S/N ratios are given in Table 4.20.

Table 4.20 Observed values of Micro-hardness and Surface roughness and their calculated S/N ratios (W1 – EL2)

Expt. No.	Micro-hardness (HV)			S/N Ratio (dB)	Surface Roughness (R_a in microns)			S/N Ratio (dB)
	R1	R2	R3		R1	R2	R3	
1	607	610	591	55.599	1.89	1.78	1.93	-5.426
2	587	598	574	55.359	1.72	1.98	1.65	-5.052
3	592	602	598	55.524	2.31	2.26	2.42	-7.351
4	665	658	679	56.485	2.12	2.08	2.31	-6.738
5	656	642	635	56.180	2.89	3.02	2.77	-9.233
6	638	646	627	56.081	3.95	3.87	4.12	-12.001
7	675	692	684	56.696	3.98	3.78	3.83	-11.741
8	651	625	639	56.097	4.85	5.11	4.80	-13.843
9	653	666	658	56.377	4.52	4.38	4.64	-13.092
Total	5724	5739	5685	504.397	28.23	28.26	28.47	-84.478
	$\overline{T}_{MH}$ = Overall mean of micro hardness = 635.11			Mean, m= 56.044	$\overline{T}_{SR}$ = Overall mean of surface roughness = 3.147			Mean, m= -9.386
R1, R2 and R3 represent the three repetitions.								

From this data, the average values of micro-hardness and the corresponding S/N ratios for the three levels of peak current, pulse on-time and pulse off-time have been calculated and are given in Table 4.21.

Table 4.21 Average values by factor levels for Micro-hardness (W1 – EL2)

Parameter / Levels	Peak Current (amperes)		Pulse on-time (µsec)		Pulse off-time (µsec)	
	Raw Data	S/N Data	Raw Data	S/N Data	Raw Data	S/N Data
L1	595.44	55.494	651.22	56.260	626.00	55.926
L2	649.56	56.248	623.00	55.879	637.56	56.074
L3	660.33	56.390	631.11	55.994	641.78	56.133

These factor effects have been plotted and presented in Fig. 4.8 (a), (b) and (c).

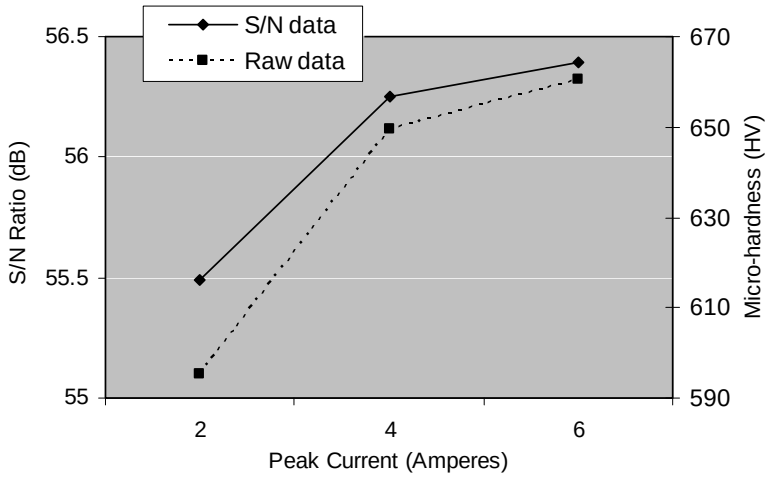

Fig. 4.8 (a) Effect of Peak Current on Micro-hardness and its S/N ratio (W1 – EL2)

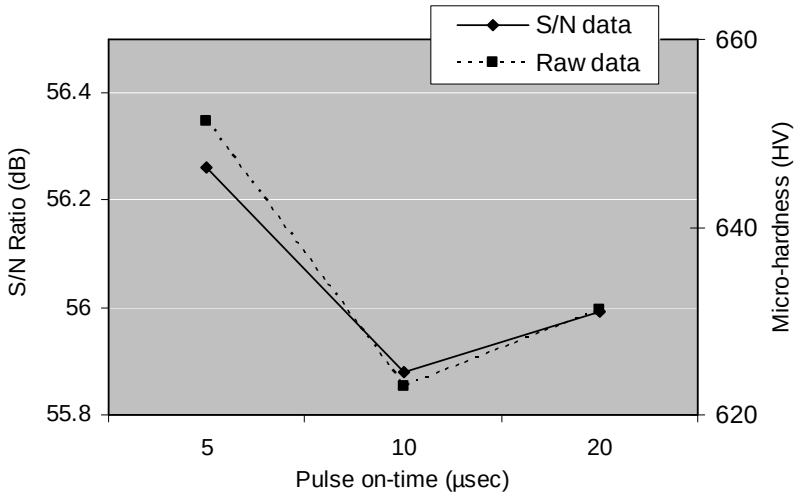

Fig. 4.8 (b) Effect of Pulse on-time on Micro-hardness and its S/N ratio (W1 – EL2)

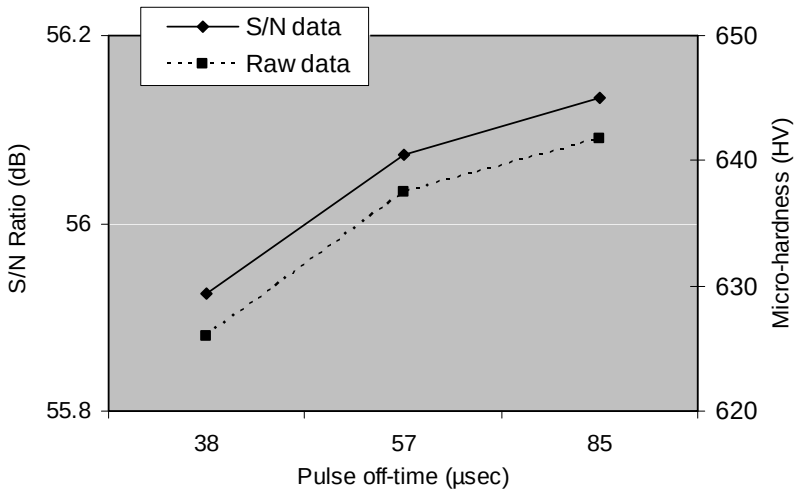

Fig. 4.8 (c) Effect of Pulse off-time on Micro-hardness and its S/N ratio (W1 – EL2)

It is observed from Fig. 4.8 (a), (b) and (c) that micro-hardness increases with increase in peak current and pulse off-time but the improvement is very less when these parameters change from level 2 to level 3. Also, its response to variation in pulse on-time is different. Micro-hardness decreases very sharply when this parameter changes from level 1 to level 2 and then shows slight improvement. It can be attributed to the transfer of carbon at level 1 and higher quenching effect at level 3. Consequently, the third level of peak current (A_3), first level of pulse on-time (B_1) and the third level of pulse off-time (C_3) give the highest values of micro-hardness. Hence, the optimum condition of input process parameters is $A_3B_1C_3$. Since this combination existed in the orthogonal array (as seventh row), a confirmation experiment was not required. The average value of micro-hardness obtained at this setting of the experiment was 683.67 HV which can be compared with the theoretical value predicted by Taguchi analysis. The theoretical value of η_{opt} under the optimum conditions is given by:

$$\eta_{opt} = m + (m_{A3} - m) + (m_{B1} - m) + (m_{C3} - m) = 56.695$$

where m is the overall mean of S/N data, m_{A3} is the mean of S/N data for factor A at level 3 and m_{B1} is the mean of S/N data for factor B at level 1, etc.

The corresponding value of micro-hardness is given by

$$y_{opt}^2 = 1 / 10^{-\eta opt / 10}$$

or, $y_{opt} = 683.48$ HV which is very close to the observed experimental value.

To obtain percentage contribution of the three factors and their significance, analysis of variance (ANOVA) of the S/N data was performed. It is presented in Table 4.22 which shows that all the three factors are significant for the response characteristic of surface roughness. The contribution of peak current is found to be very high at 82.37 % followed by pulse on-time and pulse off-time.

Table 4.22 ANOVA Table of S/N data for Micro-hardness (W1 – EL2)

Factor/Source	Sum of Squares	DOF	V	F-ratio	% Contri-bution	Remarks
Peak Current	1.3919	2	0.6959	3296.04	82.37	Significant
Pulse on-time	0.2291	2	0.1145	542.42	13.56	Significant
Pulse off-time	0.0684	2	0.0342	161.90	4.05	Significant
Error (Pooled)	0.0004	2	0.0002	-	0.02	-
Total	1.6898	8		-	100	
DOF = Degrees of Freedom, V = Variance, Tabulated F-ratio $_{0.05}$ (2, 2) = 19						

Similar analysis has now been done for surface roughness. From the experimental data given in Table 4.20, the average values of surface roughness and the corresponding S/N ratios for the three levels of input process parameters have been calculated and are given in Table 4.23.

Table 4.23 Average values by factor levels for Surface Roughness (W1 – EL2)

Parameter / Levels	Peak Current (Amperes)		Pulse on-time (µsec)		Pulse off-time (µsec)	
	Raw Data	S/N Data	Raw Data	S/N Data	Raw Data	S/N Data
L1	1.99	-5.943	2.63	-7.969	3.59	-10.423
L2	3.01	-9.324	3.20	-9.376	2.82	-8.294
L3	4.43	-12.892	3.61	-10.815	3.03	-9.442

These factor effects have been plotted and presented in Fig. 4.9 (a), (b) and (c).

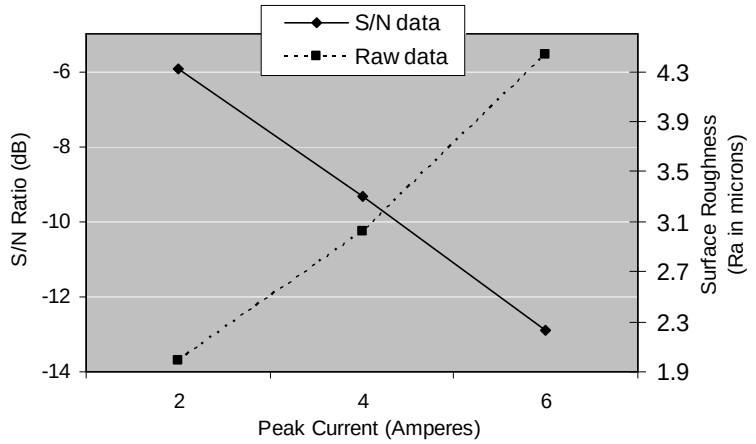

Fig. 4.9 (a) Effect of Peak Current on Surface Roughness and its S/N ratio (W1 – EL2)

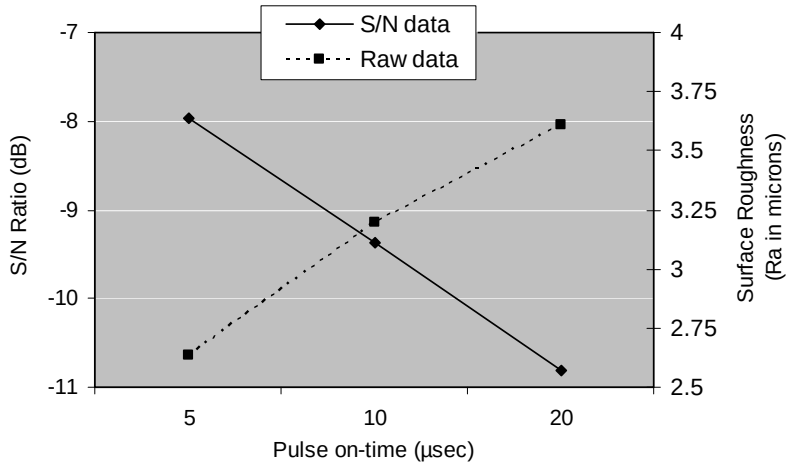

Fig. 4.9 (b) Effect of Pulse on-time on Surface Roughness and its S/N ratio (W1 – EL2)

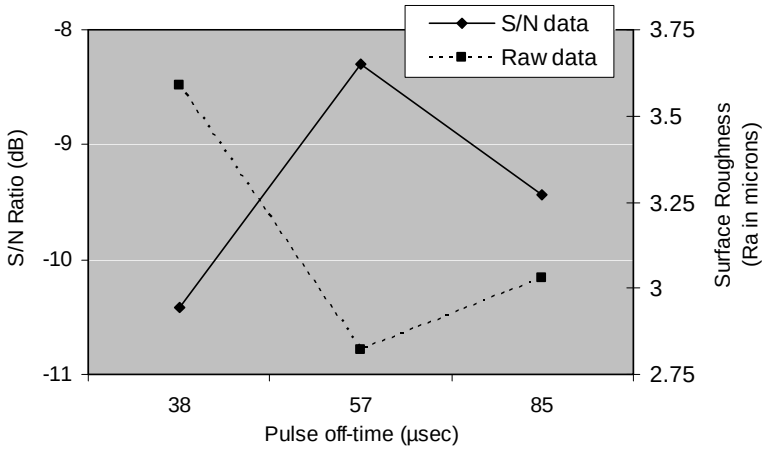

Fig. 4.9 (c) Effect of Pulse off-time on Surface Roughness and its S/N ratio (W1 – EL2)

Lower values of surface roughness are considered to be optimal. It is observed from Fig. 4.9 (a), (b) and (c) that the first level of peak current (A_1), first level of pulse on-time (B_1) and the second level of pulse off-time (C_2) give the lowest values of surface roughness. Hence, the optimum condition of input process parameters is $A_1B_1C_2$. The theoretical value of η_{opt} under the optimum conditions is given by:

$$\eta_{opt} = m + (m_{A1} - m) + (m_{B1} - m) + (m_{C2} - m) = -3.4332$$

The corresponding value of surface roughness is given by

$$y_{opt}^2 = 10^{-\eta opt / 10}$$

$$\text{or,} \quad y_{opt} = 1.48\ \mu m$$

Since this combination of input process parameters did not exist in the orthogonal array, a set of three confirmation experiments were conducted using this combination. The average value of surface roughness obtained at this setting of the experiment was 1.63 μm which is very close to the theoretical value predicted by Taguchi analysis.

Analysis of variance (ANOVA) of the S/N data was performed to obtain the percentage contribution of the factors and their significance. It is presented in Table 4.24 and it can be seen that all the three factors are significant for the response characteristic of surface roughness. Peak current is the most significant factor with 79.08 % contribution.

Table 4.24 ANOVA Table of S/N data for Surface Roughness (W1 – EL2)

Factor/Source	Sum of Squares	DOF	V	F-ratio	% Contri-bution	Remarks
Peak Current	72.4517	2	36.2258	350.27	79.08	Significant
Pulse on-time	12.1487	2	6.0743	58.73	13.26	Significant
Pulse off-time	6.8121	2	3.4061	32.93	7.44	Significant
Error (Pooled)	0.2068	2	0.1034	-	0.22	-
Total	91.6193	8		-	100	
DOF = Degrees of Freedom, V = Variance, Tabulated F-ratio $_{0.05}$ (2, 2) = 19						

4.2.2 Work Material – H13 hot die steel (W3)

The observed values of micro-hardness and surface roughness after machining H13 hot die steel with graphite electrode and calculated values of their S/N ratios are given in Table 4.25.

Table 4.25 Observed values of Micro-hardness and Surface roughness and their calculated S/N ratios (W3 – EL2)

Expt. No.	Micro-hardness (HV)			S/N Ratio (dB)	Surface Roughness (R_a in microns)			S/N Ratio (dB)
	R1	R2	R3		R1	R2	R3	
1	455	443	462	53.124	2.28	2.12	1.98	-6.568
2	434	428	447	52.792	2.51	2.62	2.65	-8.280
3	439	454	431	52.889	2.42	2.54	2.29	-7.672
4	495	482	488	53.773	2.64	2.55	2.42	-8.091
5	485	493	505	53.877	2.77	2.68	2.84	-8.831
6	452	436	451	52.990	3.01	3.11	2.98	-9.640
7	562	572	578	55.126	2.82	2.93	2.64	-8.941
8	528	519	493	54.197	3.74	3.44	3.59	-11.107
9	523	495	508	54.122	3.61	3.67	3.78	-11.334
Total	4373	4322	4363	482.890	25.80	25.66	25.17	-80.464
	$\overline{T}_{MH}$ = Overall mean of micro hardness = 483.63			Mean, m= 53.654	$\overline{T}_{SR}$ = Overall mean of surface roughness = 2.838			Mean, m= -8.940
R1, R2 and R3 represent the three repetitions.								

From this data, the average values of micro-hardness and corresponding S/N ratios for the three levels of peak current, pulse on-time and pulse off-time have been calculated and are given in Table 4.26. These average values represent the factor effects of input parameters.

Table 4.26 Average values by factor levels for Micro-hardness (W3 – EL2)

Parameter / Levels	Peak Current (amperes)		Pulse on-time (µsec)		Pulse off-time (µsec)	
	Raw Data	S/N Data	Raw Data	S/N Data	Raw Data	S/N Data
L1	443.67	52.935	504.11	54.008	471.00	53.437
L2	476.33	53.546	481.33	53.622	477.78	53.562
L3	530.89	54.482	465.44	53.334	502.11	53.964

These factor effects have been plotted and presented in Fig. 4.10 (a), (b) and (c).

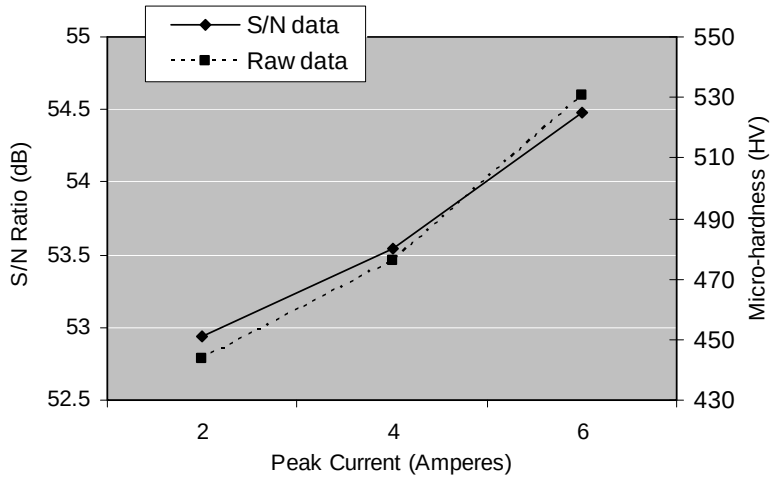

Fig. 4.10 (a) Effect of Peak Current on Micro-hardness and its S/N ratio (W3 – EL2)

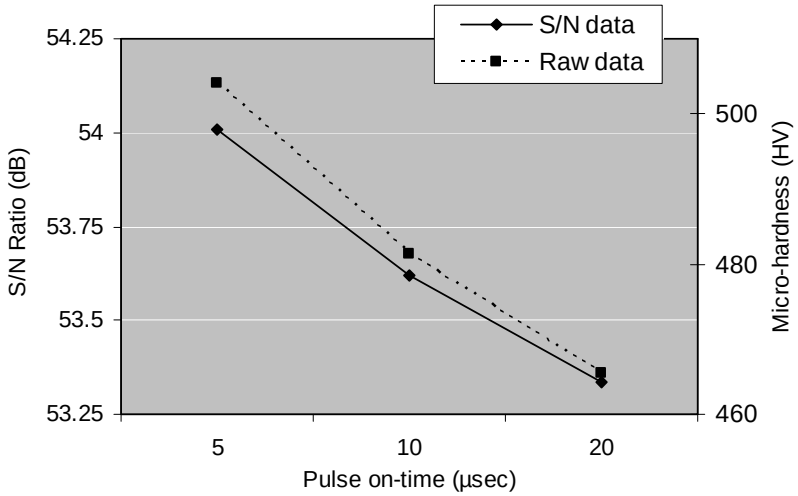

Fig. 4.10 (b) Effect of Pulse on-time on Micro-hardness and its S/N ratio (W3 – EL2)

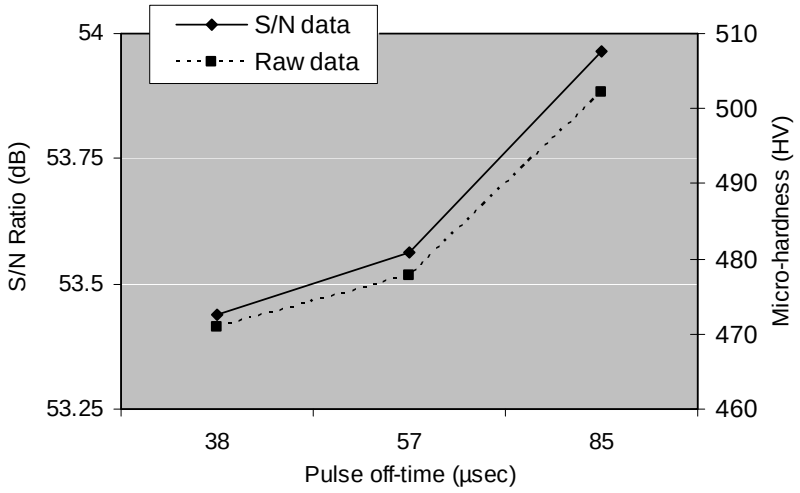

Fig. 4.10 (c) Effect of Pulse off-time on Micro-hardness and its S/N ratio (W3 – EL2)

It is observed from Fig. 4.10 (a), (b) and (c) that the response of micro-hardness to variation in pulse on-time is different from its response to the other two process parameters. It is indicative of some surface changes at lower values of pulse on-time which are responsible for the significant increase in micro-hardness. Similar effect is produced by higher values of peak current and pulse off-time. Higher values of peak current also result in more heating and consequently, more quenching of the machined surface. It is also observed that the third level of peak current (A_3), first level of pulse on-time (B_1) and the third level of pulse off-time (C_3) give the highest values of micro-hardness. Hence, the optimum condition of input process parameters is $A_3B_1C_3$. This is same as the desirable optimum condition for OHNS die steel. Since this combination exists in the orthogonal array (as seventh row), a confirmation experiment is not required. The average value of micro-hardness obtained at this setting of the experiment is 570.67 HV which can be compared with the theoretical value η_{opt} predicted by Taguchi analysis, that is:

$$\eta_{opt} = m + (m_{A3} - m) + (m_{B1} - m) + (m_{C3} - m)$$

$$= 55.145$$

The corresponding value of micro-hardness is given by

$$y_{opt}^2 = 1 / 10^{-\eta opt / 10}$$

or, $$y_{opt} = 571.77 \text{ HV}$$

which is very close to the observed experimental value.

To obtain percentage contribution of the three factors and their significance, analysis of variance (ANOVA) of the S/N data was performed. It is presented in Table 4.27 which shows that all the three factors are significant for the response characteristic of micro-hardness. The contribution of peak current is found to be very high at 75.92 % whereas error contribution is negligible.

Table 4.27 ANOVA Table of S/N data for Micro-hardness (W3 – EL2)

Factor/Source	Sum of Squares	DOF	V	F-ratio	% Contri-bution	Remarks
Peak Current	3.6393	2	1.8196	275.77	75.92	Significant
Pulse on-time	0.6862	2	0.3431	52.00	14.32	Significant
Pulse off-time	0.4548	2	0.2274	34.47	9.49	Significant
Error (Pooled)	0.0132	2	0.0066	-	0.27	-
Total	4.7935	8		-	100	
DOF = Degrees of Freedom, V = Variance, Tabulated F-ratio $_{0.05}$ (2, 2) = 19						

Similar analysis has now been done for surface roughness. From the experimental data given in Table 4.25, the average values of surface roughness and the corresponding S/N ratios for the three levels of input process parameters have been calculated and are given in Table 4.28. These average values represent the factor effects of input parameters.

Table 4.28 Average values by factor levels for Surface Roughness (W3 – EL2)

Parameter Levels	Peak Current (Amperes)		Pulse on-time (µsec)		Pulse off-time (µsec)	
	Raw Data	S/N Data	Raw Data	S/N Data	Raw Data	S/N Data
L1	2.38	-7.507	2.49	-7.867	2.91	-9.105
L2	2.78	-8.854	2.98	-9.406	2.94	-9.235
L3	3.36	-10.461	3.05	-9.549	2.66	-8.481

These factor effects have been plotted and presented in Fig. 4.11 (a), (b) and (c).

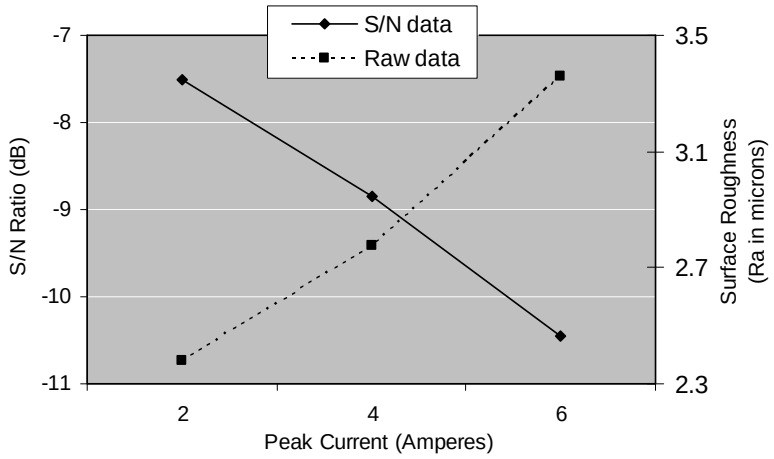

Fig. 4.11 (a) Effect of Peak Current on Surface Roughness and its S/N ratio (W3 – EL2)

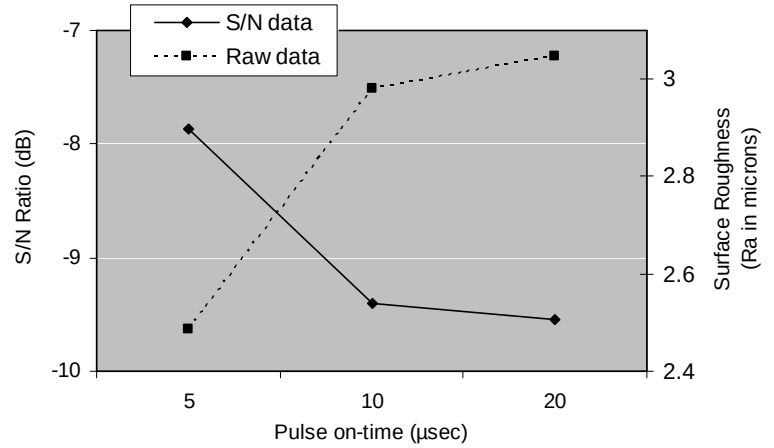

Fig. 4.11 (b) Effect of Pulse on-time on Surface Roughness and its S/N ratio (W3 – EL2)

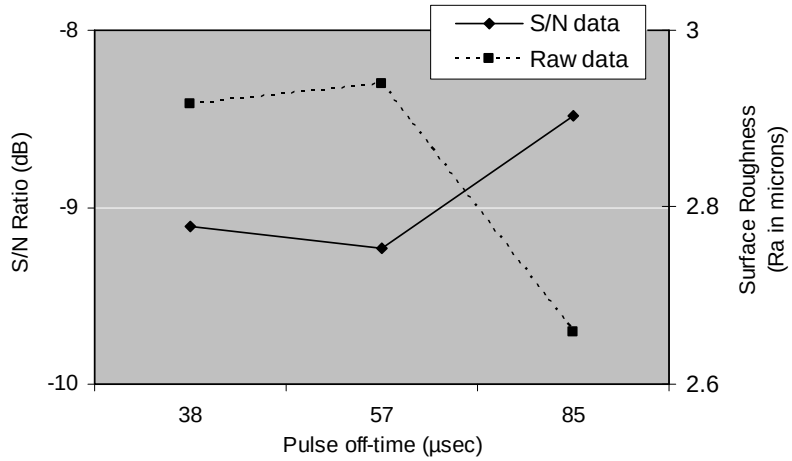

Fig. 4.11 (c) Effect of Pulse off-time on Surface Roughness and its S/N ratio (W3 – EL2)

It is observed from Fig. 4.11 (c) that there is very little change in surface roughness when the value of pulse off-time changes from level 1 to level 2 but there is a substantial improvement after that. It is also observed that the first level of peak current (A_1), first level of pulse on-time (B_1) and the third level of pulse off-time (C_3) give the lowest values of surface roughness. Hence, the optimum condition of input process parameters is $A_1B_1C_3$. The theoretical value of η_{opt} under the optimum conditions is given by:

$$\eta_{opt} = m + (m_{A1} - m) + (m_{B1} - m) + (m_{C3} - m) = -5.974$$

The corresponding value of surface roughness is given by

$$y_{opt}^2 = 10^{-\eta opt / 10}$$

or, $$y_{opt} = 1.99\ \mu m$$

Since this combination of input process parameters did not exist in the orthogonal array, a set of three confirmation experiments were conducted. The average value of surface roughness obtained at this setting of the experiment was 1.96 μm which is very close to the theoretical value predicted by the Taguchi analysis.

Analysis of variance (ANOVA) of the S/N data was performed to obtain the percentage contribution of the factors and their significance. It is presented in Table 4.29 and it can be seen that all the three factors are significant for the response characteristic of surface roughness. Error contribution is again found to be negligible.

Table 4.29 ANOVA Table of S/N data for Surface Roughness (W3 – EL2)

Factor/Source	**Sum of Squares**	**DOF**	**V**	**F-ratio**	**% Contri-bution**	**Remarks**
Peak Current	13.1228	2	6.5614	3417.01	67.93	Significant
Pulse on-time	5.2191	2	2.6095	1358.98	27.01	Significant
Pulse off-time	0.9737	2	0.4868	253.55	5.04	Significant
Error (Pooled)	0.0038	2	0.0019	-	0.02	-
Total	19.3194	8		-	100	
DOF = Degrees of Freedom, V = Variance, Tabulated F-ratio $_{0.05}(2, 2) = 19$						

4.3 MACHINING WITH COPPER-TUNGSTEN ELECTRODE (EL3)

4.3.1 Work Material – OHNS die steel (W1)

The observed values of micro-hardness and surface roughness after machining OHNS die steel with copper-tungsten electrode and calculated values of their S/N ratios are given in Table 4.30.

Table 4.30 Observed values of Micro-hardness and Surface roughness and their calculated S/N ratios (W1 – EL3)

Expt. No.	Micro-hardness (HV)			S/N Ratio (dB)	Surface Roughness (R_a in microns)			S/N Ratio (dB)
	R1	R2	R3		R1	R2	R3	
1	675	691	682	56.683	1.84	2.13	1.95	-5.920
2	692	710	685	56.845	2.11	2.05	1.74	-5.904
3	652	621	638	56.078	2.83	2.95	3.16	-9.493
4	838	863	845	58.573	4.08	3.73	4.22	-12.074
5	804	815	791	58.096	5.25	5.38	5.57	-14.650
6	738	725	717	57.225	5.76	6.15	5.83	-15.440
7	910	918	895	59.157	6.62	6.96	6.85	-16.665
8	851	864	846	58.625	6.78	6.70	6.54	-16.488
9	873	861	854	58.716	6.59	6.83	6.76	-16.557
Total	7033	7068	6953	519.997	41.86	42.88	42.62	-113.192
	$\overline{T}_{MH}$ = Overall mean of micro hardness = 779.78			Mean, m= 57.777	$\overline{T}_{SR}$ = Overall mean of surface roughness = 4.72			Mean, m= -12.577
R1, R2 and R3 represent the three repetitions.								

From this data, the average values of micro-hardness and the corresponding S/N ratios for the three levels of input process parameters have been calculated and are given in Table 4.31.

Table 4.31 Average values by factor levels for Micro-hardness (W1 – EL3)

Parameter / Levels	Peak Current (amperes)		Pulse on-time (µsec)		Pulse off-time (µsec)	
	Raw Data	S/N Data	Raw Data	S/N Data	Raw Data	S/N Data
L1	671.78	56.535	813.00	58.138	754.33	57.511
L2	792.89	57.965	784.22	57.855	802.33	58.045
L3	874.67	58.833	742.11	57.339	782.67	57.777

These factor effects have been plotted and presented in Fig. 4.12 (a), (b) and (c).

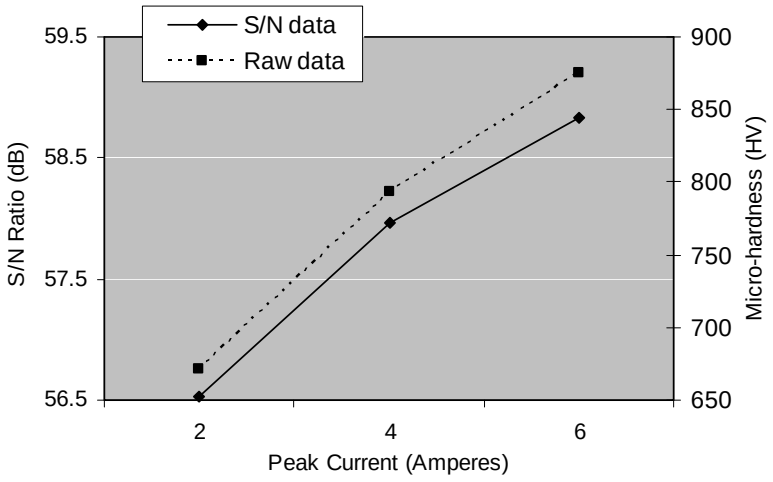

Fig. 4.12 (a) Effect of Peak Current on Micro-hardness and its S/N ratio (W1 – EL3)

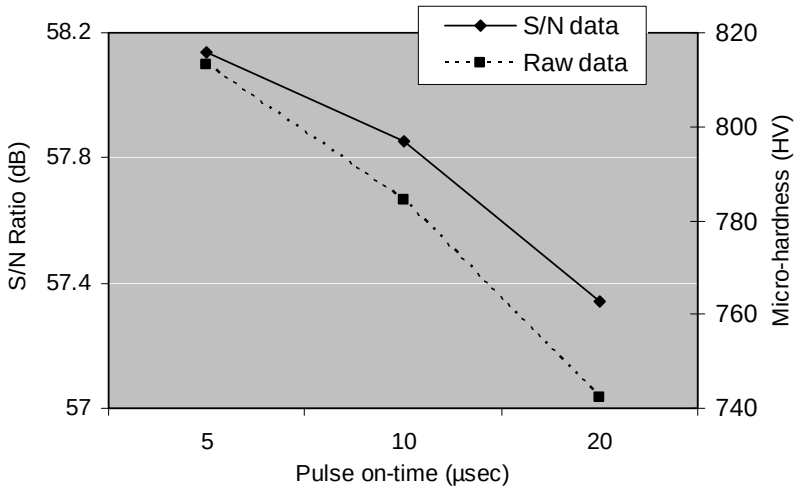

Fig. 4.12 (b) Effect of Pulse on-time on Micro-hardness and its S/N ratio (W1 – EL3)

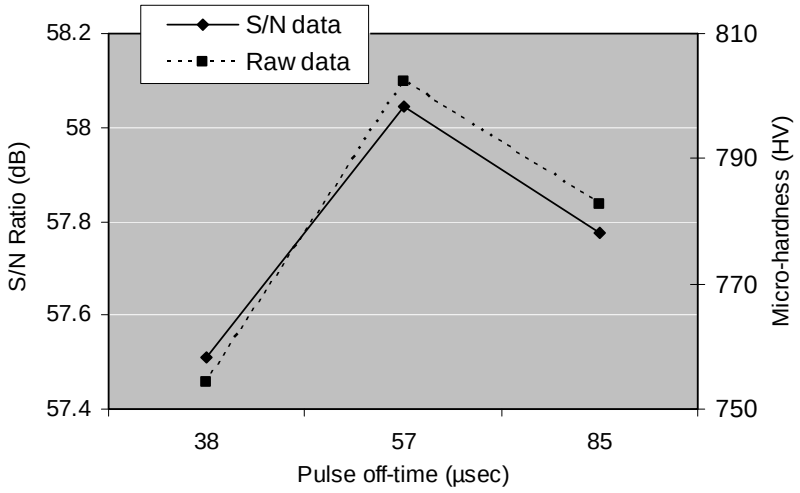

Fig. 4.12 (c) Effect of Pulse off-time on Micro-hardness and its S/N ratio (W1 – EL3)

Both the raw data and S/N data have been plotted. While the response of micro-hardness to variation in peak current and pulse on-time is on expected lines, its response to variation in pulse off-time is found to be different. The best value of micro-hardness is achieved at level 2 and then it decreases. This behaviour emphasizes the requirement of moderate pulse off-time for material transfer from this electrode. It is also noted that very high values of micro-hardness are achieved with this electrode material as compared to copper or graphite electrodes. It can be observed from Fig. 4.12 (a), (b) and (c) that that the third level of peak current (A_3), first level of pulse on-time (B_1) and second level of pulse off-time (C_2) give the highest values of micro-hardness. Hence, the optimum condition of input process parameters is $A_3B_1C_2$. The theoretical value of η_{opt} under the optimum conditions is given by:

$$\eta_{opt} = m + (m_{A3} - m) + (m_{B1} - m) + (m_{C2} - m) = 59.4598$$

The corresponding value of micro-hardness is given by

$$y_{opt}^2 = 1 / 10^{-\eta opt / 10}$$

or, $$y_{opt} = 939.70 \text{ HV}$$

Since this combination of input process parameters did not exist in the orthogonal array, a set of three confirmation experiments were conducted. The average value of micro-hardness obtained at this setting of the experiment was 923.33 HV which is very close to the theoretical value predicted by Taguchi analysis.

To obtain percentage contribution of the three factors and their significance, analysis of variance (ANOVA) of the S/N data was performed. It is presented in Table 4.32 which shows that all the three factors are significant for the response characteristic of micro-hardness. The contribution of peak current is found to be very high at 85.01 % whereas error contribution is less than 1 %.

Table 4.32 ANOVA Table of S/N data for Micro-hardness (W1 – EL3)

Factor/Source	**Sum of Squares**	**DOF**	**V**	**F-ratio**	**% Contri-bution**	**Remarks**
Peak Current	8.0740	2	4.0370	594.55	85.01	Significant
Pulse on-time	0.9829	2	0.4915	72.38	10.35	Significant
Pulse off-time	0.4272	2	0.2136	31.46	4.50	Significant
Error (Pooled)	0.0136	2	0.0068	-	0.14	-
Total	9.4977	8		-	100	
DOF = Degrees of Freedom, V = Variance, Tabulated F-ratio $_{0.05}$ (2, 2) = 19						

Similar analysis has now been done for surface roughness. From the experimental data given in Table 4.30, the average values of surface roughness and the corresponding S/N ratios for the three levels of input process parameters have been calculated and are given in Table 4.33.

Table 4.33 Average values by factor levels for Surface Roughness (W1 – EL3)

Parameter	Peak Current (Amperes)		Pulse on-time (µsec)		Pulse off-time (µsec)	
Levels	Raw Data	S/N Data	Raw Data	S/N Data	Raw Data	S/N Data
L1	2.31	-7.106	4.26	-11.553	4.85	-12.616
L2	5.11	-14.055	4.68	-12.347	4.23	-11.512
L3	6.74	-16.570	5.21	-13.830	5.06	-13.603

These factor effects have been plotted and presented in Fig. 4.13 (a), (b) and (c).

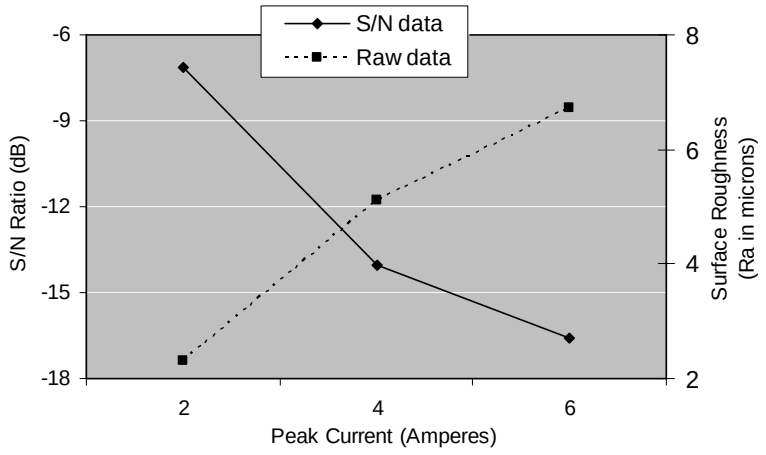

Fig. 4.13 (a) Effect of Peak Current on Surface Roughness and its S/N ratio (W1 – EL3)

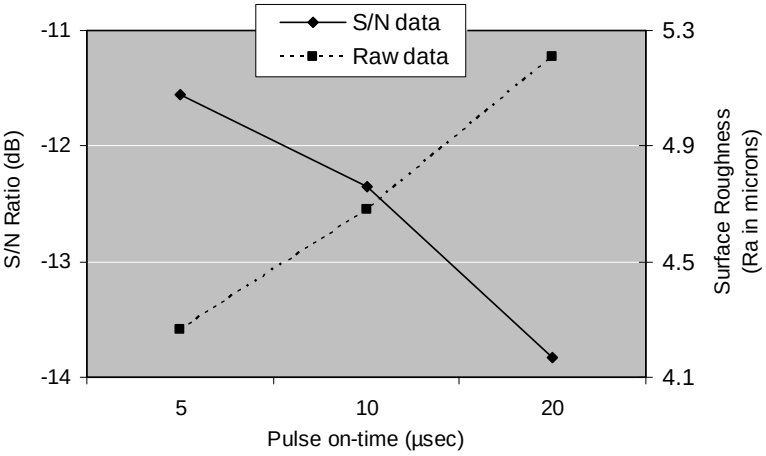

Fig. 4.13 (b) Effect of Pulse on-time on Surface Roughness and its S/N ratio (W1 – EL3)

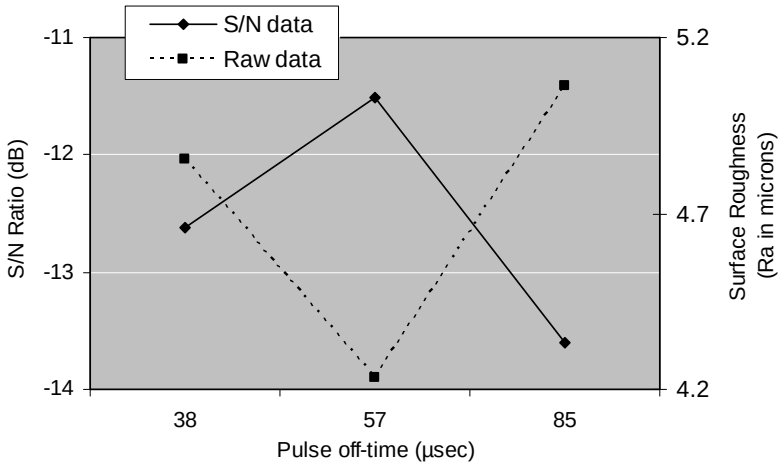

Fig. 4.13 (c) Effect of Pulse off-time on Surface Roughness and its S/N ratio (W1 – EL3)

It is observed from Fig. 4.13 (a), (b) and (c) that the first level of peak current (A_1), first level of pulse on-time (B_1) and the second level of pulse off-time (C_2) give the lowest values of surface roughness. Hence, the optimum condition of input process parameters is $A_1B_1C_2$. The theoretical value of η_{opt} under the optimum conditions is given by:

$$\eta_{opt} = m + (m_{A1} - m) + (m_{B1} - m) + (m_{C2} - m) = -5.0168$$

The corresponding value of surface roughness is given by

$$y_{opt}^2 = 10^{-\eta opt / 10}$$

or, $$y_{opt} = 1.78\ \mu m$$

Since this combination of input process parameters did not exist in the orthogonal array, a set of three confirmation experiments were conducted. The average value of surface roughness obtained at this setting of the experiment was 1.72 μm which is better than and very close to the theoretical value predicted by Taguchi analysis. It is significant to note that machining with copper-tungsten electrode has improved the micro-hardness as well as surface finish.

Analysis of variance (ANOVA) of the S/N data was performed to obtain the percentage contribution of the factors and their significance. It is presented in Table 4.34 and it can be seen that all the three factors are significant for the response characteristic of surface roughness. Contribution of peak current is very high whereas the contribution of pulse on-time and pulse off-time is almost equal.

Table 4.34 ANOVA Table of S/N data for Surface Roughness (W1 – EL3)

Factor/Source	Sum of Squares	DOF	V	F-ratio	% Contri-bution	Remarks
Peak Current	144.1851	2	72.0926	790.64	90.71	Significant
Pulse on-time	8.0152	2	4.0076	43.95	5.04	Significant
Pulse off-time	6.5660	2	3.2830	36.00	4.13	Significant
Error (Pooled)	0.1824	2	0.0912	-	0.12	-
Total	158.9487	8		-	100	
DOF = Degrees of Freedom, V = Variance, Tabulated F-ratio $_{0.05}(2, 2) = 19$						

4.3.2 Work Material – D2 High-carbon High-chromium die steel (W2)

The observed values of micro-hardness and surface roughness after machining D2 die steel with copper-tungsten electrode and the calculated values of their S/N ratios are given in Table 4.35.

Table 4.35 Observed values of Micro-hardness and Surface roughness and their calculated S/N ratios (W2 – EL3)

Expt. No.	Micro-hardness (HV)			S/N Ratio (dB)	Surface Roughness (R_a in microns)			S/N Ratio (dB)
	R1	R2	R3		R1	R2	R3	
1	687	672	718	56.796	2.16	2.52	2.37	-7.438
2	712	695	682	56.852	2.23	2.13	2.08	-6.639
3	644	671	658	56.356	2.81	2.94	2.75	-9.049
4	760	778	792	57.801	3.27	3.34	3.41	-10.476
5	726	735	747	57.336	3.71	3.92	3.85	-11.659
6	713	704	731	57.095	4.78	4.95	4.84	-13.728
7	787	812	795	58.038	5.13	5.25	5.42	-14.433
8	762	769	778	57.725	5.67	5.81	5.77	-15.194
9	796	784	768	57.869	5.89	5.72	5.47	-15.111
Total	6587	6620	6669	515.869	35.65	36.58	35.96	-103.727
	$\overline{T}_{MH}$ = Overall mean of micro hardness = 736.15			Mean, m= 57.319	$\overline{T}_{SR}$ = Overall mean of surface roughness = 4.01			Mean, m= -11.525

From this data, the average values of micro-hardness and corresponding S/N ratios for the three levels of peak current, pulse on-time and pulse off-time have been calculated and are given in Table 4.36. These average values represent the factor effects of the three input parameters.

Table 4.36 Average values by factor levels for Micro-hardness (W2 – EL3)

Parameter / Levels	Peak Current (amperes)		Pulse on-time (µsec)		Pulse off-time (µsec)	
	Raw Data	S/N Data	Raw Data	S/N Data	Raw Data	S/N Data
L1	682.11	56.668	755.67	57.545	726.00	57.206
L2	742.89	57.411	734.00	57.304	751.89	57.507
L3	783.44	57.877	718.78	57.107	730.56	57.243

These factor effects have been plotted and presented in Fig. 4.14 (a), (b) and (c).

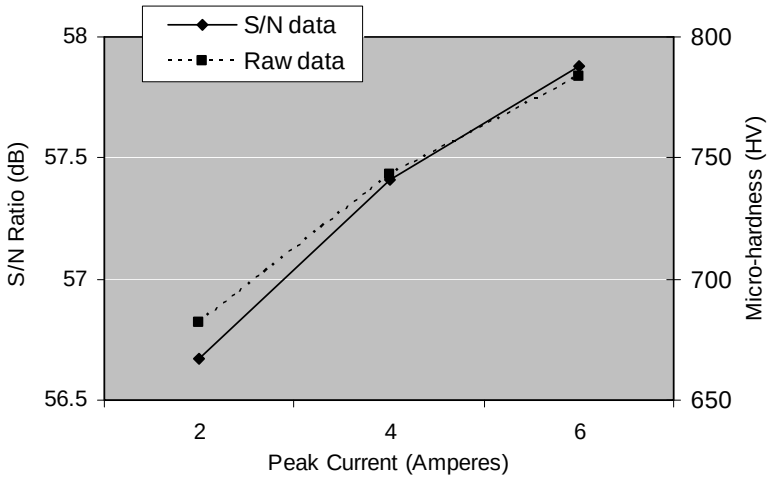

Fig. 4.14 (a) Effect of Peak Current on Micro-hardness and its S/N ratio (W2 – EL3)

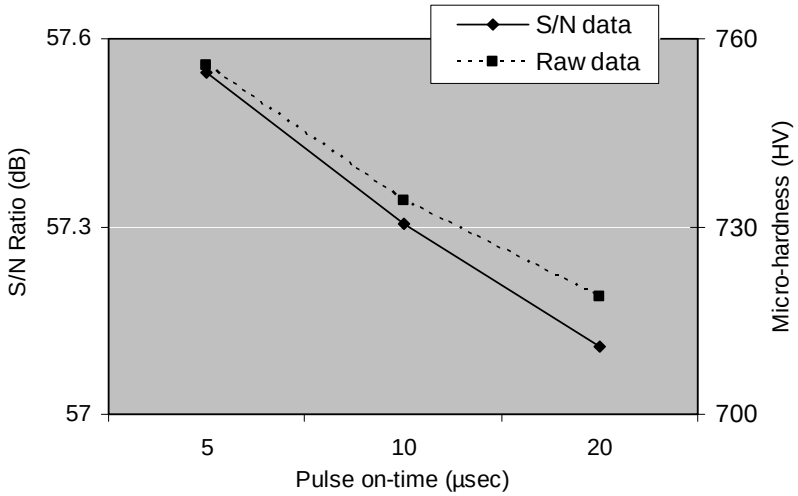

Fig. 4.14 (b) Effect of Pulse on-time on Micro-hardness and its S/N ratio (W2 – EL3)

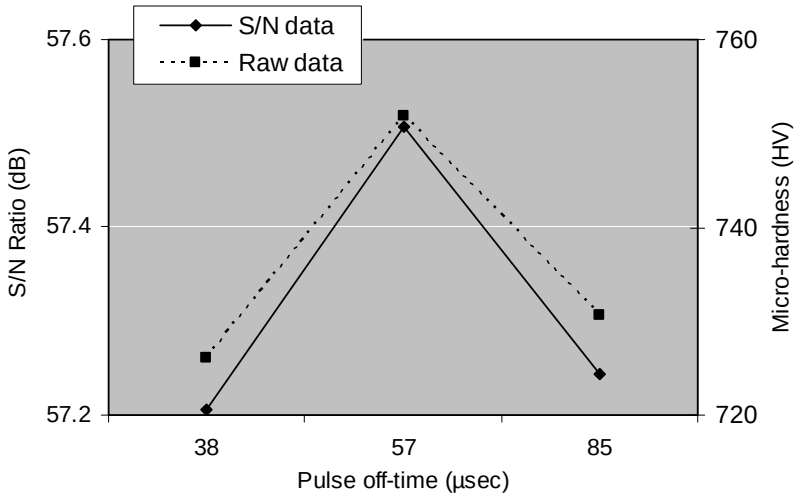

Fig. 4.14 (c) Effect of Pulse off-time on Micro-hardness and its S/N ratio (W2 – EL3)

It is observed from Fig. 4.14 (a), (b) and (c) that the response of micro-hardness to variation in the three input process parameters for this material is identical to the behaviour shown by OHNS die steel. However, the actual value of micro-hardness achieved is not significant even though the initial hardness of D2 die steel was very high. Both the other work materials show more than 50 % improvement in micro-hardness with this electrode. It is also observed that the third level of peak current (A_3), first level of pulse on-time (B_1) and second level of pulse off-time (C_2) give the highest values of micro-hardness. Hence, the optimum condition of input process parameters is $A_3B_1C_2$. The theoretical value of η_{opt} under the optimum condition is given by:

$$\eta_{opt} = m + (m_{A3} - m) + (m_{B1} - m) + (m_{C2} - m)$$

$$= 58.2922$$

The corresponding value of micro-hardness is given by

$$y_{opt}^2 = 1 / 10^{-\eta opt / 10}$$

or, $$y_{opt} = 821.50 \text{ HV}$$

Since this combination of input process parameters did not exist in the orthogonal array, a set of three confirmation experiments were conducted. The average value of micro hardness obtained at this setting of the experiment was 832.67 HV which is better than and very close to the theoretical value predicted by Taguchi analysis.

To obtain percentage contribution of the three factors and their significance, analysis of variance (ANOVA) of the S/N data was performed. It is presented in Table 4.37 which shows that all the three factors are significant for the response characteristic of micro-hardness. The contribution of peak current is found to be very high at 83.08 % followed by pulse on-time and pulse off-time. Error contribution is less than 1 %.

Table 4.37 ANOVA Table of S/N data for Micro-hardness (W2 – EL3)

Factor/Source	Sum of Squares	DOF	V	F-ratio	% Contri-bution	Remarks
Peak Current	2.2298	2	1.1149	808.44	83.08	Significant
Pulse on-time	0.2891	2	0.1446	104.83	10.77	Significant
Pulse off-time	0.1622	2	0.0811	58.80	6.04	Significant
Error (Pooled)	0.0028	2	0.0014	-	0.11	-
Total	2.6839	8		-	100	
DOF = Degrees of Freedom, V = Variance, Tabulated F-ratio $_{0.05}$ (2, 2) = 19						

Similar analysis has now been done for surface roughness. From the experimental data given in Table 4.35, the average values of surface roughness and the corresponding S/N ratios for the three levels of input process parameters have been calculated and are given in Table 4.38. These average values represent the factor effects of input parameters.

Table 4.38 Average values by factor levels for Surface Roughness (W2 – EL3)

Parameter / Levels	Peak Current (Amperes)		Pulse on-time (µsec)		Pulse off-time (µsec)	
	Raw Data	S/N Data	Raw Data	S/N Data	Raw Data	S/N Data
L1	2.44	-7.709	3.65	-10.783	4.32	-12.120
L2	4.01	-11.954	3.91	-11.164	3.73	-10.742
L3	5.57	-14.913	4.46	-12.629	3.98	-11.714

These factor effects have been plotted and presented in Fig. 4.15 (a), (b) and (c).

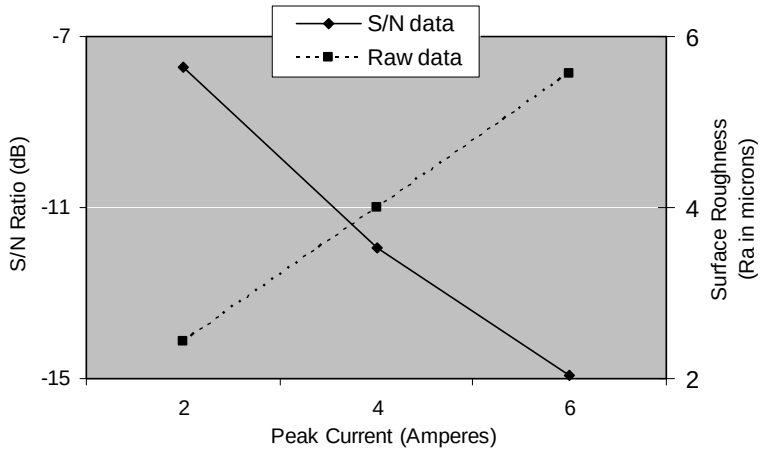

Fig. 4.15 (a) Effect of Peak Current on Surface Roughness and its S/N ratio (W2 – EL3)

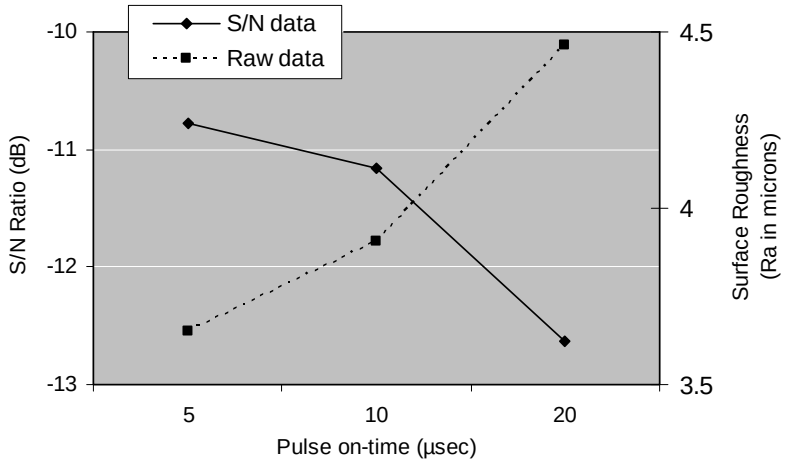

Fig. 4.15 (b) Effect of Pulse on-time on Surface Roughness and its S/N ratio (W2 – EL3)

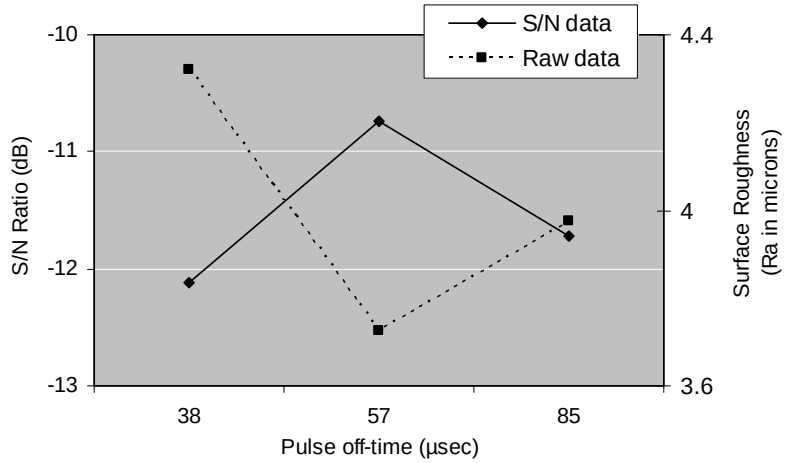

Fig. 4.15 (c) Effect of Pulse off-time on Surface Roughness and its S/N ratio (W2 – EL3)

It is observed from Fig. 4.15 (a), (b) and (c) that the first level of peak current (A_1), first level of pulse on-time (B_1) and the second level of pulse off-time (C_2) give the lowest values of surface roughness. Hence, the optimum condition of input process parameters is $A_1B_1C_2$. The theoretical value of η_{opt} at this optimum condition is given by:

$$\eta_{opt} = m + (m_{A1} - m) + (m_{B1} - m) + (m_{C2} - m) = -6.1831$$

The corresponding value of surface roughness is given by

$$y_{opt}^2 = 10^{-\eta opt / 10}$$

or, $$y_{opt} = 2.04\ \mu m$$

Since this combination of input process parameters did not exist in the orthogonal array, a set of three confirmation experiments were conducted for this combination. The average value of surface roughness obtained at this setting of the experiment was 2.15 μm which is very close to the theoretical value predicted by Taguchi analysis.

Analysis of variance (ANOVA) of the S/N data was performed to obtain the percentage contribution of the factors and their significance. It is presented in Table 4.39 and it can be seen that all the three factors are significant for the response characteristic of surface roughness. Contribution of peak current is again very high whereas the contribution of error is negligible.

Table 4.39 ANOVA Table of S/N data for Surface Roughness (W2 – EL3)

Factor/Source	**Sum of Squares**	**DOF**	**V**	**F-ratio**	**% Contri-bution**	**Remarks**
Peak Current	78.6691	2	39.3346	1147.76	89.96	Significant
Pulse on-time	5.7046	2	2.8523	83.23	6.52	Significant
Pulse off-time	3.0073	2	1.5037	43.88	3.44	Significant
Error (Pooled)	0.0686	2	0.0343	-	0.08	-
Total	87.4496	8		-	100	
DOF = Degrees of Freedom, V = Variance, Tabulated F-ratio $_{0.05}(2, 2) = 19$						

4.3.3 Work Material – H13 hot die steel (W3)

The observed values of micro-hardness and surface roughness after machining H13 hot die steel with copper-tungsten electrode and the calculated values of their S/N ratios are given in Table 4.40.

Table 4.40 Observed values of Micro-hardness and Surface roughness and their calculated S/N ratios (W3 – EL3)

Expt. No.	Micro-hardness (HV)			S/N Ratio (dB)	Surface Roughness (R_a in microns)			S/N Ratio (dB)
	R1	R2	R3		R1	R2	R3	
1	498	507	521	54.124	2.8	2.66	2.58	-8.568
2	529	492	514	54.168	3.17	3.57	3.46	-10.640
3	484	473	466	53.519	3.59	3.81	3.68	-11.351
4	598	624	637	55.834	3.78	3.95	4.13	-11.945
5	546	535	553	54.720	4.94	5.08	5.31	-14.172
6	532	512	527	54.378	4.55	4.42	4.28	-12.905
7	678	705	719	56.902	5.94	5.83	6.12	-15.512
8	648	614	625	55.966	6.57	6.28	6.35	-16.125
9	665	681	654	56.475	6.52	6.61	6.38	-16.264
Total	5178	5143	5216	496.086	41.86	42.21	42.29	-117.481
	$\overline{T}_{MH}$ = Overall mean of micro hardness = 575.44			Mean, m= 55.121	$\overline{T}_{SR}$ = Overall mean of surface roughness = 4.68			Mean, m= -13.054
R1, R2 and R3 represent the three repetitions.								

From this data, the average values of micro-hardness and the corresponding S/N ratios for the three levels of input process parameters have been calculated and are given in Table 4.41.

Table 4.41 Average values by factor levels for Micro-hardness (W3 – EL3)

Parameter / Levels	Peak Current (amperes)		Pulse on-time (µsec)		Pulse off-time (µsec)	
	Raw Data	S/N Data	Raw Data	S/N Data	Raw Data	S/N Data
L1	498.22	53.937	609.67	55.620	553.78	54.823
L2	562.67	54.977	561.78	54.952	599.33	55.492
L3	665.44	56.448	554.89	54.790	573.22	55.047

These factor effects have been plotted and presented in Fig. 4.16 (a), (b) and (c).

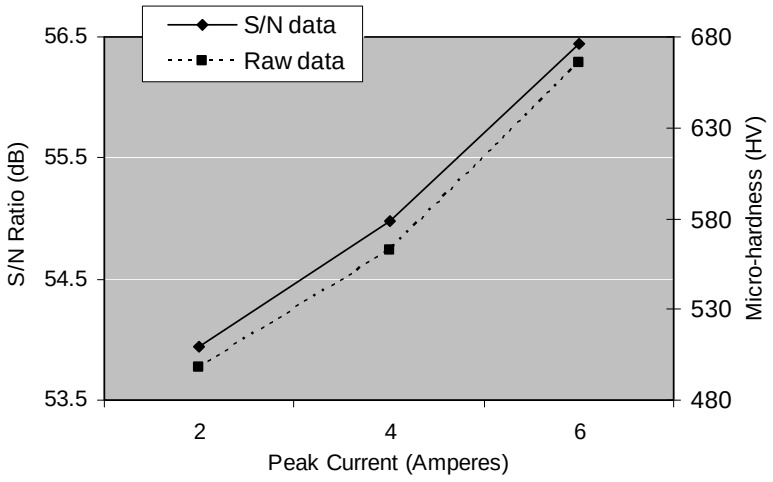

Fig. 4.16 (a) Effect of Peak Current on Micro-hardness and its S/N ratio (W3 – EL3)

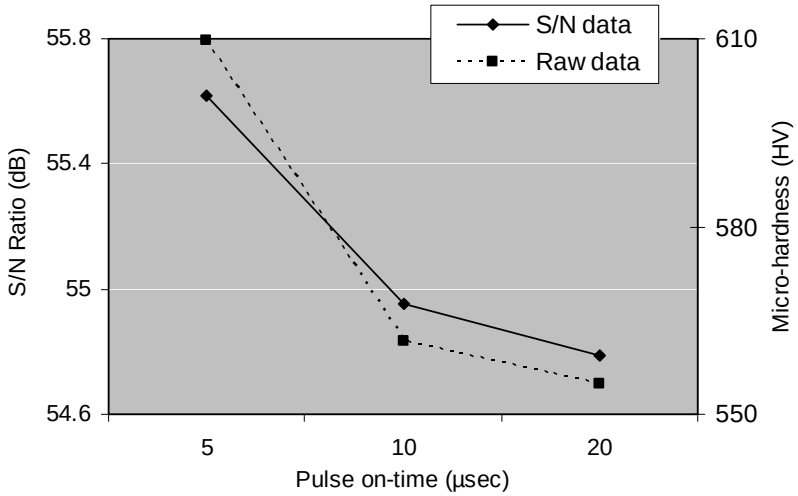

Fig. 4.16 (b) Effect of Pulse on-time on Micro-hardness and its S/N ratio (W3 – EL3)

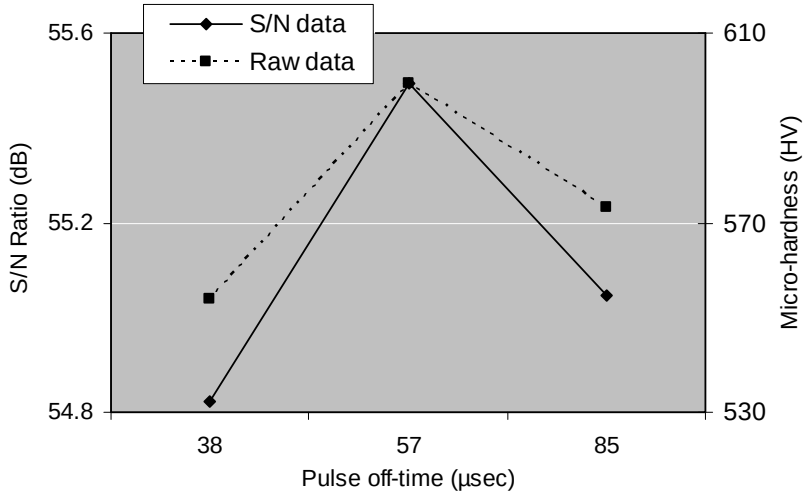

Fig. 4.16 (c) Effect of Pulse off-time on Micro-hardness and its S/N ratio (W3 – EL3)

It is observed from Fig. 4.16 (a), (b) and (c) that for this material also, the response of micro-hardness to variation in the three input process parameters is same as the other two work materials. Hence, it can be said that the pattern of response depends on the electrode material and not the work material. However, the actual value of micro-hardness achieved is the least for this material. It is also observed that the third level of peak current (A_3), first level of pulse on-time (B_1) and the second level of pulse off-time (C_2) give the highest values of micro-hardness. Hence, the optimum combination of input process parameters is $A_3B_1C_2$ which can be expected to hold good for all die steel materials when copper-tungsten electrode is used. The theoretical value of η_{opt} for this optimum combination is given by:

$$\eta_{opt} = m + (m_{A3} - m) + (m_{B1} - m) + (m_{C2} - m)$$

$$= 57.319$$

The corresponding value of micro-hardness is given by

$$y_{opt}^2 = 1 / 10^{-\eta opt / 10}$$

or, $$y_{opt} = 734.43 \text{ HV}$$

Since this combination of input process parameters did not exist in the orthogonal array, a set of three confirmation experiments were conducted for this combination. The average value of micro-hardness obtained at this setting of the experiment was 724.33 HV which is very close to the theoretical value predicted by Taguchi analysis.

To obtain percentage contribution of the three factors and their significance, analysis of variance (ANOVA) of the S/N data was performed. It is presented in Table 4.42 which shows that all the three factors are significant for the response characteristic of micro-hardness. Peak current emerges as the most significant factor with 83.68 % contribution followed by pulse on-time and pulse off-time. Error contribution is found to be negligible.

Table 4.42 ANOVA Table of S/N data for Micro-hardness (W3 – EL3)

Factor/Source	Sum of Squares	DOF	V	F-ratio	% Contri-bution	Remarks
Peak Current	9.5494	2	4.7747	2575.24	83.68	Significant
Pulse on-time	1.1621	2	0.5810	313.37	10.18	Significant
Pulse off-time	0.6968	2	0.3484	187.91	6.11	Significant
Error (Pooled)	0.0037	2	0.0019	-	0.03	-
Total	11.4120	8		-	100	
DOF = Degrees of Freedom, V = Variance, Tabulated F-ratio $_{0.05}$ (2, 2) = 19						

Similar analysis has now been done for surface roughness. From the experimental data given in Table 4.40, the average values of surface roughness and the corresponding S/N ratios for the three levels of input process parameters have been calculated and are given in Table 4.43. These average values represent the factor effects of input parameters.

Table 4.43 Average values by factor levels for Surface Roughness (W3 – EL3)

Parameter / Levels	Peak Current (Amperes)		Pulse on-time (µsec)		Pulse off-time (µsec)	
	Raw Data	S/N Data	Raw Data	S/N Data	Raw Data	S/N Data
L1	3.26	-10.186	4.20	-12.008	4.50	-12.533
L2	4.49	-13.007	4.97	-13.646	4.62	-12.950
L3	6.29	-15.967	4.87	-13.506	4.92	-13.678

These factor effects have been plotted and presented in Fig. 4.17 (a), (b) and (c).

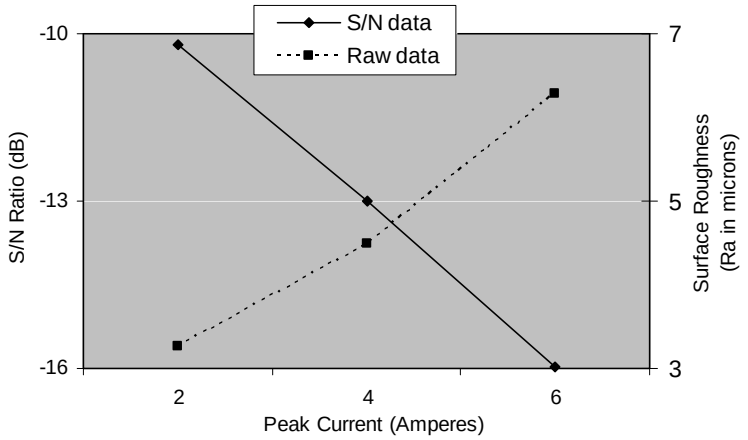

Fig. 4.17 (a) Effect of Peak Current on Surface Roughness and its S/N ratio (W3 – EL3)

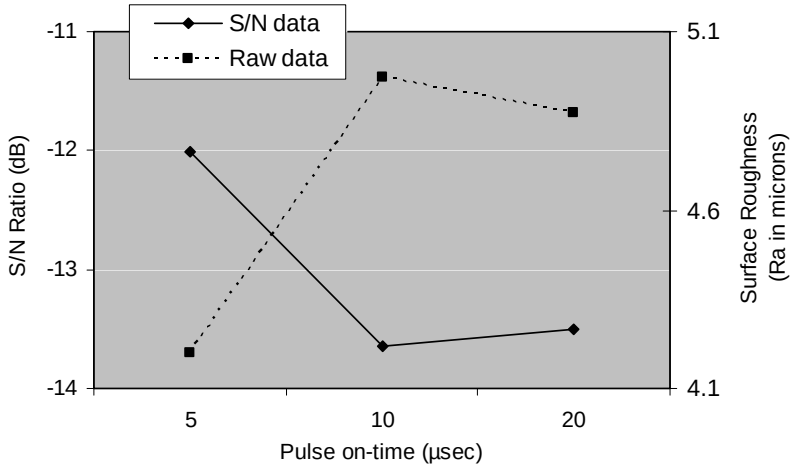

Fig. 4.17 (b) Effect of Pulse on-time on Surface Roughness and its S/N ratio (W3 – EL3)

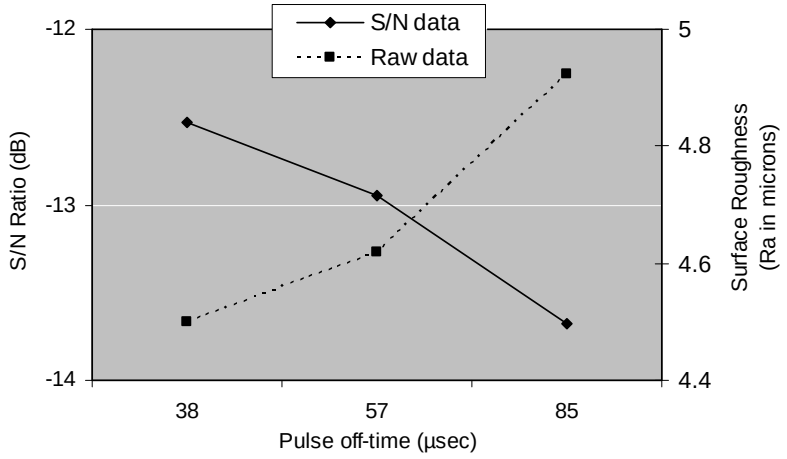

Fig. 4.17 (c) Effect of Pulse off-time on Surface Roughness and its S/N ratio (W3 – EL3)

It is observed from Fig. 4.17 (a), (b) and (c) that the first level of peak current (A_1), first level of pulse on-time (B_1) and the first level of pulse off-time (C_1) give the lowest values of surface roughness. Hence, the optimum combination of input process parameters is $A_1B_1C_1$. The theoretical value of η_{opt} for this optimum combination is given by:

$$\eta_{opt} = m + (m_{A1} - m) + (m_{B1} - m) + (m_{C1} - m) = -8.6199$$

The corresponding value of surface roughness is given by

$$y_{opt}^2 = 10^{-\eta opt / 10}$$

or, $$y_{opt} = 2.70\ \mu m$$

Since this combination existed in the orthogonal array (as first row), a confirmation experiment was not required. The average value of micro-hardness obtained at this setting of the experiment was 2.68 μm which is very close to the theoretical value predicted by Taguchi analysis.

Analysis of variance (ANOVA) of the S/N data was performed to obtain the percentage contribution of the factors and their significance. It is presented in Table 4.44 and it can be seen that all the three factors are significant for the response characteristic of surface roughness. Contribution of peak current is found to be the highest whereas the contribution of error is negligible.

Table 4.44 ANOVA Table of S/N data for Surface Roughness (W3 – EL3)

Factor/Source	Sum of Squares	DOF	V	F-ratio	% Contri-bution	Remarks
Peak Current	50.1307	2	25.0653	1454.79	87.75	Significant
Pulse on-time	4.9471	2	2.4736	143.57	8.66	Significant
Pulse off-time	2.0176	2	1.0088	58.55	3.53	Significant
Error (Pooled)	0.0345	2	0.0173	-	0.06	-
Total	57.1299	8		-	100	
DOF = Degrees of Freedom, V = Variance, Tabulated F-ratio $_{0.05}(2, 2) = 19$						

4.4 MACHINING WITH INCONEL ELECTRODE (EL4)

4.4.1 Work Material – OHNS die steel (W1)

The observed values of micro-hardness and surface roughness after machining OHNS die steel with inconel electrode and calculated values of their S/N ratios are given in Table 4.45.

Table 4.45 Observed values of Micro-hardness and Surface roughness and their calculated S/N ratios (W1 – EL4)

Expt. No.	Micro-hardness (HV)			S/N Ratio (dB)	Surface Roughness (R_a in microns)			S/N Ratio (dB)
	R1	R2	R3		R1	R2	R3	
1	782	823	835	58.195	6.82	6.91	7.11	-16.837
2	832	856	847	58.535	7.03	6.58	6.68	-16.607
3	823	765	776	57.918	6.50	6.17	6.21	-15.980
4	1098	1158	1173	61.136	9.52	9.93	9.73	-19.761
5	986	1024	1001	60.029	8.19	8.25	7.88	-18.179
6	973	990	955	59.756	9.33	8.83	9.67	-19.354
7	1005	998	983	59.958	9.91	9.76	9.65	-19.801
8	945	932	928	59.415	9.95	9.83	10.1	-19.966
9	978	982	995	59.868	10.6	10.4	10.7	-20.479
Total	8422	8522	8493	534.810	77.85	76.66	77.73	-166.963
	$\overline{T}_{MH}$ = Overall mean of micro hardness = 942.11			Mean, m= 59.423	$\overline{T}_{SR}$ = Overall mean of surface roughness = 8.601			Mean, m= -18.551
R1, R2 and R3 represent the three repetitions.								

From this data, the average values of micro-hardness and corresponding S/N ratios for the three levels of peak current, pulse on-time and pulse off-time have been calculated and are given in Table 4.46.

Table 4.46 Average values by factor levels for Micro-hardness (W1 – EL4)

Parameter / Levels	Peak Current (amperes)		Pulse on-time (µsec)		Pulse off-time (µsec)	
	Raw Data	S/N Data	Raw Data	S/N Data	Raw Data	S/N Data
L1	815.44	58.216	983.22	59.763	907.00	59.122
L2	1039.11	60.307	927.89	59.326	990.33	59.846
L3	971.78	59.747	915.22	59.181	929.00	59.301

These factor effects have been plotted and presented in Fig. 4.18 (a), (b) and (c).

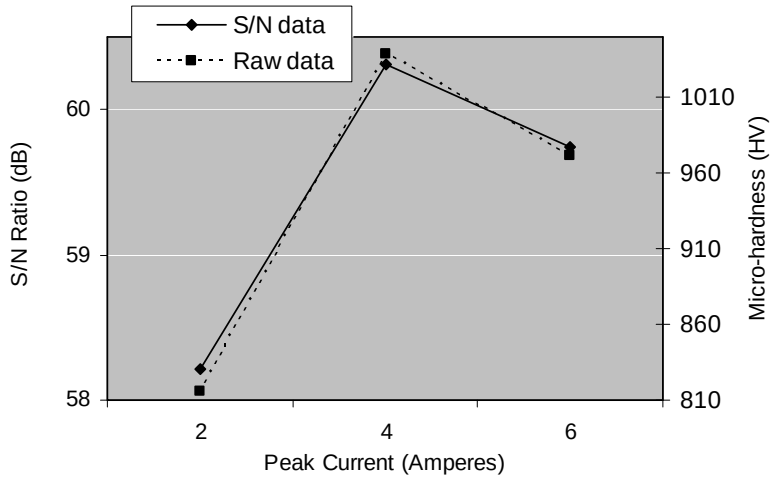

Fig. 4.18 (a) Effect of Peak Current on Micro-hardness and its S/N ratio (W1 – EL4)

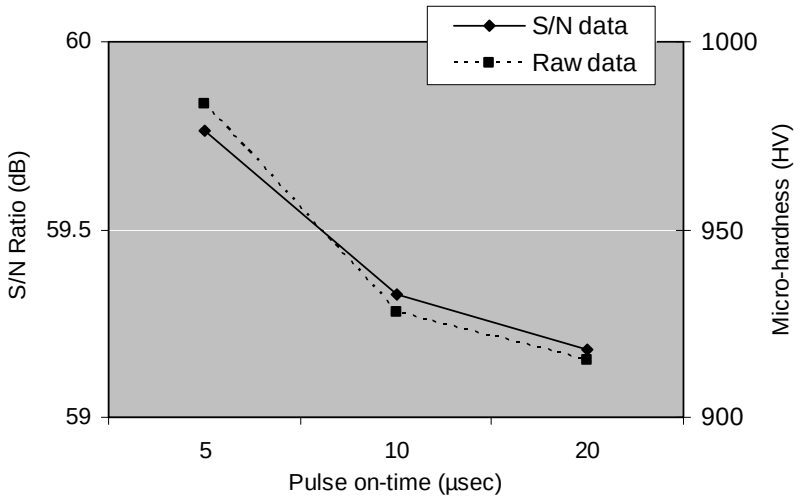

Fig. 4.18 (b) Effect of Pulse on-time on Micro-hardness and its S/N ratio (W1 – EL4)

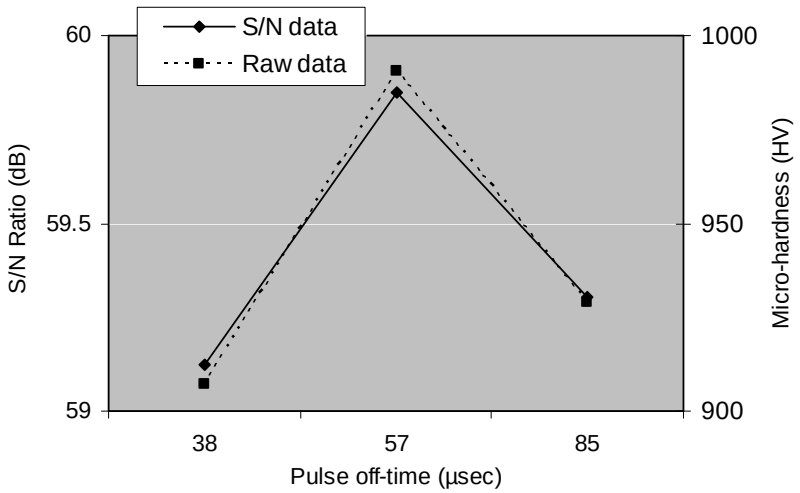

Fig. 4.18 (c) Effect of Pulse off-time on Micro-hardness and its S/N ratio (W1 – EL4)

It is observed from Fig. 4.18 (a), (b) and (c) that for the first time, micro-hardness decreases as peak current changes from level 2 (4 amperes) to level 3 (6 amperes). It can be attributed to material transfer from the inconel electrode and quenching effect at level 2 but only quenching effect at level 3. The response to variation in pulse on-time and off-time remains the same. It is also observed that the second level of peak current (A_2), first level of pulse on-time (B_1) and the second level of pulse off-time (C_2) give the highest values of micro-hardness. Hence, the optimum condition of input process parameters is $A_2B_1C_2$. Since this combination existed in the orthogonal array (as fourth row), a confirmation experiment was not required. The average value of micro-hardness obtained at this setting of the experiment was 1141 HV which can be compared with the theoretical value predicted by Taguchi analysis. The theoretical value of η under the optimum conditions, denoted by η_{opt}, is given by:

$$\eta_{opt} = m + (m_{A2} - m) + (m_{B1} - m) + (m_{C2} - m) = 61.069$$

where m is the overall mean of S/N data, m_{A2} is the mean of S/N data for factor A at level 2 and m_{B1} is the mean of S/N data for factor B at level 1, etc.

The corresponding value of micro-hardness is given by

$$y_{opt}^2 = 1 / 10^{-\eta opt / 10}$$

or, $$y_{opt} = 1131.02 \text{ HV}$$

which is very close to the observed experimental value.

To obtain percentage contribution of the three factors and their significance, analysis of variance (ANOVA) of the S/N data was performed. It is presented in Table 4.47 which shows that all the three factors are significant for the response characteristic of micro-hardness. While peak current remains the most significant factor, it is important to observe that the percentage contribution of pulse off-time exceeds that of pulse on-time. Error contribution is less than 1 %.

Table 4.47 ANOVA Table of S/N data for Micro-hardness (W1 – EL4)

Factor/Source	Sum of Squares	DOF	V	F-ratio	% Contri-bution	Remarks
Peak Current	7.0299	2	3.5149	294.44	83.12	Significant
Pulse on-time	0.5507	2	0.2753	23.07	6.51	Significant
Pulse off-time	0.8531	2	0.4265	35.73	10.09	Significant
Error (Pooled)	0.0239	2	0.0119	-	0.28	-
Total	8.4576	8		-	100	
DOF = Degrees of Freedom, V = Variance, Tabulated F-ratio $_{0.05}$ (2, 2) = 19						

Similar analysis has now been done for surface roughness. From the experimental data given in Table 4.45, the average values of surface roughness and the corresponding S/N ratios for the three levels of input process parameters have been calculated and are given in Table 4.48.

Table 4.48 Average values by factor levels for Surface Roughness (W1 – EL4)

Parameter / Levels	Peak Current (Amperes)		Pulse on-time (µsec)		Pulse off-time (µsec)	
	Raw Data	S/N Data	Raw Data	S/N Data	Raw Data	S/N Data
L1	6.67	-16.475	8.82	-18.800	8.73	-18.719
L2	9.04	-19.098	8.28	-18.250	9.02	-18.949
L3	10.10	-20.082	8.71	-18.604	8.06	-17.987

These factor effects have been plotted and presented in Fig. 4.19 (a), (b) and (c).

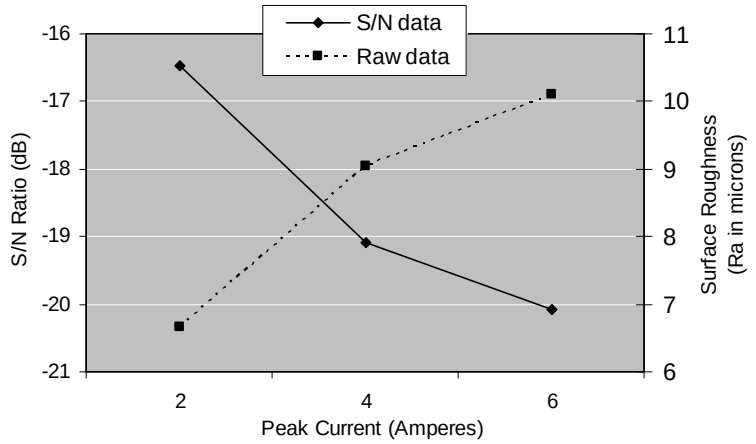

Fig. 4.19 (a) Effect of Peak Current on Surface Roughness and its S/N ratio (W1 – EL4)

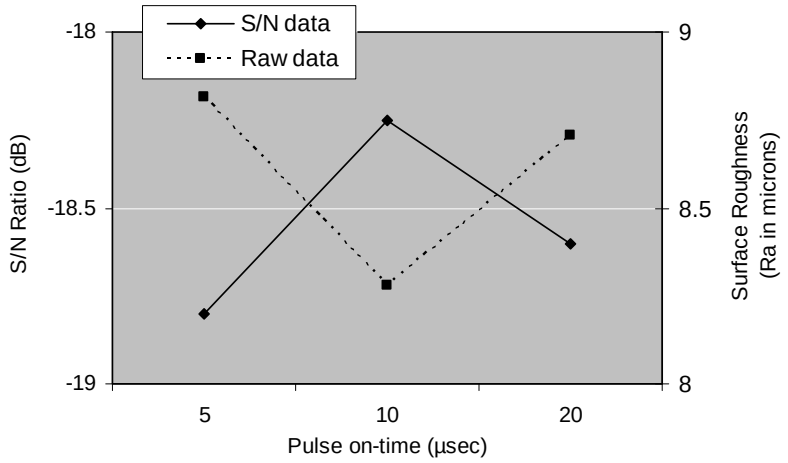

Fig. 4.19 (b) Effect of Pulse on-time on Surface Roughness and its S/N ratio (W1 – EL4)

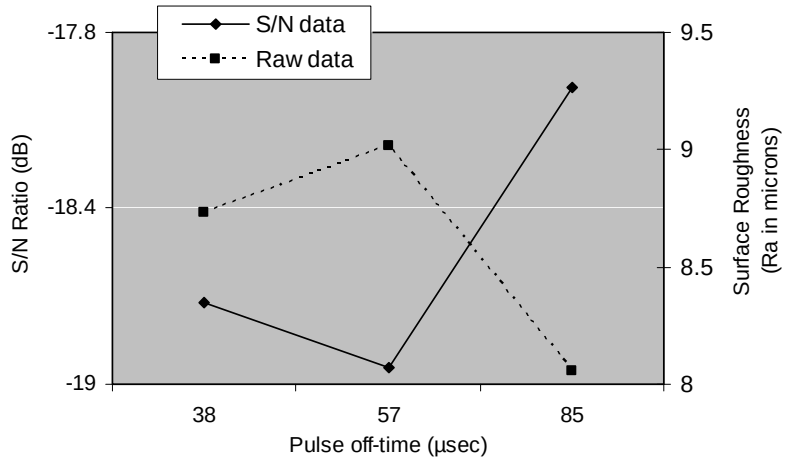

Fig. 4.19 (c) Effect of Pulse off-time on Surface Roughness and its S/N ratio (W1 – EL4)

It is observed from Fig. 4.19 (a), (b) and (c) that the first level of peak current (A_1), second level of pulse on-time (B_2) and the third level of pulse off-time (C_3) give the lowest values of surface roughness. Hence, the optimum condition of input process parameters is $A_1B_2C_3$. It is different from the optimum condition obtained for the other electrode materials. The theoretical value of η_{opt} under the optimum conditions is given by:

$$\eta_{opt} = m + (m_{A1} - m) + (m_{B2} - m) + (m_{C3} - m) = -15.609$$

The corresponding value of surface roughness is given by

$$y_{opt}^2 = 10^{-\eta opt / 10}$$

or, $$y_{opt} = 6.03\ \mu m$$

Since this combination of input process parameters did not exist in the orthogonal array, a set of three confirmation experiments were conducted. The average value of surface roughness obtained at this setting of the experiment was 5.91 μm which is better than and very close to the theoretical value predicted by Taguchi analysis.

Analysis of variance (ANOVA) of the S/N data was performed to obtain the percentage contribution of the factors and their significance. It is presented in Table 4.49 and it can be seen that all the three factors are significant for the response characteristic of surface roughness. For this response characteristic also, the contribution of pulse off-time is found to be more than pulse on-time.

Table 4.49 ANOVA Table of S/N data for Surface Roughness (W1 – EL4)

Factor/Source	Sum of Squares	DOF	V	F-ratio	% Contri-bution	Remarks
Peak Current	20.8650	2	10.4325	1575.42	91.28	Significant
Pulse on-time	0.4651	2	0.2325	35.12	2.03	Significant
Pulse off-time	1.5149	2	0.7575	114.38	6.63	Significant
Error (Pooled)	0.0132	2	0.0066	-	0.06	-
Total	22.8583	8		-	100	
DOF = Degrees of Freedom, V = Variance, Tabulated F-ratio $_{0.05}(2, 2) = 19$						

4.4.2 Work Material – H13 hot die steel (W3)

The observed values of micro-hardness and surface roughness after machining H13 hot die steel with inconel electrode and calculated values of their S/N ratios are given in Table 4.50.

Table 4.50 Observed values of Micro-hardness and Surface roughness and their calculated S/N ratios (W3 – EL4)

Expt. No.	Micro-hardness (HV)			S/N Ratio (dB)	Surface Roughness (R_a in microns)			S/N Ratio (dB)
	R1	R2	R3		R1	R2	R3	
1	604	591	623	55.643	8.32	8.53	8.47	-18.527
2	642	665	639	56.236	8.24	8.45	8.72	-18.560
3	618	632	625	55.917	9.32	9.21	8.93	-19.233
4	856	887	879	58.827	11.8	12.2	12.3	-21.657
5	827	788	803	58.122	10.9	11.4	11.5	-21.038
6	751	734	712	57.288	11.3	11.0	10.9	-20.881
7	768	738	755	57.540	11.4	11.8	11.6	-21.290
8	717	653	662	56.594	10.2	10.1	9.83	-20.039
9	738	726	743	57.332	10.9	11.4	11.6	-21.065
Total	6521	6414	6441	513.499	92.38	94.09	93.85	-182.290
	$\overline{T}_{MH}$ = Overall mean of micro hardness = 717.63			Mean, m= 57.056	$\overline{T}_{SR}$ = Overall mean of surface roughness = 10.382			Mean, m= -20.255
R1, R2 and R3 represent the three repetitions.								

From this data, the average values of micro-hardness and corresponding S/N ratios for the three levels of peak current, pulse on-time and pulse off-time have been calculated and are given in Table 4.51. These average values represent the factor effects of input parameters.

Table 4.51 Average values by factor levels for Micro-hardness (W3 – EL4)

Parameter / Levels	Peak Current (amperes)		Pulse on-time (µsec)		Pulse off-time (µsec)	
	Raw Data	S/N Data	Raw Data	S/N Data	Raw Data	S/N Data
L1	626.56	55.932	744.56	57.337	671.89	56.508
L2	804.11	58.079	710.67	56.984	752.78	57.465
L3	722.22	57.156	697.67	56.846	728.22	57.193

These factor effects have been plotted and presented in Fig. 4.20 (a), (b) and (c).

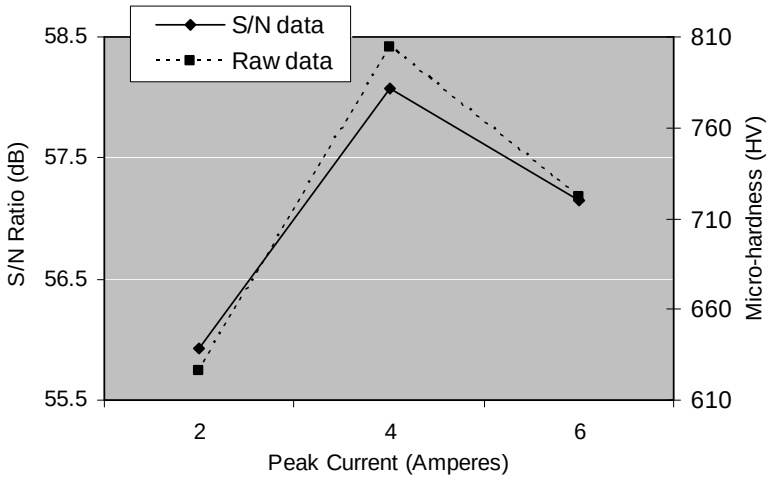

Fig. 4.20 (a) Effect of Peak Current on Micro-hardness and its S/N ratio (W3 – EL4)

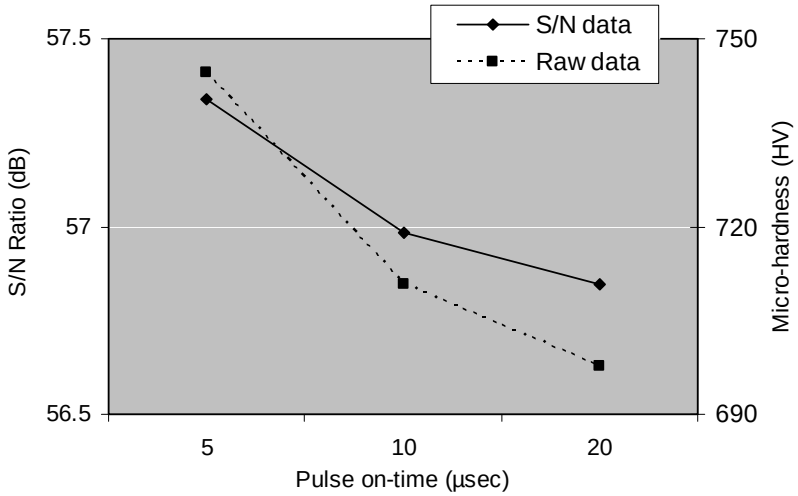

Fig. 4.20 (b) Effect of Pulse on-time on Micro-hardness and its S/N ratio (W3 – EL4)

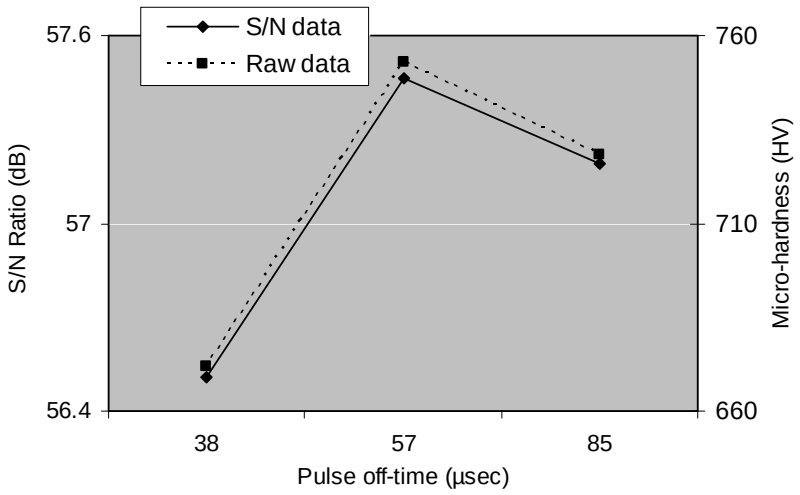

Fig. 4.20 (c) Effect of Pulse off-time on Micro-hardness and its S/N ratio (W3 – EL4)

Once again, the response of micro-hardness to variation in peak current for inconel electrode is found to be different from the other three electrode materials. But it is consistent with the behaviour of OHNS die steel and the actual value of micro-hardness achieved for both the work materials with this electrode is very high. Out of the four electrode materials, copper-tungsten and inconel give very good micro-hardness and in both cases, it is achieved at level 2 (57 μsec) of pulse off-time. It is also observed from Fig. 4.20 (a), (b) and (c) that the highest values of micro-hardness are achieved at the second level of peak current (A_2), first level of pulse on-time (B_1) and second level of pulse off-time (C_2). Hence, the optimum condition of input process parameters is $A_2B_1C_2$. Since this combination existed in the orthogonal array (as fourth row), a confirmation experiment was not required. The average value of micro-hardness obtained at this setting of the experiment was 874 HV which can be compared with the theoretical value η_{opt} predicted by Taguchi analysis.

$$\eta_{opt} = m + (m_{A2} - m) + (m_{B1} - m) + (m_{C2} - m)$$

$$= 58.770$$

The corresponding value of micro-hardness is given by

$$y_{opt}^2 = 1 / 10^{-\eta opt / 10}$$

or, $$y_{opt} = 867.97 \text{ HV}$$

which is very close to the observed experimental value.

To obtain percentage contribution of the three factors and their significance, analysis of variance (ANOVA) of the S/N data was performed. It is presented in Table 4.52 which shows that all the three factors are significant for the response characteristic of micro-hardness. For this work material also, it is important to observe that the percentage contribution of pulse off-time exceeds that of pulse on-time. Peak current is the major contributor and error contribution is found to be less than 1 %.

Table 4.52 ANOVA Table of S/N data for Micro-hardness (W3 – EL4)

Factor/Source	Sum of Squares	DOF	V	F-ratio	% Contri-bution	Remarks
Peak Current	6.9585	2	3.4792	468.24	78.92	Significant
Pulse on-time	0.3851	2	0.1925	25.91	4.37	Significant
Pulse off-time	0.4580	2	0.2290	98.11	16.54	Significant
Error (Pooled)	0.0149	2	0.0075	-	0.17	-
Total	8.8165	8		-	100	
DOF = Degrees of Freedom, V = Variance, Tabulated F-ratio $_{0.05}$ (2, 2) = 19						

Similar analysis has now been done for surface roughness. From the experimental data given in Table 4.50, the average values of surface roughness and the corresponding S/N ratios for the three levels of input process parameters have been calculated and are given in Table 4.53.

Table 4.53 Average values by factor levels for Surface Roughness (W3 – EL4)

Parameter / Levels	Peak Current (Amperes)		Pulse on-time (µsec)		Pulse off-time (µsec)	
	Raw Data	S/N Data	Raw Data	S/N Data	Raw Data	S/N Data
L1	8.69	-18.773	10.71	-20.492	9.85	-19.816
L2	11.48	-21.192	9.93	-19.879	10.62	-20.427
L3	10.98	-20.798	10.51	-20.393	10.67	-20.520

These factor effects have been plotted and presented in Fig. 4.21 (a), (b) and (c).

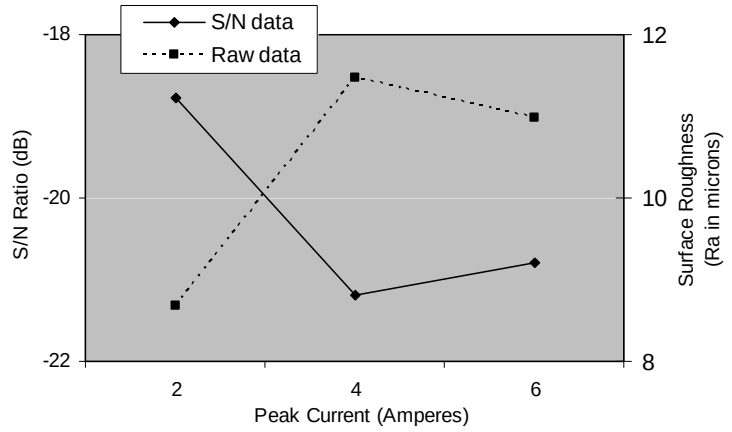

Fig. 4.21 (a) Effect of Peak Current on Surface Roughness and its S/N ratio (W3 – EL4)

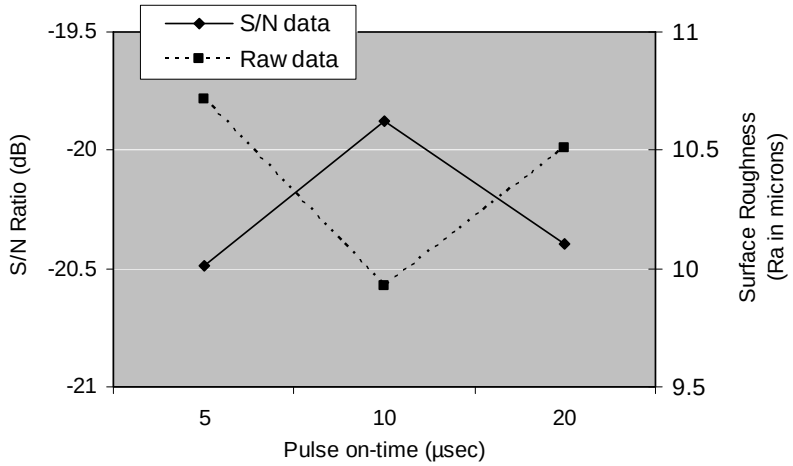

Fig. 4.21 (b) Effect of Pulse on-time on Surface Roughness and its S/N ratio (W3 – EL4)

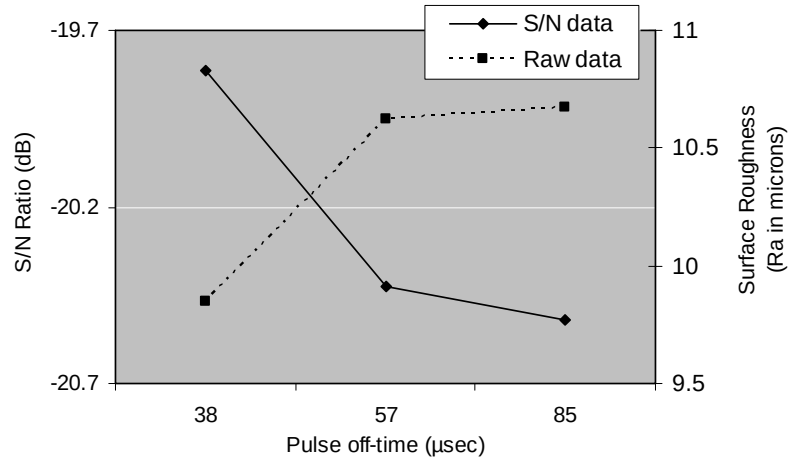

Fig. 4.21 (c) Effect of Pulse off-time on Surface Roughness and its S/N ratio (W3 – EL4)

It is observed from Fig. 4.21 (a), (b) and (c) that the first level of peak current (A_1), second level of pulse on-time (B_2) and first level of pulse off-time (C_1) give the lowest values of surface roughness. Hence, the optimum condition of input process parameters is $A_1B_2C_1$. The theoretical value of η_{opt} under the optimum conditions is given by:

$$\eta_{opt} = m + (m_{A1} - m) + (m_{B2} - m) + (m_{C1} - m) = -17.959$$

The corresponding value of surface roughness is given by

$$y_{opt}^2 = 10^{-\eta opt / 10}$$

or, $$y_{opt} = 7.91\ \mu m$$

Since this combination of input process parameters did not exist in the orthogonal array, a set of three confirmation experiments were conducted. The average value of surface roughness obtained at this setting of the experiment was 7.78 μm which is better than and very close to the theoretical value predicted by Taguchi analysis.

Analysis of variance (ANOVA) of the S/N data was performed to obtain the percentage contribution of the three factors and their significance. It is presented in Table 4.54 and it can be seen that all the three factors are significant for the response characteristic of surface roughness. It is important to note that for this response characteristic also, the contribution of pulse off-time is found to be more than pulse on-time.

Table 4.54 ANOVA Table of S/N data for Surface Roughness (W3 – EL4)

Factor/Source	Sum of Squares	DOF	V	F-ratio	% Contri-bution	Remarks
Peak Current	10.1039	2	5.0519	657.37	86.75	Significant
Pulse on-time	0.6491	2	0.3245	42.23	5.57	Significant
Pulse off-time	0.8791	2	0.4395	57.19	7.55	Significant
Error (Pooled)	0.0154	2	0.0077	-	0.13	-
Total	11.6475	8		-	100	
DOF = Degrees of Freedom, V = Variance, Tabulated F-ratio $_{0.05}(2, 2) = 19$						

CHAPTER - 5

EXPERIMENTATION WITH POWDER – MIXED DIELECTRIC

For this second stage of experimentation, the three work materials were machined using four different powders mixed in the dielectric medium. These powders were graphite, manganese, silicon and tungsten. Copper was used as the tool electrode and kerosene as the dielectric medium for all the experiments. Negative polarity was given to the tool electrode and the time for each machining cut was fixed at 10 minutes. A pictorial view of the powders is shown in Fig. 5.1.

Fig. 5.1 Pictorial view of powders used for experimentation

Composition analysis of the powders was carried out at the Chemical Analysis Lab. of Modern Steels Ltd., Mandi Gobindgarh, Punjab and the results are given in Table 5.1.

Table 5.1 Results of Chemical testing of the four powders

Powder	Chemical Composition	Particle size
Graphite	More than 99 % purity	10 – 20 μm
Manganese	More than 99.5 % purity	30 – 40 μm
Silicon	More than 99 % purity	10 – 20 μm
Tungsten	More than 99.5 % purity	30 – 40 μm

As explained in Para 3.4, a smaller tank made of mild steel was placed in the main machining tank for conducting the experiments. This tank was provided with a stirrer to keep the powder suspended uniformly in the dielectric throughout the machining cycle. A schematic diagram of the machining set-up is given in Fig. 5.2.

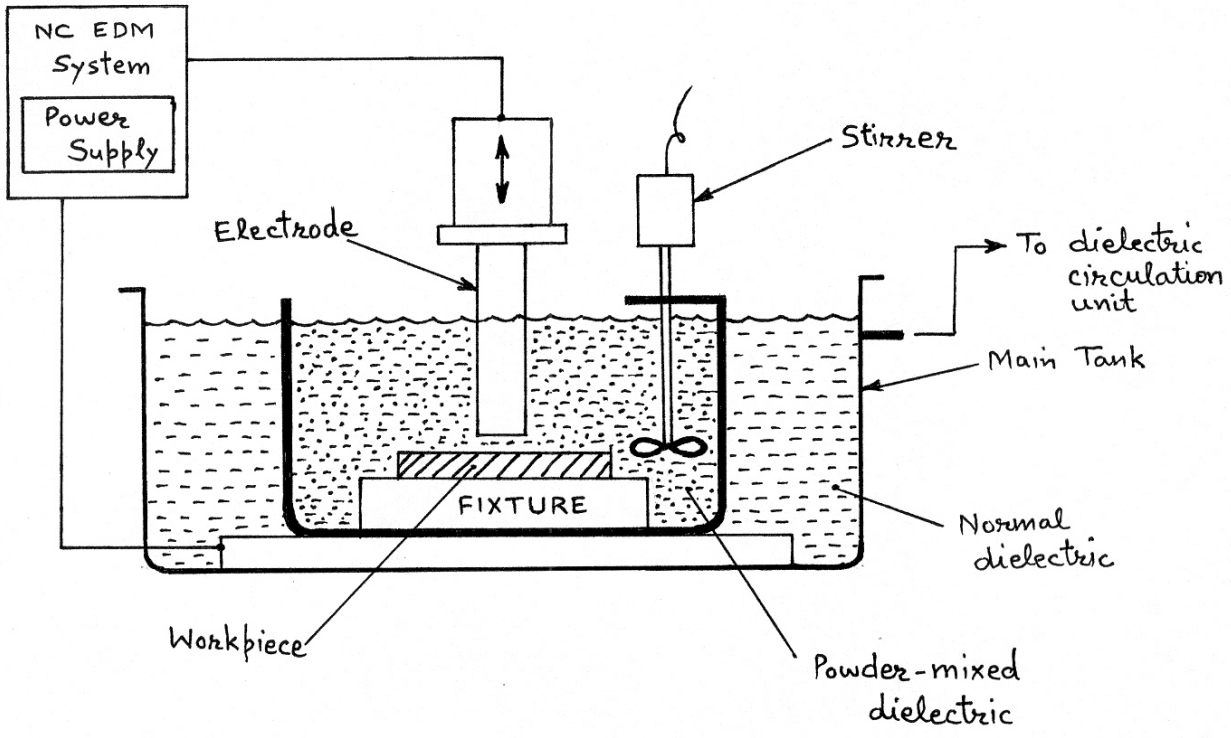

Fig. 5.2 Schematic diagram of Machining set-up for Powder-mixed dielectric

Fixture for holding the work pieces was kept in this tank. After mounting the workpiece on the fixture, the tank was filled with the dielectric flowing from the opening in the tool electrode holder. The level of the dielectric in this tank was kept at par with that of the main tank. Copper electrode was mounted in the tool holder. Desired quantity of one of the powders was then mixed in the dielectric and stirrer was switched on. The values of pulse on-time and pulse off-time were set from the control panel of the machine according to the control log given in Table 3.3. Any one row of the control log was taken at random. Copper electrode was brought near the workpiece and sparking was switched on. The setting of peak current was initially at the minimum which was gradually increased to the desired level. Since very little work material was being removed during the machining cycle and the purpose of the experimentation was to deposit the products of sparking and the suspended powder, dielectric flushing was switched off. The agitation caused by the stirrer was sufficient to keep the dielectric in motion near the machining area.

After 10 minutes of operation, the machine and the stirrer were switched off. The powder-mixed dielectric was siphoned off to a separate container and the workpiece was replaced by a new one. Copper electrode was cleaned and turned on a lathe to remove any surface irregularities and get a fresh surface for subsequent machining. It was again mounted in the tool holder, the powder-mixed dielectric was filled back and machining was started with the new set of values of the three input process parameters. Fresh powder was used after completion of each set of nine experiments.

The set of nine experiments as per Taguchi L9 orthogonal array were repeated three times for each combination of powder and work material. Thus, a total of 11 sets of experiments (with the exception that D2 high-carbon high-chromium work material was not machined using graphite powder as explained in Para 3.1.1) were conducted. The effect on the two response characteristics of micro-hardness and surface roughness has been studied and presented in this chapter. As done in the previous chapter, the experimental data was analyzed using Taguchi method to find out the optimum machining parameters for each response characteristic, their significance and percentage contribution. Verification experiments were conducted where the best combination of machining conditions as suggested by the analysis did not exist in the orthogonal array.

5.1 MACHINING WITH GRAPHITE POWDER (PW1)

5.1.1 Work Material – OHNS die steel (W1)

The observed values of micro-hardness and surface roughness after machining OHNS die steel with graphite powder mixed in the dielectric medium and the calculated values of their S/N ratios are given in Table 5.2.

Table 5.2 Observed values of Micro-hardness and Surface roughness and their calculated S/N ratios (W1 – PW1)

Expt. No.	Micro-hardness (HV)			S/N Ratio (dB)	Surface Roughness (R_a in microns)			S/N Ratio (dB)
	R1	R2	R3		R1	R2	R3	
1	671	692	667	56.604	0.83	0.97	0.78	1.272
2	685	652	678	56.537	1.09	1.02	0.95	-0.186
3	693	671	654	56.549	1.11	1.18	1.07	-0.992
4	732	745	753	57.422	1.18	1.05	1.20	-1.178
5	748	719	737	57.318	1.42	1.68	1.77	-4.244
6	716	688	703	56.927	1.63	1.95	1.81	-5.112
7	735	729	711	57.204	1.75	1.56	1.93	-4.877
8	675	713	682	56.770	2.23	2.51	2.42	-7.566
9	698	680	673	56.694	2.09	1.93	2.18	-6.316
Total	6353	6289	6258	512.025	13.33	13.85	14.11	-29.199
	$\overline{T}_{MH}$ = Overall mean of micro hardness = 700.00			Mean, m= 56.892	$\overline{T}_{SR}$ = Overall mean of surface roughness = 1.529			Mean, m= -3.244
R1, R2 and R3 represent the three repetitions.								

From this data, the average values of micro-hardness and the corresponding S/N ratios for the three levels of input process parameters have been calculated and are given in Table 5.3.

Table 5.3 Average values by factor levels for Micro-hardness (W1 – PW1)

Parameter / Levels	Peak Current (amperes)		Pulse on-time (µsec)		Pulse off-time (µsec)	
	Raw Data	S/N Data	Raw Data	S/N Data	Raw Data	S/N Data
L1	673.67	56.563	715.00	57.077	689.67	56.767
L2	726.78	57.223	698.78	56.875	699.56	56.884
L3	699.56	56.889	686.22	56.723	710.78	57.024

These factor effects have been plotted and presented in Fig. 5.3 (a), (b) and (c).

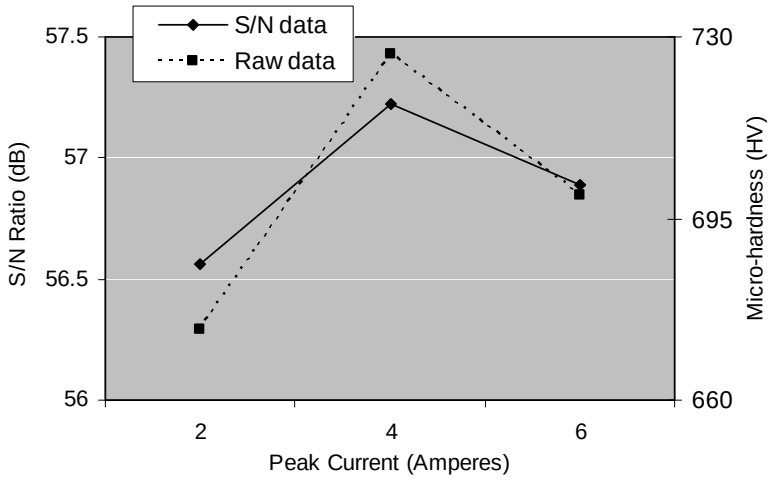

Fig. 5.3 (a) Effect of Peak Current on Micro-hardness and its S/N ratio (W1 – PW1)

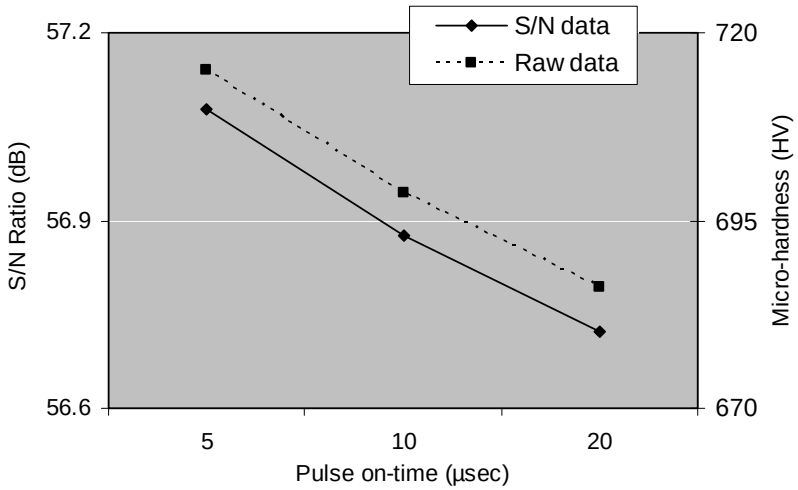

Fig. 5.3 (b) Effect of Pulse on-time on Micro-hardness and its S/N ratio (W1 – PW1)

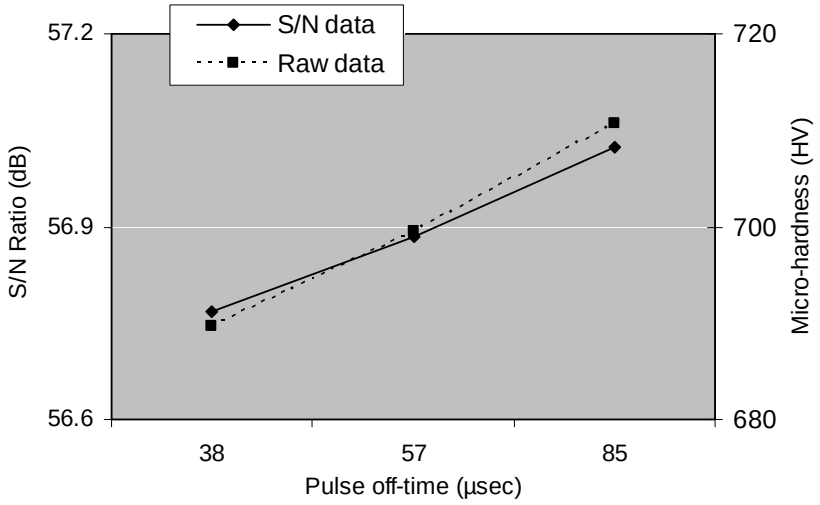

Fig. 5.3 (c) Effect of Pulse off-time on Micro-hardness and its S/N ratio (W1 – PW1)

Micro-hardness is the 'higher-the-better' type of response characteristic. Therefore, higher values of micro-hardness are considered to be optimal. It can be observed from Fig. 5.3 (a), (b) and (c) that the second level of peak current (A_2), first level of pulse on-time (B_1) and the third level of pulse off-time (C_3) give the highest values of micro-hardness. Hence, the optimum condition of input process parameters is $A_2B_1C_3$. The theoretical value of η_{opt} under the optimum conditions is given by:

$$\eta_{opt} = m + (m_{A2} - m) + (m_{B1} - m) + (m_{C3} - m)$$

$$= 57.5396$$

where m is the overall mean of S/N data, m_{A2} is the mean of S/N data for factor A at level 2 and m_{B2} is the mean of S/N data for factor B at level 2, etc.

The corresponding value of micro-hardness is given by

$$y_{opt}^2 = 1 / 10^{-\eta opt / 10}$$

or, $$y_{opt} = 753.32 \text{ HV}$$

Since this combination of input process parameters did not exist in the orthogonal array, a set of three confirmation experiments were conducted. The average value of micro-hardness obtained at this setting of the experiment was 743.33 HV which is very close to the theoretical value predicted by Taguchi analysis.

To obtain percentage contribution of the three factors and their significance, analysis of variance (ANOVA) of the S/N data was performed. It is presented in Table 5.4 which shows that all the three factors are significant for the response characteristic of micro-hardness. Peak current is found to be the major contributor at 69.19 % whereas the contribution of pulse on-time is almost double that of pulse off-time.

Table 5.4 ANOVA table of S/N data for Micro-hardness (W1 – PW1)

Factor/Source	Sum of Squares	DOF	V	F-ratio	% Contri-bution	Remarks
Peak Current	0.6519	2	0.3259	252.51	69.19	Significant
Pulse on-time	0.1886	2	0.0943	73.06	20.02	Significant
Pulse off-time	0.0990	2	0.0495	38.37	10.51	Significant
Error (Pooled)	0.0026	2	0.0013	-	0.28	-
Total	0.9421	8		-	100	
DOF = Degrees of Freedom, V = Variance, Tabulated F-ratio $_{0.05}$ (2, 2) = 19						

Similar analysis has now been done for surface roughness. From the experimental data given in Table 5.2, the average values of surface roughness and the corresponding S/N ratios for the three levels of input process parameters have been calculated and are given in Table 5.5. These average values represent the factor effects of input parameters.

Table 5.5 Average values by factor levels for Surface Roughness (W1 – PW1)

Parameter	Peak Current (Amperes)		Pulse on-time (µsec)		Pulse off-time (µsec)	
Levels	Raw Data	S/N Data	Raw Data	S/N Data	Raw Data	S/N Data
L1	1.00	0.032	1.25	-1.594	1.68	-3.802
L2	1.52	-3.512	1.68	-3.999	1.41	-2.560
L3	2.07	-6.253	1.66	-4.140	1.50	-3.371

These factor effects have been plotted and presented in Fig. 5.4 (a), (b) and (c).

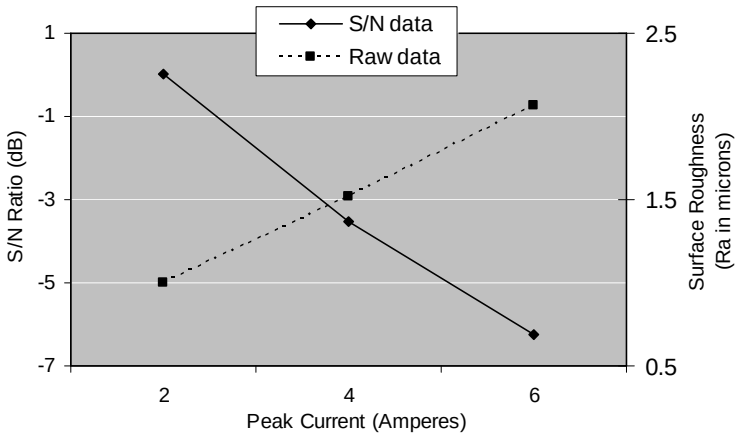

Fig. 5.4 (a) Effect of Peak Current on Surface Roughness and its S/N ratio (W1 – PW1)

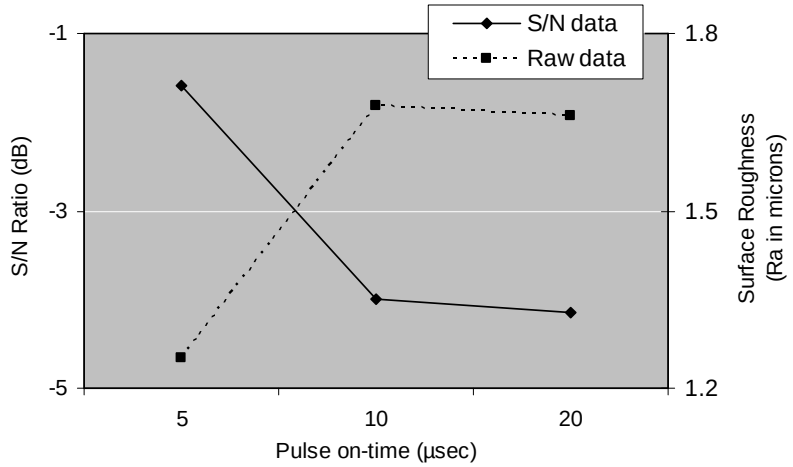

Fig. 5.4 (b) Effect of Pulse on-time on Surface Roughness and its S/N ratio (W1 – PW1)

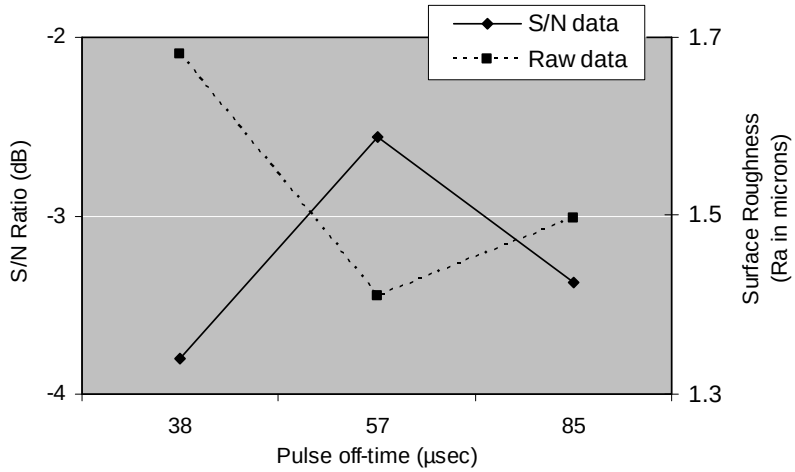

Fig. 5.4 (c) Effect of Pulse off-time on Surface Roughness and its S/N ratio (W1 – PW1)

Surface roughness is the 'lower-the-better' type of response characteristic. Therefore, lower values of surface roughness are considered to be optimal. It can be observed from Fig. 5.4 (a), (b) and (c) that the first level of peak current (A_1), first level of pulse on-time (B_1) and the second level of pulse off-time (C_2) give the lowest values of surface roughness. Hence, the optimum condition of input process parameters is $A_1B_1C_2$. The theoretical value of η_{opt} under the optimum conditions is given by:

$$\eta_{opt} = m + (m_{A1} - m) + (m_{B1} - m) + (m_{C2} - m) = 2.366$$

The corresponding value of surface roughness is given by

$$y_{opt}^2 = 10^{-\eta opt / 10}$$

or, $$y_{opt} = 0.76\ \mu m$$

Since this combination of input process parameters did not exist in the orthogonal array, a set of three confirmation experiments were conducted. The average value of surface roughness obtained at this setting of the experiment was 0.73 μm which is better than and very close to the theoretical value predicted by Taguchi analysis.

Analysis of variance (ANOVA) of the S/N data was performed to obtain the percentage contribution of the factors and their significance. It is presented in Table 5.6 and it can be seen that all the three factors are significant for the response characteristic of surface roughness. Error contribution is found to be less than 1 %.

Table 5.6 ANOVA table of S/N data for Surface Roughness (W1 – PW1)

Factor/Source	**Sum of Squares**	**DOF**	**V**	**F-ratio**	**% Contri-bution**	**Remarks**
Peak Current	59.5679	2	29.7840	455.06	80.10	Significant
Pulse on-time	12.2834	2	6.1417	93.84	16.51	Significant
Pulse off-time	2.3863	2	1.1932	18.23	3.21	≈Significant
Error (Pooled)	0.1309	2	0.0655	-	0.18	-
Total	74.3685	8		-	100	
DOF = Degrees of Freedom, V = Variance, Tabulated F-ratio $_{0.05}(2, 2) = 19$						

5.1.2 Work Material – H13 hot die steel (W3)

The observed values of micro-hardness and surface roughness after machining H13 hot die steel with graphite powder mixed in the dielectric medium and the calculated values of their S/N ratios are given in Table 5.7.

Table 5.7 Observed values of Micro-hardness and Surface roughness and their calculated S/N ratios (W3 – PW1)

Expt. No.	Micro-hardness (HV)			S/N Ratio (dB)	Surface Roughness (R_a in microns)			S/N Ratio (dB)
	R1	R2	R3		R1	R2	R3	
1	561	574	592	55.197	0.93	0.88	1.10	0.224
2	572	545	554	54.912	1.20	0.97	1.13	-0.861
3	588	571	567	55.195	1.37	1.52	1.58	-3.479
4	621	655	638	56.090	1.43	1.51	1.48	-3.368
5	627	642	615	55.955	1.66	1.93	1.87	-5.219
6	612	604	589	55.584	2.02	1.87	1.76	-5.512
7	637	626	618	55.943	2.12	2.34	2.29	-7.051
8	605	573	564	55.267	2.24	2.08	2.15	-6.680
9	567	612	581	55.355	2.55	2.46	2.38	-7.834
Total	5390	5402	5318	499.498	15.52	15.56	15.74	-39.781
	$\overline{T}_{MH}$ = Overall mean of micro hardness = 596.67			Mean, m= 55.500	$\overline{T}_{SR}$ = Overall mean of surface roughness = 1.734			Mean, m= -4.420
R1, R2 and R3 represent the three repetitions.								

From this data, the average values of micro-hardness and corresponding S/N ratios for the three levels of peak current, pulse on-time and pulse off-time have been calculated and are given in Table 5.8. These average values represent the factor effects of input parameters.

Table 5.8 Average values by factor levels for Micro-hardness (W3 – PW1)

Parameter / Levels	Peak Current (amperes)		Pulse on-time (µsec)		Pulse off-time (µsec)	
	Raw Data	S/N Data	Raw Data	S/N Data	Raw Data	S/N Data
L1	569.33	55.101	613.56	55.744	586.00	55.349
L2	622.56	55.876	588.56	55.378	593.89	55.452
L3	598.11	55.522	587.89	55.378	610.11	55.698

These factor effects have been plotted and presented in Fig. 5.5 (a), (b) and (c).

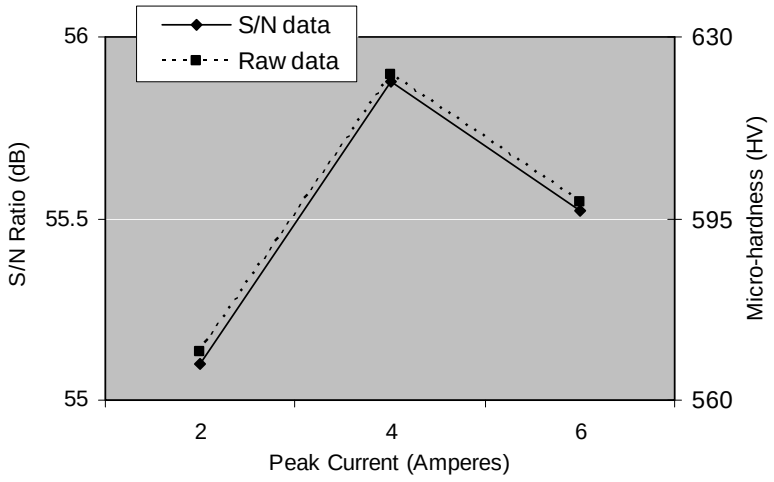

Fig. 5.5 (a) Effect of Peak Current on Micro-hardness and its S/N ratio (W3 – PW1)

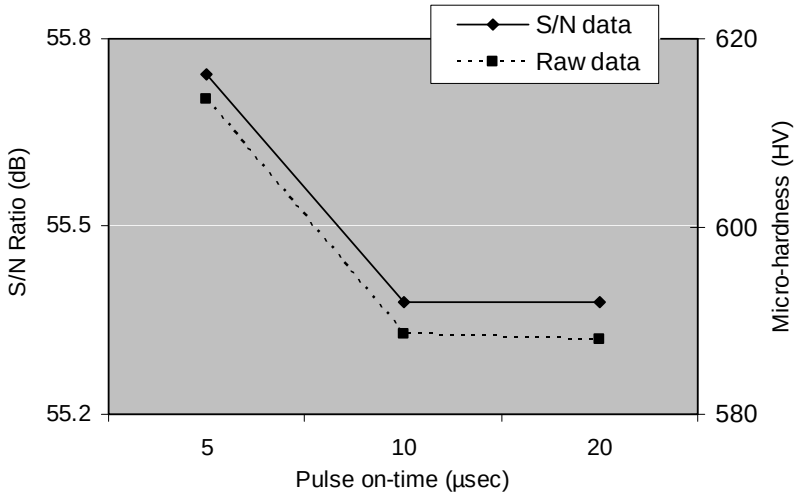

Fig. 5.5 (b) Effect of Pulse on-time on Micro-hardness and its S/N ratio (W3 – PW1)

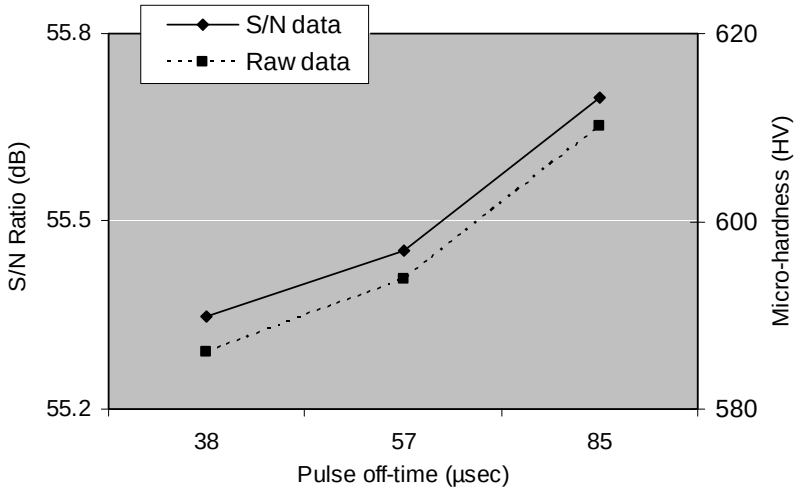

Fig. 5.5 (c) Effect of Pulse off-time on Micro-hardness and its S/N ratio (W3 – PW1)

It can be observed from Fig. 5.5 (a), (b) and (c) that the second level of peak current (A_2), first level of pulse on-time (B_1) and the third level of pulse off-time (C_3) give the highest values of micro-hardness. Hence, the optimum condition of input process parameters is $A_2B_1C_3$. When peak current changes from level 1 to level 2, there is a sharp increase in micro-hardness but after that, it shows a decline. This response can be attributed to material transfer and higher heating and quenching effect at level 2. It is also observed that micro-hardness decreases with increase in pulse-on-time but there is negligible change as pulse on-time further increases from level 2 to level 3. The theoretical value of η_{opt} under the optimum conditions is given by:

$$\eta_{opt} = m + (m_{A2} - m) + (m_{B1} - m) + (m_{C3} - m)$$

$$= 56.3183$$

The corresponding value of micro-hardness is given by

$$y_{opt}^2 = 1 / 10^{-\eta opt / 10}$$

or, $$y_{opt} = 654.51 \text{ HV}$$

Since this combination of input process parameters did not exist in the orthogonal array, a set of three confirmation experiments were conducted. The average value of micro-hardness obtained at this setting of the experiment was 663 HV which is better than and very close to the theoretical value predicted by Taguchi analysis.

To obtain percentage contribution of the three factors and their significance, analysis of variance (ANOVA) of the S/N data was performed. It is presented in Table 5.9 which shows that all the three factors are significant for the response characteristic of micro-hardness (a factor is significant if its calculated F-ratio is more than the tabulated F-ratio). Error contribution is found to be less than 1 %.

Table 5.9 ANOVA table of S/N data for Micro-hardness (W3 – PW1)

Factor/Source	Sum of Squares	DOF	V	F-ratio	% Contri-bution	Remarks
Peak Current	0.9031	2	0.4516	417.18	66.16	Significant
Pulse on-time	0.2674	2	0.1337	123.51	19.58	Significant
Pulse off-time	0.1925	2	0.0963	88.92	14.10	Significant
Error (Pooled)	0.0022	2	0.0011	-	0.16	-
Total	1.3652	8		-	100	
DOF = Degrees of Freedom, V = Variance, Tabulated F-ratio $_{0.05}$ (2, 2) = 19						

Similar analysis has now been done for surface roughness. From the experimental data given in Table 5.7, the average values of surface roughness and the corresponding S/N ratios for the three levels of input process parameters have been calculated and are given in Table 5.10. These average values represent the factor effects of input parameters.

Table 5.10 Average values by factor levels for Surface Roughness (W3 – PW1)

Parameter	Peak Current (Amperes)		Pulse on-time (µsec)		Pulse off-time (µsec)	
Levels	Raw Data	S/N Data	Raw Data	S/N Data	Raw Data	S/N Data
L1	1.19	-1.372	1.56	-3.399	1.67	-3.989
L2	1.73	-4.700	1.69	-4.253	1.68	-4.021
L3	2.29	-7.188	1.95	-5.608	1.85	-5.250

These factor effects have been plotted and presented in Fig. 5.6 (a), (b) and (c).

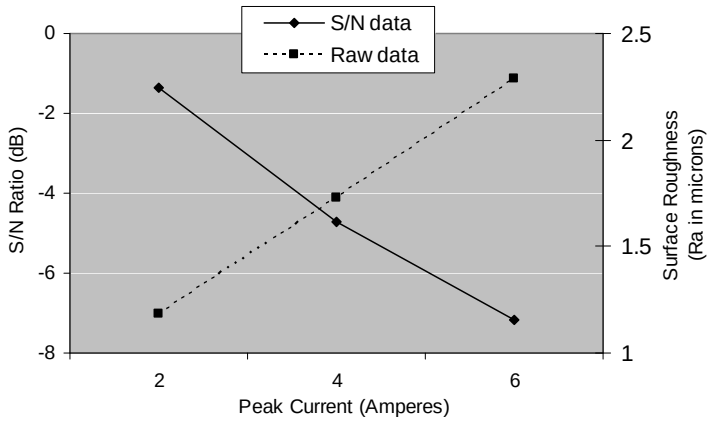

Fig. 5.6 (a) Effect of Peak Current on Surface Roughness and its S/N ratio (W3 – PW1)

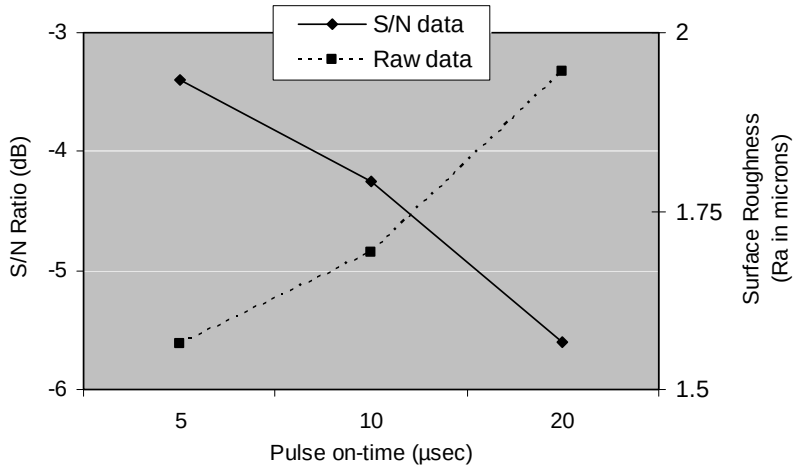

Fig. 5.6 (b) Effect of Pulse on-time on Surface Roughness and its S/N ratio (W3 – PW1)

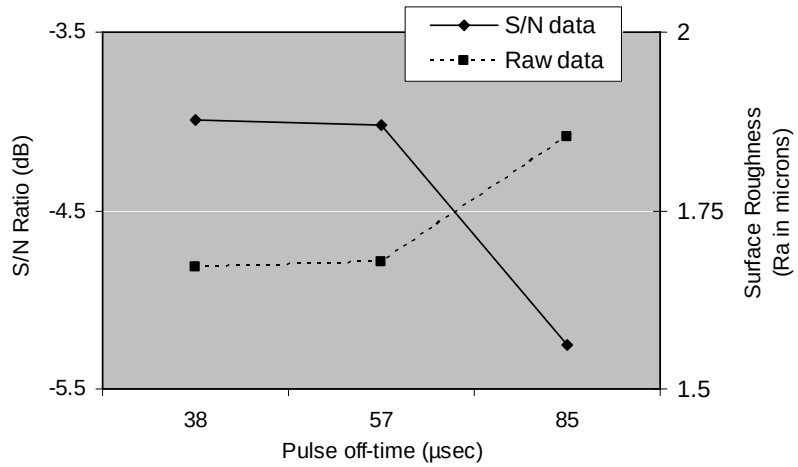

Fig. 5.6 (c) Effect of Pulse off-time on Surface Roughness and its S/N ratio (W3 – PW1)

It can be observed from Fig. 5.6 (a), (b) and (c) that the first level of peak current (A_1), first level of pulse on-time (B_1) and the first level of pulse off-time (C_1) give the lowest values of surface roughness. Hence, the optimum condition of input process parameters is $A_1B_1C_1$. However, it is significant to note that increase in surface roughness is almost negligible as pulse off-time changes from level 1 to level 2. The theoretical value of η_{opt} under the optimum conditions is given by:

$$\eta_{opt} = m + (m_{A1} - m) + (m_{B1} - m) + (m_{C1} - m) = 0.08012$$

The corresponding value of surface roughness is given by

$$y_{opt}^2 = 10^{-\eta opt / 10}$$

or, $$y_{opt} = 0.99\ \mu m$$

Since this combination of input process parameters existed in the orthogonal array (as first row), a confirmation experiment was not required. The average value of surface roughness obtained at this setting of the experiment was 0.97 μm which is better than and very close to the theoretical value predicted by Taguchi analysis.

Analysis of variance (ANOVA) of the S/N data was performed to obtain the percentage contribution of the factors and their significance. It is presented in Table 5.11 and it can be seen that all the three factors are significant for the response characteristic of surface roughness. In this case also, error contribution is found to be less than 1 %.

Table 5.11 ANOVA table of S/N data for Surface Roughness (W3 – PW1)

Factor/Source	**Sum of Squares**	**DOF**	**V**	**F-ratio**	**% Contri-bution**	**Remarks**
Peak Current	51.0952	2	25.5476	539.68	82.76	Significant
Pulse on-time	7.4507	2	3.7254	78.70	12.07	Significant
Pulse off-time	3.0991	2	1.5496	32.73	5.02	Significant
Error (Pooled)	0.0947	2	0.0474	-	0.15	-
Total	61.7397	8		-	100	
DOF = Degrees of Freedom, V = Variance, Tabulated F-ratio $_{0.05}$ (2, 2) = 19						

5.2 MACHINING WITH MANGANESE POWDER (PW2)

5.2.1 Work Material – OHNS die steel (W1)

The observed values of micro-hardness and surface roughness after machining OHNS die steel with manganese powder mixed in the dielectric medium and the calculated values of their S/N ratios are given in Table 5.12.

Table 5.12 Observed values of Micro-hardness and Surface roughness and their calculated S/N ratios (W1 – PW2)

Expt. No.	Micro-hardness (HV)			S/N Ratio (dB)	Surface Roughness (R_a in microns)			S/N Ratio (dB)
	R1	R2	R3		R1	R2	R3	
1	843	851	865	58.618	3.46	3.19	3.28	-10.402
2	820	783	794	58.046	3.57	3.85	3.72	-11.399
3	837	861	848	58.573	4.41	4.63	4.77	-13.266
4	1018	1029	1036	60.236	5.64	5.52	5.89	-15.095
5	996	1007	983	59.958	6.70	6.59	6.51	-16.392
6	978	962	971	59.738	6.38	6.63	6.55	-16.286
7	988	1011	995	59.981	6.47	6.22	6.34	-16.048
8	914	905	883	59.089	6.06	6.19	5.81	-15.595
9	939	912	921	59.312	6.92	6.75	6.83	-16.693
Total	8333	8321	8296	533.550	49.61	49.57	49.70	-131.175
	$\overline{T}_{MH}$ = Overall mean of micro hardness = 924.07			Mean, m= 59.283	$\overline{T}_{SR}$ = Overall mean of surface roughness = 5.514			Mean, m= -14.575

From this data, the average values of micro-hardness and corresponding S/N ratios for the three levels of peak current, pulse on-time and pulse off-time have been calculated and are given in Table 5.13. These average values represent the factor effects of input parameters.

Table 5.13 Average values by factor levels for Micro-hardness (W1 – PW2)

Parameter / Levels	Peak Current (amperes)		Pulse on-time (µsec)		Pulse off-time (µsec)	
	Raw Data	S/N Data	Raw Data	S/N Data	Raw Data	S/N Data
L1	833.56	58.412	959.56	59.612	908.00	59.148
L2	997.78	59.977	898.33	59.031	916.89	59.198
L3	940.89	59.460	914.33	59.207	947.33	59.504

These factor effects have been plotted and presented in Fig. 5.7 (a), (b) and (c).

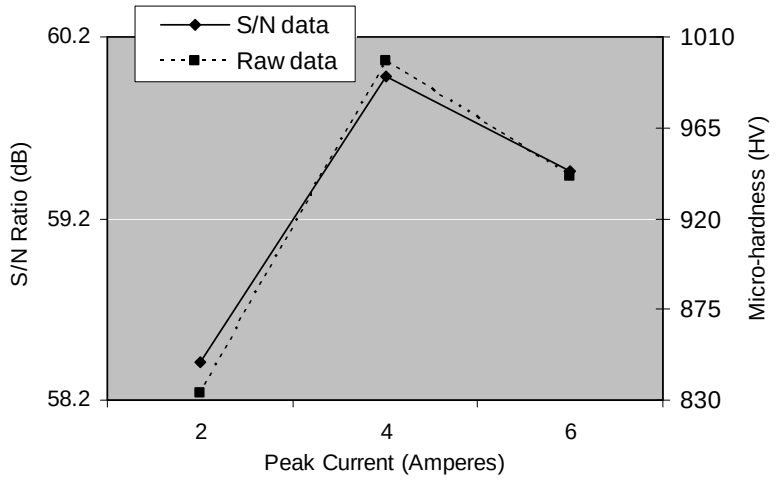

Fig. 5.7 (a) Effect of Peak Current on Micro-hardness and its S/N ratio (W1 – PW2)

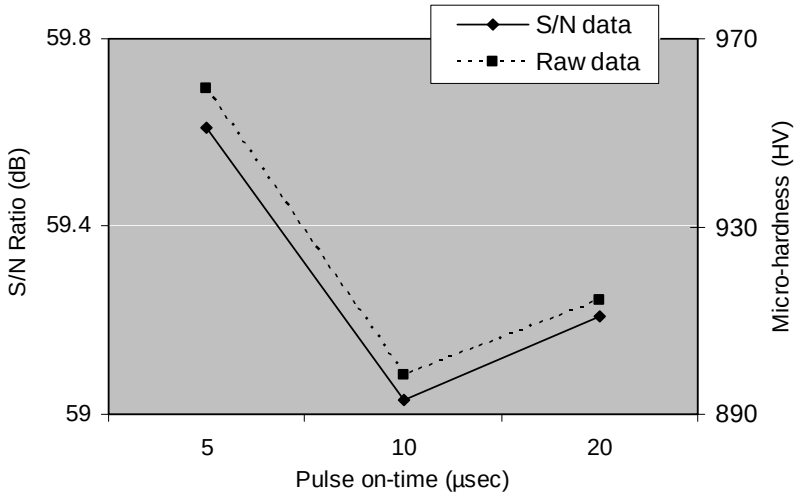

Fig. 5.7 (b) Effect of Pulse on-time on Micro-hardness and its S/N ratio (W1 – PW2)

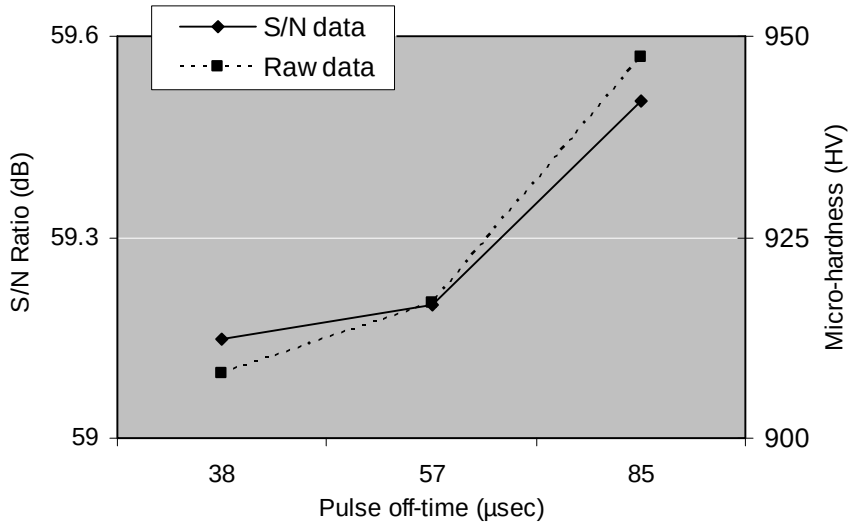

Fig. 5.7 (c) Effect of Pulse off-time on Micro-hardness and its S/N ratio (W1 – PW2)

While the response of micro-hardness to variation in peak current and pulse off-time is identical to the previous case of graphite powder, a change can be observed in its response to variation in pulse on-time. Micro-hardness decreases sharply from level 1 to level 2 of pulse on-time followed by a slight recovery. It can be stated that no material transfer is taking place at level 2 and level 3 but the higher hardening effect at level 3 is responsible for the improvement in micro-hardness. It is also observed from Fig. 5.7 (a), (b) and (c) that the second level of peak current (A_2), first level of pulse on-time (B_1) and the third level of pulse off-time (C_3) give the highest values of micro-hardness. Hence, the optimum condition of input process parameters is $A_2B_1C_3$. The theoretical value of η_{opt} under the optimum conditions is given by:

$$\eta_{opt} = m + (m_{A2} - m) + (m_{B1} - m) + (m_{C3} - m) = 60.5266$$

The corresponding value of micro-hardness is given by

$$y_{opt}^2 = 1 / 10^{-\eta opt / 10}$$

or, $$y_{opt} = 1062.5 \text{ HV}$$

Since this combination of input process parameters did not exist in the orthogonal array, a set of three confirmation experiments were conducted. The average value of micro-hardness obtained at this setting of the experiment was 1049.33 HV which is very close to the theoretical value predicted by Taguchi analysis.

To obtain percentage contribution of the three factors and their significance, analysis of variance (ANOVA) of the S/N data was performed. It is presented in Table 5.14 which shows that all the three factors are significant for the response characteristic of micro-hardness. The contribution of peak current is found to be very high at 83.41 % whereas error contribution is negligible.

Table 5.14 ANOVA table of S/N data for Micro-hardness (W1 – PW2)

Factor/Source	Sum of Squares	DOF	V	F-ratio	% Contri-bution	Remarks
Peak Current	3.8161	2	1.9081	1055.47	83.41	Significant
Pulse on-time	0.5320	2	0.2660	147.15	11.63	Significant
Pulse off-time	0.2232	2	0.1116	61.72	4.88	Significant
Error (Pooled)	0.0036	2	0.0018	-	0.08	-
Total	4.5749	8		-	100	
DOF = Degrees of Freedom, V = Variance, Tabulated F-ratio $_{0.05}$ (2, 2) = 19						

Similar analysis has now been done for surface roughness. From the experimental data given in Table 5.12, the average values of surface roughness and the corresponding S/N ratios for the three levels of input process parameters have been calculated and are given in Table 5.15.

Table 5.15 Average values by factor levels for Surface Roughness (W1 – PW2)

Parameter	Peak Current (Amperes)		Pulse on-time (µsec)		Pulse off-time (µsec)	
Levels	Raw Data	S/N Data	Raw Data	S/N Data	Raw Data	S/N Data
L1	3.88	-11.689	5.11	-13.848	5.28	-14.094
L2	6.27	-15.924	5.44	-14.462	5.41	-14.396
L3	6.40	-16.112	5.98	-15.415	5.85	-15.235

These factor effects have been plotted and presented in Fig. 5.8 (a), (b) and (c).

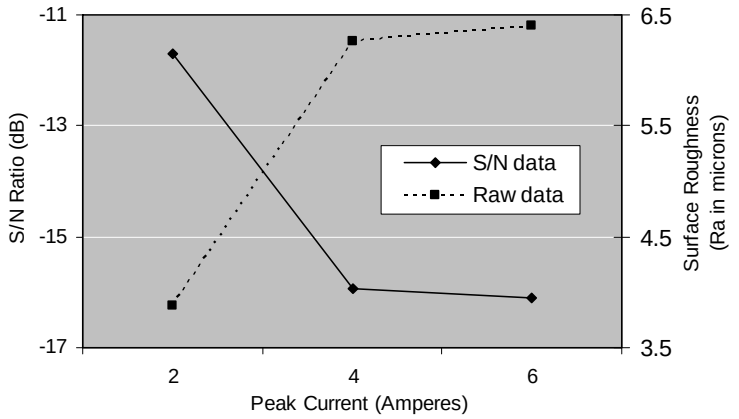

Fig. 5.8 (a) Effect of Peak Current on Surface Roughness and its S/N ratio (W1 – PW2)

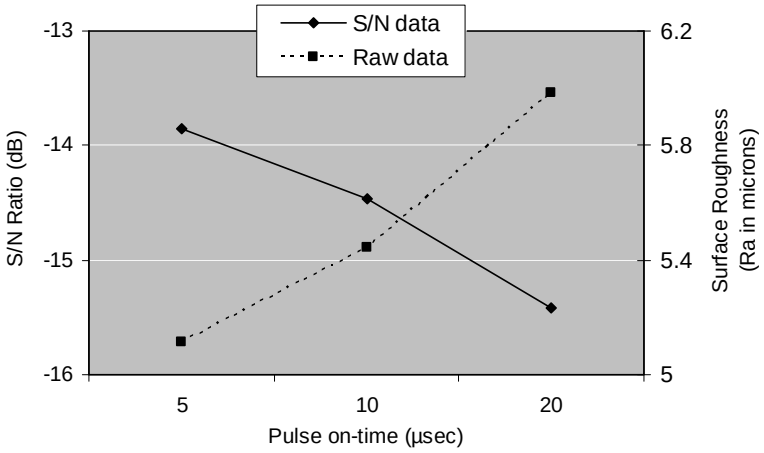

Fig. 5.8 (b) Effect of Pulse on-time on Surface Roughness and its S/N ratio (W1 – PW2)

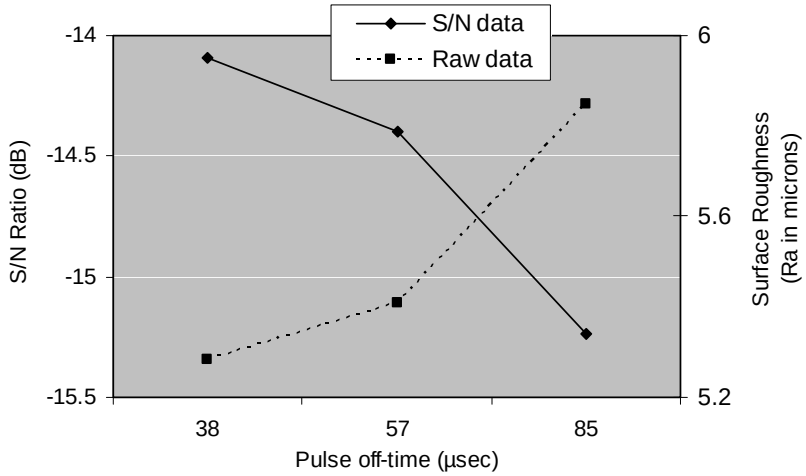

Fig. 5.8 (c) Effect of Pulse off-time on Surface Roughness and its S/N ratio (W1 – PW2)

Lower values of surface roughness are considered to be optimal. It can be observed from Fig. 5.8 (a), (b) and (c) that the first level of peak current (A_1), first level of pulse on-time (B_1) and the first level of pulse off-time (C_1) give the lowest values of surface roughness. Hence, the optimum condition of input process parameters is $A_1B_1C_1$. The theoretical value of η_{opt} under the optimum conditions is given by:

$$\eta_{opt} = m + (m_{A1} - m) + (m_{B1} - m) + (m_{C1} - m) = -10.4812$$

The corresponding value of surface roughness is given by

$$y_{opt}^2 = 10^{-\eta opt / 10}$$

$$\text{or,} \quad y_{opt} = 3.34\ \mu m$$

Since this combination of input process parameters existed in the orthogonal array (as first row), a confirmation experiment was not required. The average value of surface roughness obtained at this setting of the experiment was 3.31 μm which is better than and very close to the theoretical value predicted by Taguchi analysis.

Analysis of variance (ANOVA) of the S/N data was performed to obtain the percentage contribution of the factors and their significance. It is presented in Table 5.16 and it can be seen that all the three factors are significant for the response characteristic of surface roughness. Error contribution is found to be negligible.

Table 5.16 ANOVA table of S/N data for Surface Roughness (W1 – PW2)

Factor/Source	**Sum of Squares**	**DOF**	**V**	**F-ratio**	**% Contri-bution**	**Remarks**
Peak Current	37.5347	2	18.7674	1018.76	86.47	Significant
Pulse on-time	3.7405	2	1.8703	101.52	8.62	Significant
Pulse off-time	2.0965	2	1.0483	56.90	4.83	Significant
Error (Pooled)	0.0368	2	0.0184	-	0.08	-
Total	43.4085	8		-	100	
DOF = Degrees of Freedom, V = Variance, Tabulated F-ratio $_{0.05}(2, 2) = 19$						

5.2.2 Work Material – D2 High-carbon High-chromium die steel (W2)

The observed values of micro-hardness and surface roughness after machining D2 die steel with manganese powder mixed in the dielectric medium and calculated values of their S/N ratios are given in Table 5.17.

Table 5.17 Observed values of Micro-hardness and Surface roughness and their calculated S/N ratios (W2 – PW2)

Expt. No.	Micro-hardness (HV)			S/N Ratio (dB)	Surface Roughness (R_a in microns)			S/N Ratio (dB)
	R1	R2	R3		R1	R2	R3	
1	953	978	962	59.683	4.47	4.38	4.53	-12.988
2	905	896	883	59.032	4.50	4.76	4.62	-13.308
3	917	938	921	59.325	5.53	5.31	5.60	-14.778
4	1064	1081	1109	60.702	6.09	6.35	6.24	-15.886
5	1058	1075	1063	60.549	7.28	7.46	7.53	-17.413
6	1027	1019	1046	60.261	7.57	7.42	7.84	-17.630
7	1042	1051	1072	60.463	7.65	7.73	7.51	-17.651
8	980	963	974	59.756	7.78	7.59	7.86	-17.780
9	956	945	917	59.452	8.04	7.68	7.75	-17.870
Total	8902	8946	8947	539.223	58.91	58.68	59.48	-145.302
	$\overline{T}_{MH}$ = Overall mean of micro hardness = 992.41			Mean, m= 59.914	$\overline{T}_{SR}$ = Overall mean of surface roughness = 6.558			Mean, m= -16.145

From this data, the average values of micro-hardness and corresponding S/N ratios for the three levels of peak current, pulse on-time and pulse off-time have been calculated and are given in Table 5.18. These average values represent the factor effects at different levels of the input process parameters.

Table 5.18 Average values by factor levels for Micro-hardness (W2 – PW2)

Parameter / Levels	Peak Current (amperes)		Pulse on-time (µsec)		Pulse off-time (µsec)	
	Raw Data	S/N Data	Raw Data	S/N Data	Raw Data	S/N Data
L1	928.11	59.347	1034.67	60.283	989.11	59.900
L2	1060.22	60.504	977.44	59.779	972.89	59.729
L3	988.89	59.890	965.11	59.679	1015.22	60.112

These factor effects have been plotted and presented in Fig. 5.9 (a), (b) and (c).

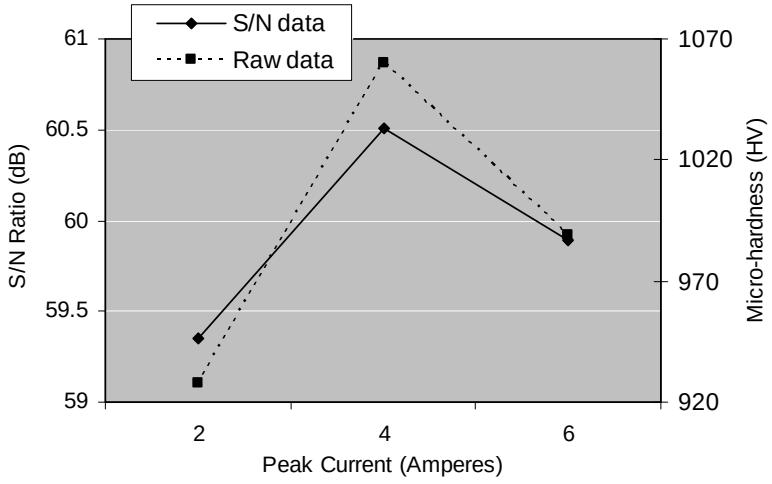

Fig. 5.9 (a) Effect of Peak Current on Micro-hardness and its S/N ratio (W2 – PW2)

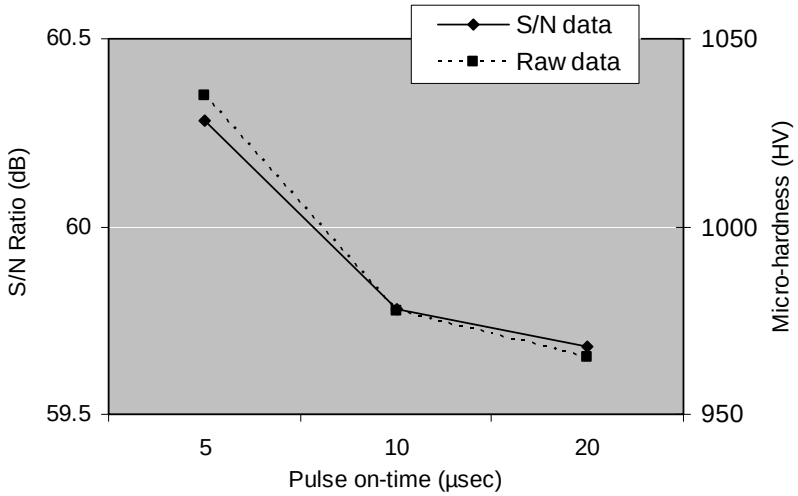

Fig. 5.9 (b) Effect of Pulse on-time on Micro-hardness and its S/N ratio (W2 – PW2)

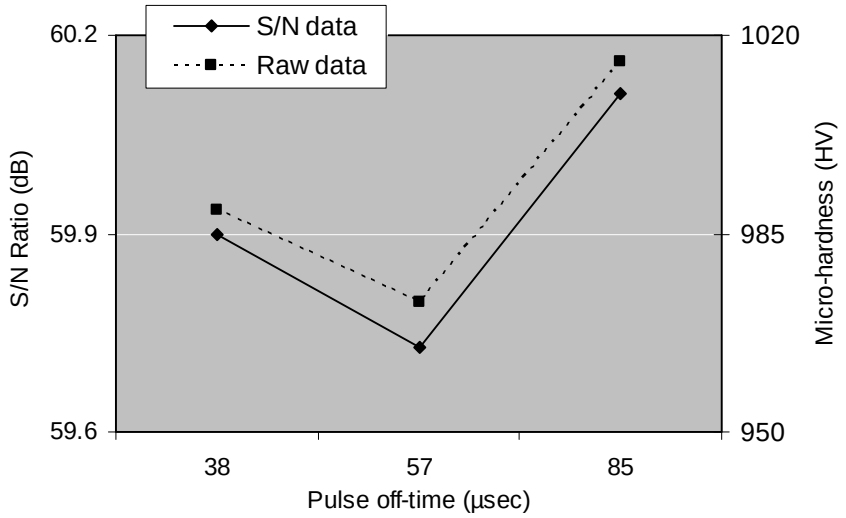

Fig. 5.9 (c) Effect of Pulse off-time on Micro-hardness and its S/N ratio (W2 – PW2)

For this material, the response of micro-hardness to variation in pulse off-time has been found to be different from the other two work materials. OHNS and H13 die steels show improvement in micro-hardness with increase in pulse off-time because sufficient deionization time results in better quenching effect. However, this material shows decrease in micro-hardness from level 1 to level 2 and significant improvement from level 2 to level 3. No apparent reason could be found for this behaviour. It is also observed from Fig. 5.9 (a), (b) and (c) that the second level of peak current (A_2), first level of pulse on-time (B_1) and the third level of pulse off-time (C_3) give the highest values of micro-hardness. Hence, the optimum condition of input process parameters is $A_2B_1C_3$. The theoretical value of η_{opt} for this optimum condition is given by:

$$\eta_{opt} = m + (m_{A2} - m) + (m_{B1} - m) + (m_{C3} - m) = 61.0719$$

The corresponding value of micro-hardness is given by

$$y_{opt}^2 = 1 / 10^{-\eta opt / 10}$$

or, $$y_{opt} = 1131.34 \text{ HV}$$

Since this combination of input process parameters did not exist in the orthogonal array, a set of three confirmation experiments were conducted. The average value of micro-hardness obtained at this setting of the experiment was 1119 HV which is very close to the theoretical value predicted by Taguchi analysis.

To obtain percentage contribution of the three factors and their significance, analysis of variance (ANOVA) of the S/N data was performed. It is presented in Table 5.19 which shows that all the three factors are significant for the response characteristic of micro-hardness. Error contribution is found to be negligible.

Table 5.19 ANOVA table of S/N data for Micro-hardness (W2 – PW2)

Factor/Source	Sum of Squares	DOF	V	F-ratio	% Contri-bution	Remarks
Peak Current	2.0121	2	1.0061	1176.98	70.27	Significant
Pulse on-time	0.6281	2	0.3141	367.40	21.93	Significant
Pulse off-time	0.2215	2	0.1108	129.59	7.74	Significant
Error (Pooled)	0.0017	2	0.0009	-	0.06	-
Total	2.8634	8		-	100	
DOF = Degrees of Freedom, V = Variance, Tabulated F-ratio $_{0.05}$ (2, 2) = 19						

Similar analysis has now been done for surface roughness. From the experimental data given in Table 5.17, the average values of surface roughness and the corresponding S/N ratios for the three levels of peak current, pulse on-time and pulse off-time have been calculated and are given in Table 5.20.

Table 5.20 Average values by factor levels for Surface Roughness (W2 – PW2)

Parameter / Levels	Peak Current (Amperes)		Pulse on-time (µsec)		Pulse off-time (µsec)	
	Raw Data	S/N Data	Raw Data	S/N Data	Raw Data	S/N Data
L1	4.86	-13.691	6.11	-15.508	6.60	-16.132
L2	7.09	-16.976	6.60	-16.167	6.23	-15.688
L3	7.73	-17.767	6.97	-16.759	6.84	-16.614

These factor effects have been plotted and presented in Fig. 5.10 (a), (b) and (c).

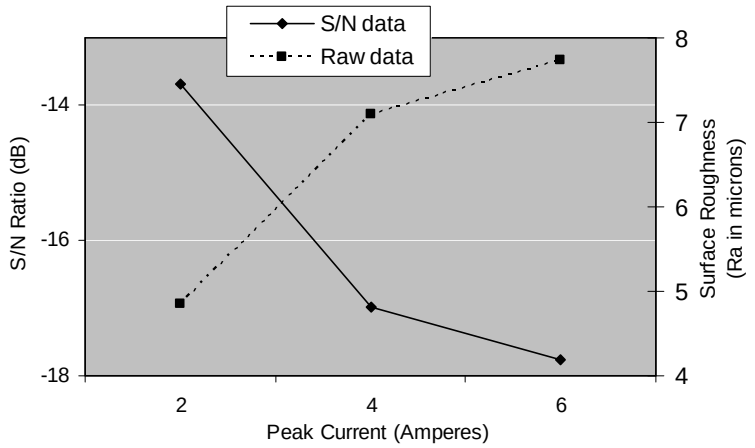

Fig. 5.10 (a) Effect of Peak Current on Surface Roughness and its S/N ratio (W2 – PW2)

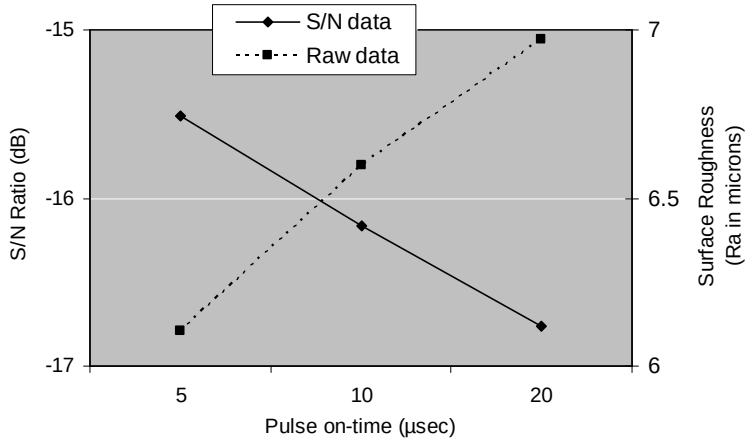

Fig. 5.10 (b) Effect of Pulse on-time on Surface Roughness and its S/N ratio (W2 – PW2)

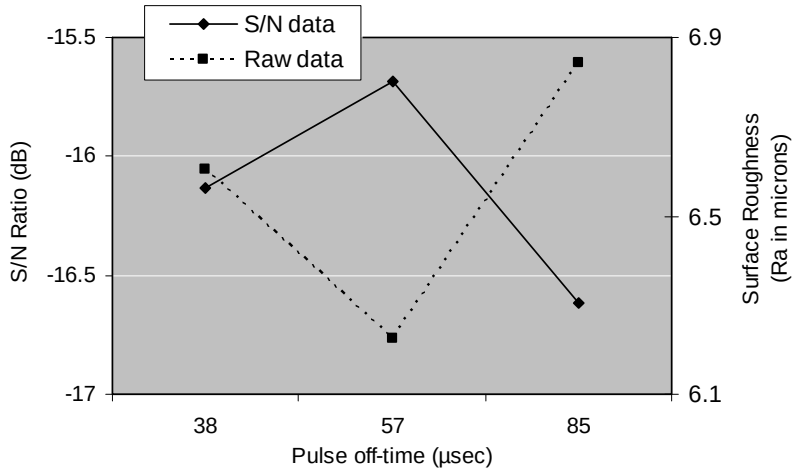

Fig. 5.10 (c) Effect of Pulse off-time on Surface Roughness and its S/N ratio (W2 – PW2)

It can be observed from Fig. 5.10 (a), (b) and (c) that the first level of peak current (A_1), first level of pulse on-time (B_1) and the second level of pulse off-time (C_2) give the lowest values of surface roughness. Hence, the optimum condition of input process parameters is $A_1B_1C_2$. The theoretical value of η_{opt} is given by:

$$\eta_{opt} = m + (m_{A1} - m) + (m_{B1} - m) + (m_{C2} - m) = -12.5978$$

The corresponding value of surface roughness is given by

$$y_{opt}^2 = 10^{-\eta opt / 10}$$

or, $$y_{opt} = 4.26\ \mu m$$

Since this combination of input process parameters did not exist in the orthogonal array, a set of three confirmation experiments were conducted. The average value of surface roughness obtained at this setting of the experiment was 4.39 μm which is very close to the theoretical value predicted by Taguchi analysis.

Analysis of variance (ANOVA) of the S/N data was performed to obtain the percentage contribution of the factors and their significance. It is presented in Table 5.21 which shows that all the three factors are significant for the response characteristic of surface roughness. Contribution of peak current is again found to be very high whereas the contribution of error is negligible.

Table 5.21 ANOVA table of S/N data for Surface Roughness (W2 – PW2)

Factor/Source	**Sum of Squares**	**DOF**	**V**	**F-ratio**	**% Contri-bution**	**Remarks**
Peak Current	28.0299	2	14.0149	1650.52	88.47	Significant
Pulse on-time	2.3488	2	1.1744	138.31	7.41	Significant
Pulse off-time	1.2871	2	0.6436	75.79	4.06	Significant
Error (Pooled)	0.0170	2	0.0085	-	0.06	-
Total	31.6828	8		-	100	
DOF = Degrees of Freedom, V = Variance, Tabulated F-ratio $_{0.05}$ (2, 2) = 19						

5.2.3 Work Material – H13 hot die steel (W3)

The observed values of micro-hardness and surface roughness after machining H13 hot die steel with manganese powder mixed in the dielectric medium and calculated values of their S/N ratios are given in Table 5.22.

Table 5.22 Observed values of Micro-hardness and Surface roughness and their calculated S/N ratios (W3 – PW2)

Expt. No.	Micro-hardness (HV)			S/N Ratio (dB)	Surface Roughness (R_a in microns)			S/N Ratio (dB)
	R1	R2	R3		R1	R2	R3	
1	674	665	646	56.409	3.87	3.72	3.64	-11.468
2	631	652	624	56.060	4.04	3.86	4.11	-12.051
3	663	655	638	56.282	4.83	5.05	4.69	-13.731
4	788	796	767	57.879	5.91	5.77	6.02	-15.418
5	804	773	791	57.942	6.75	6.93	6.86	-16.710
6	725	748	719	57.271	6.80	7.14	6.91	-16.842
7	736	753	771	57.535	6.48	6.59	6.74	-16.396
8	712	703	678	56.867	6.27	6.52	6.36	-16.102
9	660	687	695	56.652	6.83	6.68	6.95	-16.677
Total	6393	6432	6329	512.897	51.78	52.26	52.28	-135.395
	$\overline{T}_{MH}$ = Overall mean of micro hardness = 709.41			Mean, m= 56.989	$\overline{T}_{SR}$ = Overall mean of surface roughness = 5.790			Mean, m= -15.044
R1, R2 and R3 represent the three repetitions.								

From this data, the average values of micro-hardness and corresponding S/N ratios for the three levels of peak current, pulse on-time and pulse off-time have been calculated and are given in Table 5.23. These average values represent the factor effects at different levels of the input process parameters.

Table 5.23 Average values by factor levels for Micro-hardness (W3 – PW2)

Parameter / Levels	Peak Current (amperes)		Pulse on-time (µsec)		Pulse off-time (µsec)	
	Raw Data	S/N Data	Raw Data	S/N Data	Raw Data	S/N Data
L1	649.78	56.250	732.89	57.274	696.67	56.849
L2	767.89	57.697	707.56	56.956	700.00	56.864
L3	710.56	57.018	687.78	56.735	731.56	57.253

These factor effects have been plotted and presented in Fig. 5.11 (a), (b) and (c).

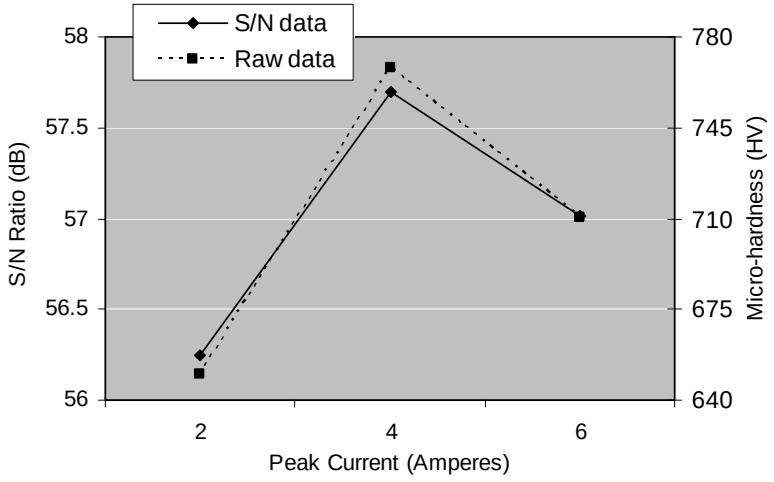

Fig. 5.11 (a) Effect of Peak Current on Micro-hardness and its S/N ratio (W3 – PW2)

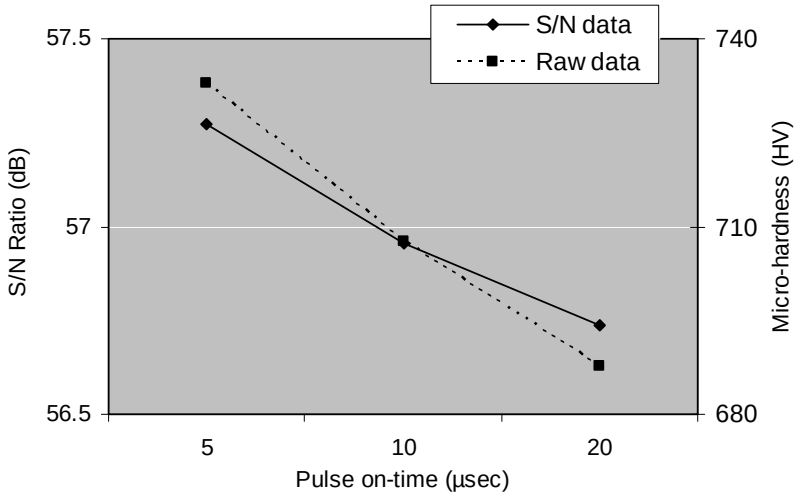

Fig. 5.11 (b) Effect of Pulse on-time on Micro-hardness and its S/N ratio (W3 – PW2)

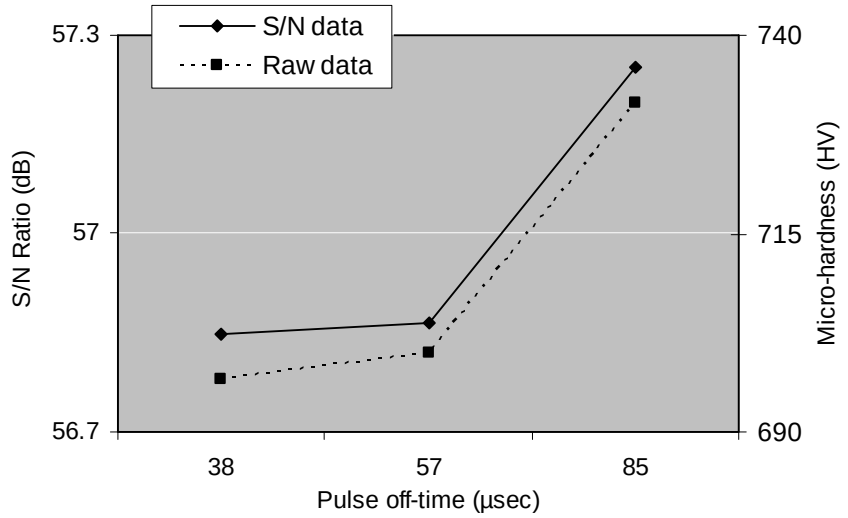

Fig. 5.11 (c) Effect of Pulse off-time on Micro-hardness and its S/N ratio (W3 – PW2)

A significant observation is that when machining was carried out with different electrode materials, maximum value of micro-hardness was achieved at level 3 of peak current (with the exception of inconel electrode). However, when machining was carried out with graphite and manganese powders, its maximum value was achieved at level 2 of peak current. This can be attributed to the need of electrode wear in the former case for which higher values of peak current are required. It is also observed from Fig. 5.11 (a), (b) and (c) that the second level of peak current (A_2), first level of pulse on-time (B_1) and the third level of pulse off-time (C_3) give the highest values of micro-hardness. Hence, the optimum condition of input process parameters is $A_2B_1C_3$. The theoretical value of η_{opt} for the optimum condition is given by:

$$\eta_{opt} = m + (m_{A2} - m) + (m_{B1} - m) + (m_{C3} - m) = 58.2474$$

The corresponding value of micro-hardness is given by

$$y_{opt}^2 = 1 / 10^{-\eta opt / 10}$$

or, $$y_{opt} = 817.28 \text{ HV}$$

Since this combination of input process parameters did not exist in the orthogonal array, a set of three confirmation experiments were conducted. The average value of micro-hardness obtained at this setting of the experiment was 808.33 HV which is very close to the theoretical value predicted by Taguchi analysis.

To obtain percentage contribution of the three factors and their significance, analysis of variance (ANOVA) of the S/N data was performed. It is presented in Table 5.24 which shows that all the three factors are significant for the response characteristic of micro-hardness. The contribution of peak current is found to be very high at 80.52 % followed by pulse on-time and pulse off-time. Error contribution is less than 1 %.

Table 5.24 ANOVA table of S/N data for Micro-hardness (W3 – PW2)

Factor/Source	Sum of Squares	DOF	V	F-ratio	% Contri-bution	Remarks
Peak Current	3.1454	2	1.5727	617.22	80.52	Significant
Pulse on-time	0.4414	2	0.2207	86.60	11.30	Significant
Pulse off-time	0.3146	2	0.1573	61.74	8.05	Significant
Error (Pooled)	0.0051	2	0.0026	-	0.13	-
Total	3.9065	8		-	100	
DOF = Degrees of Freedom, V = Variance, Tabulated F-ratio $_{0.05}$ (2, 2) = 19						

Similar analysis has now been done for surface roughness. From the experimental data given in Table 5.22, the average values of surface roughness and the corresponding S/N ratios for the three levels of input process parameters have been calculated and are given in Table 5.25.

Table 5.25 Average values by factor levels for Surface Roughness (W3 – PW2)

Parameter	Peak Current (Amperes)		Pulse on-time (µsec)		Pulse off-time (µsec)	
Levels	Raw Data	S/N Data	Raw Data	S/N Data	Raw Data	S/N Data
L1	4.20	-12.417	5.42	-14.428	5.69	-14.804
L2	6.57	-16.323	5.74	-14.955	5.57	-14.716
L3	6.60	-16.392	6.21	-15.750	6.10	-15.612

These factor effects have been plotted and presented in Fig. 5.12 (a), (b) and (c).

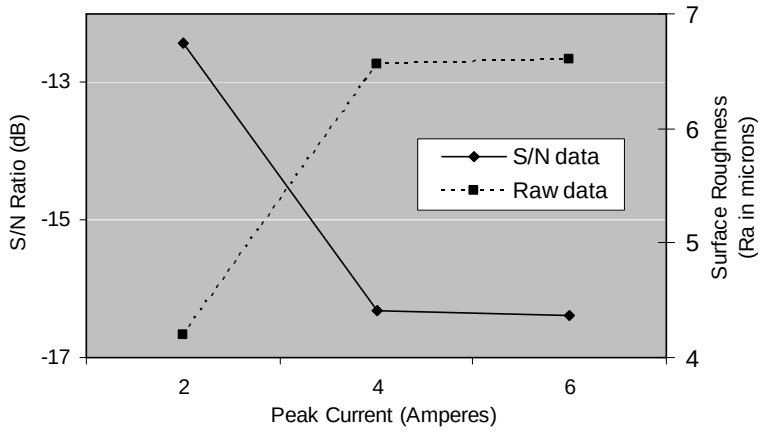

Fig. 5.12 (a) Effect of Peak Current on Surface Roughness and its S/N ratio (W3 – PW2)

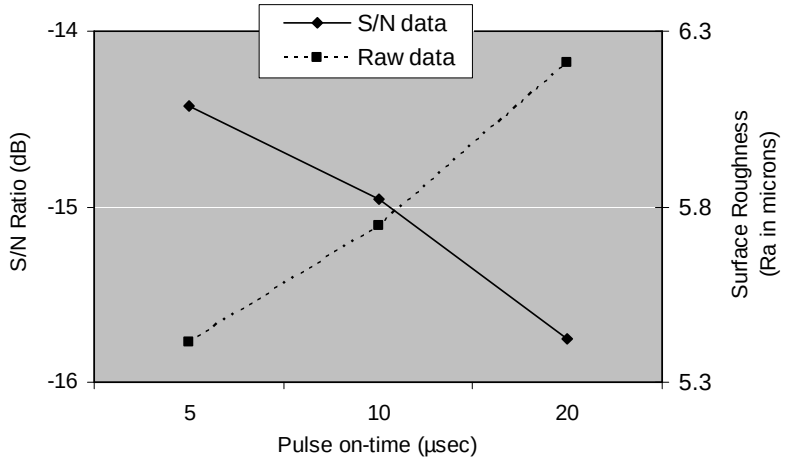

Fig. 5.12 (b) Effect of Pulse on-time on Surface Roughness and its S/N ratio (W3 – PW2)

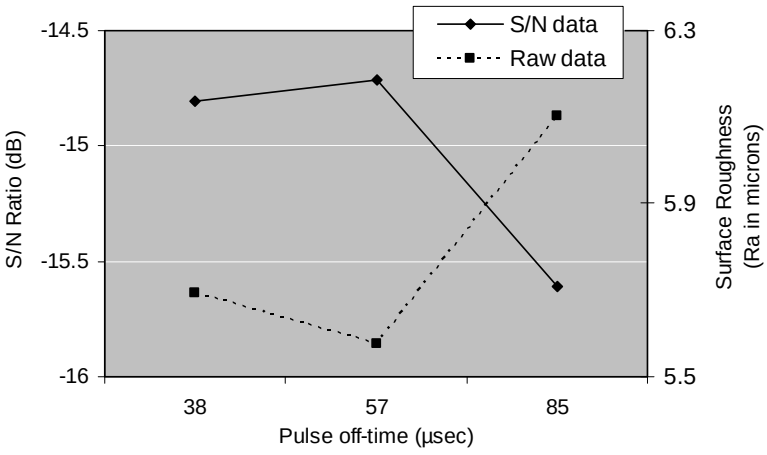

Fig. 5.12 (c) Effect of Pulse off-time on Surface Roughness and its S/N ratio (W3 – PW2)

It can be seen from Fig. 5.12 (a), (b) and (c) that the first level of peak current (A_1), first level of pulse on-time (B_1) and the second level of pulse off-time (C_2) give the lowest values of surface roughness. Hence, the optimum condition of input process parameters is $A_1B_1C_2$. Interestingly, change in surface roughness from level 1 to 2 of pulse off-time is very less.The theoretical value of η_{opt} under the optimum conditions is given by:

$$\eta_{opt} = m + (m_{A1} - m) + (m_{B1} - m) + (m_{C2} - m) = -11.472$$

The corresponding value of surface roughness is given by

$$y_{opt}^2 = 10^{-\eta opt / 10}$$

$$\text{or,} \quad y_{opt} = 3.75\ \mu m$$

Since this combination of input process parameters did not exist in the orthogonal array, a set of three confirmation experiments were conducted. The average value of surface roughness obtained at this setting of the experiment was 3.64 μm which is better than and very close to the theoretical value predicted by Taguchi analysis.

Analysis of variance (ANOVA) of the S/N data was performed to obtain the percentage contribution of the factors and their significance. It is presented in Table 5.26 and it can be seen that all the three factors are significant for the response characteristic of surface roughness. Contribution of peak current is found to be very high at 88.18 %.

Table 5.26 ANOVA table of S/N data for Surface Roughness (W3 – PW2)

Factor/Source	**Sum of Squares**	**DOF**	**V**	**F-ratio**	**% Contri-bution**	**Remarks**
Peak Current	31.0668	2	15.5334	805.16	88.18	Significant
Pulse on-time	2.6580	2	1.3290	68.89	7.55	Significant
Pulse off-time	1.4660	2	0.7330	37.99	4.16	Significant
Error (Pooled)	0.0386	2	0.0193	-	0.11	-
Total	35.2294	8		-	100	
DOF = Degrees of Freedom, V = Variance, Tabulated F-ratio $_{0.05}$ (2, 2) = 19						

5.3 MACHINING WITH SILICON POWDER (PW3)

5.3.1 Work Material – OHNS die steel (W1)

The observed values of micro-hardness and surface roughness after machining OHNS die steel with silicon powder mixed in the dielectric medium and calculated values of their S/N ratios are given in Table 5.27.

Table 5.27 Observed values of Micro-hardness and Surface roughness and their calculated S/N ratios (W1 – PW3)

Expt. No.	Micro-hardness (HV)			S/N Ratio (dB)	Surface Roughness (R_a in microns)			S/N Ratio (dB)
	R1	R2	R3		R1	R2	R3	
1	642	614	623	55.932	1.14	1.08	0.95	-0.503
2	604	581	572	55.346	1.29	1.12	1.20	-1.622
3	597	631	610	55.738	1.35	1.51	1.57	-3.403
4	636	648	659	56.224	1.42	1.26	1.33	-2.531
5	627	662	651	56.207	1.80	1.97	2.14	-5.911
6	655	619	634	56.062	2.04	1.85	1.91	-5.733
7	725	698	740	57.151	2.20	2.33	2.16	-6.971
8	691	672	656	56.554	2.47	2.78	2.63	-8.398
9	649	667	678	56.448	2.24	2.39	2.42	-7.426
Total	5826	5792	5823	505.662	15.95	16.29	16.31	-42.498
	$\overline{T}_{MH}$ = Overall mean of micro hardness = 645.96			Mean, m= 56.185	$\overline{T}_{SR}$ = Overall mean of surface roughness = 1.80			Mean, m= -4.722

From this data, the average values of micro-hardness and corresponding S/N ratios for the three levels of input process parameters have been calculated and are given in Table 5.28.

Table 5.28 Average values by factor levels for Micro-hardness (W1 – PW3)

Parameter / Levels	Peak Current (amperes)		Pulse on-time (µsec)		Pulse off-time (µsec)	
	Raw Data	S/N Data	Raw Data	S/N Data	Raw Data	S/N Data
L1	608.22	55.672	665.00	56.436	645.11	56.183
L2	643.44	56.164	635.11	56.036	632.67	56.006
L3	686.22	56.718	637.78	56.083	660.11	56.365

These factor effects have been plotted and presented in Fig. 5.13 (a), (b) and (c).

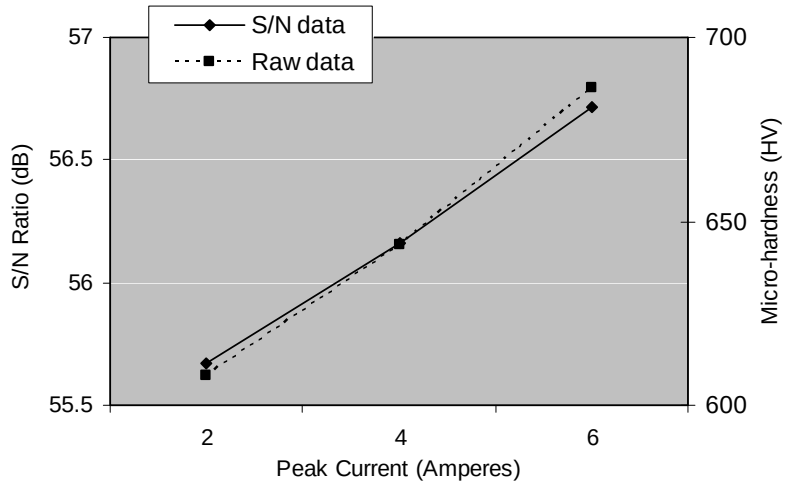

Fig. 5.13 (a) Effect of Peak Current on Micro-hardness and its S/N ratio (W1 – PW3)

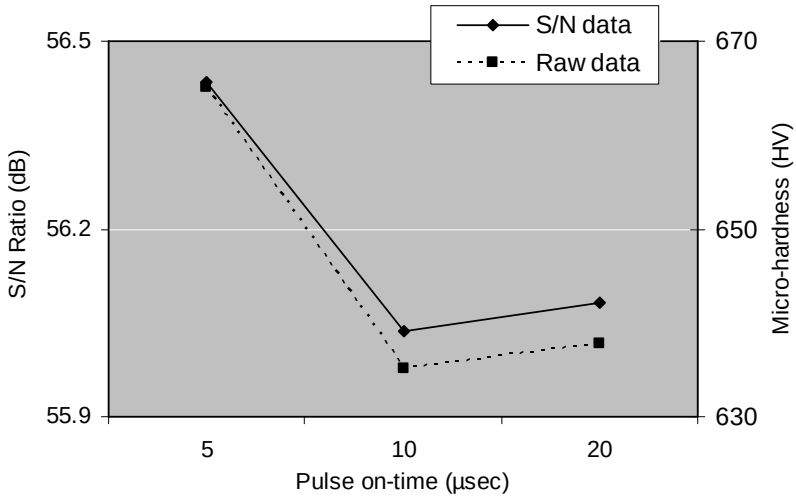

Fig. 5.13 (b) Effect of Pulse on-time on Micro-hardness and its S/N ratio (W1 – PW3)

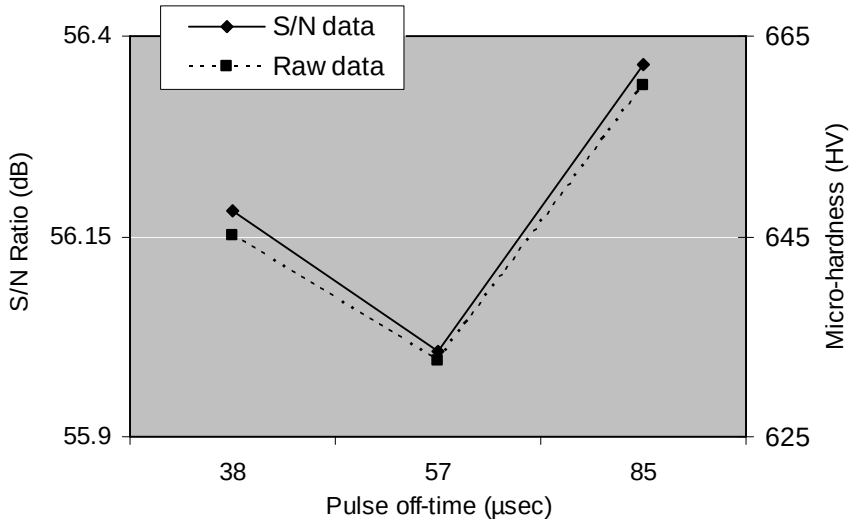

Fig. 5.13 (c) Effect of Pulse off-time on Micro-hardness and its S/N ratio (W1 – PW3)

It can be observed from Fig. 5.13 (a) that the response of micro-hardness to variation in peak current is different for silicon powder. While the highest value of micro-hardness was achieved at level 2 of peak current with the other three powders (and it declined after that), it was achieved at level 2 with silicon powder. It appears that this powder is not contributing anything to improvement in micro-hardness which is being achieved only by higher heating and quenching effect. It is also observed from Fig. 5.13 (a), (b) and (c) that the third level of peak current (A_3), first level of pulse on-time (B_1) and the third level of pulse off-time (C_3) give the highest values of micro-hardness. Hence, the optimum condition of input process parameters is $A_3B_1C_3$. Since this combination of the levels of input process parameters existed in the orthogonal array (as seventh row), a confirmation experiment was not required. The average value of micro-hardness obtained at this setting of the experiment was 721 HV which can be compared with the theoretical value predicted by Taguchi analysis. The theoretical value of best signal-to-noise ratio (η_{opt}) under the optimum conditions is given by:

$$\eta_{opt} = m + (m_{A3} - m) + (m_{B1} - m) + (m_{C3} - m) = 57.1493$$

The corresponding value of micro-hardness is given by

$$y_{opt}^2 = 1 / 10^{-\eta opt / 10}$$

or, $$y_{opt} = 720.22 \text{ HV}$$

which is very close to the observed experimental value.

To obtain percentage contribution of the three factors and their significance, analysis of variance (ANOVA) of the S/N data was performed. It is presented in Table 5.29 which shows that all the three factors are significant for the response characteristic of micro-hardness. While peak current remains the most significant factor at 77.35 %, error contribution is found to be negligible.

Table 5.29 ANOVA table of S/N data for Micro-hardness (W1 – PW3)

Factor/Source	Sum of Squares	DOF	V	F-ratio	% Contri-bution	Remarks
Peak Current	1.6427	2	0.8214	1983.04	77.35	Significant
Pulse on-time	0.2867	2	0.1434	346.10	13.50	Significant
Pulse off-time	0.1935	2	0.0968	233.52	9.11	Significant
Error (Pooled)	0.0008	2	0.0004	-	0.04	-
Total	2.1237	8		-		
DOF = Degrees of Freedom, V = Variance, Tabulated F-ratio $_{0.05}(2, 2) = 19$						

Similar analysis has now been done for surface roughness. From the experimental data given in Table 5.27, the average values of surface roughness and the corresponding S/N ratios for the three levels of input process parameters of peak current, pulse on-time and pulse off-time have been calculated and are given in Table 5.30.

Table 5.30 Average values by factor levels for Surface Roughness (W1 – PW3)

Parameter / Levels	Peak Current (Amperes)		Pulse on-time (µsec)		Pulse off-time (µsec)	
	Raw Data	S/N Data	Raw Data	S/N Data	Raw Data	S/N Data
L1	1.25	-1.843	1.54	-3.335	1.87	-4.878
L2	1.75	-4.725	1.93	-5.310	1.63	-3.860
L3	2.40	-7.598	1.92	-5.521	1.89	-5.428

These factor effects have been plotted and presented in Fig. 5.14 (a), (b) and (c).

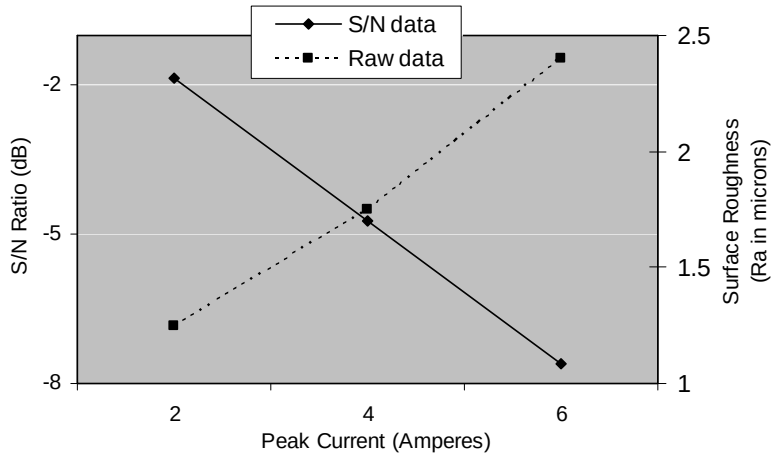

Fig. 5.14 (a) Effect of Peak Current on Surface Roughness and its S/N ratio (W1 – PW3)

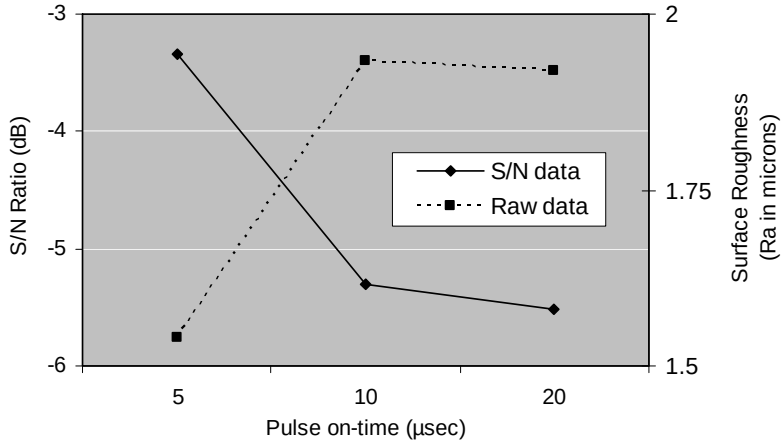

Fig. 5.14 (b) Effect of Pulse on-time on Surface Roughness and its S/N ratio (W1 – PW3)

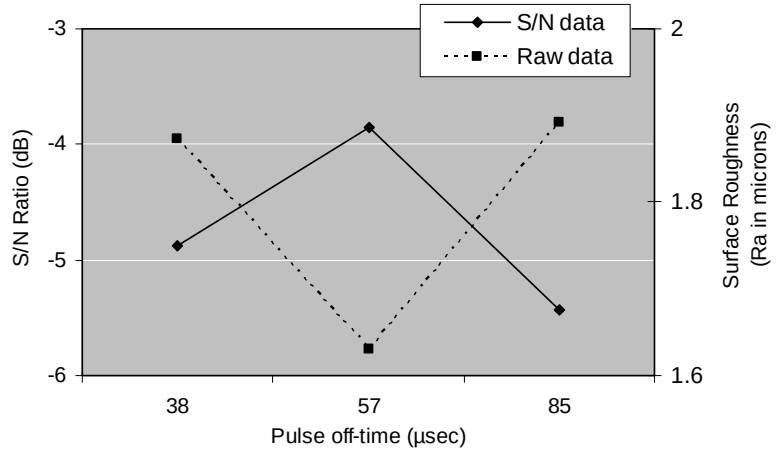

Fig. 5.14 (c) Effect of Pulse off-time on Surface Roughness and its S/N ratio (W1 – PW3)

It is observed from Fig. 5.14 (a), (b) and (c) that the first level of peak current (A_1), first level of pulse on-time (B_1) and the second level of pulse off-time (C_2) give the lowest values of surface roughness. Hence, the optimum combination of input process parameters is $A_1B_1C_2$. The theoretical value of η_{opt} under the optimum combination is given by:

$$\eta_{opt} = m + (m_{A1} - m) + (m_{B1} - m) + (m_{C2} - m)$$

$$= 0.4067$$

The corresponding value of surface roughness is given by

$$y_{opt}^2 = 10^{-\eta opt / 10}$$

or, $$y_{opt} = 0.95\ \mu m$$

Since this combination of input process parameters did not exist in the orthogonal array, a set of three confirmation experiments were conducted. The average value of surface roughness obtained at this setting of the experiment was 0.92 μm which is better than and very close to the theoretical value predicted by Taguchi analysis.

Analysis of variance (ANOVA) of the S/N data was performed to obtain the percentage contribution of the factors and their significance. It is presented in Table 5.31 and it can be seen that all the three factors are significant for the response characteristic of surface roughness. The contribution of error is found to be negligible.

Table 5.31 ANOVA table of S/N data for Surface Roughness (W1 – PW3)

Factor/Source	Sum of Squares	DOF	V	F-ratio	% Contri-bution	Remarks
Peak Current	49.6916	2	24.8458	935.64	79.80	Significant
Pulse on-time	8.7250	2	4.3625	164.28	14.01	Significant
Pulse off-time	3.7994	2	1.8997	71.54	6.10	Significant
Error (Pooled)	0.0531	2	0.0266	-	0.09	-
Total	62.2691	8		-	100	
DOF = Degrees of Freedom, V = Variance, Tabulated F-ratio $_{0.05}$ (2, 2) = 19						

5.3.2 Work Material – D2 high carbon high chromium die steel (W2)

The observed values of micro-hardness and surface roughness after machining D2 die steel with silicon powder mixed in the dielectric medium and calculated values of their S/N ratios are given in Table 5.32.

Table 5.32 Observed values of Micro-hardness and Surface roughness and their calculated S/N ratios (W2 – PW3)

Expt. No.	Micro-hardness (HV)			S/N Ratio (dB)	Surface Roughness (R_a in microns)			S/N Ratio (dB)
	R1	R2	R3		R1	R2	R3	
1	691	719	706	56.964	1.49	1.75	1.66	-4.280
2	685	668	659	56.527	1.61	1.78	1.92	-4.982
3	713	681	692	56.839	2.01	2.24	2.15	-6.590
4	744	778	753	57.593	1.94	1.83	2.06	-5.781
5	731	750	765	57.481	2.57	2.65	2.46	-8.169
6	729	722	746	57.292	2.68	2.44	2.31	-7.894
7	786	821	797	58.072	3.02	2.80	2.93	-9.302
8	738	754	771	57.547	3.11	3.17	3.36	-10.144
9	730	764	743	57.446	2.90	3.23	2.97	-9.648
Total	6547	6657	6632	515.761	21.33	21.89	21.82	-66.789
	$\overline{T}_{MH}$ = Overall mean of micro hardness = 734.67			Mean, m= 57.307	$\overline{T}_{SR}$ = Overall mean of surface roughness = 2.409			Mean, m= -7.421
R1, R2 and R3 represent the three repetitions.								

From this data, the average values of micro-hardness and corresponding S/N ratios for the three levels of peak current, pulse on-time and pulse off-time have been calculated and are given in Table 5.33.

Table 5.33 Average values by factor levels for Micro-hardness (W2 – PW3)

Parameter / Levels	Peak Current (amperes)		Pulse on-time (µsec)		Pulse off-time (µsec)	
	Raw Data	S/N Data	Raw Data	S/N Data	Raw Data	S/N Data
L1	690.44	56.777	755.00	57.543	730.67	57.268
L2	746.44	57.455	724.56	57.185	724.89	57.189
L3	767.11	57.688	724.44	57.192	748.44	57.464

These factor effects have been plotted and presented in Fig. 5.15 (a), (b) and (c).

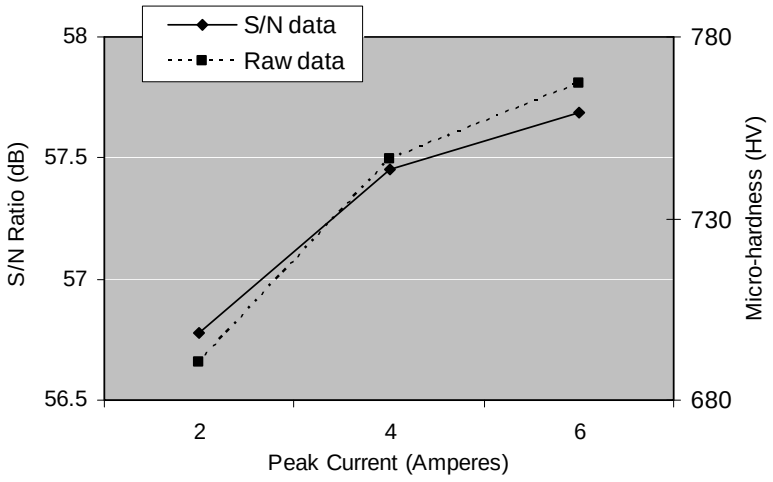

Fig. 5.15 (a) Effect of Peak Current on Micro-hardness and its S/N ratio (W2 – PW3)

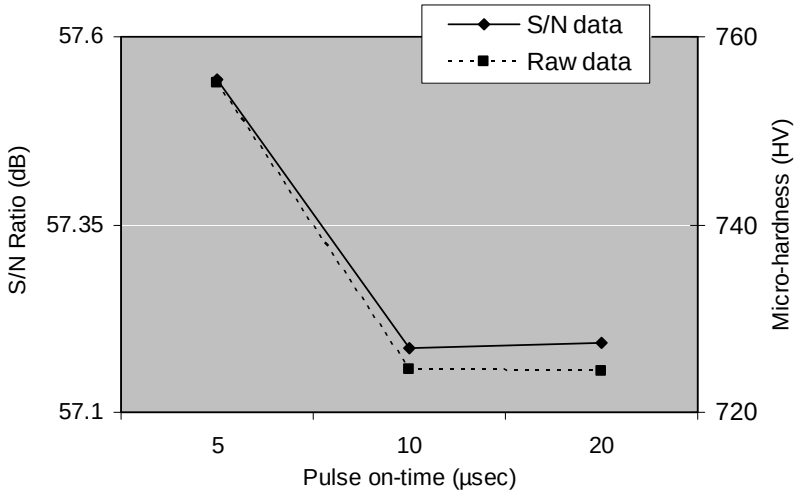

Fig. 5.15 (b) Effect of Pulse on-time on Micro-hardness and its S/N ratio (W2 – PW3)

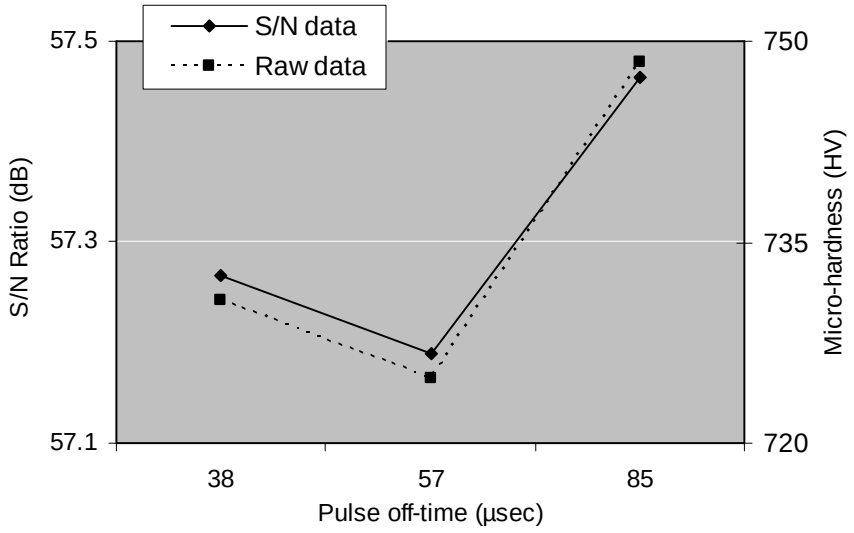

Fig. 5.15 (c) Effect of Pulse off-time on Micro-hardness and its S/N ratio (W2 – PW3)

For this work material also, similar pattern is observed in the response of micro-hardness to variation in the three input process parameters. Fig. 5.15 (b) shows that micro-hardness decreases when pulse on-time changes from level 1 to 2 and then improves marginally due to more heating and quenching effect. The high value of micro-hardness at level 1 can be attributed to the strengthening of ferrite phase by silicon and copper atoms. It is also observed from Fig. 5.15 (a), (b) and (c) that the third level of peak current (A_3), first level of pulse on-time (B_1) and the third level of pulse off-time (C_3) give the highest values of micro-hardness. Hence, the optimum condition of input process parameters is $A_3B_1C_3$. The theoretical best value of signal-to-noise ratio (η_{opt}) under the optimum condition is given by:

$$\eta_{opt} = m + (m_{A3} - m) + (m_{B1} - m) + (m_{C3} - m)$$

$$= 58.082$$

The corresponding value of micro-hardness is given by

$$y_{opt}^2 = 1 / 10^{-\eta opt / 10}$$

or, $$y_{opt} = 801.86 \text{ HV}$$

Since this combination of the levels of input process parameters existed in the orthogonal array (as seventh row), a confirmation experiment was not required. The average value of micro-hardness obtained at this setting of the experiment was 801.33 HV which is very close to the theoretical value predicted by Taguchi analysis.

To obtain percentage contribution of the three factors and their significance, analysis of variance (ANOVA) of the S/N data was performed. It is presented in Table 5.34 which shows that all the three factors are significant for the response characteristic of micro-hardness. While peak current remains the most significant factor, the percentage contribution of pulse on-time is almost double that of pulse off-time.

Table 5.34 ANOVA table of S/N data for Micro-hardness (W2 – PW3)

Factor/Source	Sum of Squares	DOF	V	F-ratio	% Contri-bution	Remarks
Peak Current	1.3458	2	0.6729	789.45	78.27	Significant
Pulse on-time	0.2511	2	0.1256	147.30	14.61	Significant
Pulse off-time	0.1207	2	0.0604	70.84	7.02	Significant
Error (Pooled)	0.0017	2	0.0009	-	0.10	-
Total	1.7193	8		-	100	
DOF = Degrees of Freedom, V = Variance, Tabulated F-ratio $_{0.05}$ (2, 2) = 19						

Similar analysis has now been done for surface roughness. From the experimental data given in Table 5.32, the average values of surface roughness and the corresponding S/N ratios for the three levels of input process parameters have been calculated and are given in Table 5.35. These average values represent the factor effects at the three levels of input parameters.

Table 5.35 Average values by factor levels for Surface Roughness (W2 – PW3)

Parameter Levels	Peak Current (Amperes)		Pulse on-time (µsec)		Pulse off-time (µsec)	
	Raw Data	S/N Data	Raw Data	S/N Data	Raw Data	S/N Data
L1	1.85	-5.284	2.16	-6.454	2.44	-7.439
L2	2.33	-7.281	2.51	-7.765	2.25	-6.804
L3	3.05	-9.698	2.55	-8.044	2.54	-8.020

These factor effects have been plotted and presented in Fig. 5.16 (a), (b) and (c).

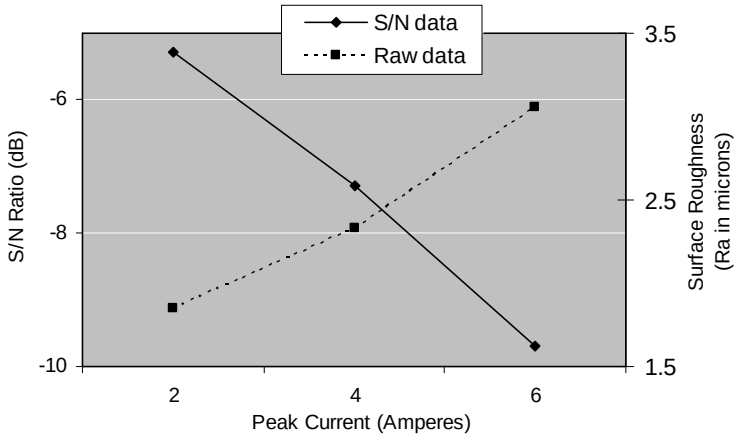

Fig. 5.16 (a) Effect of Peak Current on Surface Roughness and its S/N ratio (W2 – PW3)

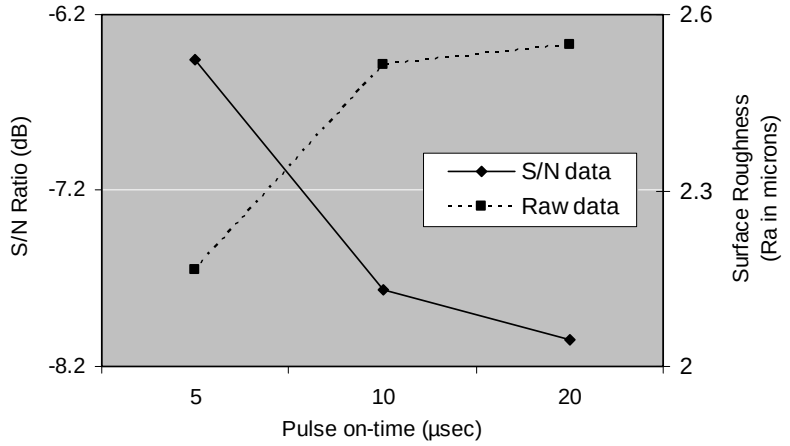

Fig. 5.16 (b) Effect of Pulse on-time on Surface Roughness and its S/N ratio (W2 – PW3)

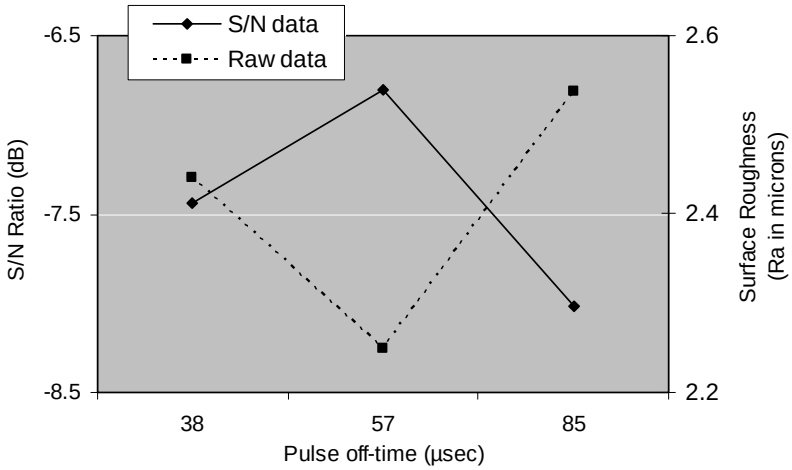

Fig. 5.16 (c) Effect of Pulse off-time on Surface Roughness and its S/N ratio (W2 – PW3)

It can be observed from Fig. 5.16 (a), (b) and (c) that the first level of peak current (A_1), first level of pulse on-time (B_1) and the second level of pulse off-time (C_2) give the lowest values of surface roughness. Hence, the optimum combination of input process parameters is $A_1B_1C_2$. The theoretical value of η_{opt} for the optimum combination is given by:

$$\eta_{opt} = m + (m_{A1} - m) + (m_{B1} - m) + (m_{C2} - m) = -3.6999$$

The corresponding value of surface roughness is given by

$$y_{opt}^2 = 10^{-\eta opt / 10}$$

$$\text{or,} \quad y_{opt} = 1.53 \ \mu m$$

Since this combination of input process parameters did not exist in the orthogonal array, a set of three confirmation experiments were conducted. The average value of surface roughness obtained at this setting of the experiment was 1.61 μm which is very close to the theoretical value predicted by Taguchi analysis.

Analysis of variance (ANOVA) of the S/N data was performed to obtain the percentage contribution of the three factors and their significance. It is presented in Table 5.36 and it can be seen that all the three factors are significant for the response characteristic of surface roughness. It is found that for this response characteristic also, the contribution of pulse on-time is almost double that of pulse off-time.

Table 5.36 ANOVA table of S/N data for Surface Roughness (W2 – PW3)

Factor/Source	**Sum of Squares**	**DOF**	**V**	**F-ratio**	**% Contri-bution**	**Remarks**
Peak Current	29.3127	2	14.6564	895.76	81.68	Significant
Pulse on-time	4.3211	2	2.1606	132.05	12.04	Significant
Pulse off-time	2.2216	2	1.1108	67.89	6.19	Significant
Error (Pooled)	0.0327	2	0.0164	-	0.09	-
Total	35.8881	8	-	-	100	-
DOF = Degrees of Freedom, V = Variance, Tabulated F-ratio $_{0.05}(2, 2) = 19$						

5.3.3 Work Material – H13 hot die steel (W3)

The observed values of micro-hardness and surface roughness after machining H13 hot die steel with silicon powder mixed in the dielectric medium and calculated values of their S/N ratios are given in Table 5.37.

Table 5.37 Observed values of Micro-hardness and Surface roughness and their calculated S/N ratios (W3 – PW3)

Expt. No.	Micro-hardness (HV)			S/N Ratio (dB)	Surface Roughness (R_a in microns)			S/N Ratio (dB)
	R1	R2	R3		R1	R2	R3	
1	524	511	489	54.107	1.13	0.95	1.06	-0.418
2	467	440	458	53.152	1.09	1.24	1.20	-1.426
3	473	486	504	53.754	1.36	1.45	1.29	-2.723
4	547	564	532	54.763	1.27	1.31	1.42	-2.509
5	528	561	542	54.699	1.84	2.00	1.73	-5.390
6	523	535	556	54.607	1.77	1.49	1.68	-4.354
7	627	594	603	55.671	1.92	1.81	2.03	-5.676
8	578	560	551	55.005	2.19	2.34	2.12	-6.921
9	519	556	542	54.621	2.08	1.96	1.87	-5.898
Total	4786	4807	4777	490.379	14.65	14.55	14.40	-35.314
	$\overline{T}_{MH}$ = Overall mean of micro hardness = 532.22			Mean, m= 54.487	$\overline{T}_{SR}$ = Overall mean of surface roughness = 1.615			Mean, m= -3.924
R1, R2 and R3 represent the three repetitions.								

From this data, the average values of micro-hardness and corresponding S/N ratios for the three levels of peak current, pulse on-time and pulse off-time have been calculated and are given in Table 5.38. These average values represent the factor effects at the three levels of input process parameters.

Table 5.38 Average values by factor levels for Micro-hardness (W3 – PW3)

Parameter / Levels	Peak Current (amperes)		Pulse on-time (µsec)		Pulse off-time (µsec)	
	Raw Data	S/N Data	Raw Data	S/N Data	Raw Data	S/N Data
L1	483.56	53.671	554.56	54.847	536.33	54.573
L2	543.11	54.690	520.56	54.285	513.89	54.179
L3	570.00	55.099	521.56	54.327	546.44	54.708

These factor effects have been plotted and presented in Fig. 5.17 (a), (b) and (c).

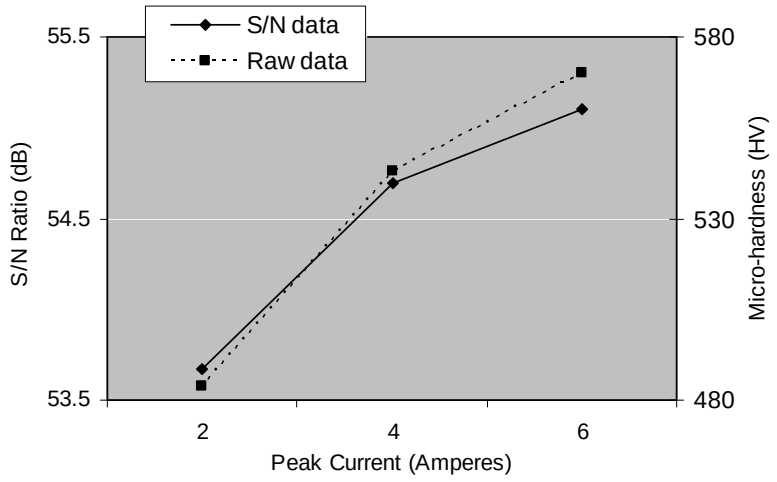

Fig. 5.17 (a) Effect of Peak Current on Micro-hardness and its S/N ratio (W3 – PW3)

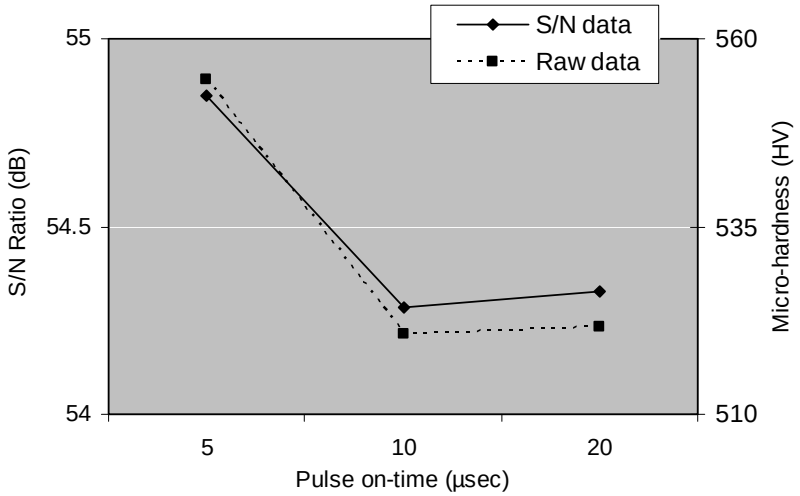

Fig. 5.17 (b) Effect of Pulse on-time on Micro-hardness and its S/N ratio (W3 – PW3)

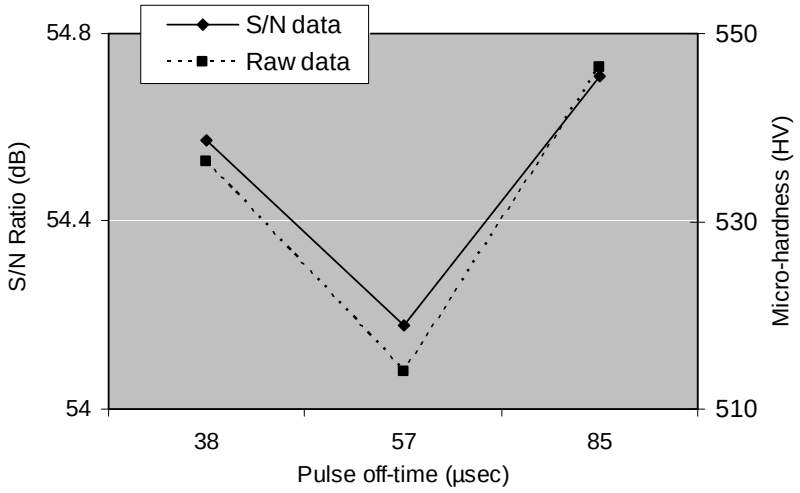

Fig. 5.17 (c) Effect of Pulse off-time on Micro-hardness and its S/N ratio (W3 – PW3)

After observing the behaviour of the three work materials, it can be stated that the response of micro-hardness to variation in the input process parameters depends on the type of powder and not the work material. It is also observed that the actual improvement in micro-hardness with silicon powder is not considerable. Hence, the use of this powder can not be recommended for improving the micro-hardness. It is also observed from Fig. 5.17 (a), (b) and (c) that the third level of peak current (A_3), first level of pulse on-time (B_1) and the third level of pulse off-time (C_3) give the highest values of micro-hardness. Hence, the optimum combination of input process parameters is $A_3B_1C_3$. The theoretical value of η_{opt} for this optimum combination is given by:

$$\eta_{opt} = m + (m_{A3} - m) + (m_{B1} - m) + (m_{C3} - m)$$

$$= 55.6809$$

The corresponding value of micro-hardness is given by

$$y_{opt}^2 = 1 / 10^{-\eta opt / 10}$$

or, $$y_{opt} = 608.20 \text{ HV}$$

Since this combination of the levels of input process parameters existed in the orthogonal array (as seventh row), a confirmation experiment was not required. The average value of micro-hardness obtained at this setting of the experiment was 608 HV which is very close to the theoretical value predicted by Taguchi analysis.

To obtain percentage contribution of the three factors and their significance, analysis of variance (ANOVA) of the S/N data was performed. It is presented in Table 5.39 which shows that all the three factors are significant for the response characteristic of micro-hardness. It is important to note that the percentage contribution of pulse off-time exceeds 10% and error contribution is negligible

Table 5.39 ANOVA table of S/N data for Micro-hardness (W3 – PW3)

Factor/Source	Sum of Squares	DOF	V	F-ratio	% Contri-bution	Remarks
Peak Current	3.2460	2	1.6230	1687.98	75.69	Significant
Pulse on-time	0.5872	2	0.2936	305.34	13.69	Significant
Pulse off-time	0.4535	2	0.2268	235.86	10.57	Significant
Error (Pooled)	0.0019	2	0.0010	-	0.05	-
Total	4.2886	8	-	-	100	-
DOF = Degrees of Freedom, V = Variance, Tabulated F-ratio $_{0.05}$ (2, 2) = 19						

Similar analysis has now been done for surface roughness. From the experimental data given in Table 5.37, the average values of surface roughness and the corresponding S/N ratios for the three levels of input process parameters have been calculated and are given in Table 5.40. These average values represent the factor effects at the three levels of input parameters.

Table 5.40 Average values by factor levels for Surface Roughness (W3 – PW3)

Parameter	Peak Current (Amperes)		Pulse on-time (µsec)		Pulse off-time (µsec)	
Levels	Raw Data	S/N Data	Raw Data	S/N Data	Raw Data	S/N Data
L1	1.20	-1.522	1.43	-2.867	1.64	-3.898
L2	1.61	-4.084	1.75	-4.579	1.49	-3.277
L3	2.04	-6.165	1.66	-4.325	1.71	-4.596

These factor effects have been plotted and presented in Fig. 5.18 (a), (b) and (c).

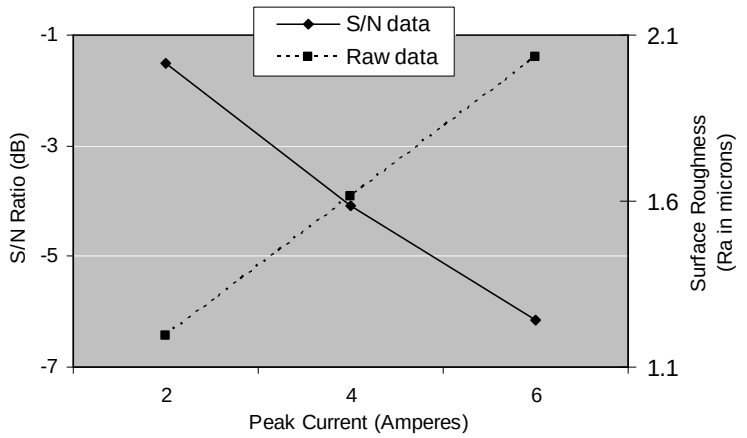

Fig. 5.18 (a) Effect of Peak Current on Surface Roughness and its S/N ratio (W3 – PW3)

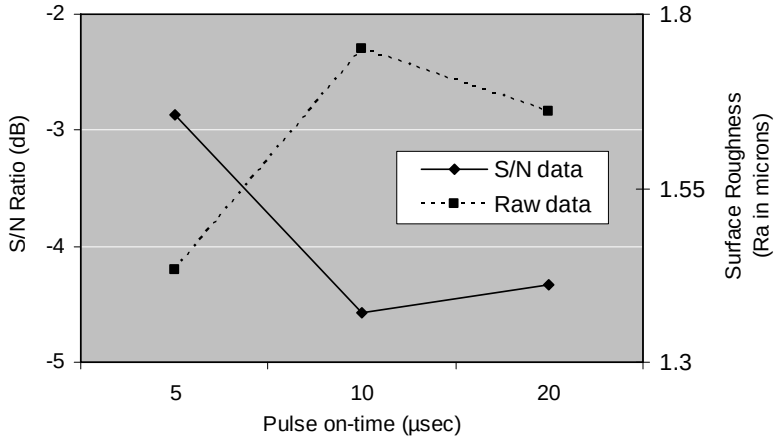

Fig. 5.18 (b) Effect of Pulse on-time on Surface Roughness and its S/N ratio (W3 – PW3)

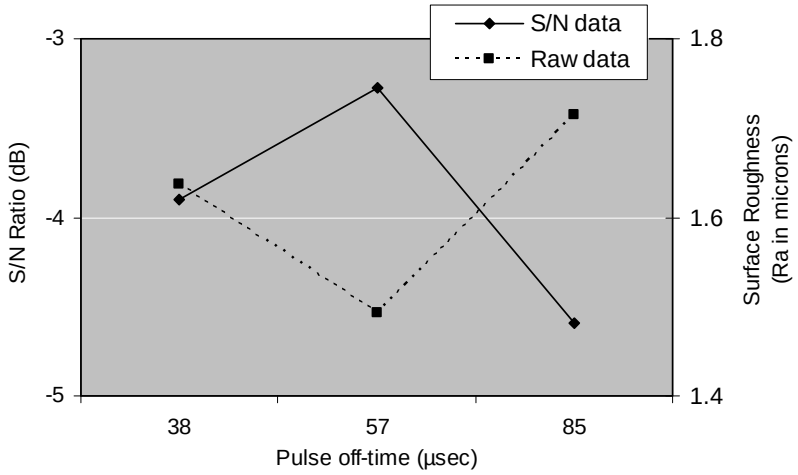

Fig. 5.18 (c) Effect of Pulse off-time on Surface Roughness and its S/N ratio (W3 – PW3)

It can be observed from Fig. 5.18 (a), (b) and (c) that the first level of peak current (A_1), first level of pulse on-time (B_1) and the second level of pulse off-time (C_2) give the lowest values of surface roughness. Hence, the optimum combination of input process parameters is $A_1B_1C_2$ which is found to be the same for all the three work materials. The theoretical value of η_{opt} for this optimum combination is given by:

$$\eta_{opt} = m + (m_{A1} - m) + (m_{B1} - m) + (m_{C2} - m)$$
$$= 0.18067$$

The corresponding value of surface roughness is given by

$$y_{opt}^2 = 10^{-\eta opt / 10}$$

or, $$y_{opt} = 0.98\ \mu m$$

Since this combination of input process parameters did not exist in the orthogonal array, a set of three confirmation experiments were conducted. The average value of surface roughness obtained at this setting of the experiment was 1.06 μm which is very close to the theoretical value predicted by Taguchi analysis.

Analysis of variance (ANOVA) of the S/N data was performed to obtain the percentage contribution of the three factors and their significance. It is presented in Table 5.41 and it can be seen that all the three factors are significant for the response characteristic of surface roughness. Peak current is the most important factor with 80.59 % contribution.

Table 5.41 ANOVA table of S/N data for Surface Roughness (W3 – PW3)

Factor/Source	Sum of Squares	DOF	V	F-ratio	% Contri-bution	Remarks
Peak Current	32.4465	2	16.2232	389.04	80.59	Significant
Pulse on-time	5.1192	2	2.5596	61.38	12.71	Significant
Pulse off-time	2.6127	2	1.3064	31.33	6.49	Significant
Error (Pooled)	0.0834	2	0.0417	-	0.21	-
Total	40.2618	8	-	-	100	-
DOF = Degrees of Freedom, V = Variance, Tabulated F-ratio $_{0.05}$ (2, 2) = 19						

5.4 MACHINING WITH TUNGSTEN POWDER (PW4)

5.4.1 Work Material – OHNS die steel (W1)

The observed values of micro-hardness and surface roughness after machining OHNS die steel with tungsten powder mixed in the dielectric medium and calculated values of their S/N ratios are given in Table 5.42.

Table 5.42 Observed values of Micro-hardness and Surface roughness and their calculated S/N ratios (W1 – PW4)

Expt. No.	Micro-hardness (HV)			S/N Ratio (dB)	Surface Roughness (R_a in microns)			S/N Ratio (dB)
	R1	R2	R3		R1	R2	R3	
1	863	846	829	58.544	4.11	3.96	3.87	-12.000
2	915	942	924	59.340	4.13	4.02	4.26	-12.336
3	939	951	927	59.452	5.24	4.80	5.09	-14.060
4	1041	1074	1087	60.562	5.46	5.74	5.87	-15.106
5	1268	1235	1253	61.951	6.81	7.18	6.96	-16.883
6	1056	1023	998	60.213	7.52	7.23	7.04	-17.226
7	940	971	927	59.513	6.54	6.88	6.79	-16.571
8	935	916	904	59.258	7.42	7.16	7.27	-17.248
9	910	859	876	58.899	7.21	7.33	7.05	-17.144
Total	8867	8817	8725	537.730	54.44	54.30	54.20	-138.573
	$\overline{T}_{MH}$ = Overall mean of micro hardness = 978.11			Mean, m= 59.748	$\overline{T}_{SR}$ = Overall mean of surface roughness = 6.035			Mean, m= -15.397

From this data, the average values of micro-hardness and corresponding S/N ratios for the three levels of peak current, pulse on-time and pulse off-time have been calculated and are given in Table 5.43.

Table 5.43 Average values by factor levels for Micro-hardness (W1 – PW4)

Parameter / Levels	Peak Current (amperes)		Pulse on-time (µsec)		Pulse off-time (µsec)	
	Raw Data	S/N Data	Raw Data	S/N Data	Raw Data	S/N Data
L1	904.00	59.112	953.11	59.539	930.00	59.338
L2	1115.00	60.908	1032.44	60.183	958.67	59.600
L3	915.33	59.223	948.78	59.521	1045.67	60.305

These factor effects have been plotted and presented in Fig. 5.19 (a), (b) and (c).

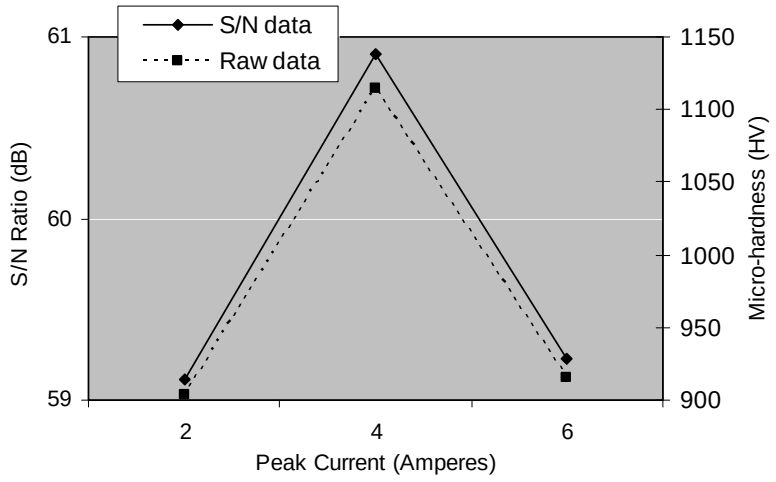

Fig. 5.19 (a) Effect of Peak Current on Micro-hardness and its S/N ratio (W1 – PW4)

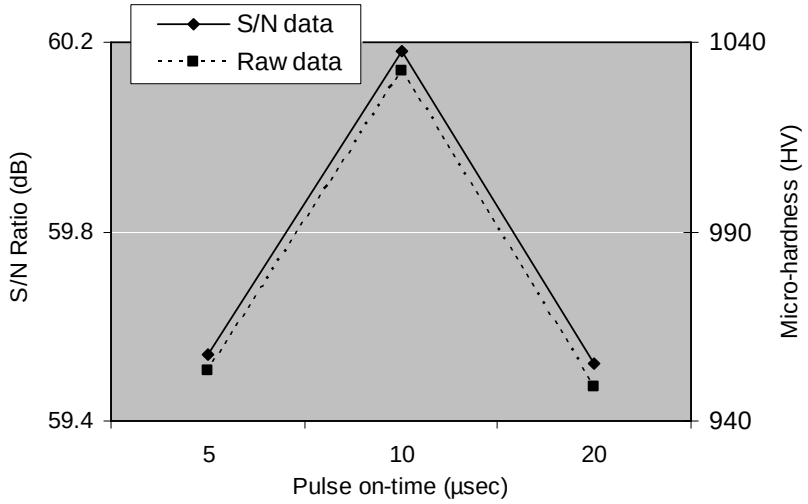

Fig. 5.19 (b) Effect of Pulse on-time on Micro-hardness and its S/N ratio (W1 – PW4)

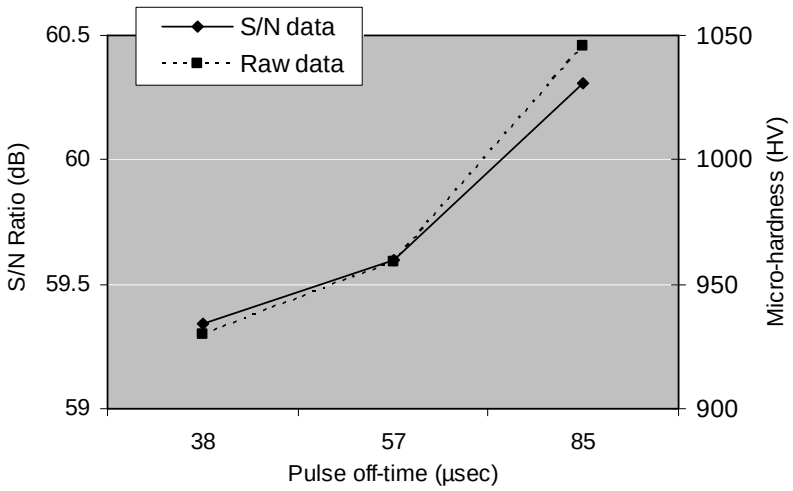

Fig. 5.19 (c) Effect of Pulse off-time on Micro-hardness and its S/N ratio (W1 – PW4)

The response of micro-hardness to variation in peak current with this powder is found to be identical to graphite and manganese powders but its response to variation in pulse on-time has undergone a change. The best value of micro-hardness has been achieved at level 2 of pulse on-time. One possible reason for this behaviour could be the high melting temperature of tungsten (Appendix-B). It can also be observed from Fig. 5.19 (a), (b) and (c) that the second level of peak current (A_2), second level of pulse on-time (B_2) and the third level of pulse off-time (C_3) give the highest values of micro-hardness. Hence, the optimum combination of input process parameters is $A_2B_2C_3$. The theoretical value of η for this optimum combination, denoted by η_{opt}, is given by:

$$\eta_{opt} = m + (m_{A2} - m) + (m_{B2} - m) + (m_{C3} - m) = 61.9006$$

where m is the overall mean of S/N data, m_{A2} is the mean of S/N data for factor A at level 2 and m_{B2} is the mean of S/N data for factor B at level 2, etc.

The corresponding best value of micro-hardness is given by

$$y_{opt}^2 = 1 / 10^{-\eta opt / 10}$$

or, $$y_{opt} = 1244.6 \text{ HV}$$

Since this combination existed in the orthogonal array (as fifth row), a confirmation experiment was not required. The average value of micro-hardness obtained at this setting of the experiment was 1252 HV which is better than and very close to the theoretical best value predicted by Taguchi analysis.

To obtain percentage contribution of the three factors and their significance, analysis of variance (ANOVA) of the S/N data was performed. It is presented in Table 5.44 which shows that all the three factors are significant for the response characteristic of micro-hardness. While peak current remains the most significant factor, it is important to note that the percentage contribution of pulse off-time exceeds that of pulse on-time. Error contribution is less than 1 %.

Table 5.44 ANOVA table of S/N data for Micro-hardness (W1 – PW4)

Factor/Source	Sum of Squares	DOF	V	F-ratio	% Contri-bution	Remarks
Peak Current	6.0810	2	3.0405	333.35	71.95	Significant
Pulse on-time	0.8513	2	0.4257	46.67	10.07	Significant
Pulse off-time	1.5007	2	0.7504	82.27	17.76	Significant
Error (Pooled)	0.0183	2	0.0092	-	0.22	-
Total	8.4513	8	-	-	100	-
DOF = Degrees of Freedom, V = Variance, Tabulated F-ratio $_{0.05}$ (2, 2) = 19						

Similar analysis has now been done for surface roughness. From the experimental data given in Table 5.42, the average values of surface roughness and the corresponding S/N ratios for the three levels of input process parameters have been calculated and are given in Table 5.45.

Table 5.45 Average values by factor levels for Surface Roughness (W1 – PW4)

Parameter / Levels	Peak Current (Amperes)		Pulse on-time (µsec)		Pulse off-time (µsec)	
	Raw Data	S/N Data	Raw Data	S/N Data	Raw Data	S/N Data
L1	4.39	-12.799	5.47	-14.559	6.18	-15.491
L2	6.65	-16.405	6.13	-15.489	5.67	-14.862
L3	7.07	-16.987	6.50	-16.143	6.25	-15.838

These factor effects have been plotted and presented in Fig. 5.20 (a), (b) and (c).

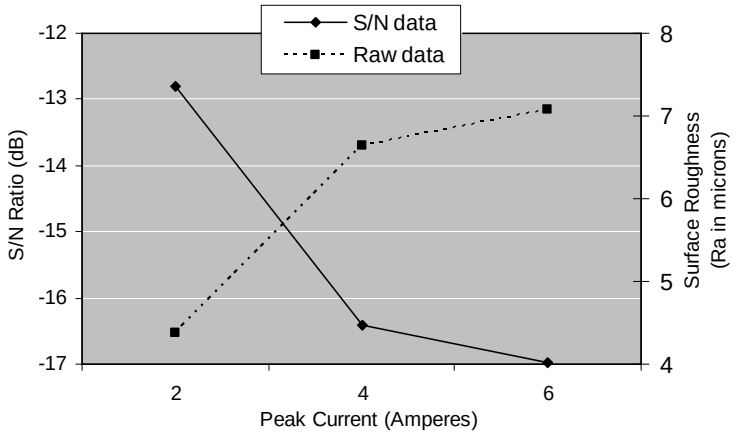

Fig. 5.20 (a) Effect of Peak Current on Surface Roughness and its S/N ratio (W1 – PW4)

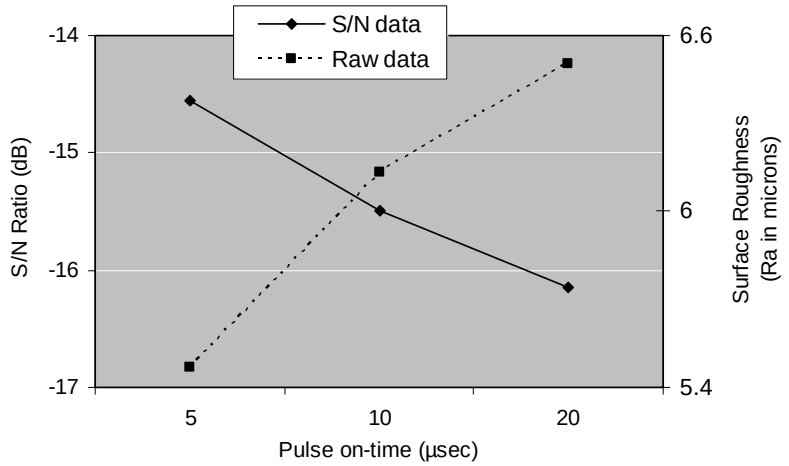

Fig. 5.20 (b) Effect of Pulse on-time on Surface Roughness and its S/N ratio (W1 – PW4)

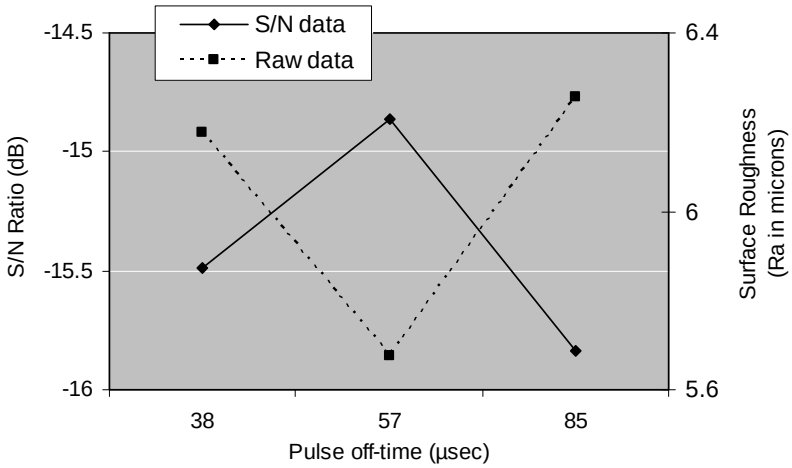

Fig. 5.20 (c) Effect of Pulse off-time on Surface Roughness and its S/N ratio (W1 – PW4)

Machining with tungsten powder is marked by deterioration in surface finish. It can be observed from Fig. 5.20 (a), (b) and (c) that the first level of peak current (A_1), first level of pulse on-time (B_1) and the second level of pulse off-time (C_2) give the lowest values of surface roughness. Hence, the optimum combination of input process parameters for this response characteristic is $A_1B_1C_2$. The theoretical value of η_{opt} for the optimum combination is given by:

$$\eta_{opt} = m + (m_{A1} - m) + (m_{B1} - m) + (m_{C2} - m) = -11.4254$$

The corresponding best value of surface roughness is given by

$$y_{opt}^2 = 10^{-\eta opt / 10} \quad \text{or,} \quad y_{opt} = 3.73\ \mu m$$

Since this combination of input process parameters did not exist in the orthogonal array, a set of three confirmation experiments were conducted. The average value of surface roughness obtained at this setting of the experiment was 3.85 μm which is very close to the theoretical best value predicted by Taguchi analysis.

Analysis of variance (ANOVA) of the S/N data was performed to obtain the percentage contribution of the factors and their significance. It is presented in Table 5.46 and it can be seen that all the three factors are significant for the response characteristic of surface roughness. However, contrary to micro-hardness, the contribution of pulse on-time for this response characteristic is found to be more than pulse off-time.

Table 5.46 ANOVA table of S/N data for Surface Roughness (W1 – PW4)

Factor/Source	Sum of Squares	DOF	V	F-ratio	% Contri-bution	Remarks
Peak Current	30.8918	2	15.4459	1160.83	85.36	Significant
Pulse on-time	3.8019	2	1.9010	142.87	10.51	Significant
Pulse off-time	1.4697	2	0.7349	55.23	4.06	Significant
Error (Pooled)	0.0266	2	0.0133	-	0.07	-
Total	36.1900	8	-	-	100	-
DOF = Degrees of Freedom, V = Variance, Tabulated F-ratio $_{0.05}(2, 2) = 19$						

5.4.2 Work Material – D2 High-carbon High-chromium die steel (W2)

The observed values of micro-hardness and surface roughness after machining D2 die steel with tungsten powder mixed in the dielectric medium and calculated values of their S/N ratios are given in Table 5.47.

Table 5.47 Observed values of Micro-hardness and Surface roughness and their calculated S/N ratios (W2 – PW4)

Expt. No.	Micro-hardness (HV)			S/N Ratio (dB)	Surface Roughness (R_a in microns)			S/N Ratio (dB)
	R1	R2	R3		R1	R2	R3	
1	953	907	925	59.349	4.76	4.43	4.65	-13.284
2	996	1019	1048	60.175	5.03	5.14	5.30	-14.249
3	1030	1065	1052	60.413	6.12	5.76	5.95	-15.483
4	1221	1208	1163	61.559	7.03	6.81	6.67	-16.699
5	1386	1412	1431	62.980	8.32	7.96	8.40	-18.307
6	1203	1157	1174	61.420	7.87	8.23	8.15	-18.153
7	1065	1048	1096	60.581	8.18	8.06	7.81	-18.082
8	1059	1021	1040	60.338	7.95	8.29	8.34	-18.271
9	952	979	937	59.605	8.62	8.23	8.47	-18.528
Total	9865	9816	9866	546.418	63.88	62.91	63.74	-151.057
	$\overline{T}_{MH}$ = Overall mean of micro hardness = 1094.3			Mean, m= 60.713	$\overline{T}_{SR}$ = Overall mean of surface roughness = 7.06			Mean, m= -16.784
R1, R2 and R3 represent the three repetitions.								

From this data, the average values of micro-hardness and corresponding S/N ratios for the three levels of peak current, pulse on-time and pulse off-time have been calculated and are given in Table 5.48.

Table 5.48 Average values by factor levels for Micro-hardness (W2 – PW4)

Parameter / Levels	Peak Current (amperes)		Pulse on-time (µsec)		Pulse off-time (µsec)	
	Raw Data	S/N Data	Raw Data	S/N Data	Raw Data	S/N Data
L1	999.44	59.979	1065.11	60.496	1048.78	60.369
L2	1261.67	61.986	1156.89	61.164	1058.11	60.446
L3	1021.89	60.174	1061.00	60.479	1176.11	61.325

These factor effects have been plotted and presented in Fig. 5.21 (a), (b) and (c).

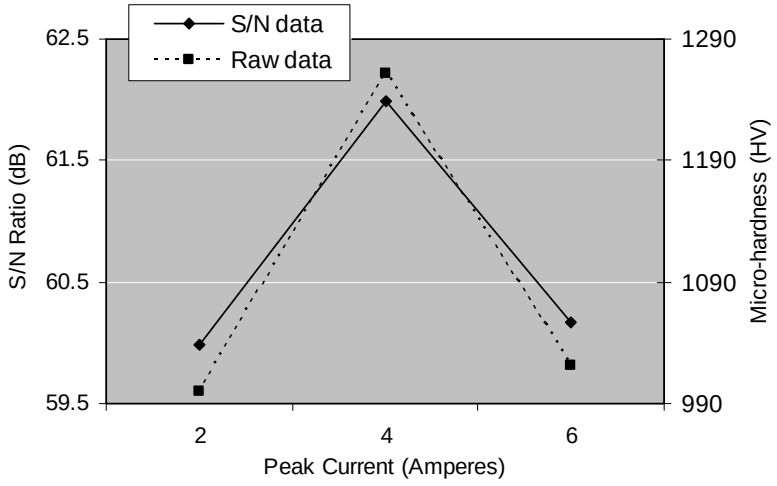

Fig. 5.21 (a) Effect of Peak Current on Micro-hardness and its S/N ratio (W2 – PW4)

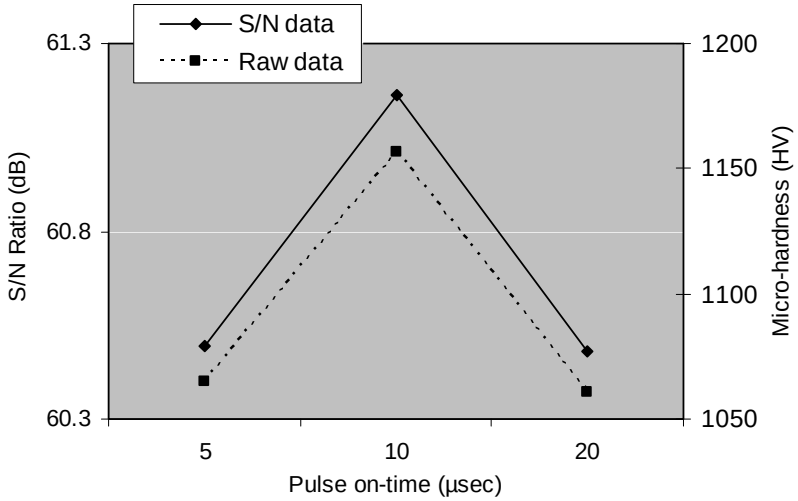

Fig. 5.21 (b) Effect of Pulse on-time on Micro-hardness and its S/N ratio (W2 – PW4)

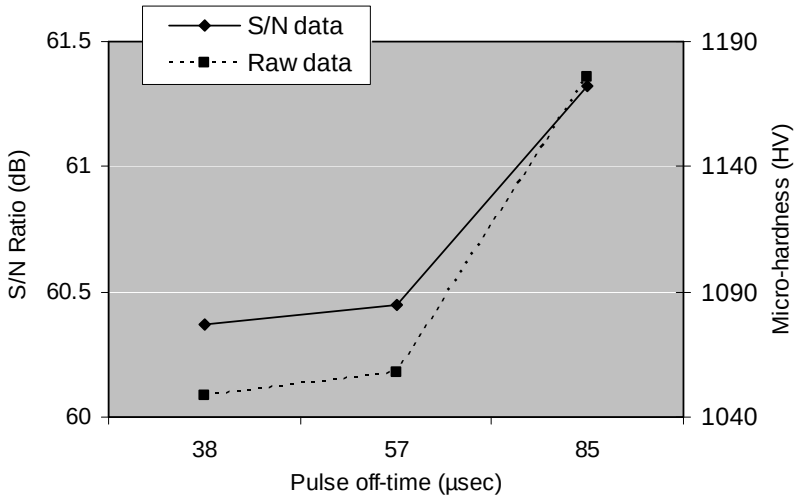

Fig. 5.21 (c) Effect of Pulse off-time on Micro-hardness and its S/N ratio (W2 – PW4)

For this material also, the response of micro-hardness to variation in peak current and pulse on-time is identical. However, a sharp improvement in micro-hardness is observed as pulse off-time changes from level 2 to 3. The actual value of micro-hardness achieved by this material is also the highest. Hence, it can be stated that sufficient off-time facilitates material transfer from the powders suspended in the dielectric medium. It is also observed from Fig. 5.21 (a), (b) and (c) that the second level of peak current (A_2), second level of pulse on-time (B_2) and the third level of pulse off-time (C_3) give the highest values of micro-hardness. Hence, the optimum combination of input process parameters is $A_2B_2C_3$. The theoretical value of η for this optimum combination, denoted by η_{opt}, is given by:

$$\eta_{opt} = m + (m_{A2} - m) + (m_{B2} - m) + (m_{C3} - m)$$

$$= 63.0486$$

The corresponding best value of micro-hardness is given by

$$y_{opt}^2 = 1 / 10^{-\eta opt / 10}$$

or, $$y_{opt} = 1420.46 \text{ HV}$$

Since this combination existed in the orthogonal array (as fifth row), a confirmation experiment was not required. The average value of micro-hardness obtained at this setting of the experiment was 1409.67 HV which is very close to the theoretical value predicted by Taguchi analysis.

To obtain percentage contribution of the three factors and their significance, analysis of variance (ANOVA) of the S/N data was performed. It is presented in Table 5.49 which shows that all the three factors are significant for the response characteristic of micro-hardness. For this work material also, it is important to note that the percentage contribution of pulse off-time is almost double that of pulse on-time.

Table 5.49 ANOVA table of S/N data for Micro-hardness (W2 – PW4)

Factor/Source	Sum of Squares	DOF	V	F-ratio	% Contri-bution	Remarks
Peak Current	7.3493	2	3.6747	304.19	73.63	Significant
Pulse on-time	0.9163	2	0.4582	37.92	9.18	Significant
Pulse off-time	1.6913	2	0.8457	70.00	16.95	Significant
Error (Pooled)	0.0242	2	0.0121	-	0.24	-
Total	9.9811	8	-	-	100	
DOF = Degrees of Freedom, V = Variance, Tabulated F-ratio $_{0.05}$ (2, 2) = 19						

Similar analysis has now been done for surface roughness. From the experimental data given in Table 5.47, the average values of surface roughness and the corresponding S/N ratios for the three levels of input process parameters have been calculated and are given in Table 5.50. These average values represent factor effects at the three levels of input process parameters.

Table 5.50 Average values by factor levels for Surface Roughness (W2 – PW4)

Parameter	Peak Current (Amperes)		Pulse on-time (µsec)		Pulse off-time (µsec)	
Levels	Raw Data	S/N Data	Raw Data	S/N Data	Raw Data	S/N Data
L1	5.24	-14.339	6.49	-16.022	6.96	-16.570
L2	7.72	-17.720	7.19	-16.943	6.81	-16.492
L3	8.22	-18.294	7.49	-17.388	7.40	-17.291

These factor effects have been plotted and presented in Fig. 5.22 (a), (b) and (c).

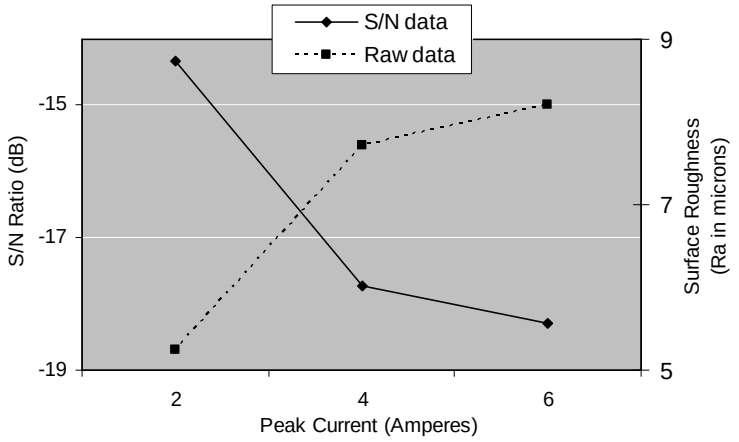

Fig. 5.22 (a) Effect of Peak Current on Surface Roughness and its S/N ratio (W2 – PW4)

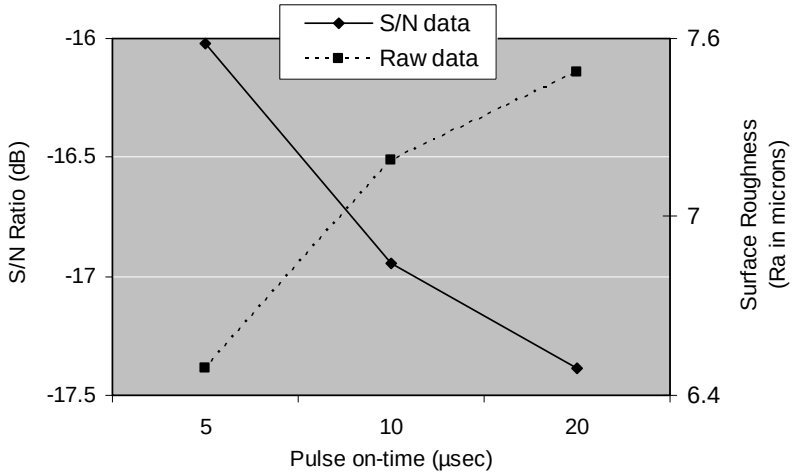

Fig. 5.22 (b) Effect of Pulse on-time on Surface Roughness and its S/N ratio (W2 – PW4)

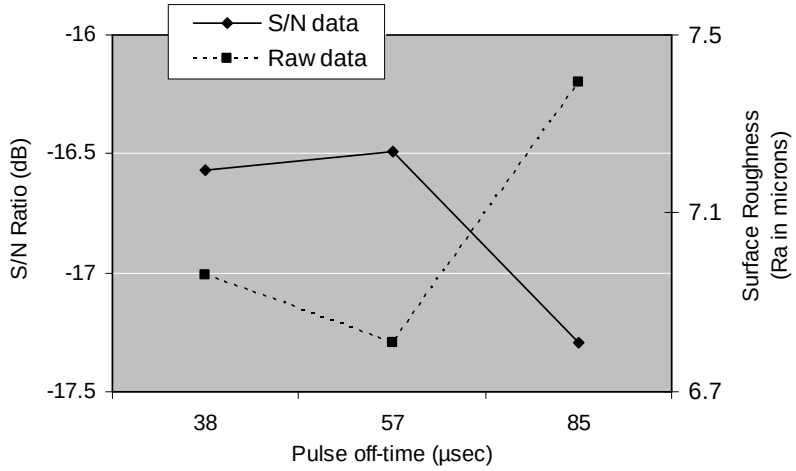

Fig. 5.22 (c) Effect of Pulse off-time on Surface Roughness and its S/N ratio (W2 – PW4)

It can be observed from Fig. 5.22 (a), (b) and (c) that the first level of peak current (A_1), first level of pulse on-time (B_1) and the second level of pulse off-time (C_2) give the lowest values of surface roughness. Hence, the optimum combination of input process parameters is $A_1B_1C_2$. The theoretical value of η_{opt} for the optimum combination is given by:

$$\eta_{opt} = m + (m_{A1} - m) + (m_{B1} - m) + (m_{C2} - m)$$
$$= -13.2845$$

The corresponding best value of surface roughness is given by

$$y_{opt}^2 = 10^{-\eta opt / 10}$$

or, $$y_{opt} = 4.62\ \mu m$$

Since this combination of input process parameters did not exist in the orthogonal array, a set of three confirmation experiments were conducted. The average value of surface roughness obtained at this setting of the experiment was 4.47 μm which is better than and very close to the theoretical value predicted by Taguchi analysis.

Analysis of variance (ANOVA) of the S/N data was performed to obtain the percentage contribution of the three factors and their significance. It is presented in Table 5.51 which shows that all the three factors are significant for the response characteristic of surface roughness. The percentage contribution of peak current is found to be very high at almost 87% whereas the contribution of pulse off-time is less than pulse on-time.

Table 5.51 ANOVA table of S/N data for Surface Roughness (W2 – PW4)

Factor/Source	**Sum of Squares**	**DOF**	**V**	**F-ratio**	**% Contri-bution**	**Remarks**
Peak Current	27.3993	2	13.6997	1003.97	86.97	Significant
Pulse on-time	2.9152	2	1.4576	106.82	9.25	Significant
Pulse off-time	1.1630	2	0.5815	42.62	3.69	Significant
Error (Pooled)	0.0273	2	0.0137	-	0.09	-
Total	31.5048	8	-	-	100	
DOF = Degrees of Freedom, V = Variance, Tabulated F-ratio $_{0.05}$ (2, 2) = 19						

5.4.3 Work Material – H13 hot die steel (W3)

The observed values of micro-hardness and surface roughness after machining H13 hot die steel with tungsten powder mixed in the dielectric medium and calculated values of their S/N ratios are given in Table 5.52.

Table 5.52 Observed values of Micro-hardness and Surface roughness and their calculated S/N ratios (W3 – PW4)

Expt. No.	Micro-hardness (HV)			S/N Ratio (dB)	Surface Roughness (R_a in microns)			S/N Ratio (dB)
	R1	R2	R3		R1	R2	R3	
1	706	735	718	57.139	3.21	3.26	3.09	-10.069
2	797	820	849	58.289	3.47	3.13	3.34	-10.413
3	832	853	814	58.408	3.85	4.21	3.72	-11.893
4	961	952	934	59.543	4.23	4.12	4.43	-12.592
5	1078	1091	1046	60.597	5.27	5.68	5.36	-14.711
6	943	905	914	59.278	5.62	5.43	5.80	-14.993
7	842	818	857	58.470	5.19	5.31	4.94	-14.234
8	790	839	811	58.197	5.73	5.85	6.08	-15.400
9	824	783	795	58.063	5.57	5.46	5.28	-14.709
Total	7773	7796	7738	527.986	42.14	42.45	42.04	-119.014
	$\overline{T}_{MH}$ = Overall mean of micro hardness = 863.22			Mean, m= 58.665	$\overline{T}_{SR}$ = Overall mean of surface roughness = 4.69			Mean, m= -13.224
R1, R2 and R3 represent the three repetitions.								

From this data, the average values of micro-hardness and corresponding S/N ratios for the three levels of peak current, pulse on-time and pulse off-time have been calculated and are given in Table 5.53.

Table 5.53 Average values by factor levels for Micro-hardness (W3 – PW4)

Parameter / Levels	Peak Current (amperes)		Pulse on-time (µsec)		Pulse off-time (µsec)	
	Raw Data	S/N Data	Raw Data	S/N Data	Raw Data	S/N Data
L1	791.56	57.945	835.89	58.384	817.89	58.205
L2	980.44	59.806	902.33	59.028	857.22	58.632
L3	817.67	58.244	851.44	58.583	914.56	59.159

These factor effects have been plotted and presented in Fig. 5.23 (a), (b) and (c).

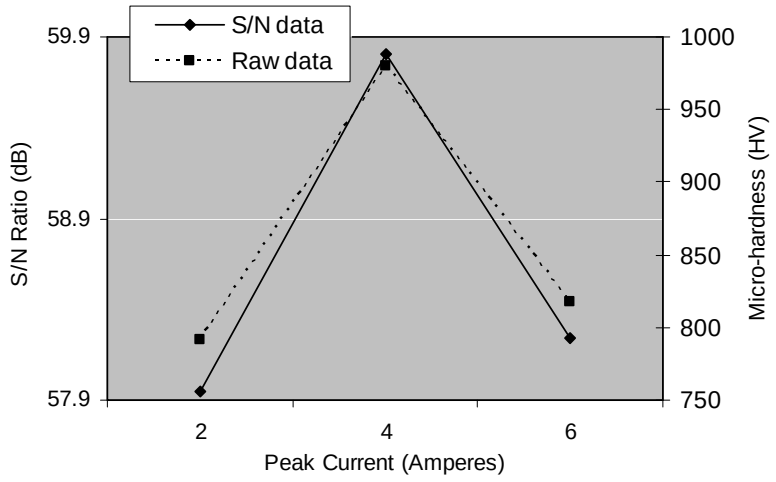

Fig. 5.23 (a) Effect of Peak Current on Micro-hardness and its S/N ratio (W3 – PW4)

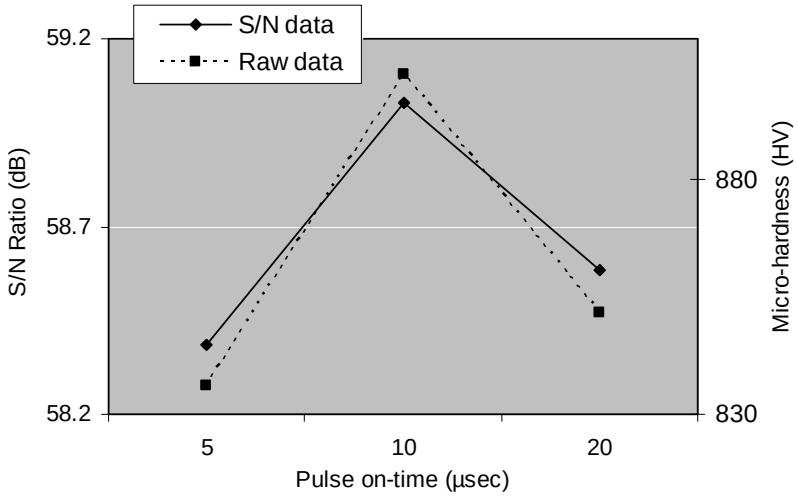

Fig. 5.23 (b) Effect of Pulse on-time on Micro-hardness and its S/N ratio (W3 – PW4)

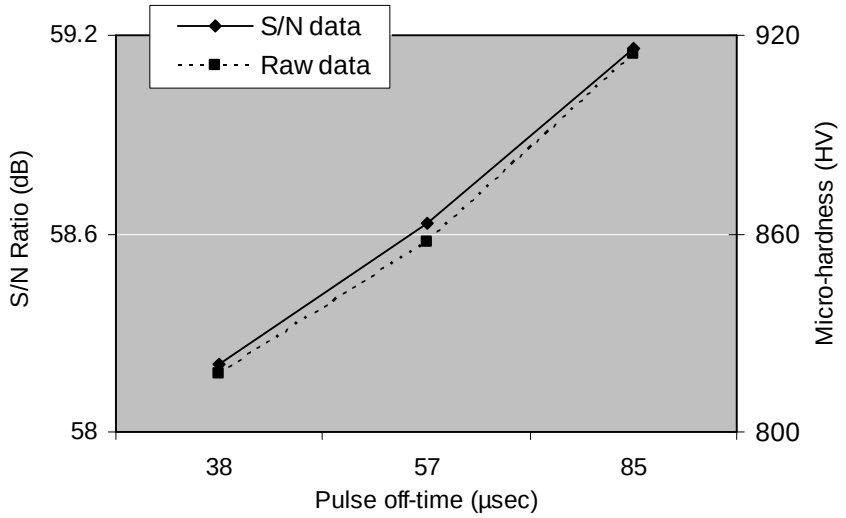

Fig. 5.23 (c) Effect of Pulse off-time on Micro-hardness and its S/N ratio (W3 – PW4)

Amongst the four powders, the best improvement in micro-hardness has been reported by tungsten powder for all the three work materials, followed by manganese powder. It was accompanied by some deterioration in surface finish but that does not have a major negative influence on the performance of dies and press tools. Hence, this powder can be recommended for improvement in surface hardness of die steels. It is also observed from Fig. 5.23 (a), (b) and (c) that the second level of peak current (A_2), second level of pulse on-time (B_2) and the third level of pulse off-time (C_3) give the highest values of micro-hardness. Hence, the optimum combination of input process parameters is $A_2B_2C_3$. The theoretical value of η for the optimum c combination, denoted by η_{opt}, is given by:

$$\eta_{opt} = m + (m_{A2} - m) + (m_{B2} - m) + (m_{C3} - m)$$

$$= 60.6624$$

The corresponding best value of micro-hardness is given by

$$y_{opt}^{2} = 1 / 10^{-\eta opt / 10}$$

or, $$y_{opt} = 1079.24 \text{ HV}$$

Since this combination existed in the orthogonal array (as fifth row), a confirmation experiment was not required. The average value of micro-hardness obtained at this setting of the experiment was 1071.67 HV which is very close to the theoretical best value predicted by Taguchi analysis.

To obtain percentage contribution of the three factors and their significance, analysis of variance (ANOVA) of the S/N data was performed. It is presented in Table 5.54 which shows that all the three factors are significant for the response characteristic of micro-hardness. The percentage contribution of pulse off-time is almost double that of pulse on-time for all the three work materials which emphasizes the importance of sufficient cooling time. Error contribution is again found to be less than 1 %.

Table 5.54 ANOVA table of S/N data for Micro-hardness (W3 – PW4)

Factor/Source	Sum of Squares	DOF	V	F-ratio	% Contri-bution	Remarks
Peak Current	5.9935	2	2.9968	281.63	74.59	Significant
Pulse on-time	0.6513	2	0.3257	30.60	8.10	Significant
Pulse off-time	1.3692	2	0.6846	64.34	17.04	Significant
Error (Pooled)	0.0213	2	0.0107	-	0.27	-
Total	8.0353	8		-	100	
DOF = Degrees of Freedom, V = Variance, Tabulated F-ratio $_{0.05}$ (2, 2) = 19						

Similar analysis has now been done for surface roughness. From the experimental data given in Table 5.52, the average values of surface roughness and the corresponding S/N ratios for the three levels of input process parameters have been calculated and are given in Table 5.55.

Table 5.55 Average values by factor levels for Surface Roughness (W3 – PW4)

Parameter	Peak Current (Amperes)		Pulse on-time (µsec)		Pulse off-time (µsec)	
Levels	Raw Data	S/N Data	Raw Data	S/N Data	Raw Data	S/N Data
L1	3.48	-10.792	4.20	-12.299	4.90	-13.487
L2	5.10	-14.099	4.88	-13.508	4.34	-12.571
L3	5.49	-14.781	4.99	-13.865	4.84	-13.613

These factor effects have been plotted and presented in Fig. 5.24 (a), (b) and (c).

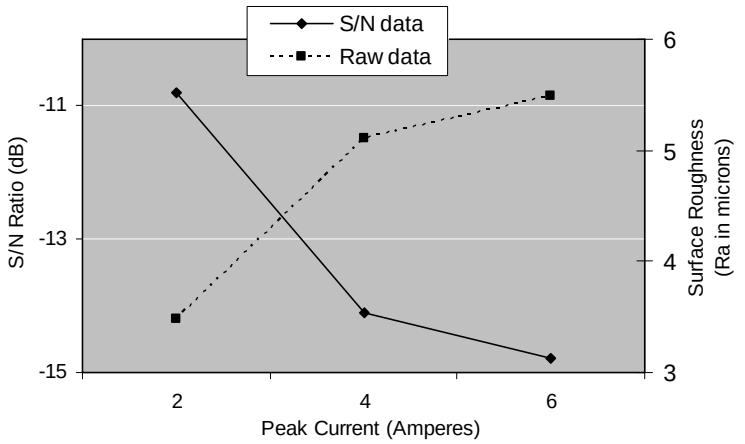

Fig. 5.24 (a) Effect of Peak Current on Surface Roughness and its S/N ratio (W3 – PW4)

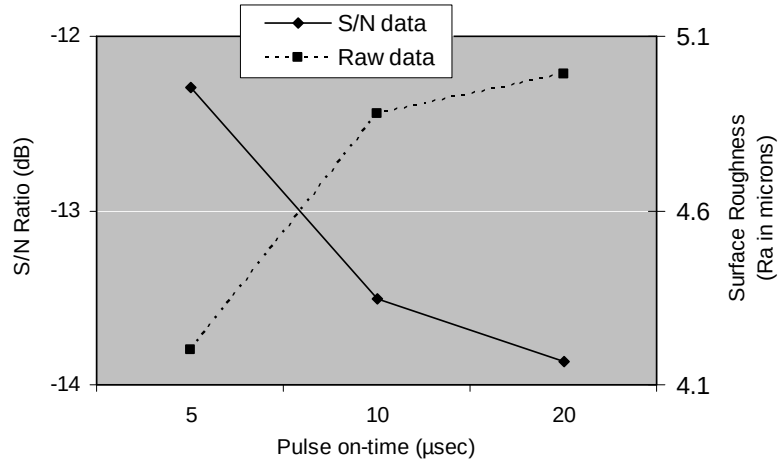

Fig. 5.24 (b) Effect of Pulse on-time on Surface Roughness and its S/N ratio (W3 – PW4)

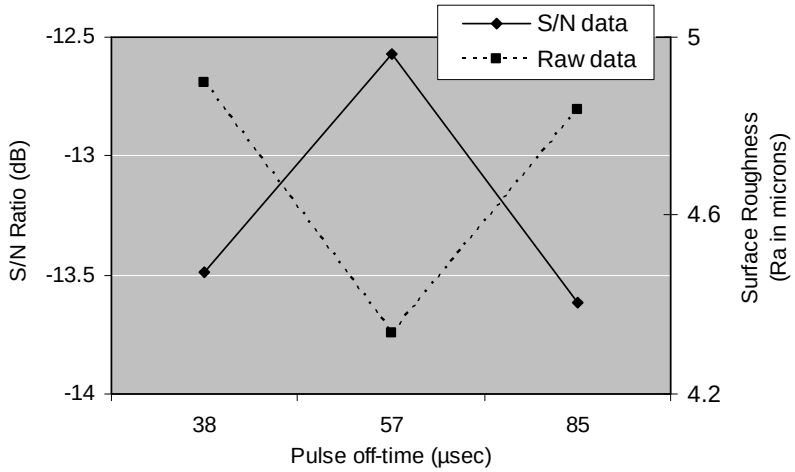

Fig. 5.24 (c) Effect of Pulse off-time on Surface Roughness and its S/N ratio (W3 – PW4)

It can be observed from Fig. 5.24 (a), (b) and (c) that the first level of peak current (A_1), first level of pulse on-time (B_1) and the second level of pulse off-time (C_2) give the lowest values of surface roughness. Hence, the optimum combination of input process parameters for this response characteristic is $A_1B_1C_2$. In general, level 2 of pulse off-time is found to be the most suitable for good surface finish. Lower value of this parameter shows a sharp deterioration in surface finish which is indicative of unstable machining conditions in the sparking zone. The theoretical value of η_{opt} for the optimum combination is given by:

$$\eta_{opt} = m + (m_{A1} - m) + (m_{B1} - m) + (m_{C2} - m) = -9.2138$$

The corresponding value of surface roughness is given by

$$y_{opt}^2 = 10^{-\eta opt / 10}$$

or, $$y_{opt} = 2.89\ \mu m$$

Since this combination of input process parameters did not exist in the orthogonal array, a set of three confirmation experiments were conducted. The average value of surface roughness obtained at this setting of the experiment was 2.96 μm which is very close to the theoretical value predicted by Taguchi analysis.

Analysis of variance (ANOVA) of the S/N data was performed to obtain the percentage contribution of the three factors and their significance. It is presented in Table 5.56.

Table 5.56 ANOVA table of S/N data for Surface Roughness (W3 – PW4)

Factor/Source	Sum of Squares	DOF	V	F-ratio	% Contri-bution	Remarks
Peak Current	27.3196	2	13.6598	1027.03	81.97	Significant
Pulse on-time	4.0432	2	2.0216	152.00	12.13	Significant
Pulse off-time	1.9392	2	0.9696	72.90	5.82	Significant
Error (Pooled)	0.0266	2	0.0133	-	0.08	-
Total	33.3286	8		-	100	
DOF = Degrees of Freedom, V = Variance, Tabulated F-ratio $_{0.05}$ (2, 2) = 19						

It can be observed that all the three factors are significant for the response characteristic of surface roughness. While the contribution of pulse off-time was found to be higher than pulse on-time for the response characteristic of micro-hardness, the behaviour is opposite for surface roughness. For all the four powders, the optimum combination of the levels of input process parameters was found to be dependent on the type of powder and not the work material. Hence, it can be stated that the same combination will hold good for any die steel material if a particular powder is used.

CHAPTER - 6

ANALYSIS AND DISCUSSION OF THE RESULTS

During the experimentation, three die steel work materials were machined using four electrode materials and four different powders suspended in the dielectric medium under process conditions favouring material transfer to the workpiece surface. Machining was done by varying peak current, pulse on-time and pulse off-time according to L9 orthogonal array of Taguchi design of experiments. All the machined surfaces were subjected to micro-hardness and surface roughness measurements. The data was analyzed to find out the desirable combination of levels of the three input process parameters, their significance and relative contribution. Wherever the desirable combination of factors did not exist as one of the experiments in the orthogonal array, confirmation experiments were conducted to find out the best experimental results and they were compared with the theoretical values predicted by Taguchi analysis. The results of experimentation with different electrode materials and powders have been presented in Chapters 4 and 5 respectively.

Further analysis of the machined surfaces after confirmation experiments was done to find out surface composition and microstructure and it has been presented in this chapter. Surface composition was determined with the help of X-ray diffraction (XRD) analysis and then it was quantitatively confirmed by optical emission spectrometry. Microstructural studies were carried out on a Scanning Electron Microscope (SEM). Since peak current emerged as the major factor influencing both micro-hardness and surface roughness, some more experiments were conducted by varying the peak current and keeping the other two factors constant, to study the effect of peak current on the chemical composition of the machined surface.

The analysis has been divided into two parts – in the first part, effect of machining in different environments on each work material has been discussed (Para 6.1 to 6.3); and in the second part, favourable conditions for the migration of important alloying elements to the workpiece surface have been discussed (Para 6.4 to 6.8). A comparison between the two methods of surface modification has also been drawn.

Pictorial views of some of the machined samples of the three die steel materials are shown in Fig. 6.1.

Fig. 6.1 (a) Some machined samples of OHNS die steel

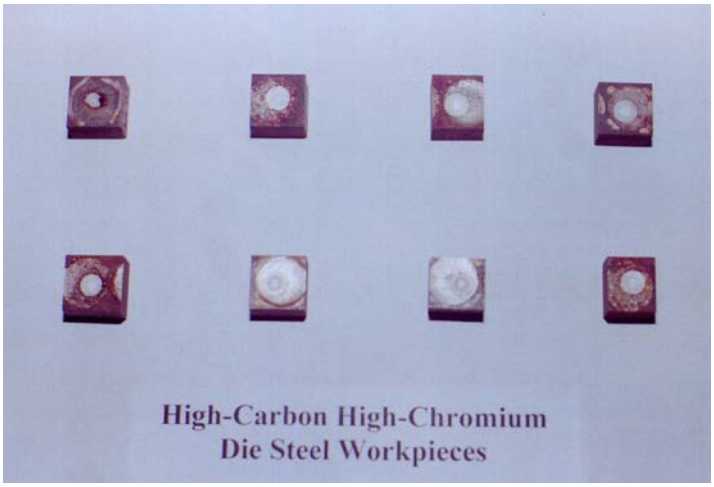

Fig. 6.1 (b) Some machined samples of D2 die steel

Fig. 6.1 (c) Some machined samples of H13 hot die steel

Before the start of experimentation, photomicrographs of the three die steel materials were taken on a Scanning Electron Microscope. The samples were polished and etched as per standard metallographic procedure before taking the pictures. These micrographs are presented in Fig. 6.2. In the micrograph of OHNS die steel {Fig. 6.2 (a)}, cementite phase appears as small white spots and the gray matrix is tempered martensite. In the micrograph of D2 high-carbon high-chromium die steel {Fig. 6.2 (b)}, large undissolved carbides can be seen in a tempered martensite matrix. In the micrograph of H13 hot die steel {Fig. 6.2 (c)}, the cementite particles are fewer and smaller as compared to OHNS die steel and the gray matrix is tempered martensite.

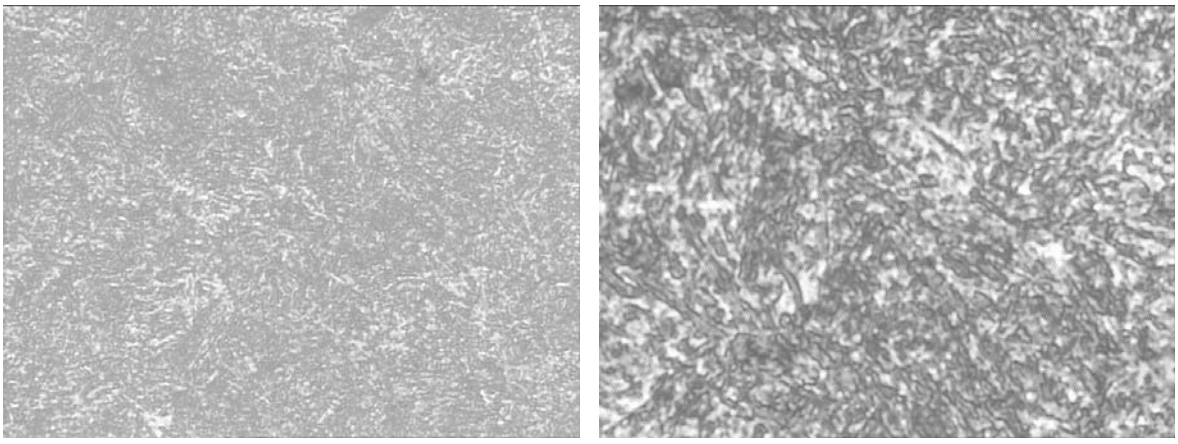

at 400X **at 1000X**

Fig. 6.2 (a) SEM micrograph of the original microstructure of OHNS die steel

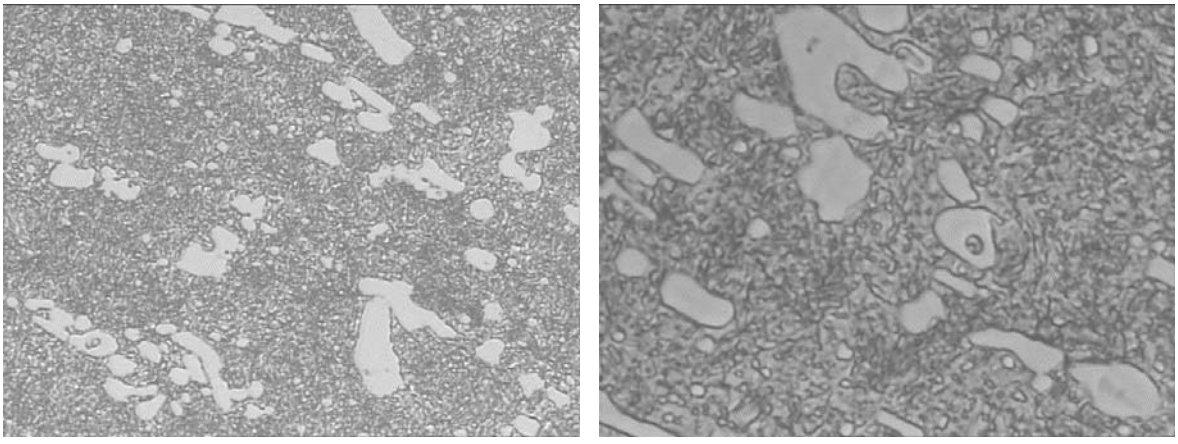

at 400X **at 1000X**

Fig. 6.2 (b) SEM micrograph of the original microstructure of D2 die steel

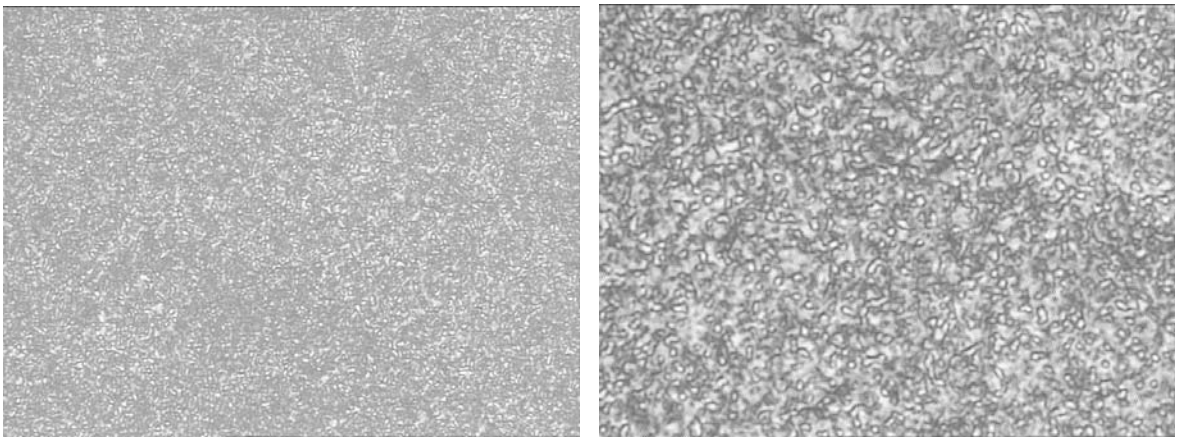

at 400X **at 1000X**

Fig. 6.2 (c) SEM micrograph of the original microstructure of H13 hot die steel

The XRD pattern of a surface of OHNS die steel after machining with copper electrode was also taken for reference purposes and it is presented in Fig. 6.3. The pattern shows the presence of ferrite (Fe-C) and cementite (Fe_3C) phases and some traces of copper. Peaks of only those alloying elements which were significant for this research work and their compounds were taken up for identification and others were ignored.

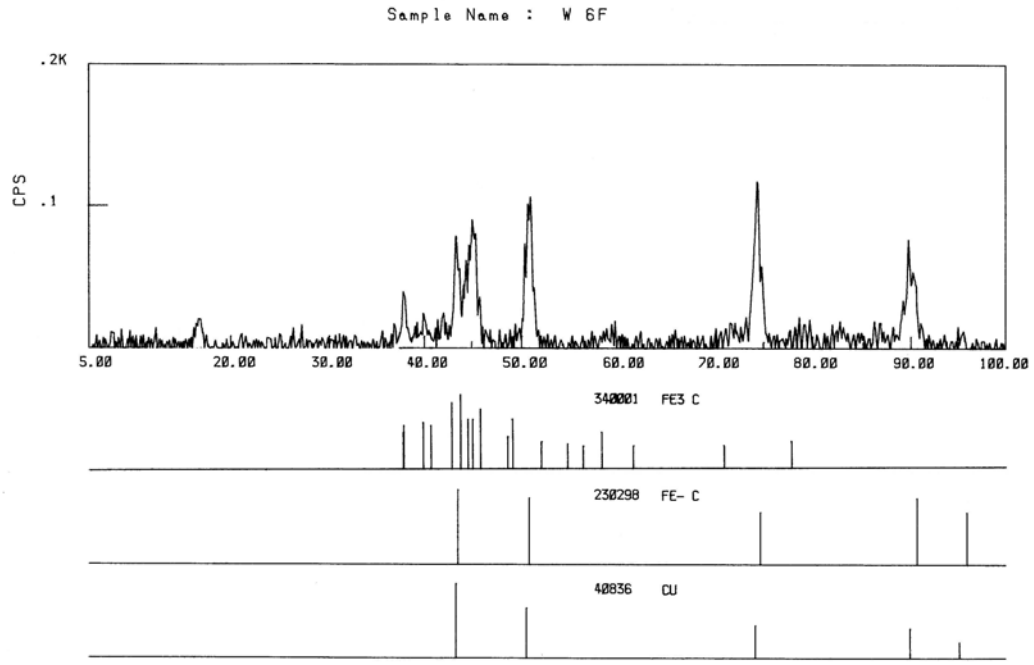

Fig. 6.3 XRD pattern of OHNS die steel after machining with Copper electrode (at I_p = 6 amp, P_{on} = 5 µsec and P_{off} = 85 µsec)

The spectrometric analysis of the work surface showed an increase in percentages of copper and carbon. There was no copper present in the material initially but after machining, it was found to be 0.15 % and the percentage of carbon increased from 0.82 % to 1.02 %. The corresponding SEM micrograph of the same surface is shown in Fig. 6.4. Compared to the microstructure given in Fig. 6.2 (a), significant surface changes can be observed in this micrograph. The large craters are characteristic of electrical discharge machined surface at high values of peak current.

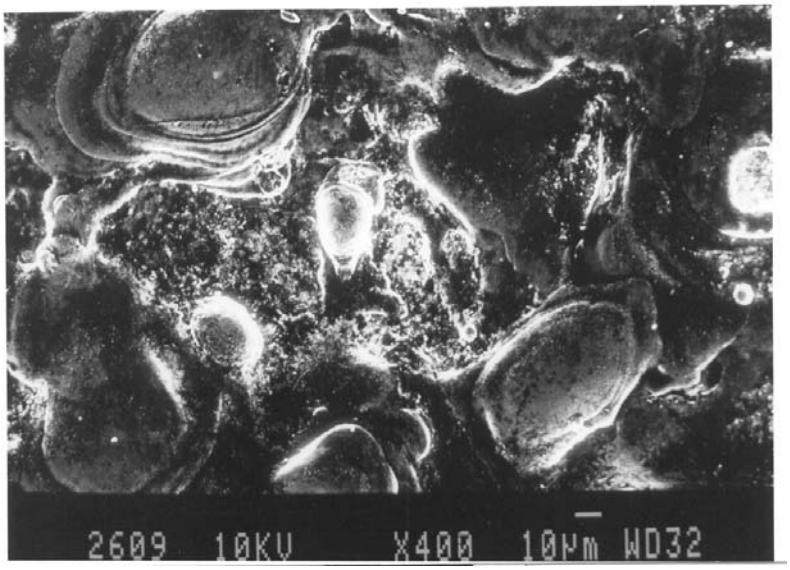

Fig. 6.4 SEM micrograph of OHNS die steel after machining with Copper electrode (at I_p = 6 amp, P_{on} = 5 µsec and P_{off} = 85 µsec)

6.1 RESPONSE OF OHNS DIE STEEL

6.1.1 Effect on Micro-hardness

The response of OHNS die steel in terms of improvement in micro-hardness after machining with different electrode materials and powders has been summarized in Table 6.1 and comparison has been done with the original value of micro-hardness recorded before the start of experimentation. It can be seen that all the eight methods result in an increase in micro-hardness, ranging from 12.5 % with copper electrode to 106.3 % with tungsten powder. Peak current is found to be the most significant factor with 56 % contribution when copper electrode is used and more than 70 % in all other cases, followed by pulse on-time and pulse off-time.

Table 6.1 Comparative analysis of Micro-hardness for OHNS die steel

Electrode Material / Powder	**Micro-hardness on OHNS Die Steel (Vickers Hardness Number, HV)**		
	Best Value achieved	% improvement	Optimum Process Parameters
Before machining	607.00	-	-
Copper Electrode	682.67	12.5 %	$A_3B_1C_3$
Graphite Electrode	683.67	12.6 %	$A_3B_1C_3$
Copper-Tungsten Electrode	923.33	52.1 %	$A_3B_1C_2$
Inconel alloy Electrode	1143.00	88.3 %	$A_2B_1C_2$
Graphite Powder	743.33	22.5 %	$A_2B_1C_3$
Manganese Powder	1049.33	72.9 %	$A_2B_1C_3$
Silicon Powder	721.00	18.8 %	$A_3B_1C_3$
Tungsten Powder	1252.00	106.3 %	$A_2B_2C_3$
Factor A represents Peak current and level A_1 = 2 A, A_2 = 4 A, A_3 = 6 A Factor B represents Pulse on-time and level B_1 = 5 µs, B_2 = 10 µs, B_3 = 20 µs Factor C represents Pulse off-time and level C_1 = 38 µs, C_2 = 57 µs, C_3 = 85 µs			

This increase in micro-hardness can be attributed to three reasons:

- More heating and quenching of the work surface results in more hardening.
- The increase in carbon in the work surface results in formation of more cementite which has high hardness.

- Transfer of alloying elements to the work surface results in formation of their solid solutions in ferrite and cementite phases or their independent hard carbides or both. This aspect has been analyzed with more details later in this chapter when migration of individual alloying elements is taken up for discussion.

The best value of peak current is found to be 4 A or 6 A in all cases (A_2 or A_3). It means that very little transfer of material is taking place at 2 A value of peak current. Low value of peak current means less energy in the discharge channel and also less heating and quenching effect. The best value of pulse on-time is found to be 5 μsec (B_1) in all cases with the exception of tungsten powder where it is 10 μsec (B_2). One possible reason for this occurrence can be the very high melting point of tungsten as compared to the other elements taken up in this work (Appendix-B). Higher value of pulse on-time means that heat energy in the discharge channel is available for a longer period of time. It is also observed that machining with tungsten powder gives the best increase in micro-hardness which is due to the presence of tungsten and tungsten carbide in the work surface (Fig. 6.18). The best value of pulse off-time is found to be 57 μsec (C_2) or 85 μsec (C_3). However, it is significant to note that this value is 57 μsec when material transfer is to take place from copper-tungsten and inconel electrodes, and it is 85 μsec in case of all the powders. It means that more idle time is required for products of sparking to settle in the work surface when machining is done in powder-mixed dielectric. On the other hand, when material transfer is desired from the electrode bodies, less idle time means that the electrode is still hot when the next sparking cycle starts and it can disintegrate easily.

Amongst the electrode materials, inconel reports the best performance with approximately 88% increase in micro-hardness which has been made possible by the transfer of chromium and nickel to the work surface. Both these elements form intermetallic compounds as well as solid solution with iron (Fig. 6.25 and 6.27) and strengthen it. The transfer of these elements has been further confirmed by spectrometric analysis. Since melting point of chromium and nickel is lower than that of tungsten, the optimum value of peak current for this electrode material is found to be less than that required by copper-tungsten electrode. Though tungsten is more effective in improving the hardness, but very little transfer of tungsten has taken place from the electrode body. Hence, it can be stated that inconel alloy is a better electrode material if surface improvement is desired only by material transfer from the tool electrode.

6.1.2 Effect on Surface Roughness

The response of OHNS die steel in terms of improvement in surface roughness has been summarized in Table 6.2. The comparison has been done with the value of surface roughness achieved with copper electrode.

Table 6.2 Comparative analysis of Surface roughness for OHNS die steel

Electrode Material / Powder	**Surface Roughness on OHNS Die Steel (R_a in microns)**		
	Best Value achieved	% improvement	Optimum Process Parameters
Copper Electrode	2.46	-	$A_1B_1C_2$
Graphite Electrode	1.63	33.7 %	$A_1B_1C_2$
Copper-Tungsten Electrode	1.72	30.1 %	$A_1B_1C_2$
Inconel alloy Electrode	5.91	-	$A_1B_2C_3$
Graphite Powder	0.73	70.3 %	$A_1B_1C_2$
Manganese Powder	3.31	-	$A_1B_1C_1$
Silicon Powder	0.92	62.6 %	$A_1B_1C_2$
Tungsten Powder	3.85	-	$A_1B_1C_2$
Factor A represents Peak current and level A_1 = 2 A, A_2 = 4 A, A_3 = 6 A Factor B represents Pulse on-time and level B_1 = 5 µs, B_2 = 10 µs, B_3 = 20 µs Factor C represents Pulse off-time and level C_1 = 38 µs, C_2 = 57 µs, C_3 = 85 µs			

It is observed that graphite and copper-tungsten electrodes improve the surface finish whereas a sharp deterioration takes place when machining is done with inconel electrode.

This can be attributed to high wear of inconel electrode. As was observed during pilot experimentation (para 3.3.3), electrode wear of inconel was 1.912 % - the highest amongst the four electrode materials. This results in an uneven electrode surface and uneven sparking. Since machined surface is a mirror image of the electrode surface, deterioration of surface finish takes place.

The optimum machining parameters for best surface finish are on expected lines, that is, minimum value of peak current (2 A), minimum value of pulse on-time (5 μsec) and moderate value of pulse off-time (57 μsec); the only exceptions being inconel electrode and manganese powder. But even in those two cases, the change in surface roughness from C_1 to C_2 is only marginal. Peak current emerges as the most important factor and its contribution is higher for this response characteristic as compared to micro-hardness (more than 80 % in all cases). It was expected that the transfer of material would result in deterioration of surface finish and wherever significant increase in micro-hardness took place, surface finish would not be good. However, this did not happen. Despite the transfer of material, it was found that surface finish depended on the values of peak current and pulse on-time to a large extent; and on pulse off-time to a very limited extent.

Machining with graphite and silicon powders suspended in the dielectric medium resulted in significant improvement of R_a values of surface roughness (also R_z values as observed in subsequent experiments). This was made possible due to lowering of the breakdown strength of the dielectric medium by these powders. As a result, gap distance between the workpiece and tool electrode increased and spark energy reduced. The performance of graphite powder was found to be better than silicon powder (Tables 6.11 and 6.18).

6.2 RESPONSE OF D2 HIGH CARBON HIGH CHROMIUM DIE STEEL

6.2.1 Effect on Micro-hardness

The response of D2 die steel in terms of improvement in micro-hardness has been summarized in Table 6.3. Amongst the three work materials, it has the highest initial value of hardness because of the high amount of carbon and chromium present in it. Since this work material was already rich in carbon (1.57 %), it was not machined with graphite electrode or graphite powder suspended in the dielectric medium. Once again, manganese and tungsten powders gave very good improvement in micro-hardness. Machining with manganese

powder resulted in the formation of manganese carbide (Mn_7C_3) in the workpiece surface (Fig. 6.31). When tungsten powder was used, the best value of 1409 HV for the whole experimentation was achieved by this material. It can be stated that even during electrical discharge machining, the actual value of hardness achieved depends on the type of work material. This has been made possible due the formation of double carbide of iron and tungsten (Fe_6W_6C) along with tungsten carbide (WC) in the workpiece surface (Fig. 6.20). Copper-tungsten electrode does not show a good performance for this material even though some material transfer has taken place (Fig. 6.14). The impact of machining with silicon powder on micro-hardness is also very less. No traces of silicon or silicon carbide can be seen in the XRD pattern of the work surface and it can be said that the 23 % increase in micro-hardness is only due to the heating and quenching cycle.

Table 6.3 Comparative analysis of Micro-hardness for D2 die steel

Electrode Material / Powder	**Micro-hardness on D2 Die Steel (Vickers Hardness Number, HV)**		
	Best Value achieved	% improvement	Optimum Process Parameters
Before machining	652.00	-	-
Copper Electrode	748.00	14.7 %	$A_3B_2C_3$
Copper-Tungsten Electrode	832.67	27.7 %	$A_3B_1C_2$
Manganese Powder	1119.00	71.6 %	$A_2B_1C_3$
Silicon Powder	801.33	22.9 %	$A_3B_1C_3$
Tungsten Powder	1409.67	116.2 %	$A_2B_2C_3$
Factor A represents Peak current and level A_1 = 2 A, A_2 = 4 A, A_3 = 6 A Factor B represents Pulse on-time and level B_1 = 5 µs, B_2 = 10 µs, B_3 = 20 µs Factor C represents Pulse off-time and level C_1 = 38 µs, C_2 = 57 µs, C_3 = 85 µs			

The optimum parameters are found to be same as that for OHNS die steel for each machining condition. Hence, it may be concluded that the optimum machining parameters depend on the electrode material or suspended powder being used and not on the work material.

6.2.2 Effect on Surface Roughness

The response of D2 die steel in terms of improvement in surface roughness has been summarized in Table 6.4. The comparison has been done with the surface roughness values achieved with copper electrode. Amongst the three work materials, the initial value of surface roughness is the highest for this material which can be attributed to the presence of high amounts of cementite and chromium carbide. However, this surface roughness has been improved considerably by copper-tungsten electrode and silicon powder. Copper-tungsten emerges as an ideal electrode material which gives the desired combination of good micro-hardness and superior surface finish. Since machining with graphite powder is not recommended for D2 die steel (Para 3.1.1), silicon powder can be mixed in the dielectric for achieving good surface finish on this material. The optimum process parameters were consistently found to be $A_1B_1C_2$. It is also observed that the deterioration in surface finish is almost the same for manganese and tungsten powders.

Table 6.4 Comparative analysis of Surface roughness for D2 die steel

Electrode Material / Powder	**Surface Roughness on D2 Die Steel (R_a in microns)**		
	Best Value achieved	% improvement	Optimum Process Parameters
Copper Electrode	3.54	-	$A_1B_1C_2$
Copper-Tungsten Electrode	2.15	39.3 %	$A_1B_1C_2$
Manganese Powder	4.39	-	$A_1B_1C_2$
Silicon Powder	1.61	54.5 %	$A_1B_1C_2$
Tungsten Powder	4.47	-	$A_1B_1C_2$

6.3 RESPONSE OF H13 HOT DIE STEEL

6.3.1 Effect on Micro-hardness

The response of H13 hot die steel in terms of improvement in micro-hardness has been summarized in Table 6.5. The performance of this material is found to be similar to OHNS die steel with the only difference being that the hardness values achieved are correspondingly

Table 6.5 Comparative analysis of Micro-hardness for H13 die steel

Electrode Material / Powder	**Micro-hardness on H13 Die Steel (Vickers Hardness Number, HV)**		
	Best Value achieved	% improvement	Optimum Process Parameters
Before machining	465.00	-	-
Copper Electrode	582.67	25.3 %	$A_3B_1C_3$
Graphite Electrode	570.67	22.7 %	$A_3B_1C_3$
Copper-Tungsten Electrode	724.33	55.8 %	$A_3B_1C_2$
Inconel alloy Electrode	874.00	87.9 %	$A_2B_1C_2$
Graphite Powder	663.00	42.6 %	$A_2B_1C_3$
Manganese Powder	808.33	73.8 %	$A_2B_1C_3$
Silicon Powder	608.00	30.7 %	$A_3B_1C_3$
Tungsten Powder	1071.67	130.5 %	$A_2B_2C_3$
Factor A represents Peak current and level A_1 = 2 A, A_2 = 4 A, A_3 = 6 A Factor B represents Pulse on-time and level B_1 = 5 µs, B_2 = 10 µs, B_3 = 20 µs Factor C represents Pulse off-time and level C_1 = 38 µs, C_2 = 57 µs, C_3 = 85 µs			

lower. This difference emanates from the initial composition of the work materials. H13 die steel contains 0.44 % carbon as compared to 0.82 % carbon in OHNS die steel. Thus, very little cementite is present in its microstructure and the initial value of hardness obtained by this material after heat treatment is also less. But it has good resistance to softening effect of heat due to the presence of medium chromium content. The addition of tungsten can further improve its hot strength. For this material, it is important to note that the percentage improvement in micro-hardness is much more than the other two work materials in most of the conditions. The reason for this behaviour is that, irrespective of the electrode material or suspended powder, the percentage of carbon in the work surface is increasing by contribution from the pyrolysis of the hydrocarbon dielectric. Since H13 contains less carbon initially, the scope for improvement in micro-hardness by increasing the carbon percentage is higher. Spectrometric analysis also indicates increase in percentage of carbon (Tables 6.14 and 6.15). The presence of carbide forming elements such as molybdenum (0.9%) and vanadium (1.1%) also help in improving the hardness but it could not be confirmed in this analysis.

Amongst the electrode materials, inconel alloy again improves the micro-hardness by almost 88 % but the best value of micro-hardness is achieved by machining with tungsten powder. In this particular material, machining with tungsten powder also improves the surface finish slightly (Table 6.6). The presence of tungsten carbide (W_2C) can be seen in the XRD pattern of the sample (Fig. 6.22). Except minor changes, the optimum process parameters remain the same for each machining condition, further confirming that the process parameters are independent of the work material.

6.3.2 Effect on Surface Roughness

The response of H13 die steel in terms of improvement in surface roughness has been summarized in Table 6.6. The comparison has been done with the value of surface roughness achieved with copper electrode. It can be seen that a surface finish of $R_a < 1$ μm is obtained when machining is carried out in graphite powder. The performance of silicon powder is also similar (1.06 μm). The levels of the two most significant optimum process parameters (more than 74 % contribution of peak current and more than 12 % contribution by pulse on-time) are also the same in both cases. The impact of peak current on surface finish is already well known (lower values give good surface finish) and it can be concluded from this research

work that lower values of pulse on-time also improve the surface finish. However, the levels of pulse off-time for best surface finish are found to be different for the two powders (C_1 for graphite powder and C_2 for silicon powder) but it can be observed from Fig. 5.6 (c) that there is an insignificant change in this parameter from level C_1 to C_2 (raw data value changes from 1.67 µm to 1.68 µm). Taking into consideration the response of other work materials also for this response characteristic (Tables 6.2 and 6.4), it can be concluded that moderate values of pulse off-time are conducive for good surface finish (57 µsec in this work).

Table 6.6 Comparative analysis of Surface roughness for H13 die steel

Electrode Material / Powder	**Surface Roughness on H13 Die Steel (R_a in microns)**		
	Best Value achieved	% improvement	Optimum Process Parameters
Copper Electrode	3.05	-	$A_1B_1C_2$
Graphite Electrode	1.96	35.7 %	$A_1B_1C_3$
Copper-Tungsten Electrode	2.68	12.1 %	$A_1B_1C_1$
Inconel alloy Electrode	7.78	-	$A_1B_2C_1$
Graphite Powder	0.97	68.2 %	$A_1B_1C_1$
Manganese Powder	3.64	-	$A_1B_1C_2$
Silicon Powder	1.06	65.2 %	$A_1B_1C_2$
Tungsten Powder	2.96	2.9 %	$A_1B_1C_2$
Factor A represents Peak current and level A_1 = 2 A, A_2 = 4 A, A_3 = 6 A Factor B represents Pulse on-time and level B_1 = 5 µs, B_2 = 10 µs, B_3 = 20 µs Factor C represents Pulse off-time and level C_1 = 38 µs, C_2 = 57 µs, C_3 = 85 µs			

There is a slight improvement in surface finish by tungsten powder for this material, but it can be treated as an exception. In general, it is found that machining with manganese and tungsten powders improve the micro-hardness considerably but the surface finish deteriorates to some extent. However, in the case of press tools and dies, some amount of surface roughness is desirable for good lubrication retention and smooth functioning of the dies. A mirror-like surface finish promotes sticking situations between the workpiece and the die.

6.4 MIGRATION OF CARBON

Carbon is an essential ingredient of all types of steels. It imparts strength, hardness and wear resistance to steels but reduces ductility and toughness. Carbon can exist in three different forms in steels – as an interstitial solid solution with iron known as ferrite (Fe-C), as chemical compound iron carbide (Fe_3C) known as cementite, or as free graphite. While ferrite is soft and ductile, cementite is very hard and brittle. When the carbon percentage in steel is 0.8 %, a simultaneous precipitation of ferrite and cementite phases in the form of a eutectoid mixture (known as pearlite) takes place. All steels containing more than 0.8 % carbon will have some amount of cementite present in the microstructure along with pearlite. The iron atoms in cementite can be substituted by atoms of manganese, chromium and tungsten. Elements like nickel form a solid solution with ferrite and strengthen it. Carbon also forms hard carbides with other alloying elements such as tungsten, vanadium, manganese and chromium etc. When the percentage of carbon in steel is very high (above 1.5%); it may be present in the free graphite form.

In this experimental work, two work materials were machined using graphite electrode and graphite powder to find out their effect on micro-hardness, surface roughness and the chemical composition of the machined surface. The third work material, namely D2 die steel, already contained more than 1.5 % carbon, so it was not machined by any of these methods. Though machining with graphite electrode resulted in an improvement in micro-hardness (12.6 % for OHNS die steel and 22.7 % for H13 die steel), no distinctive feature was observed in the XRD analysis of any of the work materials. As already explained, the relatively higher improvement in case of H13 die steel can be attributed to the difference in initial composition of the two work materials. The spectrometric analysis presented in Table 6.7 shows an increase in percentage of carbon for both the materials after machining with

graphite electrode. The additional carbon might have been contributed by electrode wear as well as by the pyrolysis of dielectric.

Table 6.7 Percentage of Carbon after machining with Graphite electrode

	% Carbon (at I_p = 6 amp, P_{on} = 5 µsec and P_{off} = 85 µsec)	
	OHNS Die Steel	**H13 Die Steel**
Before Machining	0.82	0.44
After Machining	1.16	0.69
% Increase	41.5 %	56.8 %

When machining was carried out with graphite powder, both the work materials showed comparatively higher improvement in micro-hardness (22.5 % for OHNS die steel and 42.6% for H13 die steel). The spectrometric analysis shows very high increase in the percentage of carbon in the work surface of both the materials (Table 6.8). However, much of it is present in the free graphite form as observed from the XRD pattern of the two materials (Fig. 6.5 and 6.7). In OHNS die steel, ferrite can be seen and a new phase of iron carbide in the form of Fe_5C_2 has emerged**.** However, in case of H13 die steel, cementite has not formed despite significant increase in percentage of carbon. As a result, not much improvement in micro-hardness takes place.

Table 6.8 Percentage of Carbon after machining with Graphite powder

	% Carbon (at I_p = 4 amp, P_{on} = 5 µsec and P_{off} = 85 µsec)	
	OHNS Die Steel	H13 Die Steel
Before Machining	0.82	0.44
After Machining	4.11	3.23
% Increase	401.2 %	634.1 %

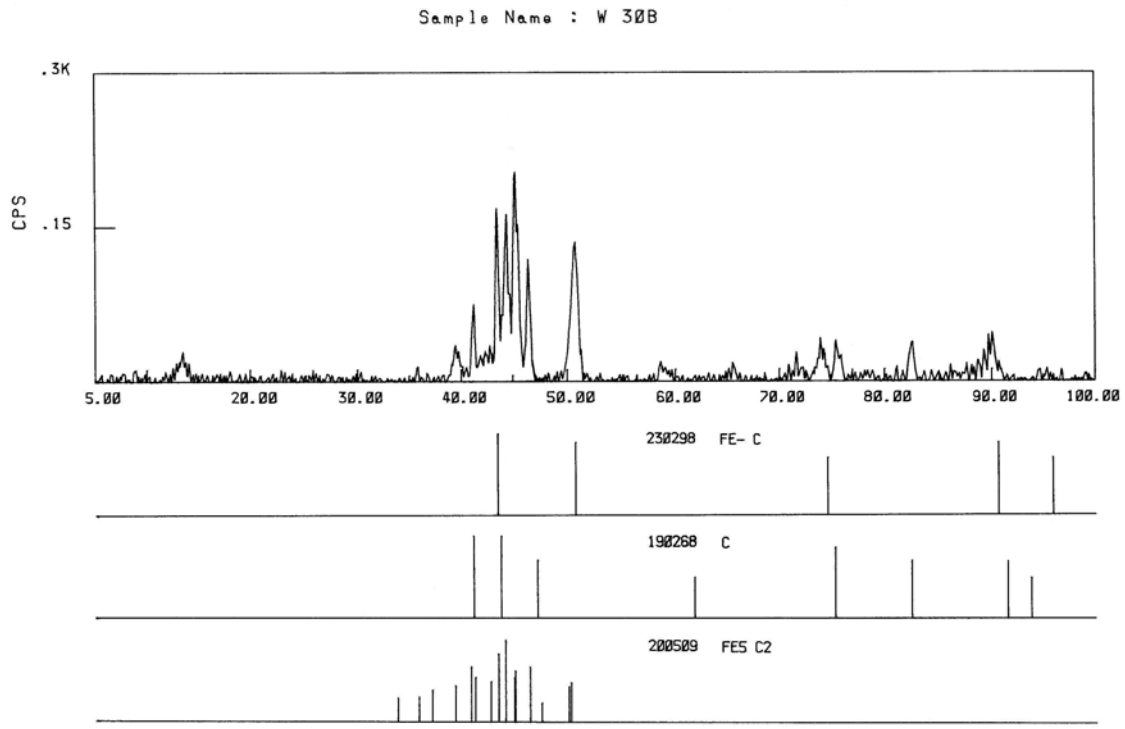

Fig. 6.5 XRD pattern of OHNS die steel after machining with Graphite powder (at I_p = 4 amp, P_{on} = 5 µsec and P_{off} = 85 µsec)

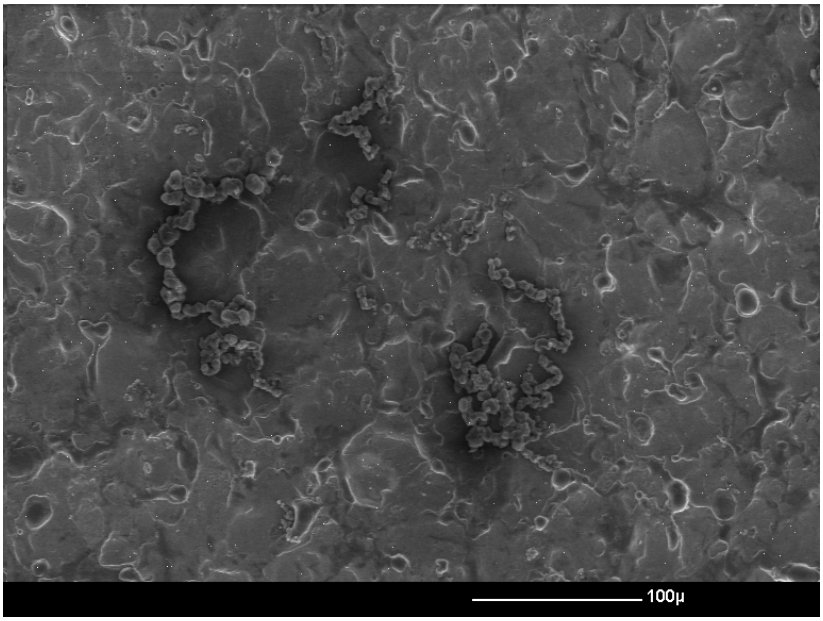

Fig. 6.6 SEM micrograph of OHNS die steel after machining with Graphite powder (at I_p = 4 amp, P_{on} = 5 µsec and P_{off} = 85 µsec)

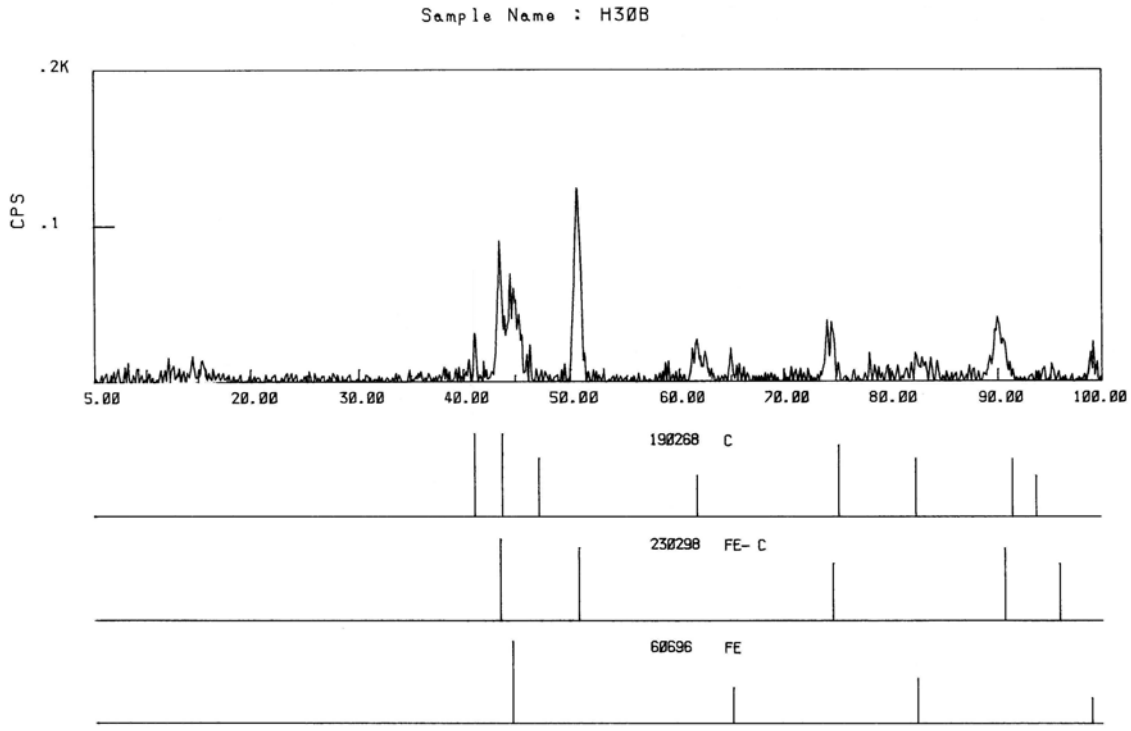

Fig. 6.7 XRD pattern of H13 die steel after machining with Graphite powder (at I_p = 4 amp, P_{on} = 5 µsec and P_{off} = 85 µsec)

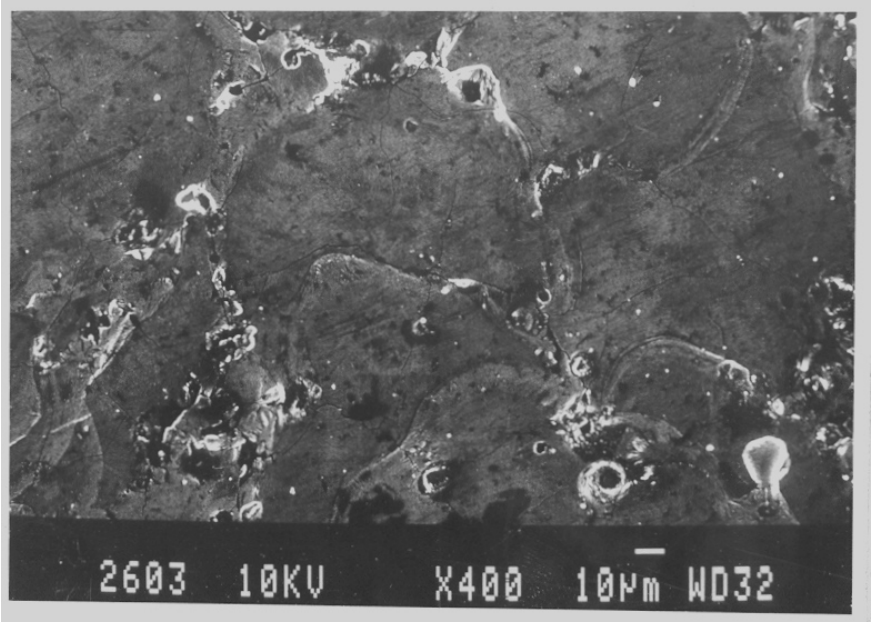

Fig. 6.8 SEM micrograph of H13 die steel after machining with Graphite powder (at I_p = 4 amp, P_{on} = 5 µsec and P_{off} = 85 µsec)

The corresponding microstructures of the two work materials after machining with graphite powder (Fig. 6.6 and 6.8) show smooth surfaces devoid of any craters. Nodules of free graphite can also be seen. Based on these observations, it can be concluded that by this method of machining, existing phases get disturbed and infusion of carbon takes place but formation of the cementite can not be ensured. Hence, this method can be recommended for improvement in surface finish only and not for increasing the micro-hardness.

When OHNS die steel was machined with graphite electrode, the optimum condition for maximum micro-hardness was found to be $A_3B_1C_3$ with the percentage contribution of peak current being 82.37 %, followed by pulse on-time at 13.56 % and pulse off-time at 4.05 %. Since the contribution of peak current was very high as compared to the other two factors, it was decided to conduct experiments at different values of peak current to find out the percentage of carbon in the workpiece surface while keeping the other two factors constant (that is, pulse on-time = 5 µsec and pulse off-time = 85 µsec). The results of the spectrometric analysis of these samples are given in Table 6.9.

Table 6.9 Chemical composition of OHNS die steel after machining with Graphite electrode at different values of Peak current (P_{on} = 5 µsec and P_{off} = 85 µsec)

Composition	**Before machining**	**After machining with Graphite Electrode**		
		I_p = 2 amp	**I_p = 4 amp**	**I_p = 6 amp**
% Carbon	0.82	0.91	1.07	1.16

Similarly, experiments were conducted with graphite powder also at different values of peak current by keeping the other two factors constant. The results of the spectrometric analysis of these samples are given in Table 6.10.

Table 6.10 Chemical composition of OHNS die steel after machining with Graphite Powder at different values of Peak current (P_{on} = 5 µsec and P_{off} = 85 µsec)

Composition	**Before machining**	**After machining with Graphite Powder**		
		I_p = 2 amp	**I_p = 4 amp**	**I_p = 6 amp**
% Carbon	0.82	3.53	4.11	2.35

These results have been compared graphically in Fig. 6.9.

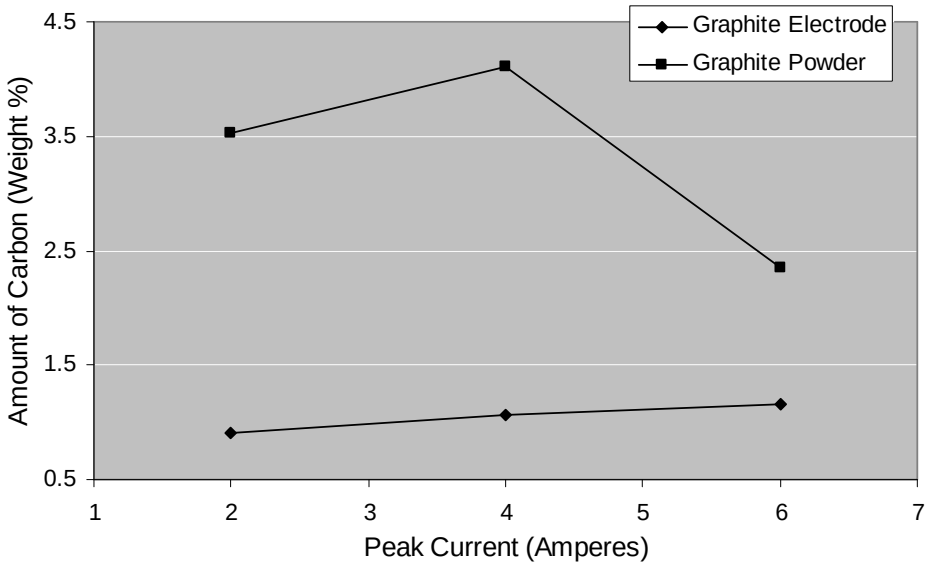

Fig. 6.9 Comparison of carbon percentage with change in Peak current after machining with Graphite Electrode and Graphite powder (Work material – OHNS die steel)

It is observed that the percentage of carbon in workpiece surface undergoes a sharp decline from 4.11 % to 2.35 % as the peak current changes from 4 A to 6 A. This is in contrast with the observation from Fig. 5.3 (a) that the effect of this variation in peak current on micro-hardness is very less {micro-hardness changes from 727 HV to 700 HV as the level of peak current changes from A_2 (4 A) to A_3 (6 A)}. This difference can be attributed to the hardening of the workpiece surface by more heating and subsequently, higher quenching effect at 6 A peak current which results in an increase in hardness.

Since graphite powder resulted in very good surface finish, more experiments were conducted to find out R_a and R_z values of surface roughness on the samples machined with graphite powder. R_z is a measure of mean peak-to-valley height of surface asperities and is considered to be a better representative of overall surface finish than R_{max} which is a measure of maximum roughness depth. Extreme values of R_{max} can be the result of random causes and may not be a true indicator of good machining conditions. The optimum condition for least surface roughness after machining OHNS die steel with graphite powder was found to be $A_1B_1C_2$ with the percentage contribution of peak current being 80.1 %, followed by pulse on-time at 16.5 % and pulse off-time at 3.2 %. The optimum condition for least surface

roughness with copper electrode (reference value) was also found to be $A_1B_1C_2$. So, the experiments were conducted with and without graphite powder using copper electrode at different values of peak current by keeping the other two factors constant and surface roughness measurements were taken. The results of these experiments are given in Table 6.11 and presented graphically in Fig. 6.10.

Table 6.11 R_a and R_z values of Surface Roughness after machining OHNS die steel with and without Graphite powder-mixed dielectric (P_{on} = 5 µsec and P_{off} = 57 µsec)

Peak Current (amperes)	Surface Roughness values achieved with Copper electrode		Surface Roughness values achieved with Graphite powder under same machining conditions	
	R_a (in µm)	R_z (in µm)	R_a (in µm)	R_z (in µm)
2 A	2.46	11.8	0.73	3.81
4 A	3.01	14.1	1.14	5.23
6 A	4.43	21.7	1.69	7.16

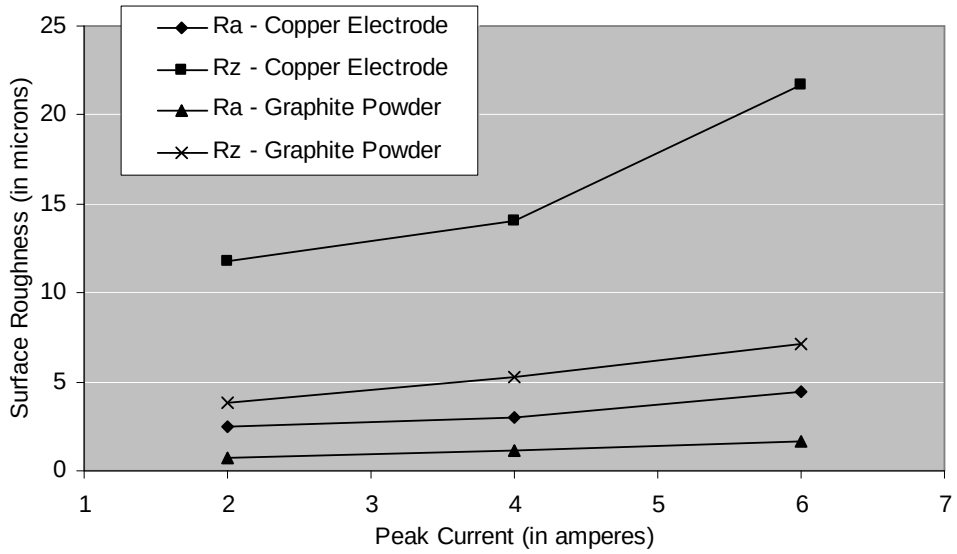

Fig. 6.10 Comparison of R_a and R_z values of Surface Roughness after machining OHNS die steel with graphite powder-mixed dielectric (P_{on} = 5 µsec and P_{off} = 57 µsec)

A sharp reduction in R_a and R_z values of surface roughness is observed when machining is carried out with graphite powder. More important is the decrease in R_z value from 11.8 μm to 3.81 μm at 2 A peak current which reflects a very good surface finish. Even at higher values of peak current, a significant decrease in R_a and R_z values takes place. This is a very important benefit of machining with graphite powder. SEM micrograph of the surface machined with graphite powder at 2 A peak current in Fig. 6.11 shows a very smooth, crack-free surface without the typical craters of EDM. The presence of graphite particles help in lowering the breakdown strength of the insulating dielectric fluid. For the same applied voltage, the spark gap between the tool and workpiece increases and the current is easily established. The sparking is uniformly distributed among the powder particles and electric density of the spark decreases. Crater size and depth diminishes and surface finish is improved. White spots of cementite and black nodules of free graphite are also visible in the micrograph. Nodules of free graphite are expected to provide self-lubricating property to the workpiece surface.

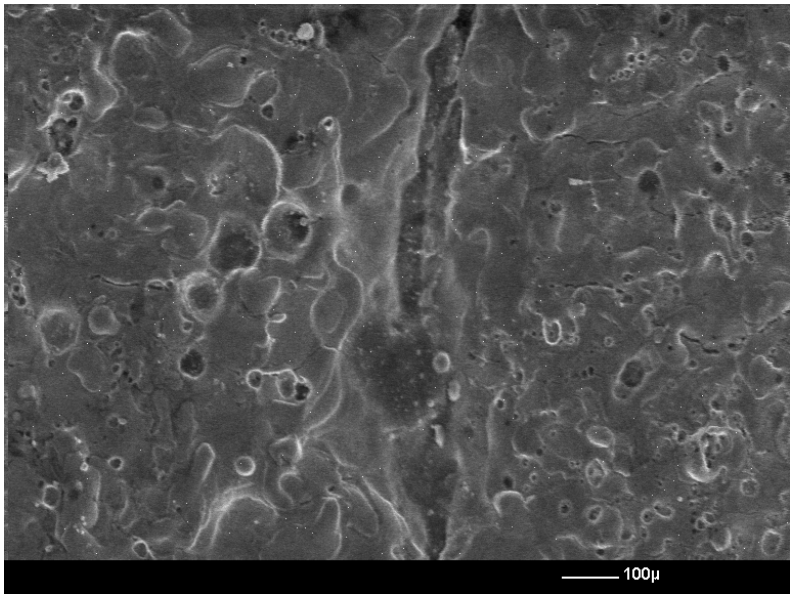

Fig. 6.11 SEM micrograph of OHNS die steel after machining with Graphite powder (at I_p = 2 amp, P_{on} = 5 μsec and P_{off} = 57 μsec)

6.5 MIGRATION OF TUNGSTEN

Tungsten forms hard, abrasion-resistant particles in tool steels and promotes hardness and strength at elevated temperatures. It can exist in different forms in die steels. It may dissolve

in the ferrite or cementite phases of the iron-carbon system or it may be present as independent carbide in the form of WC, W_2C etc. The iron atoms of the cementite phase can be substituted by tungsten atoms. It may also form intermetallic compounds with iron such as Fe_3W_2 or Fe_2W [20]. In general, the effect of tungsten on properties of steel is similar to that of molybdenum, although large quantities are required. The contribution of approximately 2 to 3 percent tungsten is equivalent to 1 percent molybdenum. Higher tungsten and molybdenum contents increase red hardness but slightly reduce toughness.

Experiments for the migration of tungsten were conducted by using copper-tungsten electrode and then by suspending tungsten powder in the dielectric. The XRD patterns of the three work materials after machining with copper-tungsten electrode and the corresponding microstructures are given in Fig. 6.12 to Fig. 6.17. Fine dispersion of hard particles can be seen in the three microstructures. SEM micrograph of OHNS die steel (Fig. 6.13) shows small black particles of intermetallic compound Fe_7W_6 surrounded by white regions of cementite. Compared to Fig. 6.4, the size of craters is smaller which results in better surface finish.

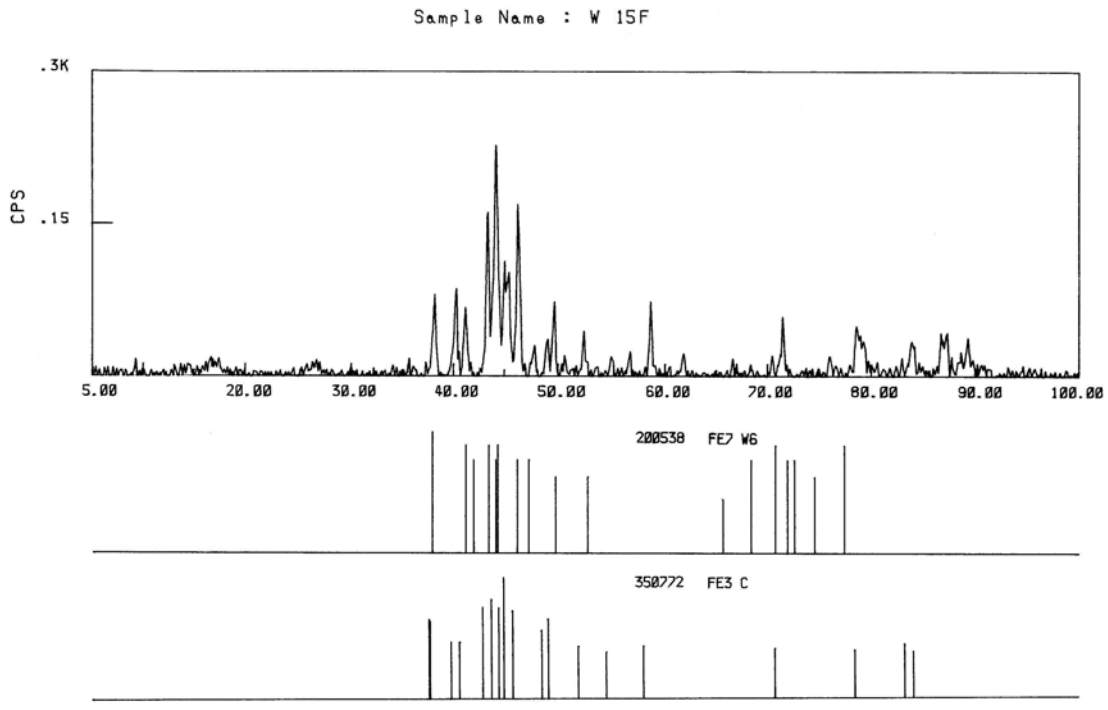

Fig. 6.12 XRD pattern of OHNS die steel after machining with Copper-tungsten electrode (at I_p = 6 amp, P_{on} = 5 µsec and P_{off} = 57 µsec)

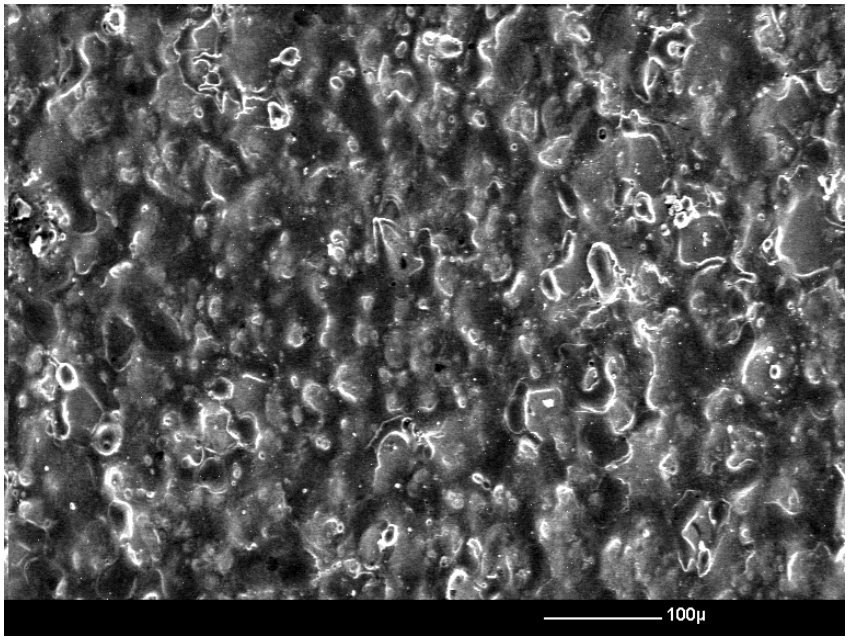

Fig. 6.13 SEM micrograph of OHNS die steel after machining with copper-tungsten electrode (at I_p = 6 amp, P_{on} = 5 µsec and P_{off} = 57 µsec)

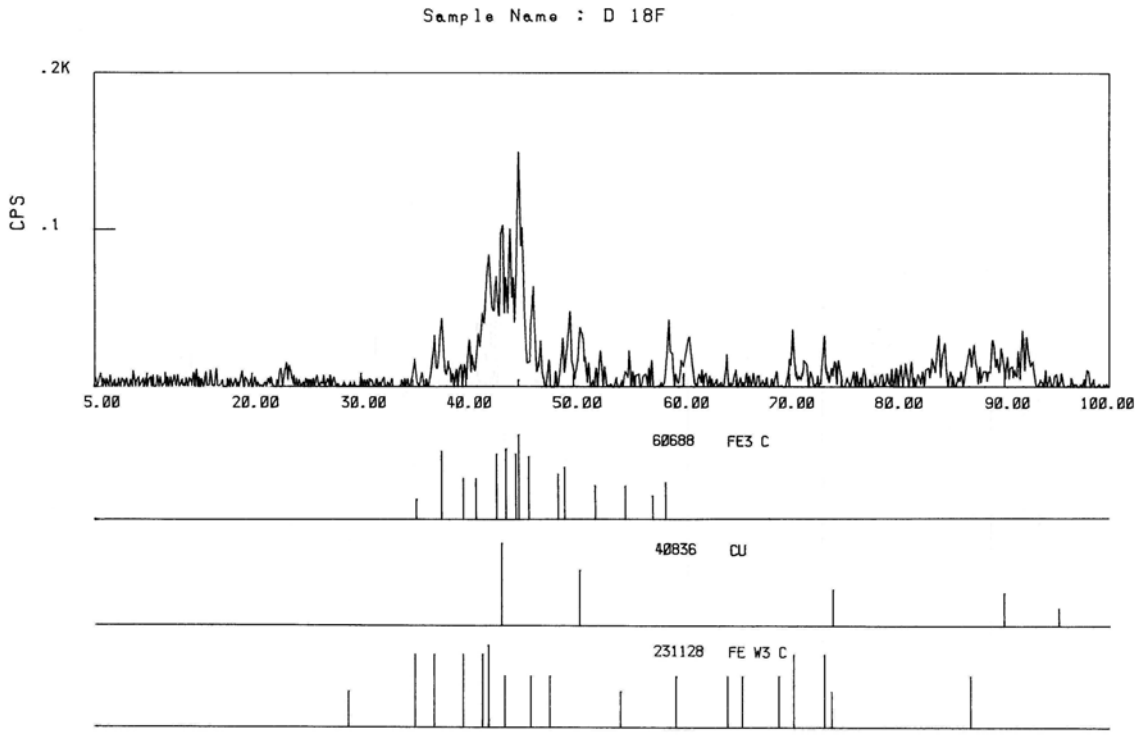

Fig. 6.14 XRD pattern of D2 die steel after machining with Copper-tungsten electrode (at I_p = 6 amp, P_{on} = 5 µsec and P_{off} = 57 µsec)

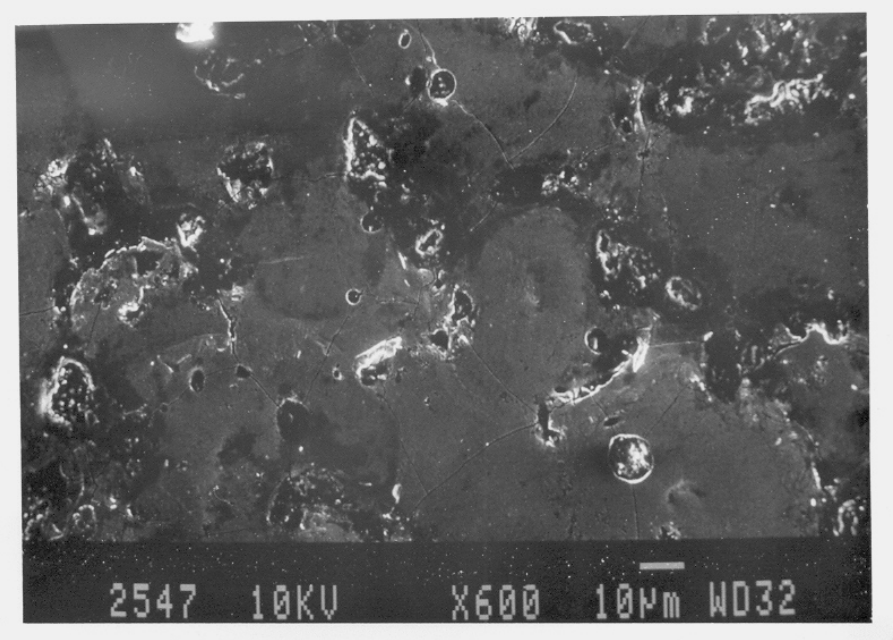

Fig. 6.15 SEM micrograph of D2 die steel after machining with Copper-tungsten electrode (at I_p = 6 amp, P_{on} = 5 µsec and P_{off} = 57 µsec)

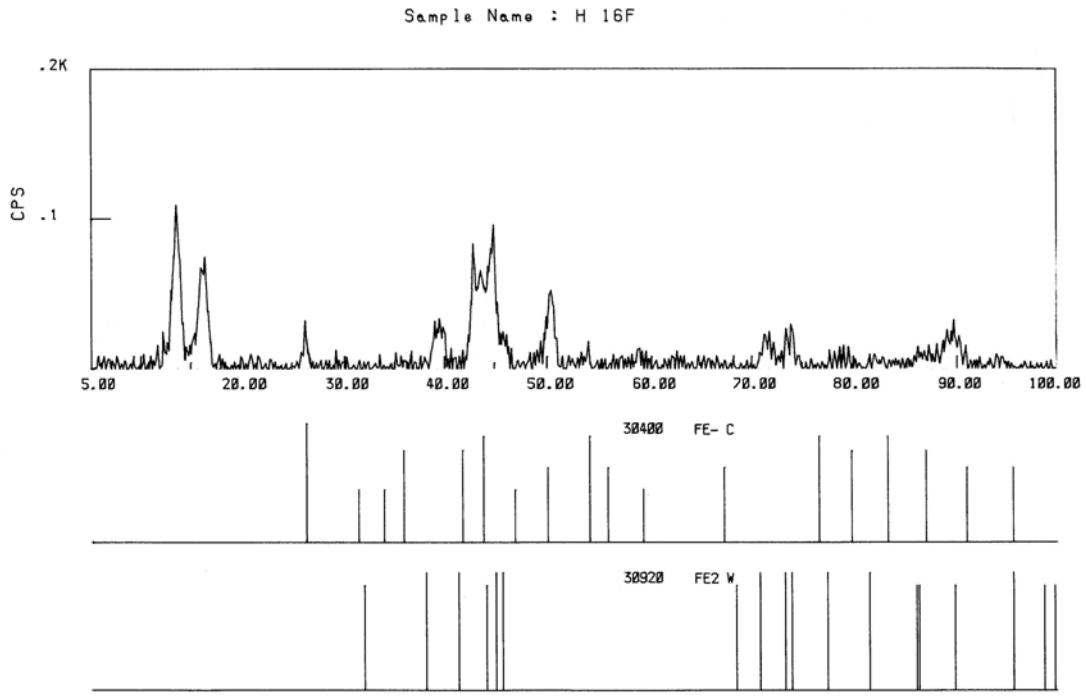

Fig. 6.16 XRD pattern of H13 die steel after machining with Copper-tungsten electrode (at I_p = 6 amp, P_{on} = 5 µsec and P_{off} = 57 µsec)

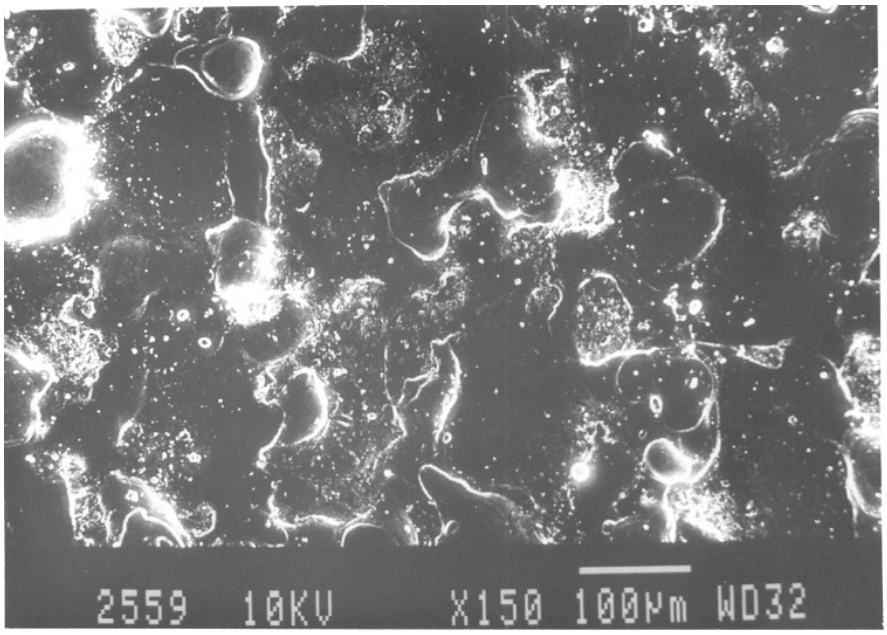

Fig. 6.17 SEM micrograph of H13 die steel after machining with Copper-tungsten electrode (at I_p = 6 amp, P_{on} = 5 µsec and P_{off} = 57 µsec)

However, the micrograph of D2 die steel (Fig. 6.15) shows some micro-cracks and improvement in micro-hardness is also not significant. While the increase in micro-hardness is more than 50 % in case of OHNS and H13 die steels, it is only 28 % in case of D2 die steel. This difference has come due to the manner in which tungsten has migrated to the workpiece surface. The XRD patterns of OHNS and H13 die steels show the formation of intermetallic compounds of tungsten with iron (Fe_7W_6 and Fe_2W) which are very hard. Whereas, in case of D2 die steel, tungsten has entered the cementite phase already present in the structure and replaced some of the iron atoms to form alloyed cementite {$(Fe, W)_3C$}. Hence, the improvement in micro-hardness for this material is not substantial.

Surface finish after machining with copper-tungsten electrode is also much better (more than 40 % improvement in case of D2 die steel). Traces of copper can be seen in the XRD pattern of D2 die steel only. It was subjected to spectrometric analysis to confirm the presence of copper and a small percentage of copper was noticed. The results of this analysis are given in Table 6.12. Copper, nickel, silicon and aluminum do not form carbides in steel and are generally found as a solid solution with iron. The effect of copper in improving the mechanical properties of ferrite phase is only marginal, but in any case, its presence is not

detrimental to the properties. Thus, there was no need of any attempt to eliminate copper from the workpiece surface when machining was done with copper-tungsten electrode. Moreover, copper is not seen in the XRD pattern of the other two work materials, even though the machining process parameters are the same. Thus, the presence of copper in D2 die steel can be treated as an exception and it may be concluded that significant amount of copper can not be alloyed to the machined surface by this method.

Besides the increase in the percentage of tungsten in the workpiece surface and presence of copper, the spectrometric analysis also shows an increase in the percentage of carbon and some loss of chromium. Carbon has come from the breakdown of the dielectric. Chromium, like tungsten, replaces some of the iron atoms in cementite to form alloyed cementite {(Fe, $Cr)_3C$}, besides forming carbides. Loss of chromium in this case can be attributed to the replacement of chromium by tungsten on the workpiece surface.

Table 6.12 Chemical composition of D2 die steel after machining with Copper-tungsten electrode (at I_p = 6 amp, P_{on} = 5 µsec and P_{off} = 57 µsec)

Composition	Before machining	After machining	Significant changes
% Carbon	**1.57**	**1.72**	**+ 0.15**
% Silicon	0.19	0.14	-
% Manganese	0.07	0.09	-
% Chromium	**12.38**	**11.77**	**– 0.61**
% Molybdenum	0.76	0.75	-
% Vanadium	0.96	1.01	-
% Tungsten	**-**	**1.10**	**+ 1.10**
% Nickel	0.09	0.11	-
% Copper	**-**	**0.43**	**+ 0.43**
% Iron	Balance	Balance	-

When machining was carried out with tungsten powder, the improvement in micro-hardness was much higher as compared to copper-tungsten electrode. All the three work materials reported more than 100 % increase in micro-hardness. Even D2 die steel, which did not show much improvement with copper-tungsten electrode, showed 116 % increase in micro-hardness with tungsten powder. The XRD patterns of the three work materials after machining with tungsten powder-mixed dielectric and the corresponding microstructures are given in Fig. 6.18 to Fig. 6.23. The microstructures show significant surface changes as a result of machining with tungsten powder. Surface finish has deteriorated and the dispersion of hard particles is not uniform. But none of the surfaces show any presence of micro-cracks. SEM micrograph of H13 die steel (Fig. 6.23) shows relatively uniform size of tungsten carbide (W_2C) particles which gives this material the highest micro-hardness amongst the three work materials. Though the XRD pattern (Fig. 6.22) does not show cementite, some unmarked peaks indicate the presence of this phase.

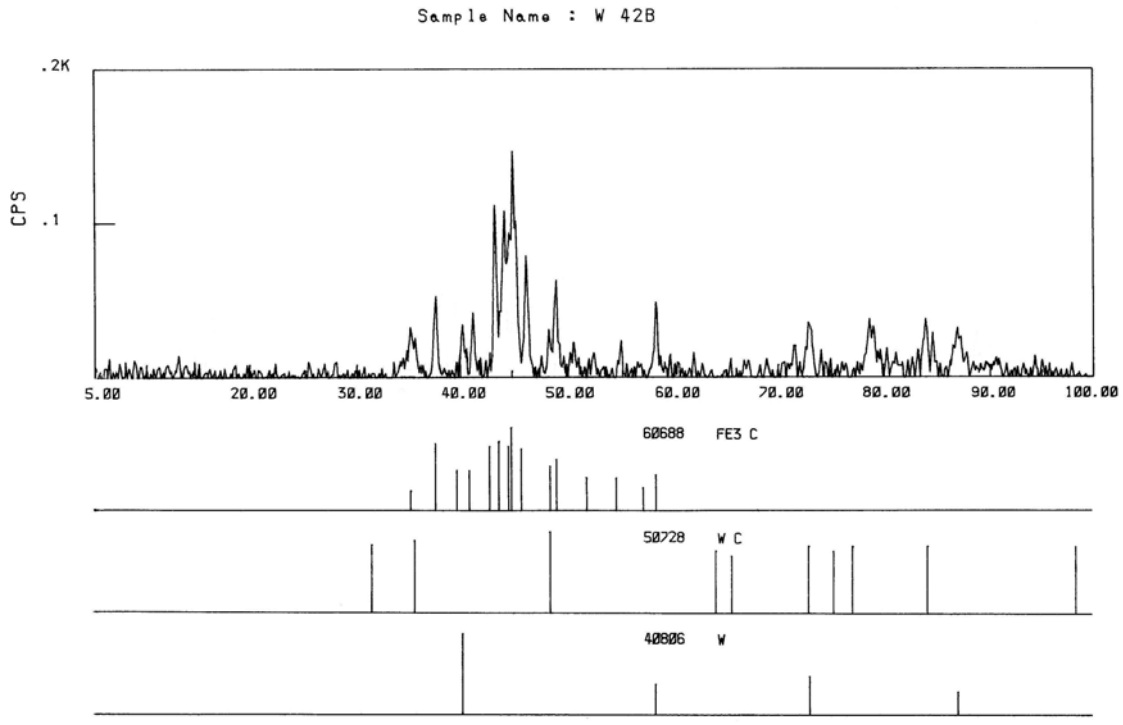

Fig. 6.18 XRD pattern of OHNS die steel after machining with Tungsten powder (at I_p = 4 amp, P_{on} = 10 µsec and P_{off} = 85 µsec)

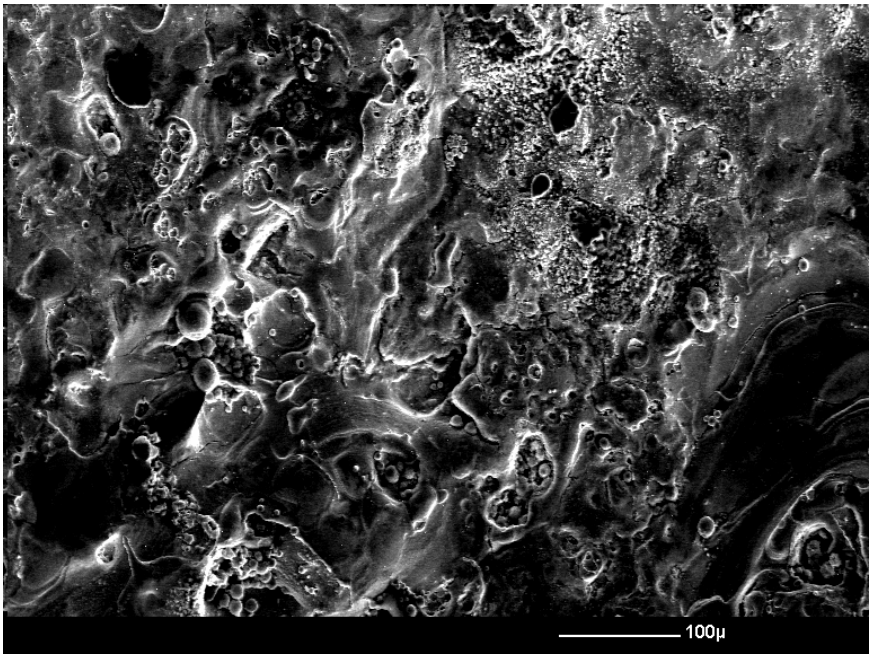

Fig. 6.19 SEM micrograph of OHNS die steel after machining with Tungsten powder (at I_p = 4 amp, P_{on} = 10 µsec and P_{off} = 85 µsec)

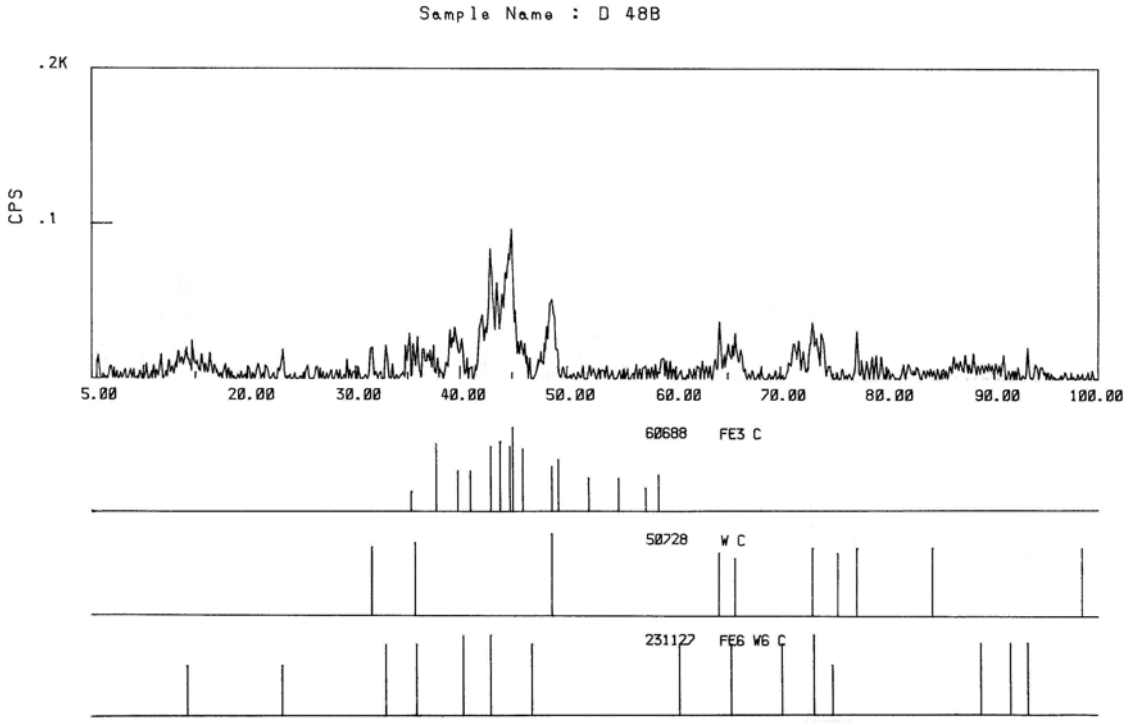

Fig. 6.20 XRD pattern of D2 die steel after machining with Tungsten powder (at I_p = 4 amp, P_{on} = 10 µsec and P_{off} = 85 µsec)

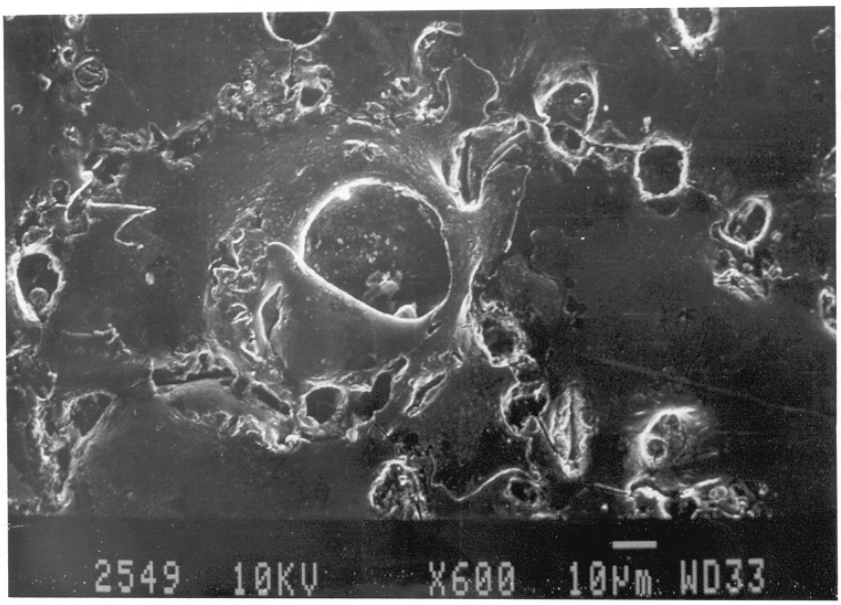

Fig. 6.21 SEM micrograph of D2 die steel after machining with Tungsten powder (at I_p = 4 amp, P_{on} = 10 µsec and P_{off} = 85 µsec)

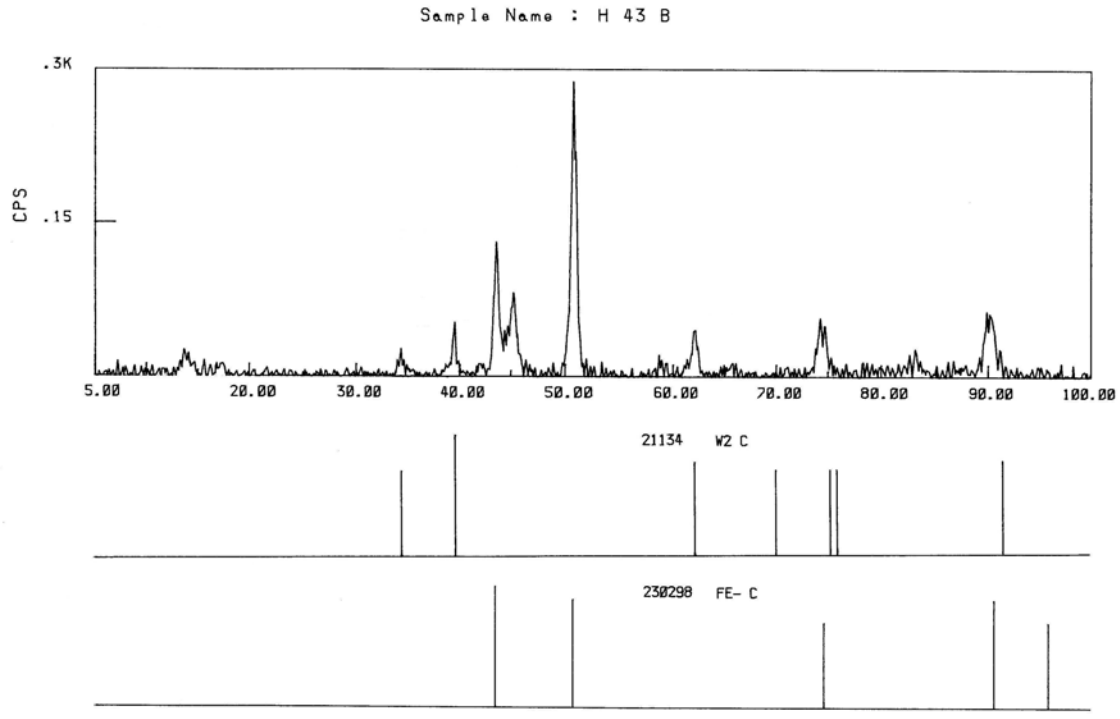

Fig. 6.22 XRD pattern of H13 die steel after machining with Tungsten powder (at I_p = 4 amp, P_{on} = 10 µsec and P_{off} = 85 µsec)

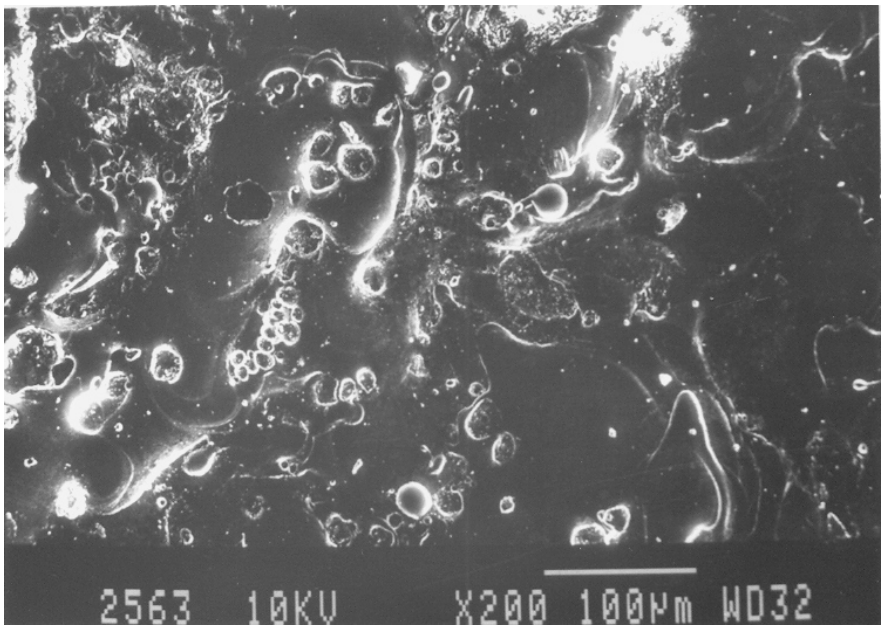

Fig. 6.23 SEM micrograph of H13 die steel after machining with Tungsten powder (at I_p = 4 amp, P_{on} = 10 µsec and P_{off} = 85 µsec)

Only this material has reported improvement in surface finish by machining with tungsten powder which is corroborated by the smooth surface shown in the micrograph. All the three XRD patterns show presence of tungsten carbide either in the form of WC or W_2C. Free tungsten is observed on the surface of OHNS die steel. A double carbide (Fe_6W_6C) has formed on the surface of D2 die steel which is responsible for the much improved hardness.

The optimum machining parameters for the three work materials and the relative contribution of the factors have been summarized in Table 6.13. It is found that the optimum machining parameters for an electrode material or suspended powder are the same for all work materials. Even the relative contribution of the factors is almost identical. Hence, it can be conclusively inferred from this data that the input process parameters are independent of the work material and the same values will hold good for any work material. However, the optimum combination of levels of the three input parameters is found to be different for the two methods of machining. The level of peak current is A_3 (6 A) for copper-tungsten electrode as compared to level A_2 (4 A) for tungsten powder. In the first case, tungsten has to come from the disintegration of the tool electrode for which higher current is required. Higher current means more energy in the spark channel and more pulse on-time means that

Table 6.13 Optimum Process Parameters and their Relative Contribution for Micro-hardness with Copper-tungsten electrode and Tungsten Powder

Method of Machining	Input Process Parameters	Work Materials		
		OHNS Die Steel	D2 Die Steel	H13 Die Steel
With Copper-tungsten Electrode	Optimum Setting	$A_3B_1C_2$	$A_3B_1C_2$	$A_3B_1C_2$
	Peak Current	85.0 %	83.1 %	83.7 %
	Pulse on-time	10.3 %	10.8 %	10.2 %
	Pulse off-time	4.5 %	6.0 %	6.1 %
With Tungsten Powder	Optimum Setting	$A_2B_2C_3$	$A_2B_2C_3$	$A_2B_2C_3$
	Peak Current	71.9 %	73.6 %	74.6 %
	Pulse on-time	10.1 %	9.2 %	8.1 %
	Pulse off-time	17.7 %	16.9 %	17.0 %
Factor A represents Peak current and level A_1 = 2 A, A_2 = 4 A, A_3 = 6 A Factor B represents Pulse on-time and level B_1 = 5 µs, B_2 = 10 µs, B_3 = 20 µs Factor C represents Pulse off-time and level C_1 = 38 µs, C_2 = 57 µs, C_3 = 85 µs				

this energy is sustained for a longer time. In EDM process, it is well known that lower pulse on-times provoke electrode wear [3, 121] which is desirable in the case of copper-tungsten electrode. Thus, the optimum setting of pulse on-time is found to be its lowest value for the experimentation, that is B_1 (5 µsec). Also, the contribution of pulse on-time has been consistent at about 10 % for both the methods of machining. Another important observation is that the contribution of pulse off-time is more than pulse on-time (at the expense of peak current) when machining is carried out with tungsten powder. It means that pulse off-time is more significant and sufficient idle time is essential for the work surface to cool down and absorb the products of sparking. As already explained in Para 6.1.1, when material transfer is desired from the electrode bodies, less idle time means that the electrode remains hot for the next sparking cycle. Hence, the optimum value of pulse off-time for copper-tungsten electrode is found to be C_2 (57 µsec).

Some more experiments were conducted on H13 die steel to draw a comparison between the two methods of machining on the percentage of tungsten in the workpiece surface. Since the contribution of peak current towards micro-hardness with copper-tungsten electrode was found to be very high (more than 83 %) as compared to the other two factors, it was decided to conduct experiments at different values of peak current while keeping the other two factors constant. The results of the spectrometric analysis of these samples are given in Table 6.14.

Table 6.14 Significant changes in chemical composition of H13 die steel after machining with Copper-tungsten electrode (P_{on} = 5 µsec and P_{off} = 57 µsec)

Composition	Before machining	After machining with Copper-tungsten Electrode		
		I_p = 2 amp	I_p = 4 amp	I_p = 6 amp
% Carbon	0.44	0.50	0.63	0.54
% Tungsten	-	0.082	0.629	0.872

Similarly, the optimum condition for machining with tungsten powder was found to be $A_2B_2C_3$ with 74.6 % contribution of peak current. So, the experiments were conducted at different values of peak current while keeping the other two factors constant. The result of spectrometric analysis of these samples is given in Table 6.15.

Table 6.15 Significant changes in chemical composition of H13 die steel after machining with Tungsten Powder (P_{on} = 10 µsec and P_{off} = 85 µsec)

Composition	Before machining	After machining with Tungsten Powder		
		I_p = 2 amp	I_p = 4 amp	I_p = 6 amp
% Carbon	0.44	0.57	0.76	0.65
% Tungsten	-	1.986	3.252	1.102

The effect of the two methods of machining on the percentage of carbon and tungsten in the workpiece surface has been presented graphically in Fig. 6.24.

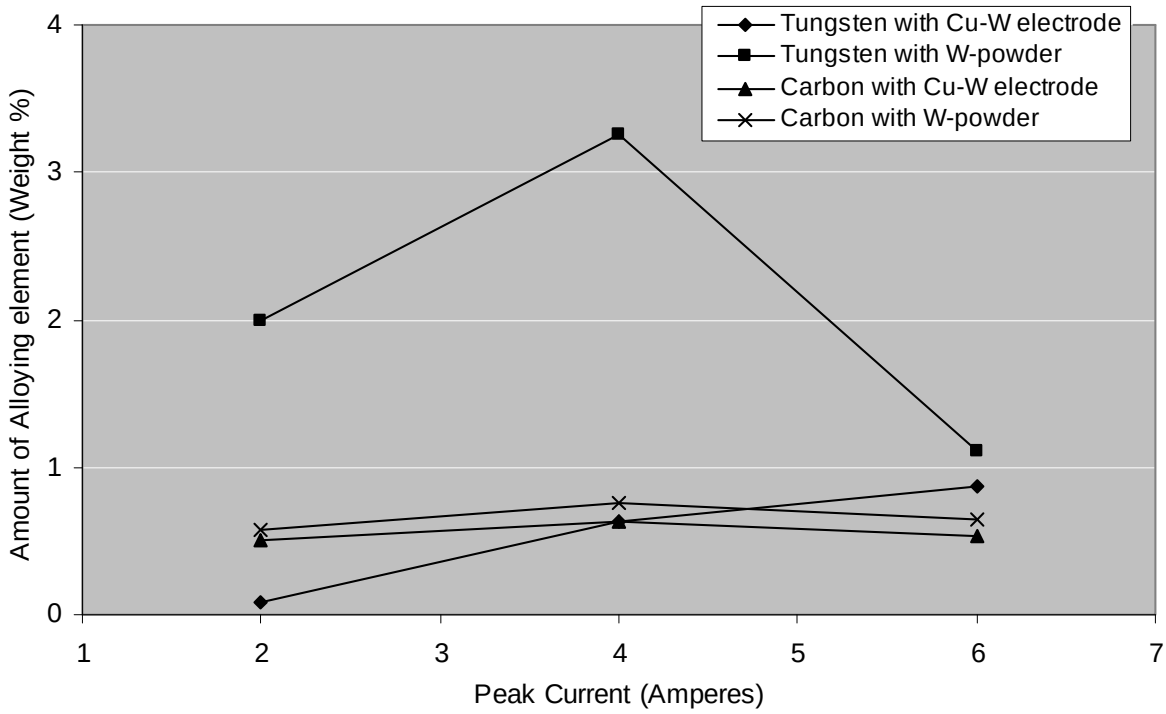

Fig. 6.24 Comparison of Tungsten percentage with change in Peak current for Copper-tungsten Electrode and Tungsten powder (Work material – H13 die steel)

It is observed from the graph that the pattern of material transfer is different for the two methods of machining, that is, machining with copper-tungsten electrode and machining with tungsten powder mixed in the dielectric. When machining is done with tungsten powder, the percentage of tungsten is highest at 4 A peak current and then shows a decline. On the other hand, there is a steady increase from 2 A to 6 A with copper-tungsten electrode. The reason for this behaviour is that while tungsten powder is readily available in the dielectric medium in the former case; it has to come from electrode wear in the latter case for which higher current is more conducive. This is in agreement with the results of pilot experimentation shown in Fig. 3.12.

A sharp reduction in the percentage of tungsten from 3.252 % to 1.102 % is observed as the peak current changes from 4 A to 6 A. The corresponding change in micro-hardness is very less {from 980 HV to 818 HV as shown in Fig. 5.23 (a)}. This behaviour is found to be similar to machining with graphite powder, and here also, the difference can be attributed to more heating and higher quenching effect at 6 A peak current which results in an increase in hardness. This hardening partially offsets the effect of decrease in tungsten percentage.

Regarding the increase in percentage of carbon, it is found that in both the cases, the increase is not substantial and maximum amount of carbon is seen at the peak current value of 4 A. This is in consonance with the behaviour of powders which have all shown maximum impact at the peak current value of 4 A. In general, the percentage of carbon is more when machining is carried out with tungsten powder. This observation leads to the inference that carbon for the formation of tungsten carbide has come from the breakdown of the dielectric and not from the workpiece surface.

6.6 MIGRATION OF CHROMIUM AND NICKEL

Inconel alloy was used as the tool electrode with the aim of providing chromium and nickel to the workpiece surface. This alloy chiefly contains 74 % nickel, 16 % chromium and 9 % iron. Both chromium and nickel impart strength, toughness and corrosion resistance to steel. Chromium may form solid solution with iron and has high solubility in α-ferrite as well as gamma iron. The iron atoms of the cementite phase can be substituted by chromium atoms. It may also form simple carbides (Cr_4C, Cr_7C_3) or complex carbides $\{(FeCr)_3C\}$ in steels. When chromium is present in excess of 5 percent, the high temperature properties and corrosion resistance of steel are greatly improved.

Nickel is also highly soluble in ferrite and contributes to the strength and toughness of this phase. It is a universal grain refiner in alloy steels and improves the hardness even without heat treatment. However, nickel does not form any carbides. It has only a mild effect on hardenability but is outstanding in its ability to improve toughness, particularly at low temperatures [33]. When both nickel and chromium are added together, the effect of nickel in increasing toughness and ductility is combined with the effect of chromium in improving hardenability and wear resistance.

Amongst the four electrode materials, machining with inconel electrode accounted for the maximum improvement in micro-hardness – around 88 % for both OHNS as well as H13 die steel. The third work material, D2 high-carbon high-chromium die steel, was not machined with this electrode because it contained 12.38 % chromium and 1.57 % carbon and addition of nickel to chromium and carbon rich die steel leads to deterioration of properties [19, 120]. The optimum parameters for maximum value of micro-hardness were found to be $A_2B_1C_2$ for

both the work materials. The corresponding values for copper-tungsten were $A_3B_1C_2$ which also resulted in very good improvement of micro-hardness. The spectrometric analysis of the two samples is given in Table 6.16 and the results show that significant amounts of chromium and nickel have migrated to the workpiece surface.

Table 6.16 Significant changes in chemical composition of OHNS and H13 die steels after machining with Inconel electrode (at I_p = 4 A, P_{on} = 5 µsec and P_{off} = 57 µsec)

Composition	Work Materials			
	OHNS Die Steel		H13 Die Steel	
	Before machining	After machining	Before machining	After machining
% Carbon	0.82	0.97	0.44	0.61
% Chromium	0.49	1.20	5.39	6.52
% Nickel	0.05	5.40	0.19	4.87

Hence, it may be concluded that for material transfer to take place from electrode bodies, lower values of pulse on-time (5 µsec in this case) and moderate values of pulse off-time (57 µsec in this case) are appropriate. While peak current remains the most significant factor, the contribution of pulse off-time has been found to be more than pulse on-time. Regarding the difference in optimum values of peak current for copper-tungsten and inconel electrodes, it can be stated that disintegration of tungsten requires more current because of its high melting point. The results also show an increase in the percentage of carbon but formation of chromium carbide has not taken place. The XRD patterns of the work materials after machining with inconel electrode and the corresponding microstructures are given in Fig. 6.25 to Fig. 6.28. The microstructures show a coarse surface with uneven distribution of phases. Some micro-cracks are also present. The XRD pattern of OHNS die steel shows an intermetallic compound of iron, chromium and nickel (FeCrNi) besides ferrite (Fe-C) and cementite (Fe_3C) phases.

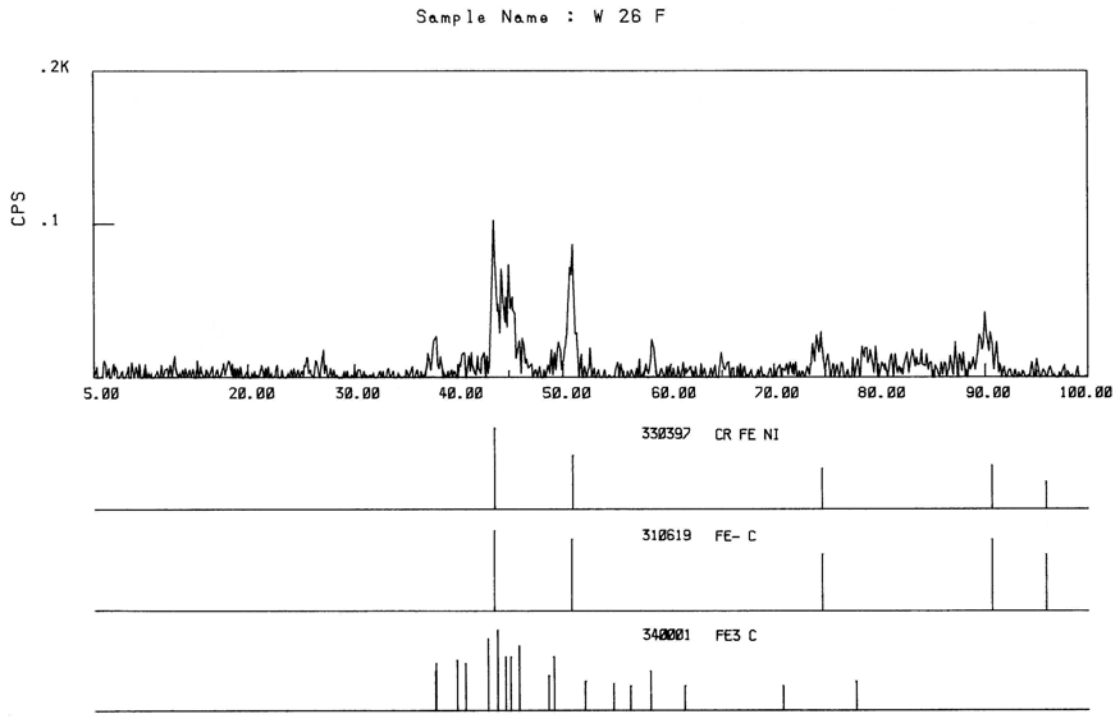

Fig. 6.25 XRD pattern of OHNS die steel after machining with Inconel electrode (at I_p = 4 amp, P_{on} = 5 µsec and P_{off} = 57 µsec)

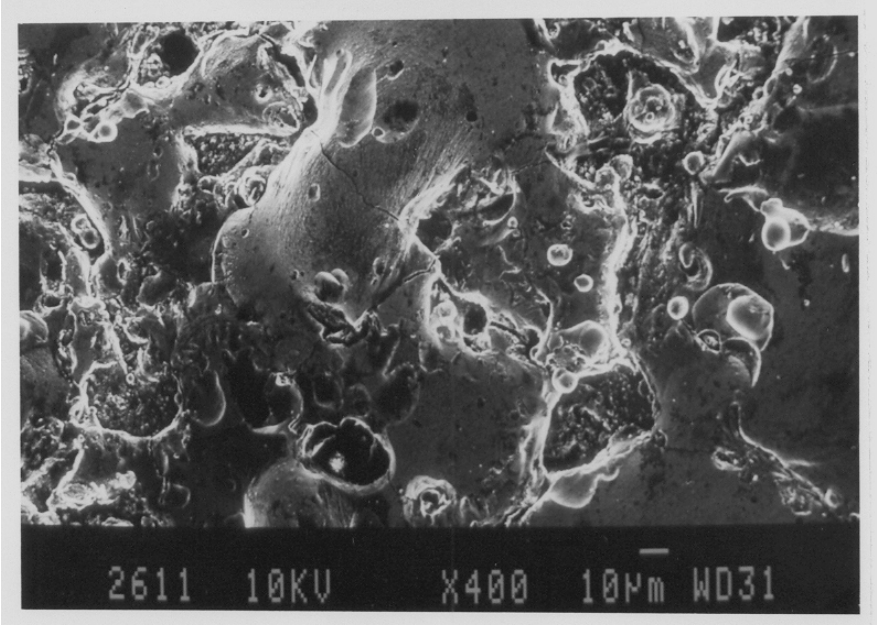

Fig. 6.26 SEM micrograph of OHNS die steel after machining with Inconel electrode (at I_p = 4 amp, P_{on} = 5 µsec and P_{off} = 57 µsec)

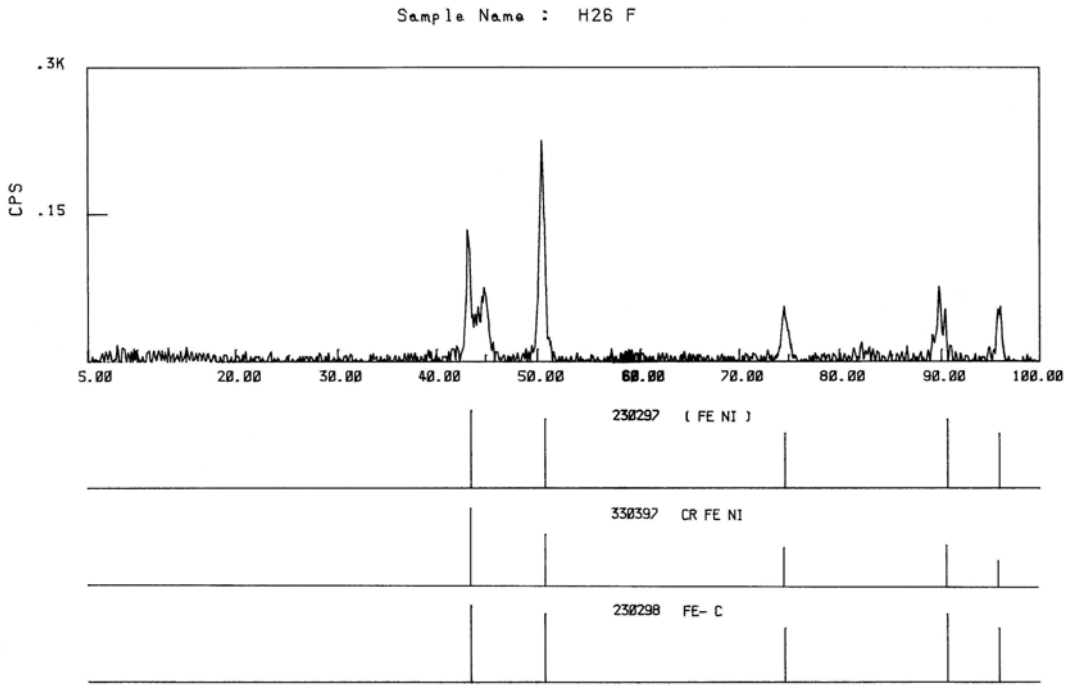

Fig. 6.27 XRD pattern of H13 die steel after machining with Inconel electrode (at I_p = 4 amp, P_{on} = 5 µsec and P_{off} = 57 µsec)

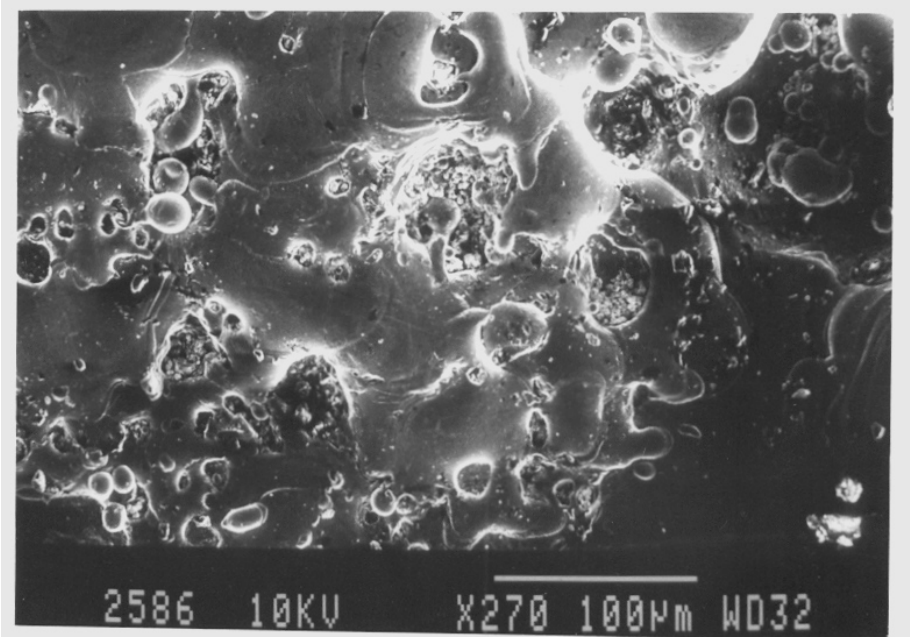

Fig. 6.28 SEM micrograph of H13 die steel after machining with Inconel electrode (at I_p = 4 amp, P_{on} = 5 µsec and P_{off} = 57 µsec)

This intermetallic compound (FeCrNi) is also seen in the XRD pattern of H13 die steel along with ferrite (Fe-C) and a solid solution phase of iron and nickel (Fe-Ni). Though cementite has not been shown, some unmarked peaks indicate a weak presence of this phase. As far as the improvement in micro-hardness is concerned, the absence of cementite in H13 die steel gets compensated by the formation of the solid solution of iron and nickel. It is also observed that despite the availability of carbon from the dielectric and presence of significant amount of chromium, chromium carbide could not be formed on the workpiece surface. Thus, it can be inferred that these machining conditions are not suitable for the formation of chromium carbide. The microstructures indicate that surface finish has deteriorated substantially after machining with inconel electrode. As the deterioration was more than 100 % in both the materials, further analysis of this aspect was not done.

6.7 MIGRATION OF MANGANESE

Manganese is present in all steels as a deoxidizer. It improves strength and hardness, but to a lesser degree than carbon, and is most effective in high carbon steels. Its carbide-forming tendency is greater than iron but less than chromium. It has a moderate effect on hardenability and reduces brittleness at high temperatures. The iron atoms of the cementite phase can also be substituted by manganese atoms [119].

Though manganese is classified as a weak carbide former in steels, but machining with manganese powder has resulted in the formation of its carbides in the machined surface of all the three work materials. The results of the spectrometric analysis done on D2 die steel are given in Table 6.17. The increase in percentages of manganese as well as carbon indicate that the formation of manganese carbide is taking place in the sparking channel which gets deposited on the work surface after the plasma channel collapses. The optimum combination of the input process parameters for all the work materials is found to be $A_2B_1C_3$ in which the need for longer pulse off-time has been reflected. When compared to the optimum combination for tungsten powder ($A_2B_2C_3$), there is difference in the value of pulse on-time only which can be attributed to the difference in melting points of manganese (1244 ^{0}C) and tungsten (3410 ^{0}C). A small amount of copper is also seen in the spectrometric analysis (but not in the XRD pattern due to the low percentage) which indicates that electrode material is

an integral part of the sparking channel under all machining conditions. Some loss of chromium has taken place in this case also.

Table 6.17 Chemical composition of D2 die steel after machining with Manganese Powder (at I_p = 4 amp, P_{on} = 5 µsec and P_{off} = 85 µsec)

Composition	Before machining	After machining with Manganese Powder	Significant changes
% Carbon	**1.57**	**1.92**	**+ 0.35**
% Silicon	0.19	0.21	-
% Manganese	**0.07**	**0.62**	**+ 0.55**
% Chromium	**12.38**	**12.04**	**– 0.34**
% Molybdenum	0.76	0.79	-
% Vanadium	0.96	0.94	-
% Tungsten	-	-	-
% Nickel	0.09	0.13	-
% Copper	**-**	**0.15**	**+ 0.15**
% Iron	Balance	Balance	-

The XRD patterns of the work materials after machining with manganese powder and the corresponding microstructures are given in Fig. 6.29 to Fig. 6.34. Microstructures show relatively smoother surfaces with uniform dispersion of phases as compared to the surfaces generated by machining with inconel electrode and tungsten powder (which are the other two cases of very high improvement in micro-hardness). There are even no micro-cracks. Manganese carbide in different forms ($Mn_4C_{1.06}$, Mn_7C_3 and Mn_5C_2) can be seen in the XRD analysis of the workpiece surfaces.

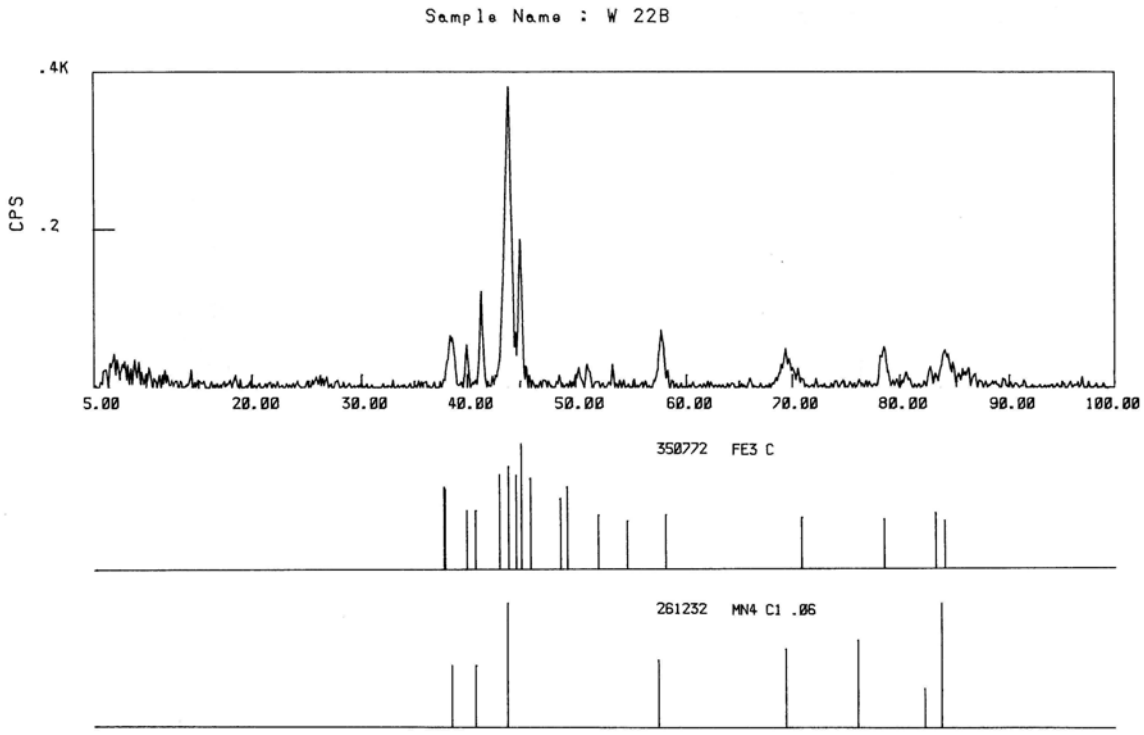

Fig. 6.29 XRD pattern of OHNS die steel after machining with Manganese powder-mixed dielectric (at I_p = 4 amp, P_{on} = 5 µsec and P_{off} = 85 µsec)

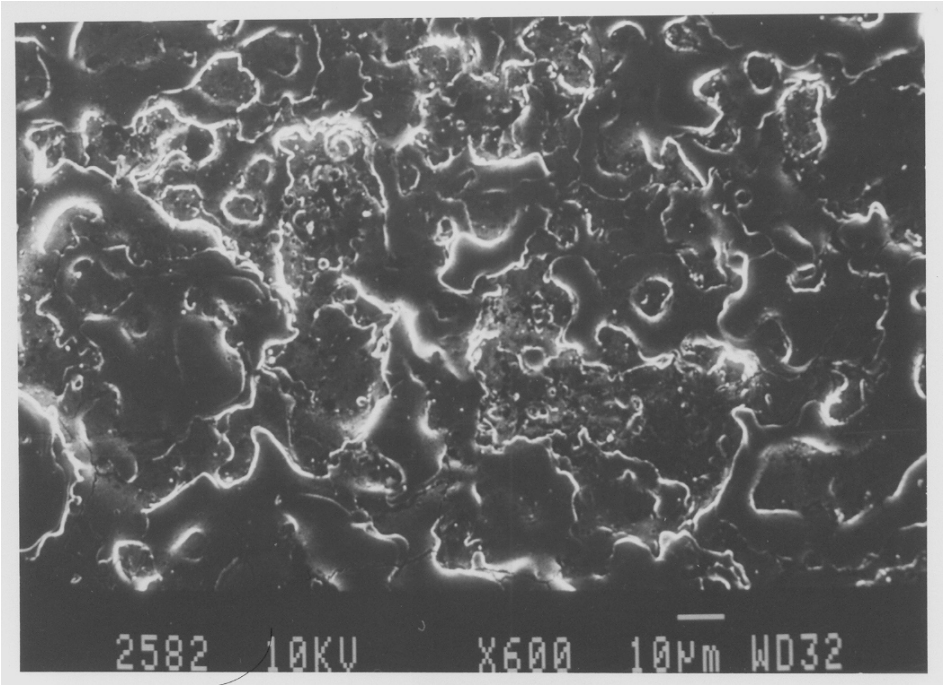

Fig. 6.30 SEM micrograph of OHNS die steel after machining with Manganese powder-mixed dielectric (at I_p = 4 amp, P_{on} = 5 µsec and P_{off} = 85 µsec)

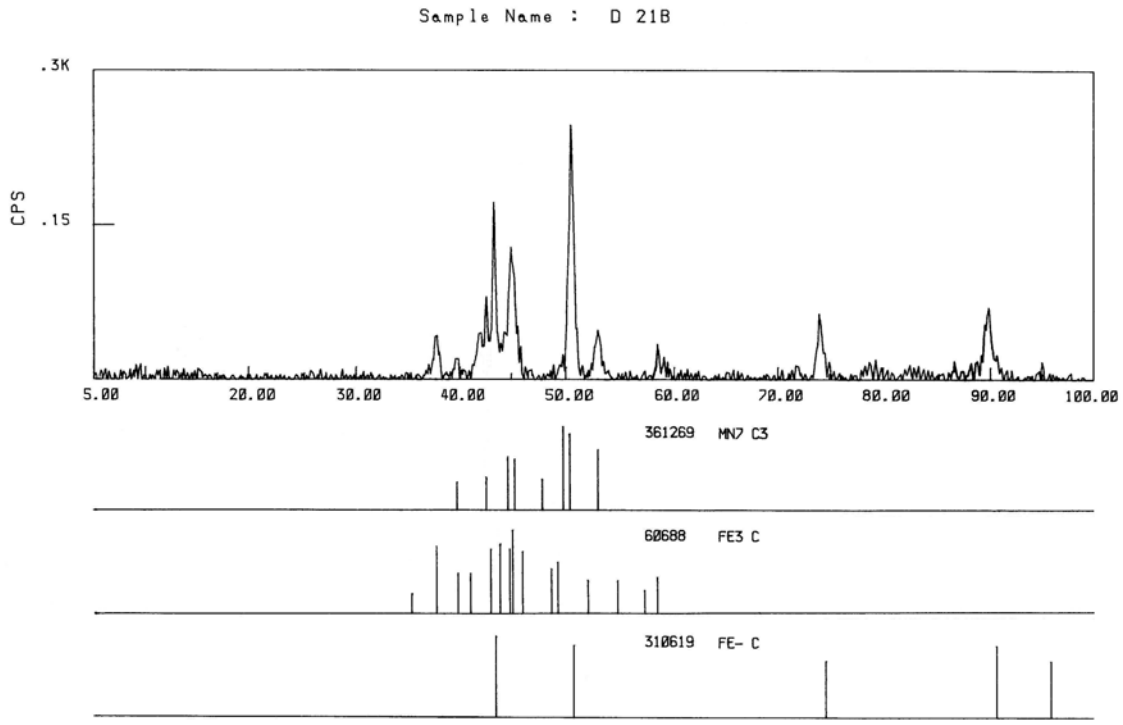

Fig. 6.31 XRD pattern of D2 die steel after machining with Manganese powder-mixed dielectric (at I_p = 4 amp, P_{on} = 5 µsec and P_{off} = 85 µsec)

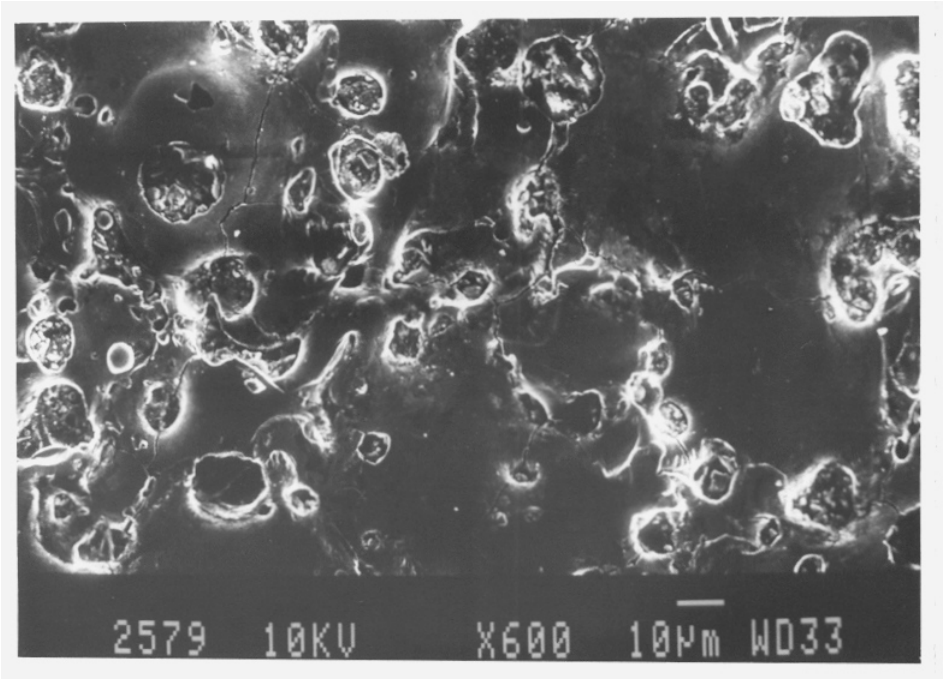

Fig. 6.32 SEM micrograph of D2 die steel after machining with Manganese powder-mixed dielectric (at I_p = 4 amp, P_{on} = 5 µsec and P_{off} = 85 µsec)

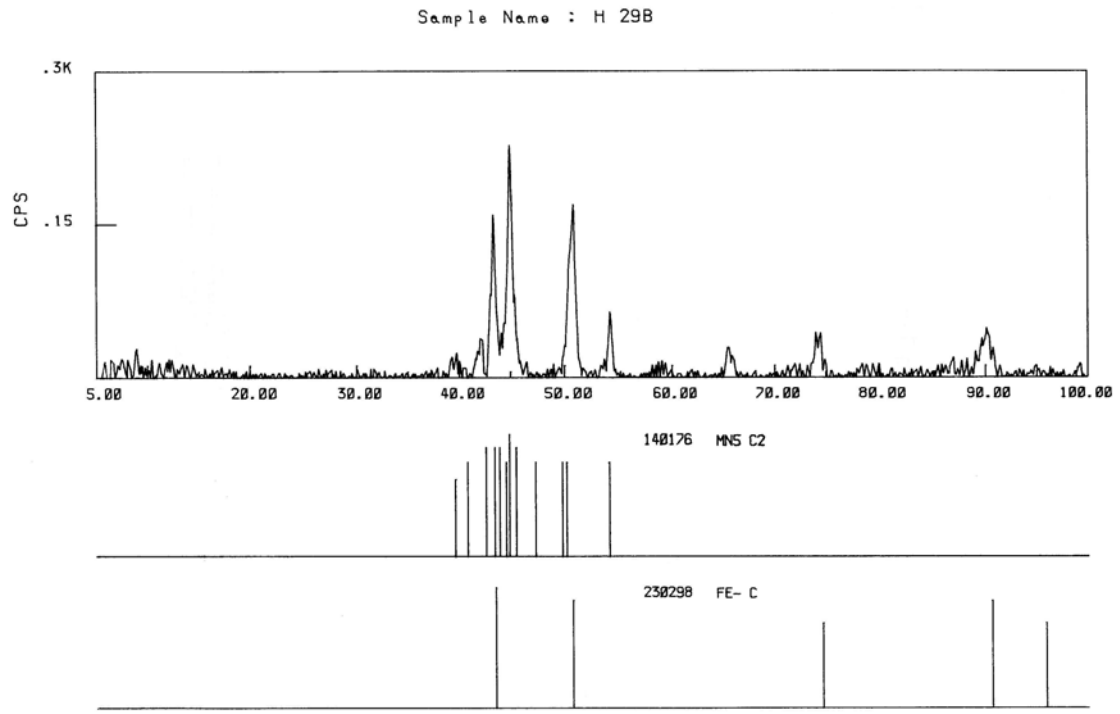

Fig. 6.33 XRD pattern of H13 die steel after machining with Manganese powder-mixed dielectric (at I_p = 4 amp, P_{on} = 5 µsec and P_{off} = 85 µsec)

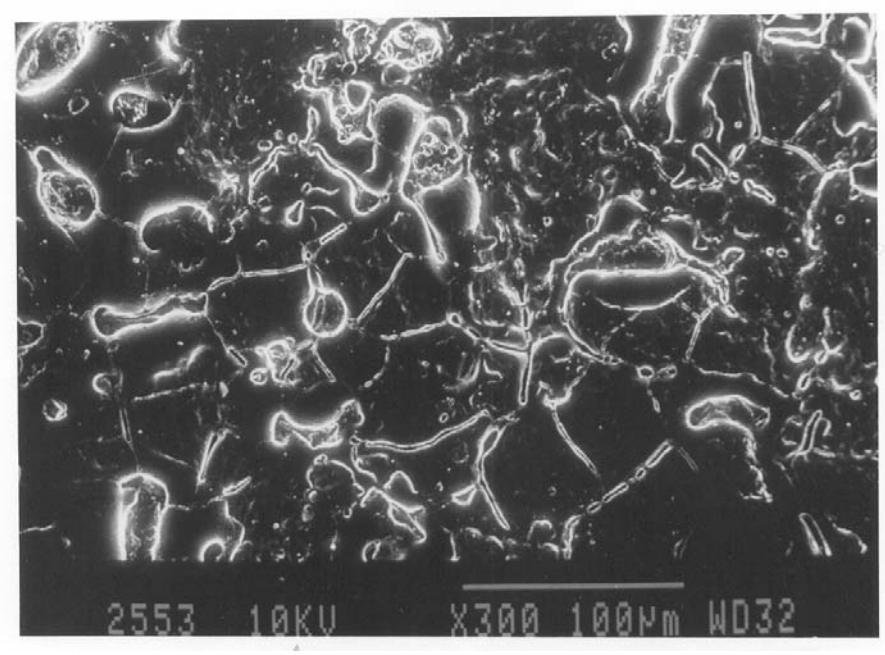

Fig. 6.34 SEM micrograph of H13 die steel after machining with Manganese powder-mixed dielectric (at I_p = 4 amp, P_{on} = 5 µsec and P_{off} = 85 µsec)

It is interesting to note that despite the different forms of manganese carbide, the improvement in micro-hardness is almost identical (72.9 % in case of OHNS die steel, 69.8 % in case of D2 die steel and 73.8 % in case of H13 die steel). Similar to the behaviour of tungsten powder, surface finish deteriorates with manganese powder also, but to a lesser extent for OHNS and D2 die steels (in case of H13 die steel, surface finish actually improves when machining is done with tungsten powder). It is evident from the microstructures also. Keeping in view the overall results, both tungsten and manganese powders can be recommended for carrying out surface modification of die steels.

6.8 MIGRATION OF SILICON

Silicon is present in all steels as a cheap deoxidizer. Like nickel, silicon is not a carbide former but dissolves in ferrite, increasing the strength and toughness of this phase. It also improves the oxidation resistance. A properly balanced combination of manganese and silicon produces a steel of unusually high strength, good ductility and toughness. Silicon has a strong graphitizing influence and is generally not desirable in high carbon steels.

The XRD patterns of OHNS and H13 die steels are given in Fig. 6.35 and Fig. 6.36. No traces of silicon or silicon carbide were seen in the XRD pattern of the D2 die steel sample machined with silicon powder and due to this reason, it has not been included here. Solid solution of silicon with iron (Fe-Si) along with cementite is observed in the XRD pattern of OHNS die steel and some traces of silicon with ferrite are seen in the XRD pattern of H13 die steel. However, the improvement in micro-hardness is almost the same as that achieved with copper electrode only (18.8 % for OHNS die steel with silicon powder and 12.5 % with copper electrode). As the increase in micro-hardness was only marginal but machining with silicon powder improved the surface finish considerably; further exploration was restricted to the study of surface roughness only.

Just like graphite powder, machining with silicon powder also resulted in a very good surface finish. Amongst the three work materials, minimum R_a value of 0.92 μm was reported for OHNS die steel. So, more experiments were conducted on OHNS die steel with silicon powder to find out R_a and R_z values of surface roughness.

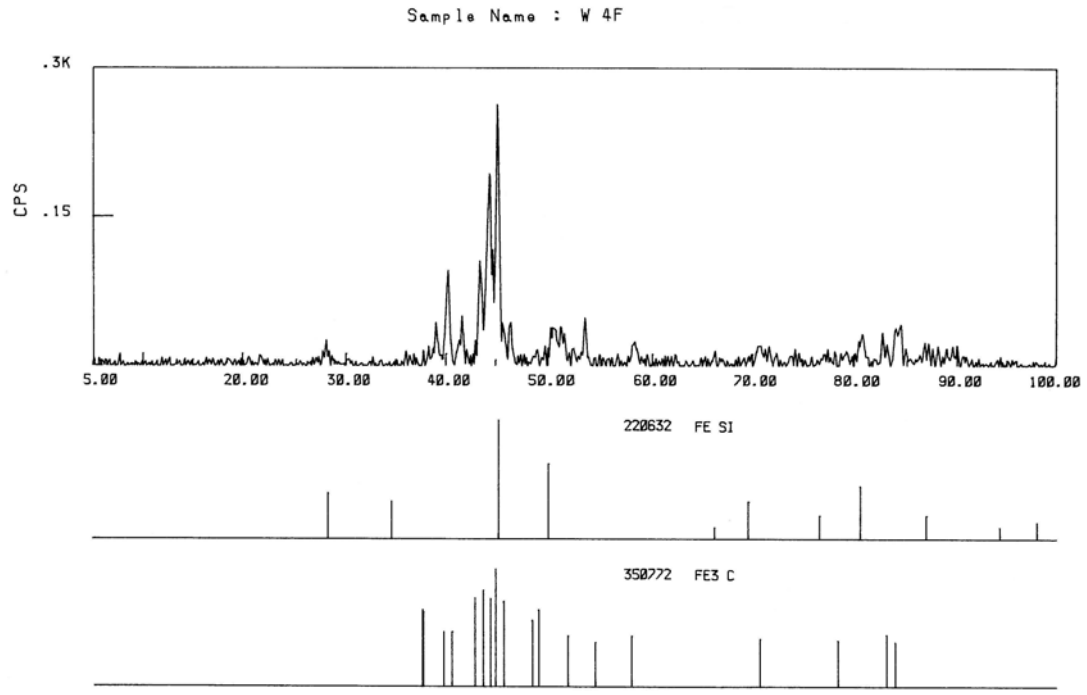

Fig. 6.35 XRD pattern of OHNS die steel after machining with Silicon powder-mixed dielectric (at I_p = 6 amp, P_{on} = 5 µsec and P_{off} = 85 µsec)

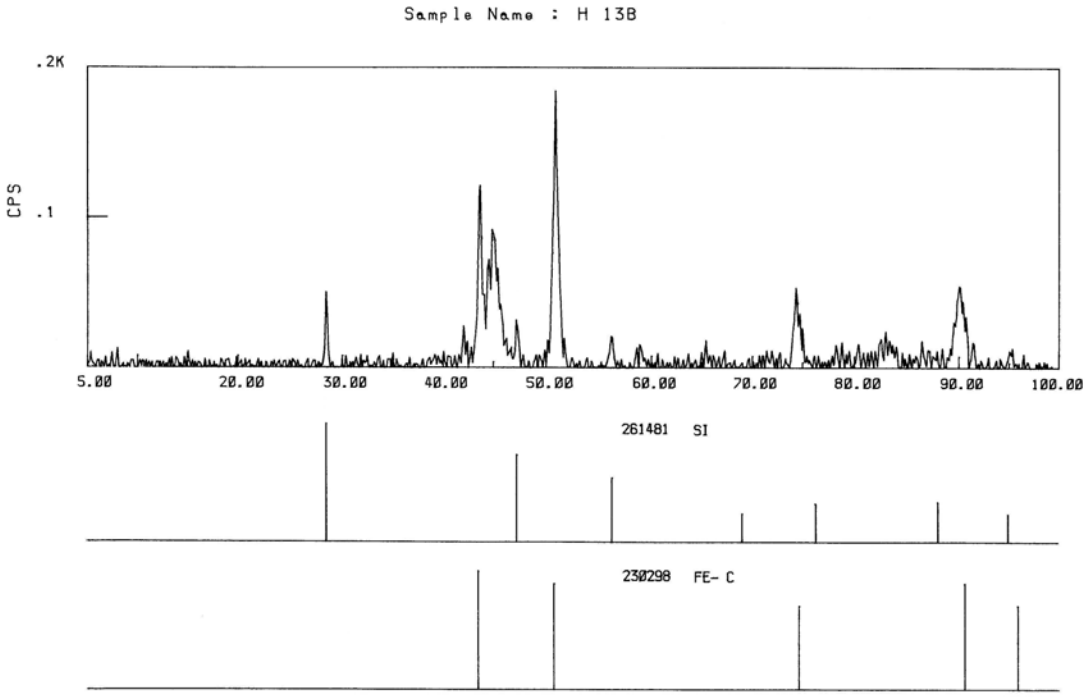

Fig. 6.36 XRD pattern of H13 die steel after machining with Silicon powder-mixed dielectric (at I_p = 6 amp, P_{on} = 5 µsec and P_{off} = 85 µsec)

The optimum condition for least surface roughness with silicon powder was found to be $A_1B_1C_2$ with the percentage contribution of peak current being 79.8 %, followed by pulse on-time at 14 % and pulse off-time at 6.1 %. The optimum condition for least surface roughness with copper electrode (reference value) was also found to be $A_1B_1C_2$. Therefore, experiments were conducted with and without silicon powder using copper electrode at different values of peak current by keeping the other two factors constant (pulse on-time = 5 µsec and pulse off-time = 57 µsec). The average R_a and R_z values of surface roughness were measured and they are given in Table 6.18. These values have been presented graphically in Fig. 6.37.

Table 6.18 R_a and R_z values of Surface Roughness after machining OHNS die steel with and without Silicon powder-mixed dielectric (P_{on} = 5 µsec and P_{off} = 57 µsec)

Peak Current (amperes)	Surface Roughness values achieved with Copper electrode		Surface Roughness values achieved with Silicon powder under same machining conditions	
	R_a (in µm)	R_z (in µm)	R_a (in µm)	R_z (in µm)
2 A	2.46	11.8	0.92	4.97
4 A	3.01	14.1	1.33	7.06
6 A	4.43	21.7	2.14	10.3

Substantial reduction in R_a and R_z values of surface roughness is observed when machining is carried out with silicon powder. While graphite powder reported a decrease in R_z value from 11.8 µm to 3.81 µm at 2 amperes peak current, the corresponding value achieved with silicon powder is 4.97 µm which is slightly inferior but still reflects a very good surface finish. SEM micrograph of this surface is given in Fig. 6.38 which shows a crack-free smooth surface. Similar to the surface machined with graphite powder, no craters are visible. Powder particles improve the sparking efficiency by lowering the dielectric strength and help in the uniform dispersion of discharges throughout the surface. The increased gap between the tool and workpiece due to lower dielectric breakdown resistance also results in wider discharge passages. This generates a lower discharge power density, a lower plasma pressure and a

lower impact force on the melted material of the surface craters [102]. The capacitive effect between the tool and workpiece also gets reduced [95]. The combined effect specifically improves the surface finish by reducing asperities (lower R_z value) which is evident in the micrograph also.

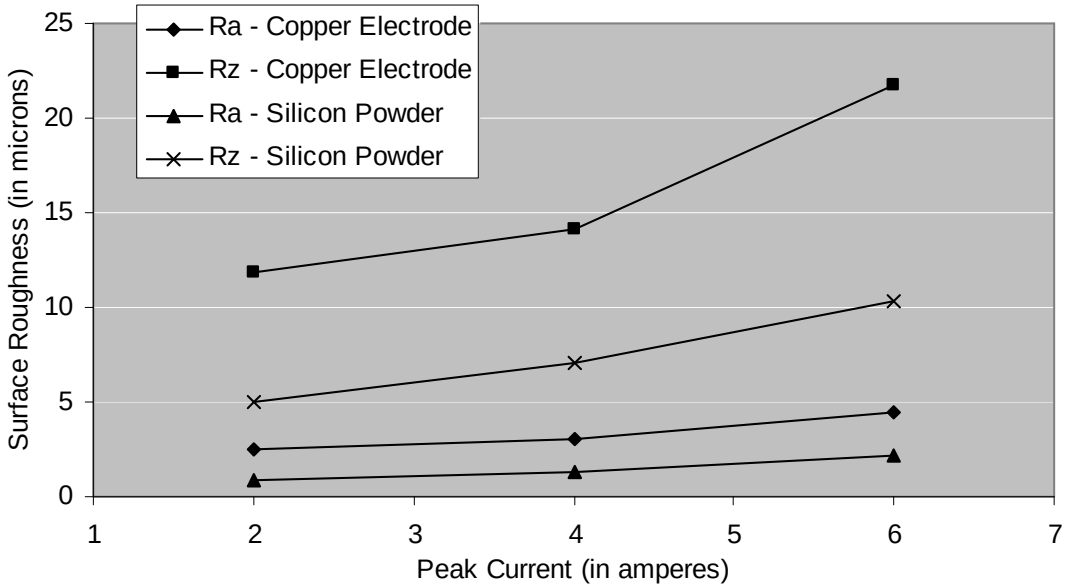

Fig. 6.37 Comparison of R_a and R_z values of Surface Roughness after machining OHNS die steel with silicon powder-mixed dielectric (P_{on} = 5 µsec and P_{off} = 57 µsec)

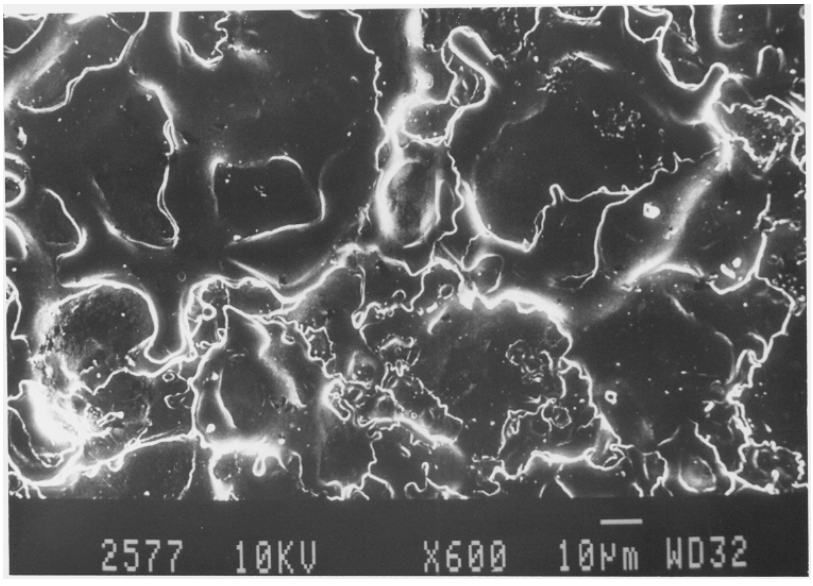

Fig. 6.38 SEM micrograph of OHNS die steel after machining with Silicon powder-mixed dielectric (at I_p = 2 amp, P_{on} = 5 µsec and P_{off} = 57 µsec)

The absence of craters is an important outcome of machining with these powders. As compared to silicon powder, the improvement in micro-hardness achieved by graphite powder is also higher (743 HV as compared to 721 HV by silicon powder for OHNS die steel and 663 HV as compared to 608 HV by silicon powder for H13 die steel). Hence, it can be suggested that graphite powder is a better option for improving the surface finish of die steels and silicon powder can be recommended only for die steels containing high amounts of carbon, for example, D2 die steel.

CHAPTER - 7

CONCLUSIONS AND SCOPE FOR FUTURE WORK

7.1 CONCLUSIONS

Experimental investigations were conducted into the phenomenon of material transfer during electrical discharge machining of three die steel materials using four different tool electrodes and four powders suspended in the dielectric medium. The important conclusions drawn from this research work are:

- The favourable machining conditions for material transfer by EDM were found to be low discharge current (less than 5 amperes), shorter pulse on-time (less than 10 μsec), longer pulse off-time (more than 50 μsec) and negative polarity of the tool electrode. In general, it was observed that within the given conditions, less current and more pulse on-time were required for material transfer from suspended powders as compared to material transfer from tool electrode bodies.
- Inconel alloy emerged as a very important electrode material from the point of view of surface modification of die steel materials. It contributed chromium and nickel to the workpiece surface under appropriate machining conditions. From the base values of 0.49 % chromium and 0.05 % nickel in OHNS die steel, the maximum percentages achieved were 1.20 % chromium and 5.4 % nickel. This electrode material improved the micro-hardness of OHNS and H13 die steel materials by approximately 88 %. However, this was accompanied by deterioration of surface finish.
- Tungsten was found in the workpiece surface in different forms when machining was carried out with copper-tungsten electrode or with tungsten powder suspended in the dielectric medium. In case of H13 hot die steel, from a negligible percentage (0.005%) of tungsten in the base material, it increased to a maximum of 0.872% when machining was carried out with copper-tungsten electrode and to a maximum of 3.252% with tungsten powder. But the optimum machining parameters were found to be different in each case. When machining was carried out with copper-tungsten electrode, the best value of micro-hardness was achieved at peak current of 6

amperes, pulse on-time of 5 μsec and pulse off-time of 57 μsec; whereas in case of tungsten-mixed dielectric, the corresponding values were 4 amperes peak current, 10 μsec pulse on-time and 85 μsec pulse off-time. The difference in peak current and pulse on-time values can be attributed to the need of electrode wear in case of copper-tungsten electrode for which higher current and lower pulse on-time are required. Regarding shorter pulse off-time for copper-tungsten electrode, it can be said that the electrode is still hot when the next sparking cycle starts and it can disintegrate easily.

- All the three work materials showed more than 100 % improvement in micro-hardness when machining was carried out with tungsten powder mixed in the dielectric and the highest value of 1409 HV was achieved by D2 die steel. Tungsten was found in the form of intermetallic compounds with iron (Fe_2W, Fe_7W_6) when machining was carried out with copper-tungsten electrode and as carbides (WC, W_2C) when machining was done with tungsten powder. In one of the cases, atoms of tungsten replaced the iron atoms in cementite to form alloyed cementite [$(FeW)_3C$]. When OHNS die steel was machined with tungsten powder, free tungsten was seen on the surface along with tungsten carbide. Hence, it can be concluded that migration of tungsten successfully takes place by both these methods of surface modification.
- The optimum values and relative contribution of the three input process parameters for each electrode material or the type of powder suspended in the dielectric medium were found to be almost the same irrespective of the work material. Thus, it can be concluded that the desirable values of input process parameters depend on the type of electrode material or powder and not on the work material. On the other hand, the best values of micro-hardness and surface roughness depend on the type of work material. Peak current was found to be the most important parameter (more than 50 % contribution in all cases) for both the response characteristics of micro-hardness and surface roughness.
- This study establishes the significance of pulse off-time along side current and pulse on-time for the phenomenon of surface modification. In general, it was observed that the percentage contribution of this parameter for the response characteristic of micro-hardness was more as compared to its contribution for the other response

characteristic of surface roughness. When machining was carried out with inconel electrode or with tungsten powder suspended in the dielectric, pulse off-time was found to be second most important parameter (after peak current) for micro-hardness. In both these cases, the improvement in micro-hardness was very high. The best values of micro-hardness were achieved at level 2 (57 μsec) or level 3 (85 μsec) of pulse off-time and the best values of surface roughness were achieved at level 1 (38 μsec) or level 2 (57 μsec) of this parameter. Hence, it can be concluded that moderate values of pulse off-time are suitable for improving the surface properties of die steels.

- The use of graphite powder improved the surface finish without considerable effect on micro-hardness. Though the carbon percentage was found to be more than 4% in some cases, micro-hardness did not show much improvement. The study corroborates the earlier findings that conductive powders improve the surface finish significantly [94-95, 99-101, 106]. When using graphite powder with OHNS die steel, a surface roughness (R_a) value of 0.73 μm was achieved. Another important observation is the major reduction in R_z values under these machining conditions which is indicative of excellent surface finish. Moreover, the presence of free graphite is expected to provide self-lubricating property to the workpiece surface which is highly beneficial for dies and press tools. Hence, it is recommended that graphite powder should be added to the dielectric during electrical discharge machining of die steels. The lack of improvement in micro-hardness might be due to the use of copper electrode with graphite powder. It can also be suggested that graphite powder should be used with suitable tungsten / titanium electrodes to obtain the right combination of high micro-hardness and good surface finish.

- It was possible to transfer a significant amount of manganese element into the workpiece surface by suspending its powder in the dielectric medium. The percentage of this element in D2 (high carbon high chromium) die steel increased from 0.07 % to 0.62 %. Manganese carbide in different forms was observed in the machined surfaces of all the three work materials. Hence, it can be inferred that transfer of manganese is possible by EDM in powder-mixed dielectric.

- Machining with tungsten and manganese powders improved the micro-hardness considerably, but surface finish deteriorated. The highest value of micro-hardness achieved in this experimentation was 1409 HV (an improvement of 116 %) when D2 die steel was machined with tungsten powder and the best improvement in micro-hardness (130 % increase from 465 HV to 1071 HV) took place in the case of H13 die steel. The low percentage of carbon in H13 die steel initially provides more scope for improvement in surface properties by infusion of carbon. An increase in percentage of carbon was found in this material under all machining conditions and it can be concluded that carbon from the pyrolysis of the hydrocarbon dielectric migrates to the workpiece surface.
- Silicon powder improved the surface finish and gave a crack-free surface, but its effect on improving the micro-hardness was negligible. Like graphite powder, significant improvements in both R_a as well as R_z values were observed. Very small traces of silicon in elemental form and as a solid solution with iron (Fe-Si) were seen in the X-ray diffraction pattern of the surfaces machined with silicon powder. However, no traces of silicon carbide were seen. It can be concluded that silicon powder may be used for improving the surface finish only. In general, the performance of graphite powder in improving the surface finish as well as micro-hardness was found to be better than silicon powder. Hence, silicon powder can be recommended only for die steels containing high amounts of carbon.
- Copper-tungsten was found to be the only electrode material that provided significant improvement in micro-hardness along with superior surface finish. It improved the micro-hardness of OHNS and H13 die steels by more than 50 % and that of D2 die steel by 28 %. While improvement in micro-hardness by inconel electrode was much higher, it was accompanied by a substantial deterioration of surface finish. If surface improvement is desired to be achieved only from tool electrodes without using any powder, then copper-tungsten can be recommended as a good electrode material.

(12) Finally, it can be concluded from this research work that the method of surface modification by electrical discharge machining is technically feasible and has the potential of becoming a cost effective and time saving alternative to the surface

modification techniques currently being used by the tool and die making industry. It is pertinent to note that EDM process is already being used in the industry for machining hardened work materials, and simple modifications in the existing set-up can lead to substantial improvement in surface properties. Consequently, the working life of dies and press tools can be significantly enhanced.

7.2 RECOMMENDATIONS FOR FUTURE WORK

After completing this research work, it is felt that the method of surface modification by electrical discharge machining opens a vast number of avenues for further exploration. Future work may be in the direction of:

(1) Three important die steel materials were chosen for this experimental work. Other die and tool steel materials such as Tungsten hot work die steels (H2x-series), Molybdenum high speed tool steels (M-series), Air-hardening medium- alloy cold work die steels (A-series), Water-hardening die steels (W-series) and Shock resisting tool steels (S-series) etc. can be tried for the surface modification process.

(2) Powder metallurgy electrodes of various desirable powders may be prepared in different compositions and used under negative polarity favouring high electrode wear for surface alloying. The sintering temperature and pressure for the fabrication of these electrodes can also be varied.

(3) In this experimental work, area of the electrodes was kept fixed. It is well known that in EDM, the short distance between electrode and workpiece creates a capacitive effect, which increases with the electrode area and disturbs the discharge process. The use of powders in the dielectric increases this electrode-workpiece distance. Hence, there is a need to study the effect of change in electrode area on the response characteristics of micro-hardness and surface roughness.

(4) In this experimental work, machining was carried out in powder-mixed dielectric using graphite, manganese, tungsten and silicon powders. Other important alloying elements in tool and die steels such as cobalt, chromium, nickel, molybdenum and vanadium can be taken in the powder form and suspended in the dielectric medium. Particle size of the powders and their concentration in dielectric can also be varied.

(5) Some other organic liquids (such as ethylene glycol) or deionized water (already used in wire-EDM) may be tried as dielectric medium. In such a medium, graphite electrode can be used as a source for providing carbon when tungsten powder is suspended in the dielectric.

(6) The methods of surface modification with the help of material transfer from the electrode bodies and from powders suspended in the dielectric medium are not mutually exclusive. Both methods can be attempted simultaneously and it may yield better results. For example, chromium carbide and vanadium carbide are known to provide very good hardness and wear resistance to tool steel [20]. When machining was carried out with inconel electrode in this work, transfer of chromium took place but chromium carbide could not be obtained. It is suggested that inconel electrode should be used with graphite powder suspended in the dielectric medium to explore the possibility of getting chromium carbide in the workpiece surface.

(7) Machining with graphite electrode has given very good surface finish (in the range of 1-2 μm). Likewise, machining with graphite powder has given very good surface finish (< 1 μm), but the electrode used was copper in this case. If an attempt is made by using graphite electrode with graphite powder suspended in the dielectric medium, the resultant surface finish is expected to be still better.

(8) Like inconel, some other readily available alloys of desirable elements can be tried as electrode materials for this application. Examples of such materials are Haynes alloy (containing cobalt, chromium and molybdenum), Hastalloy (containing nickel, chromium, molybdenum and iron), Cupronickel (containing copper and nickel) and Silicon Bronze (containing copper, silicon and manganese) etc.

(9) An attempt was made in this research work to infuse silicon carbide into the machined surface by carrying out machining in silicon powder-mixed dielectric but success could not be achieved. Some amount of silicon was observed in the workpiece surface in the form of intermetallic compound Fe-Si but no traces of SiC were found. As silicon carbide is known to impart surface hardness as high as 4000 HV, efforts should be made to find out the machining conditions in which this compound may get deposited on the machined surface.

REFERENCES

[1] Dewes R, Aspinwall D, Simao J and Lee H G (2003), "Electrical Discharge Machining and Surface Alloying – The Process, Parameters and State of Play", *Materials World,* Vol. 11, No. 5, pp 16-18

[2] Altan T, Lilly B W, Konig W, Tonshoff H K, Luttervelt C A van, Khairy A B (1993), "Advanced techniques for Die and Mold Manufacturing", *Annals of the CIRP*, Vol. 42 (2), pp 707-716

[3] Fuller John E. (1996), "Electrical Discharge Machining", in ASM Machining Handbook, Vol. 16, pp 557-564

[4] Pandey P C and Shan H S (1995), "Modern Machining Processes", Tata McGraw Hill, New Delhi, India, ISBN 0-07-096518-8

[5] Jain V K (2004), "Advanced Machining Processes", Allied Publishers, New Delhi, India, ISBN 81-7764-294-4

[6] Lahiri B N (2001), "Understanding EDM technology", Lecture notes of Summer Programme on Advanced Manufacturing, IIT Kharagpur, pp 61-77

[7] Zolotykh B N (1995), "Modern physical theory of electric erosion of metals- the basis of development of new directions in EDM", *Proceedings of ISEM-XI,* pp 114-116

[8] Lucca D A, Brinksmeirer E and Goch G (1998), "Progress in assessing surface and subsurface integrity", *Annals of the CIRP,* Vol. 47(2), pp 669-693.

[9] Tsukahara H and Sone T (2000), "Surface hardening of titanium using EDM process,' Titan. Japan, Vol. 48 (2), pp 47-49

[10] Tzeng Y F, Lee C Y (2001), "Effects of powder characteristics on electro-discharge machining efficiency" *Int. J. of Adv. Manuf. Technology,* Vol. 17 (8), pp 586-592

[11] Marafona J. and Wykes C. (2000), "A new method of optimizing material removal rate using EDM with copper tungsten electrodes", *Int. J. of Machine tools & manufacture,* Vol. 40 (2), pp 153-164

[12] Mohri N, Saito N and Tsunekawa Y (1993), "Metal Surface modification by electrical discharge machining with composite electrodes," *Annals of the CIRP,* Vol. 42 (1), pp 219-222

[13] Soni J S and Chakraverti G (1996), "Experimental investigation on migration of material during EDM of T 215 Cr12 die steel," *J. of Mat. Proc. Tech.,* Vol. 56, pp 439-451

[14] Lahiri B N, Mukherjee S K and Mullick B K (1981), "Loss of energy in pyrolysis of dielectric in EDM process", *Journal of Institution of Engineers (I),* pt ME2, Vol. 62, pp 66-69

[15] Quan Y M, Liu Y H (1995), "Powder-suspension dielectric fluid for EDM", *J. of Mat. Proc. Tech.,* Vol. 52, No. 1, pp 44-54

[16] Furutani K, Saneto A, Takezawa H, Mohri N and Miyake H (2001), "Accretion of titanium carbide by electrical discharge machining with powder suspended in working fluid", *Precision Engg.,* Vol. 25, pp 138-144

[17] ASM Specialty Handbook: Tool Materials (1995), 1st Edition, ASM International, USA, ISBN : 0-87170-545-1

[18] ASM Handbook : Surface Engineering (1999), Vol. 5, ASM International, USA, ISBN : 0-87170-384-X

[19] Prabhudev K H (2000), "Handbook of Heat Treatment of Steels", Tata McGraw Hill Publishing Company, New Delhi, India. ISBN 0-07-451831-3

[20] Lakhtin Y (1983), "Engineering Physical Metallurgy", Mir Publishers, Moscow, ISBN : 81-239-0602-1

[21] Kalpakjian S and Schmid S R (2001), "Manufacturing Engineering & Technology", 4th Edition, Pearson Education Inc., USA. ISBN 81-7808-157-1

[22] DeGarmo E Paul, Black J T and Kohser R A (1997), "Materials and Processes in Manufacturing", 8th Edition, Pearson Education Inc., USA. ISBN 81-203-1243-0

[23] Galerie A, Pons M and Caillet M (1989), "Surface modification using lasers and ion beams", *Material Science and Technology,* Vol. 5, pp 806-812

[24] Mishra P K (2005), "Non Conventional Machining", Narosa Publishing House, New Delhi. ISBN 81-7319-192-1

[25] Sommer C (2000), "Non-traditional Machining Handbook", Advance Publishing Inc., Houston, USA, 1st Edition, ISBN 1-57537-325-4

[26] Shankar N U and Krishnan A (1979), "Polarity Effect in Spark Erosion Machining", *Indian J. Technol.,* Vol. 17 (9), pp 363-364

[27] Benedict Gary F (1987), "Nontraditional Manufacturing Processes", Marcel Dekker Inc., New York, ISBN 0-8247-7352-7

[28] Ho K H and Newman S T (2003), "State of the art electrical discharge machining", *Int. J. of Machine Tools & Manufacture,* Vol. 43, pp 1287-1300

[29] Kuneida M, Lauwers B, Rajurkar K P and Schumacher B M (2005), "Advancing EDM through fundamental insight into the process", *Annals of CIRP,* Vol. 54(2), pp 599-622

[30] Pandit S M and Rajurkar K P (1983), "A stochastic approach to thermal modeling applied to electro-discharge machining", *Tr. of ASME, Journal of Heat Transfer,* Vol. 105, pp 555-562

[31] Toren M, Zvirin Y and Winograd Y (1975), "Melting and Evaporation phenomena during Electrical Erosion", *Tr. of ASME, Journal of Heat Transfer,* Vol. 97, pp 576-581

[32] Roberts G A and Cary R A (1980), "Tool Steels", 4th Edition, American Society for Metals, Ohio, USA, ISBN 0-87170-096-4

[33] Avner S H (1997), "Introduction to Physical Metallurgy", 2nd Edition, Tata McGraw Hill Publishing Company, New Delhi, India. ISBN 0-07-463006-7

[34] Roy R K (1990), "A primer on the Taguchi method", Van Nostrand Reinhold, New York, USA, ISBN 0-442-23729-4

[35] Singh Sehijpal, Shan H S and Kumar Pradeep (2002), "Parametric optimization of magnetic field assisted abrasive flow machining by Taguchi method", *Journal of Quality and Reliability engineering International",* Vol. 18, pp 273-283

[36] Lazarenko B R (1943), "To invert the effect of wear on electric power contacts", Dissertation of The All-Union Institute for Electro Technique in Moscow / CCCP (in Russian).

[37] Jameson E C (2001), "Description and development of electrical discharge machining", Society of Manufacturing Engineers, Dearbern, Michigan, USA.

[38] Abu Zeid O A (1997), "On the effect of electrodischarge machining parameters on the fatigue life of AISI D6 tool steel", *Int. Journal of Materials Processing Technology,* Vol. 68 (1), pp 27-32

[39] Schumacher B M (2004), "After 60 years of EDM, the discharge process remains still disputed", *Int. Journal of Materials Processing Technology,* Vol. 149, pp 376-381

[40] Tsai K M and Wang P J (2001), "Predictions on surface finish in electrical discharge machining based upon neural network models", *Int. J. of Machine tools & manufacture,* Vol. 41 (10), pp 1385-1403

[41] McGeough J A (1988), "Advanced Methods of Machining", Chapman and Hall, USA, 1st Edition, ISBN 0-412-31970-5

[42] Crookall J R and Heuvelman C J (1971), "Electro-discharge machining – the state of the art", *Annals of the CIRP*, Vol. 20 (1), pp 113-120

[43] Bruyn H E De (1968), "Slope control – a great improvement in spark erosion", *Annals of the CIRP*, Vol. 16, pp 183-186

[44] Wong Y S, Lim L C and Lee L C (1995), "Effect of flushing on electro-discharge machined surfaces", *Int. Journal of Materials Processing Technology,* Vol. 48, pp 299-305

[45] Levy G N and Ferroni B (1975), "Planetary spark erosion – applications and optimization", *Proc. of 16th MDR Conference*, pp 291-297

[46] Schumacher B M (1983), "EDM technology for precision workpieces with excellent surface quality", *Proc. of ISEM-7*, pp 124-135

[47] Kruth J P, Stevens L, Froyen L and Lauwers B (1995), "Study on the white layer of a surface machined by die sinking electro-discharge machining", *Annals of the CIRP*, Vol. 44 (1), pp 169-172

[48] Kruth J P, Tonshoff H K and Klocke F (1998), "Surface and sub-surface quality in material removal process for tool making", *Proc. of ISEM-12*, pp 33-64

[49] Kruth J P (1995), "Rapid prototyping, a new application of physical and chemical processes for material accretion manufacturing", *Proc. of ISEM-XI,* pp 3-28.

[50] Mohri N, Takezawa H, Furutani K, Ito Y and Sata T (2000), "A new process of additive and removal machining by EDM with a thin electrode", *Annals of CIRP,* Vol. 40 (1), pp 123-126.

[51] Roethel F and Garbajs V (1976), "Contributions to the micro-analysis of spark eroded surfaces", *Annals of the CIRP,* vol 25 (1), pp 135-140.

[52] Lee L C, Lim L C, Narayanan V and Venkatesh V C (1988), "Quantification of surface damage of tool steels after EDM", *Int. J. of Mach. Tools & manufacture,* vol. 28 (4), pp 359-372.

[53] Venkatesh V C and Parasnis S (1972), "Surface transformation in high speed steel after electro discharge machining." *Proc. of the 5th AIMTDR conference*, IIT, Roorkee, pp 639-649

[54] Jeswani M L and Basu S (1976), "Electron microprobe study of deposition and diffusion of tool material in electrical discharge machining", *Int. J. of Production Research,* Vol. 17 (1), pp 1-14

[55] Kunieda M and Yoshida M (1997), **"**Electric Discharge Machining in Gas**"**, *Annals of the CIRP*, Vol. 46 (1), pp 143-146

[56] Barash M M and Kahlon C S (1965), "Experiments with electric spark toughening", *Int. J. of Machine Tool Design & Research*, Vol. 4, pp 1-8

[57] Koshy G, Philip P K and Geddam A (1983), "Hardening of surface layers using electric discharge techniques", *Proc. of 11th AIMTDR Conf.,* IIT Madras, pp 315-319

[58] Erden A and Bilgin S (1980), "Role of impurities in EDM", *Proc. of 21st IMTDR Conference,* pp 345-350

[59] Gangadhar A, Shunmugam M S and Philip P K (1991), "Surface modification in electrodischarge processing with a powder compact tool electrode", *Wear,* Vol. 143, pp 45-55

[60] Shunmugam M S, Philip P K and Gangadhar A (1994), "Improvement of wear resistance by EDM with tungsten carbide powder metallurgy electrode", *Wear,* Vol. 171, pp 1-5

[61] Cao G, Zhao W, Wang Z and Guo Y (2005), "Instantaneous fabrication of tungsten micro-electrode based on single electrical discharge", *Int. J. of Materials Processing Technology,* Vol. 168, pp 83-88

[62] Tsunekawa Y, Okumiya M, Mohri N and Takahashi I (1994), "Surface modification of aluminum by electrical discharge alloying", *Materials Science and Engg.,* Vol. A174, pp 193-198

[63] Tsai H C, Yan B H and Huang F Y (2003), "EDM performance of Cr/Cu-based composite electrodes", *Int. Journal of Machine Tools and Manufacture,* Vol. 43, pp 245-252

[64] Miyazaki T, Yoshioka S, Kimura T and Kinoshita N (1995), "Surface modification of steel by a small diameter plasma arc", *Annals of CIRP,* Vol. 44 (1), pp 161-164

[65] Samuel M P and Philip P K (1997), "Powder metallurgy tool electrodes for electrical discharge machining", *Int. J. of Machine Tools & Manufacture*, Vol. 37 (11), pp 1625-1633

[66] Pantelis D I, Vaxevanidis N M, Houndri A E, Dumas P and Jeandin M (1998), "Investigation into application of electrodischarge machining as steel surface modification technique", Surface Engineering, Vol. 14 (1), pp 55-61

[67] Mohri N, Fukusima Y, Fukuzawa Y, Tani T and Saito N (2003), "Layer generation process on workpiece in electrical discharge machining", *Annals of the CIRP*, Vol. 52 (1), pp 157-160

[68] Lin Y C, Yan B H and Huang F Y (2001), "Surface improvement using a combination of electrical discharge machining with ball burnish machining based on the Taguchi method", *Int. Journal of Advanced Manufacturing Technology,* vol. 18, pp 673-682

[69] Yan B H, Lin Y C and Huang F Y (2002), "Surface modification of Al-Zn-Mg alloy by combined electrical discharge machining with ball burnish machining", *Int. J. of Machine Tools & Manufacture,* Vol. 42, pp 925-934

[70] Simao J, Aspinwall D, El-Menshawy F and Meadows K (2002), "Surface alloying using PM composite electrode materials when electrical discharge texturing hardened AISI D2", *Int. Journal of Materials Processing Technology,* Vol. 127, pp 211-216

[71] Curodeau A, Marceau L F, Richard M and Lessard J (2005), "New EDM polishing and texturing process with conductive polymer electrodes", *Int. Journal of Materials Processing Technology,* Vol. 159, pp 17-26

[72] Aspinwall D K, Dewes R C, Lee H G and Simao J (2003), "Electrical Discharge surface alloying of Ti and Fe workpiece materials using refractory powder compact electrodes and Cu wire", *Annals of the CIRP,* Vol. 52 (1), pp 151-160

[73] Lee H G, Simao J, Aspinwall D K, Dewes R C and Voice W (2004), "Electrical discharge surface alloying", *Int. Journal of Materials Processing Technology,* Vol. 149, pp 334-340

[74] Wang Z L, Fang Y, Wu P N, Zhao W S and Cheng K (2002), "Surface modification process by electrical discharge machining with a Ti powder green compact electrode", *Int. Journal of Materials Processing Technology,* Vol. 129, pp 139-142

[75] Miyake H, Imai A, Goto A, Saito N and Mohri N (1998), "Improvement of tool life through surface modification by electrical discharge machining", *Proc. of ISEM-12*, pp 261-270

[76] Moro T, Goto A, Mohri N, Saito N, Matsukawa K and Miyake H (2001), "Surface modification process by electrical discharge machining with TiC semi-sintered electrode", *J. of Jpn. Soc. Prec. Engg.,* Vol. 67 (1), pp 114-119

[77] Simao J, Lee H G, Aspinwall D K, Dewes R C and Aspinwall E M (2003), "Workpiece surface modification using electrical discharge machining", *Int. J. of Machine Tools & Manufacture,* Vol. 43, pp 121-128

[78] Bai Ching-Yuan and Koo Chun-Hao (2006), "Effects of kerosene or distilled water as dielectric on electrical discharge alloying of superalloy Haynes 230 with Al-Mo composite electrode", *Surface & Coatings Technology,* Vol. 200, pp 4127-4135

[79] Patowari P K, Mishra U K, Saha P and Mishra P K (2006), "Surface modification of C-40 steel using WC-Cu P/M green compact electrodes in EDM", *Proc. of the 1st International and 22nd AIMTDR conference*, IIT Roorkee, pp 875-879

[80] Panda D K and Bhoi R K (2006), "Experimental investigation of relative erosion of electrodes in electrical discharge machining", *Proc. of the 1st Int. and 22nd AIMTDR Conference,* IIT, Roorkee, pp 929-934

[81] Patel M R, Barrufet M A and Eubank P T (1989), "Theoretical model of the electrical discharge machining process – II. The anode erosion model", *Journal of Applied Physics*, Vol. 66 (9), pp 4104-4111

[82] Eubank P T, Patel M R, Barrufet M A and Bozkurt B (1993), "Theoretical model of the electrical discharge machining process – III. The variable mass, cylindrical plasma model", *Journal of Applied Physics*, Vol. 73 (11), pp 7900-7909

[83] Zimanyi J (1975), "Photometric determination of the spatial and chronological structure variations of the discharge by spark erosion metalworking" *Annals of the CIRP,* Vol. 24 (1), pp 89-94

[84] Shankar P, Jain V K and Sundararajan T (1997), "Analysis of Spark Profiles during EDM process", *Machin. Sci. Technology,* Vol. 1, No. 2, pp 195-217

[85] Kaldes F (1983), **"**Flushing the gap in EDM**"**, EDM Digest, Part-I

[86] George V and Venkatesh V C (1980), **"**Investigations on Optimum Machining conditions for Electric Discharge Machining of 5 Cr Die Steel**"**, *Proc. of 9th AIMTDR Conference*, IIT Kanpur, pp 327

[87] Kuppan P, Rajadurai A and Narayanan S (2006), "Experimental investigation into electrical discharge deep hole drilling of Inconel 718 using Graphite electrode", *1st Int. and 22nd AIMTDR Conference,* IIT, Roorkee, pp 923-928

[88] Ahmad M, A Senthil Kumar and Lim H S (2006), "A study on machining parameters of guided micro-EDM tool with focus on minimizing spark gap", *22nd AIMTDR Conference,* IIT, Roorkee, pp 869-873

[89] Van Dijck F (1973)**, "**Physico-mathematical analysis of EDM process**"**, Ph. D. Thesis, Katholieke University, Heverlee, Netherlands

[90] Raghunathan V (1980), "Performance representation and Optimization of Electric Discharge Machining", Diss. Abstr, Int. State University of New York

[91] Soni J S and Chakraverty G (1995), "Effect of Electrode Material Properties on Surface Roughness and Dimensional Accuracy in Electrical Discharge Machining of High carbon High chromium Die Steel" , *J. of Inst. of Engineers (I) – PR,* Vol. 76

[92] George V and Philip P K (1978), "Analysis of EDM Performance and Tool Wear in Cu-Die Steel system – A Review", *Proceedings of the 8th AIMTDR Conference,* IIT Bombay

[93] Kansal H K, Singh S and Kumar P (2005), "Parametric optimization of powder mixed electrical discharge machining by response surface methodology", *Int. Journal of Materials Processing Technology,* Vol. 169, pp 427-436

[94] Rehbein W, Schulze H P, Mecke K, Wollenberg G and Storr M (2004), "Influence of selected groups of additives on breakdown in EDM sinking", *Int. Journal of Materials Processing Technology,* Vol. 149, pp 58-64

[95] Pecas P and Henriques E (2003), "Influence of silicon powder-mixed dielectric on conventional electrical discharge machining", *Int. J. of Machine Tools & Manufacture,* Vol. 43, pp 1465-1471

[96] Okada A, Uno Y and Hirao K (2000), "Formation of hard layer by EDM with carbon powder mixed fluid using titanium electrode", *Proceedings of the Int. Conf. on Progress of Machining Technology,* pp 464-469

[97] Narumiya H, Mohri N, Saito N, Ootake H, Tsunekawa Y, Takawashi T and Kobayashi K (1989), "EDM by powder suspended working fluid", *Proceedings of the ISEM-9,* Nagoya, Japan, pp 5-8

[98] Tzeng Y F and Lee C Y (2001), "Effect of powder characteristics on electrodischarge machining efficiency", *Int. Journal of Advanced Manufacturing Technology,* Vol. 17 (8), pp 586-592

[99] Kozak J, Rozenek M and Dabrowski L (2003), "Study of electrical discharge machining using powder-suspended working media", *Journal of Engg. Manufacture,* Proc. Instn. Mech. Engrs, Vol. 217 part B, pp 1597-1602

[100] Zhao W S, Meng Q G and Wang Z L (2002), "The application of research on powder mixed EDM in rough machining", *Int. Journal of Materials Processing Technology,* Vol. 129, pp 30-33

[101] Jeswani M L (1981), "Effect of addition of graphite powder to kerosene used as a dielectric fluid in electrical discharge machining", *Wear,* Vol. 70, pp 133-139

[102] Uno Y, Okada A and Cetin S (2001), "Surface modification of EDMed surface with powder mixed fluid", *Proceedings of the 2nd Int. Conf. on Design and Production of Dies and Molds*

[103] Furutani K and Shimizu Y (2003), "Experimental analysis of deposition process of lubricant surface by EDM with molybdenum disulphide powder suspended in working oil", *Proc. of American Soc. For Prec. Engg.,* Vol. 30, pp 547-550

[104] Yan B H, Tsai H C and Huang F Y (2005), "The effect in EDM of a dielectric of a urea solution in water on modifying the surface of titanium", *Int. Journal of Machine Tools and Manufacture,* vol. 45, pp 194-200

[105] Wu K L, Yan B H, Huang F Y and Chen S C (2005), "Improvement of surface finish on SKD steel using electro-discharge machining with aluminum and surfactant added dielectric", *Int. J. of Machine Tools & Manufacture,* Vol. 45, pp 1195-1201

[106] Wong Y S, Lim L C, Rahuman I and Tee W M (1998), "Near mirror-finish phenomenon in EDM using powder-mixed dielectric", *Int. Journal of Materials Processing Technology,* Vol. 79, pp 30-40

[107] Tzeng Y and Chen F (2005), "Investigation into some surface characteristics of electrical discharge machined SKD-11 using powder-suspension dielectric oil", *Int. Journal of Materials Processing Technology,* Vol. 170, pp 385-391

[108] Klocke F, Lung D, Antonoglou G and Thomaidis D (2004), "The effects of powder suspended dielectrics on the thermal influenced zone by electrodischarge machining with small discharge energies", *Int. Journal of Materials Processing Technology,* Vol. 149, pp 191-197

[109] Fredriksson G and Hogmark S (1995), **"**Influence of dielectric temperature in EDM of hot worked tool steel**"**, *Surface Engg.,* Vol. 11 (4), pp 324-330

[110] Lin Y C, Yan B H and Huang F Y (2001), "Surface modification of Al-Zn-Mg aluminum alloy using the combined process of EDM with USM", *Int. J. of Materials Processing Technology,* Vol. 115, pp 359-366

[111] Montgomery D C (2005), "Design & Analysis of Experiments", 5th Edition, John Wiley & Sons, ISBN 9971-51-329-3

[112] Phadke Madhav S (1989), "Quality engineering using robust design", AT & T Bell Laboratories, P T R Prentice Hall Inc, New Jersey, USA, ISBN 0-13-745167-9

[113] Bagchi T (1993), "Taguchi methods explained : Practical steps to robust design", Prentice Hall of India, ISBN 0-87692-808-4

[114] Singh H and Kumar Pradeep (2005), "Optimizing cutting force for turned parts by Taguchi's parameter design approach", *Indian Journal of Engg. & Mat. Sciences,* vol. 12, pp 97-103

[115] Ross Phillip J (1988), "Taguchi techniques for quality engineering", McGraw Hill Book Company, ISBN 0-07-053866-2

[116] Gupta N B, Shahabadkar P K and Nandurkar K N (2006), "Experimental investigations on EDM using Taguchi technique for optimization of process parameters", *1st Int. and 22nd AIMTDR Conference,* IIT, Roorkee, pp 941-946

[117] Garcia-Diaz A, Philips D T (1995), "Principles of Experimental Design and Analysis", Chapman and Hall, London.

[118] Cahn R W (2005), "Concise Encyclopaedia of Materials Characterization", 2nd Edition, Elsevier Ltd., Oxford, UK, ISBN 0-08-044547-0.

[119] Pollack H W (1988), "Materials Science and Metallurgy", 4th Edition, Prentice Hall Inc., USA, ISBN 0-8359-4287-2.

[120] Tottle C R (1984), "An Encyclopaedia of Metallurgy and Materials", Macdonald & Evans Ltd., UK, ISBN 0-7121-0571-9.

[121] Victory Electromech, "Operation manual for T-3822M Electric Discharge Machine", Kolhapur, India.

APPENDIX – A

TECHNICAL SPECIFICATIONS OF THE EDM MACHINE [121]

The experimentation has been conducted on Electric Discharge Machine model T-3822M, make Victory Electromech, Kolhapur, India. It is a ram type vertical sinking EDM machine equipped with a solid state Pulse Generation Circuit. Technical data of the machine is as under:

1. ELECTRICAL DATA

Supply Volts	:	415 V, 3 Ø, 50 Hz
Connected Load	:	3 KVA
Open Gap Output Voltage	:	135 ± 5 % V
Machine Current (Max.)	:	12 A
Rotary Switch Current Range	:	3 ranges of 4 A each
Rotary Knob Current Adjust	:	Fine current adjustment from 0-4 A in each current range
Pulse Duration	:	2, 5, 10, 20, 50, 100, 200, 500 µsec
Pulse Interval	:	2 to 3840 µsec in various steps depending on selection of pulse on-time

2. MACHINE TOOL

Height	:	1300 mm
Width	:	730 mm
Depth	:	840 mm
Net Weight	:	325 Kg.
Travel of the Quill	:	150 mm
Reading accuracy of the dial gauge	:	0.01 mm
Maximum load lifting capacity including accessories	:	10 Kg

3. WORK TANK

Length	:	600 mm
Width	:	350 mm
Height	:	240 mm

4. COORDINATE TABLE

Mounting Surface (Length x Width)	:	380 x 220 mm
Maximum Workpiece Height	:	125 mm
Maximum Workpiece Weight	:	80 Kg.
Longitudinal Travel (X-axis)	:	200 mm
Transverse Travel (Y-axis)	:	125 mm
Maximum Table-Quill distance	:	340 mm
Minimum Table-Quill distance	:	190 mm
Low Level Indicator	:	40 mm above sparking point.

5. DIELECTRIC UNIT

Length	:	1000 mm
Width	:	780 mm
Height	:	675 mm
Capacity	:	150 Liters
Weight without Dielectric Fluid	:	65 Kg.
Filter Elements type	:	Paper
Filter Number	:	One
Filter Rating	:	Below 20 microns
Motor Specifications	:	1 HP, 415 V, 3 Ø, 50 Hz

APPENDIX – B

IMPORTANT PROPERTIES OF ELEMENTS INVOLVED IN EXPERIMENTATION [120]

(All values at 25 ^{0}C)

Element	Atomic Number	Atomic Weight	Density (g/cm^3)	Melting Point (^{0}C)	Thermal Conductivity (W/cm ^{0}C)	Electrical Resistivity (μΩ cm)	Specific Heat (J/g ^{0}C)
Carbon	6	12.011	2.25	3550	0.238	1375	0.712
Chromium	24	51.996	7.20	1857	0.91	12.9	0.448
Copper	29	63.55	8.96	1083.4	3.98	1.673	0.385
Iron	26	55.84	7.86	1535	0.803	9.71	0.444
Manganese	25	54.938	7.20	1244	1.59	185.0	0.477
Nickel	28	58.7	8.90	1453	0.90	6.84	0.444
Silicon	14	28.09	2.33	1410	0.835	10.0	0.703
Tungsten	74	183.85	19.35	3410	1.78	5.65	0.133

APPENDIX – C

IMPORTANT SPECIFICATIONS OF MEASURING INSTRUMENTS USED IN EXPERIMENTATION

---

1. Perthometer

Make and model	:	Mahr, M4Pi, Germany
Measurement method	:	Stylus
Profile resolution	:	100 nm
Measuring range	:	Up to 100 μm
Profile resolution	:	12 nm
Cut-off wavelength	:	0.8 mm
Tracing length	:	4.8 mm
Evaluation length	:	4.0 mm

2. Optical Emission Spectrometer

Make and model	:	Baird, DV-6, USA
Base	:	Iron, Copper, Aluminium
Medium	:	Argon gas
Accuracy	:	0.0001%

3. Micro Hardness Tester

Make and model	:	Shimadzu Corporation, HMV-2, Kyoto, Japan
Indenter	:	Diamond Pyramid Indenter (face angle $136^0 \pm 0.5^0$)
Optical Monitor	:	Objective lens 40x, Eyepiece 10x
Loads available	:	98.07 mN, 245.2 mN, 490.3 mN, 980.7 mN, 1.96 N, 2.942 N, 4.903 N, **9.807 N**, 19.614 N
Load duration time	:	20 sec
Units	:	Vickers, Rockwell
Vickers Hardness, HV	=	$0.1891\ F/d^2$, where F is test load in Newtons, d is mean of indentation diagonal length (mm)

4. X-Ray Diffractometer System

Make and model	:	Rigaku Corporation, ME210LA2, Japan
Scanning Angle Range	:	-100 to $+160^0$
Step Used	:	0.02^0
Scan speed	:	5^0 /min
Range of 2θ	:	5^0 to 100^0

5. Scanning Electron Microscope

Make and model	:	JEOL, JSM-840A, Japan
Magnification	:	10x to 3,00,000x
EDS attachment	:	TRACOR NORTHERN, TN-5500

APPENDIX – D

STANDARD L9 ORTHOGONAL ARRAY AND ITS LINEAR GRAPH [115]

Experiment Number	Column			
	1	**2**	**3**	**4**
1	1	1	1	1
2	1	2	2	2
3	1	3	3	3
4	2	1	2	3
5	2	2	3	1
6	2	3	1	2
7	3	1	3	2
8	3	2	1	3
9	3	3	2	1

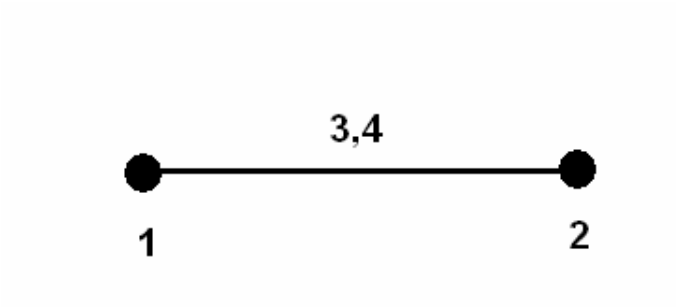

Linear Graph for L9

APPENDIX – E

FORMULAE USED FOR ANOVA CALCULATIONS [112]

The analysis of the data has been performed using Microsoft Excel® Spreadsheet software. The formulae used for the calculations are as under:

For micro-hardness, which is higher-the-better type of response characteristic, the value of signal-to-noise ratio η, has been calculated as

$$\eta = -10 \log \left[\frac{1}{R} \sum_{j=1}^{R} (1/y_j^2) \right]$$

where y_j is the measured value of response characteristic

and R is the number of repetitions

For surface roughness, which is lower-the-better type of response characteristic, the value of signal-to-noise ratio η, has been calculated as

$$\eta = -10 \log \left[\frac{1}{R} \sum_{j=1}^{R} (y_j^2) \right]$$

Overall mean value of η, $m = \frac{1}{9} \sum_{i=1}^{9} \eta_i$

Effect of factor A at level 1, $m_{A1} = \frac{1}{3} (\eta_1 + \eta_2 + \eta_3)$

where η_1 is the signal-to-noise ratio of the first row of OA

where η_2 is the signal-to-noise ratio of the second row, etc.

Effect of factor A at level 2, $m_{A2} = \frac{1}{3} (\eta_4 + \eta_5 + \eta_6)$

Effect of factor A at level 3, $m_{A3} = \frac{1}{3} (\eta_7 + \eta_8 + \eta_9)$

Effect of factor B at level 1, $m_{B1} = \frac{1}{3} (\eta_1 + \eta_4 + \eta_7)$

Effect of factor B at level 2, $m_{B2} = \frac{1}{3} (\eta_2 + \eta_5 + \eta_8)$

Effect of factor B at level 3, $m_{B3} = \frac{1}{3}(\eta_3 + \eta_6 + \eta_9)$

Effect of factor C at level 1, $m_{C1} = \frac{1}{3}(\eta_1 + \eta_6 + \eta_8)$

Effect of factor C at level 2, $m_{C2} = \frac{1}{3}(\eta_2 + \eta_4 + \eta_9)$

Effect of factor C at level 3, $m_{C3} = \frac{1}{3}(\eta_3 + \eta_5 + \eta_7)$

Grand total sum of squares $= \sum_{i=1}^{9} \eta_i^2$

Sum of squares due to mean = (number of experiments) x m^2

Total sum of squares $= \sum_{i=1}^{9} (\eta_i - m)^2$

Also, total sum of squares = (grand total sum of squares)
– (sum of squares due to mean)

Sum of squares due to factor A = $3(m_{A1} - m)^2 + 3(m_{A2} - m)^2 + 3(m_{A3} - m)^2$

Sum of squares due to factor B = $3(m_{B1} - m)^2 + 3(m_{B2} - m)^2 + 3(m_{B3} - m)^2$

Sum of squares due to factor C = $3(m_{C1} - m)^2 + 3(m_{C2} - m)^2 + 3(m_{C3} - m)^2$

Total sum of squares = (sum of the sum of squares due to various factors)
+ (sum of squares due to error)

$$\text{Variance} = \frac{\text{Sum of squares due to a factor}}{\text{Degrees of freedom of that factor}}$$

$$\text{Error variance} = \frac{\text{Sum of squares due to error}}{\text{Degrees of freedom for error}}$$

$$\text{F-ratio for a factor} = \frac{\text{Variance of that factor}}{\text{Error variance}}$$

$$\% \text{ contribution of a factor} = \frac{\text{Sum of squares due to that factor}}{\text{Total sum of squares}} \times 100$$

Assuming the optimum condition of the three input process parameters is $A_3B_1C_3$, then the theoretical value of η under the optimum conditions, denoted by η_{opt}, is given by:

$$\eta_{opt} = m + (m_{A3} - m) + (m_{B1} - m) + (m_{C3} - m)$$

The corresponding optimum value of higher-the-better type of response characteristic is given by

$$y_{opt}^2 = 1 / 10^{-\eta opt / 10}$$

And the optimum value of lower-the-better type of response characteristic is given by

$$y_{opt}^2 = 10^{-\eta opt / 10}$$